University of Strathclyde

Strathclyde Institute of Pharmacy and Biomedical Sciences

PHARMACOMETRIC MODELS OF ORAL CIPROFLOXACIN FOR CHILDREN WITH MALNUTRITION

WANCHANA UNGPHAKORN

A thesis presented in fulfilment of the requirements for the degree of Doctor of Philosophy

2012

This thesis is the result of the author's original research. It has been composed by the author and has not been previously submitted for examination which has led to the award of a degree

Signed:

Date:

SUMMARY

Children with severe malnutrition typically suffer from numerous associated complications. Among these, septicaemia, especially with Gram-negative organisms, remains the major concern because it is associated with a high mortality rate. The World Health Organization (WHO) has been releasing standard guidelines for the treatment of bacterial infections for many years; however, it has been found that the mortality rate remains high even if these guidelines are followed. Ciprofloxacin is a fluoroquinolone antimicrobial agent that has been considered as alternative treatment option. However, to date, data around the pharmacokinetics (PK) of ciprofloxacin, as well as other drugs, are limited in malnourished children. The aim of this thesis was to develop pharmacokinetic models for describing and predicting the PK of drugs in such children.

A population analysis was performed by using ciprofloxacin concentration-time data obtained from 52 malnourished children. It was found that a one-compartment model, with first-order absorption and a lag, adequately described the data. The final population model included the effect of body weight, high mortality risk and serum sodium concentration on clearance (CL), and the effect of body weight and sodium concentration on volume of distribution (V). Inclusion of these factors reduced inter-individual variability in CL from 50% to 38%, and in V from 49% to 43%. Absorption rate (ka) was poorly estimated and highly variable.

Internal validation techniques, including nonparametric bootstrap, a visual predictive check, normalised prediction distribution error and a jackknife analysis, were used to assess the stability and robustness of the final population model. The results of these analyses indicated that the model was stable and had a favourable predictive performance for CL and V.

To develop new dosage regimens, the population model was used to perform a 10,000-patient Monte Carlo simulation. The probabilities of achieving the therapeutic target $AUC_{0\text{-}24}$/MIC ratio and the expected population response were then

determined. The results showed that PK-PD breakpoints were 0.06-0.125 mg/L and 0.25-0.5 mg/L for Gram-negative and Gram-positive organisms, respectively. The overall response with the 30 mg/kg/day dose was 80% for *Escherichia coli*, *Klebsiella pneumoniae* and *Salmonella* species, but <60% for *Pseudomonas aeruginosa* and *Streptococcus pneumoniae.* The results suggested that an oral dose of ciprofloxacin 10 mg/kg three times daily (30 mg/kg/day) may be appropriate for the management of septicaemia in severely malnourished children. Discrepancies of susceptibility breakpoints between reference sources were also found, i.e., PK-PD, CLSI and EUCAST, and these discrepancies were most pronounced for *P. aeruginosa* and *S. pneumoniae*.

The population model was also used to determine optimal design for future population PK studies. A number of design options and design variables were examined. The results suggest that the optimal number of groups was three and two for three- and four-sample designs, respectively. When using two groups, it was possible to vary the number of individuals in each group. If permission was given to obtain up to five samples from each patient, one group of participants would be adequate. Only samples taken after the first dose gave sufficient information. The expected coefficient of variation (CV) of all parameters was under 10% with sample sizes of 25 and 40 for five- and four-sample designs, respectively. For three samples, the CV for ka remained above 20%, although the sample size was increased to 100. It was also found that the optimal designs were highly dependent on the prior information, so prior knowledge of drug concentration-time profiles should be used with optimal design methods when designing population PK studies.

In order to predict the disposition of other drugs in a malnourished population, whole body physiologically based pharmacokinetic (WBPBPK) models were developed by using ciprofloxacin as a model drug. The WBPBPK model was initially developed for healthy adults and then scaled to healthy and malnourished children. Kp values were calculated using the Poulin method, the Rodgers method and empirical method. The results showed that, for healthy adults and children, the predicted versus observed concentration-time profiles were well described with intravenous (IV bolus

and short infusion) models. Oral predictions were also in good agreement with the data from the literature, but peak concentrations were more rapidly achieved with a higher dose. Unlike the Poulin method, the concentration-time profiles predicted using Kp from the Rodgers method and the empirical methods were similar, and closely resembled the observed data. When models were scaled for malnutrition, inter-individual variability was higher, especially during the absorption phase. However, PK profiles were still adequately described.

The models developed in this thesis are useful tools for describing and predicting drug PK in malnourished children. However, due to the scarcity of data, further studies to characterise the alteration of drug kinetics, particularly during the absorption process, might improve the performance of the models. Application of these models to other drugs and data is also required to substantiate the predictive performance of the model.

Dedicated to my parents Paiboon and Thararat Ungphakorn

ACKNOWLEDGEMENTS

Three years ago, when I was starting my PhD, my sister told me that ‘doing a PhD is like walking through a dark tunnel because you never see the light until you are approaching the end’. I am now at the end of this journey and do not hesitate to acknowledge the following people for their help and support:

My sincere thanks must firstly go to the people who have always believed in my ability and have given me the great opportunity of pursuing my doctoral degree; Dr Alison Thomson and Dr Anne Boyter. They always motivate and encourage me to keep going and produce such good work. I would like to express my especial gratitude to Dr Alison Thomson for her time in reviewing this thesis and for her patience when I was lazy.

I would also like to thank Dr Nahashon Thuo, Professor Kathryn Maitland and all my colleagues from Kenya for providing me with the clinical data set. My experiments would not have been possible without these interesting data.

I would like to express my gratitude to Dr Joachim Grevel, Dr Kayode Ogungbenro, Professor Simon Mackay, Dr Andrea Edginton, and Esther Yun for their kindly support and advice.

My everyday life in SIPBS was not totally alone, thanks to my colleagues, Sarah Alghanem and Adel Alghamdi.

I am indebted to my best friends, Suppanut Taechakumponsarakij, Chananya Chanthes, and Wichai Piboon. We are a thousand miles apart, but they are always there with me.

Lastly, I would like to thank my dearest family – my father, mother, sister, grandmother and aunt for their unconditional love and understanding, as well as financial support.

TABLE OF CONTENTS

LIST OF TABLES

Chapter 1

Chapter 2

Chapter 3

Chapter 4

Chapter 5

Chapter 6

Chapter 7

LIST OF FIGURES

Chapter 4

Chapter 5

Chapter 6

Chapter 7

LIST OF PUBLICATIONS AND PRESENTATIONS

PUBLICATIONS

- Thuo, N., Ungphakorn, W., Karisa, J., Muchohi, S., Muturi, A., Kokwaro, G., Thomson, A. H., & Maitland, K. (2011). Dosing regimens of oral ciprofloxacin for children with severe malnutrition: a population pharmacokinetic study with Monte Carlo simulation. *Journal of Antimicrobial and Chemotherapy*. 66(10): 2336-2345.

PRESENTATIONS

- Poster presentation – PKUK, Bristol, UK (2010). Population pharmacokinetics of oral ciprofloxacin in paediatric patients with severe malnutrition.
- Oral presentation – ATPER, Copenhagen, Denmark (2011). Population pharmacokinetics modeling: An example of oral ciprofloxacin in malnourished children.
- Poster presentation – 20th PAGE, Athens, Greece (2011**).** Population pharmacokinetics and use of Monte Carlo simulation to determine optimal dosing regimen of oral ciprofloxacin in paediatric patients with severe malnutrition.
- Poster presentation – PKUK, Durham, UK (2011). Optimal study design for oral ciprofloxacin in malnourished children.
- Poster presentation – 21st PAGE, Venice, Italy (2012). Development of Sparse Sampling Study of Oral Ciprofloxacin for Severely Malnourished Children.
- Oral presentation – PKUK, Surrey, UK (2012). Development of a Whole-Body Physiologically Based Pharmacokinetics Model for Children with Severe Malnutrition.
- Poster presentation – PKUK, Surrey, UK (2012). Comparison of PK-PD Susceptibility Breakpoints for Healthy and Patient Subjects

LIST OF ABBREVIATIONS

Symbol	Definition
AIC	Akaike information criteria
AUC	Area under the curve
BMI	Body mass index
BSA	Body surface area
C_{AP}	Concentration of acidic phospholipids
CDC	Center for Disease Control
CFR	Cumulative fraction of response
CI	Confidence interval
CLcr	Creatinine clearance
CL_H	Hepatic clearance
$CLu_{int,H}$	Unbound intrinsic hepatic clearance
CL_{NR}	Non-renal clearance
CL_R	Renal clearance
CLSI	Clinical and Laboratory Standards Institute
CL_T	Total clearance
C_{max}	Maximum concentration
CO	Cardiac output
CV	Coefficient of variation
CWRES	Conditional weighted residual
DV	Dependent variable
$D_{OV:W}$	Olive oil:buffer PC of both non-ionised and ionised forms
EBE	Empirical Bayes estimates
EUCAST	European Committee on Antimicrobial Susceptibility Testing
EX	Exchange algorithm
F	Bioavailability
*f*BW	Body weight fraction
FDA	Food and Drug Administration
FIM	Fisher information matrix
FO	First-order estimation method

Symbol	Definition
FOCE	First-order conditional estimation method
FOCE-I	First-order conditional estimation method with interaction
*f*OW	Organ weight fraction
fu	Fraction unbound
GAM	Generalised assistive modelling
GFR	Glomerular filtration rate
HB	Hybrid algorithm
Hct	Haematocrit
IBW	Ideal body weight
ICRP	International Committee on Radiological Protection
IM	Intramuscular administration
IPRED	Individual predicted concentration
IRES	Individual residual
IV	Intravenous administration
IWRES	Individual weighted residual
k	Elimination rate constant
ka	Absorption rate constant
Ka_{AP}	Affinity constant for the acidic phospholipids
Kp	Tissue:plasma partition coefficient
Kpu	Tissue:unbound partition coefficient
k_{tr}	Transfer rate constant
$K_{VO:W}$	Olive oil:buffer PC of the non-ionised form
LBW	Lean body weight
LODE	Linear ordinary differential equation
MBC	Minimum bactericidal concentration
me	Mean error
MIC	Minimum inhibitory concentration
MTT	Mean transit time
MUAC	Mid upper-arm circumference
npde	Normalised prediction distribution error
OFV	Objective function value

Symbol	Definition
PAE	Post-antibiotic effect
PBPK	Physiologically based pharmacokinetics
PD	Pharmacodynamics
pe	Prediction error
PK	Pharmacokinetics
PO	Oral administration
$P_{O:W}$	*n*-octanol:buffer partition coefficient (PC) of the non-ionised form
PRED	Population predicted concentration
PTA	Probability of target attainment
R	Blood-to-plasma ratio
RES	Residual
rmse	Root mean squared error
Scr	Serum creatinine
SD	Standard deviation
se	Standard error
SM	Simplex algorithm
T_{max}	Time to maximum concentration
TS	Tubular secretion
TV	Typical value
V	Volume of distribution
VPC	Visual predictive check
Vss	Volume of distribution at steady state
WBPBPK	Whole-body physiologically based pharmacokinetics
WHO	Who Health Organization
WHZ	Weight-for-height Z-score
WRES	Weighted residual
ε	Residual error
η	Inter-individual error
σ^2	Variance of ε
ω^2	Variance of η

CHAPTER 1

INTRODUCTION

INTRODUCTION TO CHAPTER

This chapter gives a general background to the research conducted in this thesis. Firstly, a concept of drug therapy individualisation is described in Section 1.1. Section 1.2 gives a brief introduction to pharmacokinetics (PK) and pharmacodynamics (PD), followed by Section 1.3, which provides information on how to use the PK-PD approach to optimise antimicrobial therapy, focusing mainly on the fluoroquinolone antibiotics. A background review of ciprofloxacin, the antimicrobial agent that is the focus of this thesis, is given in Section 1.4. Section 1.5 provides information on malnutrition in children, which is the patient population used in this research. Finally, the influences of age, particularly neonates and children, and malnutrition on the pharmacokinetics of drugs are reviewed.

1.1 CONCEPT OF DRUG THERAPY INDIVIDUALISATION

The goal of antimicrobial therapy is to eradicate pathogens at the site of infection while minimizing toxicities and the emergence of bacterial resistance. The antimicrobial dosage regimen should be selected to achieve this goal effectively. There are numerous references that provide excellent sources of drug information and dosage recommendations; however, these references of drug information may be ill-suited for clinical use. This was highlighted in the study of Vidal *et al.* (2005), who conducted a systemic comparison of four references commonly used in clinical practice: *American Hospital Formulary Service Drug Information, the British National Formulary*, *Drug Prescribing in Renal Failure*, and *Martindale: The Complete Drug Reference*. They found a remarkable variation in recommendations, and a lack of primary literature in these references. The results from this work suggest a need for a more consistent, quantitative approach to dosage regimen design.

1.2 PHARMACOKINETICS AND PHARMACODYNAMICS

Pharmacokinetics is the study of the disposition of drugs within the body, which depend on the processes of drug absorption, distribution and elimination. It is reflected most often by the serum concentration against time profile. Pharmacodynamics is the study of the relationship between drug concentration and

pharmacological or toxicological effects. For antimicrobial agents, this refers to the relationship between drug concentration and antimicrobial activity or toxicity (Figure 1.1). Two fundamental pharmacodynamic parameters most commonly used to quantify antimicrobial activity are the minimum inhibitory concentration (MIC), which is defined as the lowest antimicrobial concentration that prevents visible growth of the organism, and the minimum bactericidal concentration (MBC), which is defined as the lowest antimicrobial concentration that kills 99.9% of the initially viable cells.

Figure 1.1 Relationship between drug dose and response

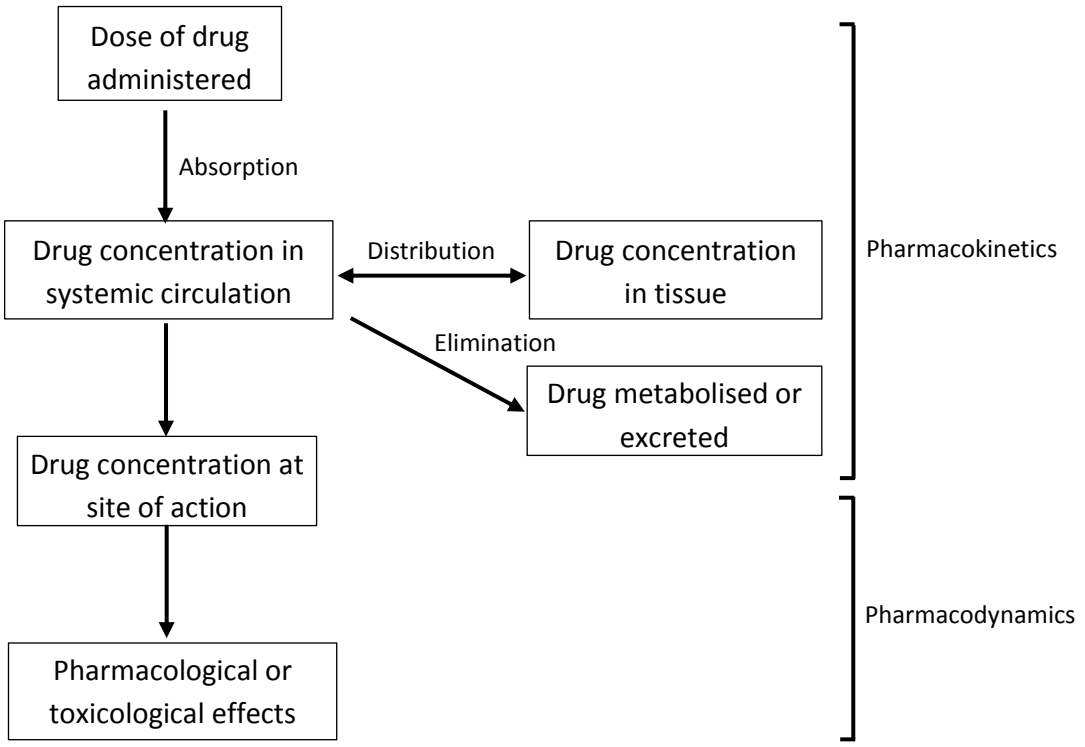

1.3 OPTIMISATION OF ANTIMICROBIAL THERAPY USING A PK-PD APPROACH

Although both MIC and MBC are good parameters to predict antimicrobial efficacy, they have limitations when applied to a clinical setting because they do not describe antimicrobial activity as a function of time. The MBC does not provide information on the killing rate or whether this rate increases at higher concentrations. MIC and

MBC do not describe antimicrobial activity at concentrations below these values, which may have initial inhibitory or bactericidal activity that is not maintained throughout the typical incubation period of 18-24 hours. Additionally, the process to determine MIC and MBC by using fixed and constant concentrations ignores the fact that concentrations of antimicrobial agents *in vivo* fluctuate with time and antimicrobial effects may persist after drug exposure (post-antibiotic effect). A better approach to determine antimicrobial efficacy is by integrating PK and PD parameters. The concepts of PK-PD for antimicrobial therapy were first described in the 1940s and 1950s by Eagle and his colleagues (Eagle *et al.*, 1950a; Eagle *et al.*, 1950b). Through experiments conducted on rodents, they found that antimicrobials can be categorised on the basis of their patterns of antimicrobial activity as either 'time-dependent' or 'concentration-dependent' agents.

Time-dependent drugs, such as β-lactams, demonstrate no additional killing activity when drug concentrations exceed the MIC. Increasing the dosage of these agents above the MIC of the organisms will therefore not enhance the killing rate. For these types of antimicrobials, the frequency of administration and the dose are both important determinants of their antimicrobial activity. The PK-PD parameter that best correlates with the therapeutic efficacy is the duration of time in which drug concentration remains above the MIC (T>MIC) (Ambrose *et al.*, 2007). Results from an animal model revealed that T>MIC of 40-50% of the dosing interval is required for amoxicillin and amoxicillin-clavulanate against *Streptococcus pneumoniae* (Andes & Craig, 1998; Woodnutt & Berry, 1999). A similar magnitude for T>MIC to achieve 85-100% bacteriologic efficacy has been reported in children with acute otitis media (MacGowan *et al.*, 1996). For time-dependent drugs that also have a prolonged post-antibiotic effect (PAE), such as macrolides, clindamycin and glycopeptides, a key predictor of outcome is the ratio of the area under the concentration time-curve at 24 h to the MIC value (AUC_{24}/MIC).

The aminoglycosides and fluoroquinolones are drugs that exhibit concentration-dependent killing and produce a prolonged PAE. That is, higher doses will result in better bacterial killing. The frequency of the dose is usually not a major factor in the

efficacy of these drugs. It has been proven that the maximum drug concentration (C_{max}) to MIC ratio (C_{max}/MIC) and AUC_{0-24}/MIC ratio are parameters that correlate with the efficacy of these agents (Ambrose *et al.*, 2007). Regarding the question of which parameter will have the highest correlation for predicting outcomes, Rodvold (2001) has suggested that if a C_{max}/MIC of 10 or greater is achieved, then C_{max}/MIC is the parameter most likely to be linked to a successful outcome. However, if C_{max}/MIC is less than 10, then AUC_{0-24}/MIC is more likely to correlate with a successful outcome. Indeed, it is difficult to justify which parameter is more important because of the correlation between parameters. A fixed dosing interval of 24 hours used in most studies, therefore an increase or decrease in dose will usually result in similar directional changes for C_{max} and AUC_{0-24}. Since the magnitude of the PK-PD parameters is a function of the physicochemical properties of the drugs and the biological properties of the target organisms, the optimal value varies between organisms. The magnitude of the PK-PD parameters that have been reported for fluoroquinolones are summarised in Table 1.1. In general, for Gram-negative organisms, a C_{max}/MIC of >8 and AUC_{0-24}/MIC of >125 is needed to obtain the highest rates of bacteriologic and clinical cures. For Gram-positive organisms, such as *S. pneumoniae*, a magnitude of 30 or greater has been suggested.

Table 1.1 PK-PD data for fluoroquinolones

Antimicrobial agents	Organism	PK-PD parameter and magnitude	Source of data	Reference
Ciprofloxacin	*P. aeruginosa*	C_{max}/MIC >8	*in vitro* model	Dudley *et al.* (1991)
Ciprofloxacin, ofloxacin	*P. aeruginosa*	AUC_{0-24}/MIC>100	*in vitro* model	Madaras-Kelly *et al.* (1996)
Ciprofloxacin, levofloxacin	*S. pneumoniae*	AUC_{0-24}/MIC 30-55	*in vitro* model	Lacy *et al.* (1999)
Ciprofloxacin, ofloxacin, trovafloxacin	*S. pneumoniae*	AUC_{0-24}/MIC 44-49	*in vitro* model	Lister and Sanders (1999a)
Ciprofloxacin, levofloxacin	*S. pneumoniae*	AUC_{0-24}/MIC 32-64	*in vitro* model	Lister and Sanders (1999b)
Lomefloxacin	*P. aeruginosa*	C_{max}/MIC >10	neutropenic rat	Drusano *et al.* (1993)
Ciprofloxacin	82% Gram-negative	AUC_{0-24}/MIC>125	human	Forrest *et al.* (1993)

1.4 CIPROFLOXACIN

1.4.1 Structure

Ciprofloxacin is a 1-cyclopropyl-6-fluoro-1,4-dihydro 4-oxo-7-(1-piperazinyl)-3-quinoline carboxylic acid (Figure 1.2). The fluorine atom at position C-6 in combination with the piperazine moiety group at position C-7 increases antimicrobial activity compared to the older agents nalidixic acid, oxolinic acid and cinoxacin (Wolfson & Hooper, 1989; Domagala *et al.*, 1986). The substitution of the piperazine group also enhances potency against Gram-negative bacteria, including many strains of *P. aeruginosa* (Stein, 1988). An N-1-cyclopropyl substituent has been shown to affect DNA gyrase activity and antimicrobial potency due to the steric effect mechanism (Chu *et al.*, 1989).

Figure 1.2 Chemical structure of ciprofloxacin

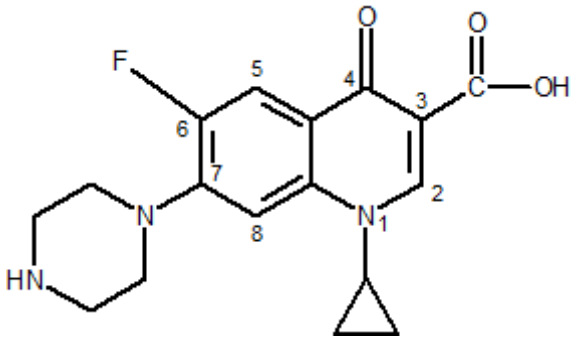

1.4.2 Mechanism of action

It is currently known that fluoroquinolone antibiotics interact with 2 enzyme targets, DNA gyrase and topoisomerase IV. Both of these enzymes are important for bacterial DNA replication (Drlica & Zhao, 1997). DNA gyrase is responsible for introducing negative supercoils into DNA, which is the initial step of DNA replication (Wang, 1996). Topoisomerase IV acts in the final step by allowing separation of daughter chromosomes into daughter cells (Adams *et al.*, 1992). Fluoroquinolones inhibit these enzymes by stabilizing enzyme-DNA complex. Fluoroquinolone-gyrase-DNA complex formation rapidly inhibits DNA replication

and is consistent with DNA gyrase acting ahead of replication forks. However, inhibition of replication by fluoroquinolone-topoisomerase IV-DNA complexes occurs slowly, consistent with the enzyme being located behind the replication forks.

The affinity to enzymes differs for Gram-negative and Gram-positive organisms. For Gram-negative bacteria it is the DNA gyrase, whereas it is topoisomerase IV for Gram-positive organisms. However, the new generation fluoroquinolones, i.e. clinafloxacin and moxifloxacin, have similar affinity for both targets for both types of organism (Takei *et al.*, 2001).

1.4.3 Mechanism of resistance

The rate of fluoroquinolone resistance is rising and is related to the increasing use of these drugs both in the community and the hospital *(*Neuhauser *et al.*, 2003*;* Polk *et al.*, 2004). Acquisition of resistance has been most frequent with *E. coli* (Ko & Hsueh, 2009), *K. pneumoniae* (Fu *et al.*, 2008), and *P. aeruginosa (*Polk *et al.*, 2004). Three mechanisms have been discovered to date: alterations in DNA gyrase and topoisomerase IV (Friedman & Lu, 2001; Ruiz, 2003; Willmott & Maxwell, 1993; Yoshida *et al.*, 1991), decreased drug accumulation due to impermeability of the membrane and/or overexpression of an efflux pump system (Ruiz, 2003; Jacoby, 2005), and plasmid-mediated resistance (Martínez-Martínez *et al.*, 1998; Tran *et al.*, 2005). The development of fluoroquinolone resistance is thought to be more common in Gram-negative bacteria, which have a more complex cell wall, than in Gram-positive bacteria and has been related to the intensity and duration of therapy (Tam *et al.*, 2007).

Cross-resistance among quinolones appears to be related to the enzyme target. For example, topoisomerase IV is the primary target for ciprofloxacin and levofloxacin, while DNA gyrase is the primary target for sparfloxacin, moxifloxacin and gatifloxacin. Therefore, ciprofloxacin resistance may have little effect on sparfloxacin and vice versa (Fukuda *et al.*, 2001; Li *et al.*, 2002). Cross-resistance to other antimicrobials is generally due to efflux mutations and plasmid-mediated resistance (Giraud *et al.*, 2000).

1.4.4 Antimicrobial activity

Ciprofloxacin has a wide spectrum of activity. It is highly active against aerobic Gram-negative bacilli, particularly *Enterobacteriaceae*, *H. influenzae* and Gram-negative cocci, such as *Neisseria* spp. and *M. catarrhalis* (Rolston *et al.*, 2003; Wolfson & Hooper, 1989). The guideline published by the Clinical and Laboratory Standards Institute (CLSI) indicates that ciprofloxacin remains the most potent fluoroquinolone against *P. aeruginosa* with the *in vitro* MIC breakpoints established as ≤1, 2 and ≥4 for susceptible, intermediate and resistant organisms, respectively (CLSI, 2012). The current recommendations of the European Committee on Antimicrobial Susceptibility Testing (EUCAST) are consistent with the CLSI values but a slightly lower MIC value of ≤0.5 has been suggested as the susceptible breakpoint (EUCAST, 2012). Ciprofloxacin has a limited activity against Gram-positive organisms, such as *S. aureus* and *S. pneumoniae*, and many anaerobes (Balfour & Wiseman, 1999; Blondeau, 1999; Perry *et al.*, 1999).

The post-antibiotic effect (PAE) of ciprofloxacin is usually long (Gould *et al.*, 1990), but there is a high variation among species (Drabu & Blakemore, 1991). At four times the MIC, the PAE was 58 minutes for *S. pneumoniae*, 39-82 minutes for *H. influenza*, 45-76 minutes for *M. catarrhalis*, and 17-37 minutes for *S. aureus* (Dubois & St-Pierre, 2000). Fuursted (1987) reported a PAE of approximately 2.2 hours for *P. aeruginosa*, which was exposed to 5-10 times the MIC for 1-2 hours.

1.4.5 Pharmacokinetics

1.4.5.1 Adults

1.4.5.1.1 Absorption

Table 1.2 summarises PK data for oral ciprofloxacin collected from several studies. Ciprofloxacin is well absorbed after oral administration. The reported oral bioavailability is around 70% with the mean ranging from 56-84%. Davis *et al.* (1985) found a significant difference in the bioavailability between dosage forms of ciprofloxacin. The 250 mg tablet had a bioavailability of 59%, which was low compared to the 500 mg tablet and a solution formulation (75% and 79%, respectively). The time to reach peak concentration (T_{max}) is approximately 1-2

hours, depending on the dose. Previous studies have demonstrated that T_{max} appears to increase when increasing the oral dose (Hoffken *et al.*, 1985; Tartaglione *et al.*, 1986). The authors suggest that it is probably due to a saturation process of drug absorption of ciprofloxacin and the variability in disintegration/dissolution rates between drug formulations. Bergan *et al.* (1987) and Höffler *et al*. (1984) have shown that ciprofloxacin has a linear relationship between oral dose and C_{max}. In contrast, a nonlinear relationship was observed in some studies (Hoffken *et al.*, 1985; Borner *et al.*, 1986). A linear relationship between dose and concentration has been reported for intravenous administration of ciprofloxacin (Borner *et al.*, 1986; Drusano *et al.*, 1986b; Dudley *et al.*, 1987) and it has been found that the concentrations following a single oral dose are similar to those at the steady state (Table 1.2).

The presence of food has been shown to decrease C_{max} and also delay T_{max} (Neuvonen *et al.*, 1991; Ledergerber *et al.*, 1985). However, other investigators found no statistically significant changes on either parameter when ciprofloxacin was administered with food (Shah, 1999) or enteral feeding (Yuk *et al.*, 1989).

1.4.5.1.2 Distribution

Ciprofloxacin is widely distributed throughout the body. The volume of distribution at a steady state (V_{ss}) ranges from 1.74 to 5 L/kg (Table 1.2 and 1.3). Protein binding of ciprofloxacin is relatively low at approximately 30% (Dudley *et al.*, 1987). The degree of binding does not appear to be significantly affected by pH or concentration (Vance-Bryan *et al.*, 1990). Ciprofloxacin is concentrated in lung, kidney, intestine, hepatic tissue and bile. The concentrations in fat, skin, muscle, bone and cerebrospinal fluid (CSF) tend to be lower than those in serum but there are wide variations between individuals (Table 1.4).

1.4.5.1.3 Elimination

Ciprofloxacin is eliminated by metabolism, renal glomerular filtration, active tubular secretion and the transintestinal route. Approximately one-third of an administered ciprofloxacin dose is metabolised. There are four metabolites that have been

identified: desethyleneciprofloxacin (M1), sulfociprofloxacin (M2), oxociprofloxacin (M3) and formylciprofloxacin (M4) (Vance-Bryan *et al.*, 1990). M3 is the major metabolite found in urine, accounting for about 6% of the oral and intravenous dose. M2 is a primarily a faecal metabolite with 5.9% of an oral dose and 1.3% of an intravenous dose recovered in the faeces. M1 and M4 can be detected in very small amounts. The total amount of metabolite of ciprofloxacin excreted in the urine increased from 30% after intravenous administration to 43% after oral administration (Hoffken *et al.*, 1985). This suggests that ciprofloxacin has a first-pass effect; however, it is thought to be clinically unimportant (Vance-Bryan *et al.*, 1990).

Elimination of ciprofloxacin and its metabolites in the urine comprises approximately 60-70% of the dose, and the remainder is secreted directly through the intestinal mucosa (Rohwedder *et al.*, 1990). Biliary excretion is relatively low (<1%) compared to other pathways but exceeds the concentrations in serum (Parry *et al.*, 1988). Renal clearance of ciprofloxacin accounts for approximately two-thirds of the total clearance (Davis *et al.*, 1996). Studies in healthy subjects have shown that renal clearance of ciprofloxacin greatly exceeds creatinine clearance, indicating a significant contribution of tubular secretion (Wingender *et al.*, 1984). Jaehde *et al.* (1995) have demonstrated that coadministration of ciprofloxacin with probenecid decreased total clearance and renal clearance by approximately 60%. Generally, the apparent total clearance and renal clearance of different dosing regimens are comparable and are similar following single or multiple doses (Table 1.2 and 1.3). However, some investigators reported a trend of decreasing renal clearance with a large dose (Höffler *et al.*, 1984).

1.4.5.2 Children

Due to ethical restrictions, only a few studies of ciprofloxacin pharmacokinetics in children have been published to date. Peltola and coworkers (1992) performed a study on 7 infants (aged 9-14 weeks) and 9 children (aged 1-5 years). All patients received a single dose of 15 mg/kg ciprofloxacin to treat *Salmonella* infections. The authors reported that the elimination of ciprofloxacin is faster in children than in infants (1.28 versus 2.73 hours), requiring an oral dose of 10-15 mg/kg three times

daily for this age group. In the study of Rubio (1997), 18 children with cystic fibrosis (aged 5-17 years) received intravenous ciprofloxacin 10 mg/kg every 8 hours followed by oral ciprofloxacin 10 mg/kg every 12 hours. Average elimination half-life values were 2.6 and 3.4 hours after IV and oral administration, respectively, and no significant difference in elimination rate between age groups was observed. The authors suggested that oral dosing of 40 mg/kg/day or intravenous dosing of 30 mg/kg/day is needed to maintain adequate therapeutic concentrations in children with cystic fibrosis.

In 1998, Peltola *et al.* studied the disposition of ciprofloxacin in 16 children, ages 0.3-7.1 years, with various types of infections, including urinary tract infections, chronic otitis media and endocarditis. The dose was 10 mg/kg given every 8 hours. The oral clearance was lower in children <6 years of age (16.4-17.3 mL/min/kg) than in those ≥6 years (24.4 mL/min/kg). The elimination half-life did not significantly differ between age groups, ranging from 4.2 hours in patients 1 year of age to 5.1 in children 2-5 years. The results of this study suggest that the oral suspension form of ciprofloxacin 10 mg/kg given orally three times daily would be the appropriate regimen for children. In another study, 20 children with severe sepsis were treated with intravenous ciprofloxacin 10 mg/kg every 12 hours for 7 days (Lipman *et al.*, 2002). The authors reported an elimination half-life of 3.3-4.2 hours in children aged 3 months to 1 year and of 2.8-3.1 in older children (1-5 years). No evidence of drug accumulation was observed after 7 days of drug administration. The authors advised a dosing regimen of 10 mg/kg ciprofloxacin every 8 hours for some resistant ICU organisms.

1.4.5.3 Renal failure

In patients with renal impairment, neither absorption nor distribution of ciprofloxacin are significantly changed (Plaisance *et al.*, 1990; Webb *et al.*, 1986). Mild to moderate renal impairment does not significantly affect clearance (MacGowan *et al.*, 1994), but in patients with severe renal impairment, the AUC and elimination half-life are double those of patients with normal renal function (Gasser *et al.*, 1987; Boelaert *et al.*, 1985). Therefore, a dose reduction to 50% or a doubling of the dosing

interval was recommended. In contrast, MacGowan *et al*. (1994) demonstrated that ciprofloxacin did not greatly accumulate when giving to patients with moderate or severe renal failure. The trough concentrations were 0.6 mg/L in moderate renal failure and 0.5 mg/L in severe renal failure compared with 0.3 mg/L in patients with normal renal function. On the basis of these findings and in order to avoid subtherapeutic levels of drug, they recommend that the dose should not be reduced in a patient with renal failure.

1.4.5.4 Liver failure

There is little information available on the effect of liver failure on the pharmacokinetics of ciprofloxacin. Following a single oral dose of 500 mg, slightly increased maximum concentration and AUC values have been observed only in patients with severe liver failure; in these patients, the elimination half-life was increased by approximately 35% compared to controls (Esposito *et al.*, 1989). The pharmacokinetics of ciprofloxacin in patients with lesser degrees of liver failure did not significantly alter. Frost *et al.* (1989b) found no significant difference in pharmacokinetic parameters (C_{max}, T_{max}, AUC, elimination half-life and clearance) between cirrhotic patients and the control group. The formation of M1 and M2 metabolites was unaffected, but the maximum concentration of M3 was reduced by approximately 50%. The investigators concluded that dose adjustment may not be required for patients with liver failure.

Table 1.2 Pharmacokinetics of ciprofloxacin in healthy subjects after oral administration

No. of subjects (sex)	Dose (mg)	C_{max} (mg/L)	T_{max} (h)	AUC (mg·h/L)	V_{ss}/F (L/kg)	V/F (L/kg)	CL_T/F (L/h)	CL_R/F (L/h)	fu (%)	F (%)	Reference
6(M)	500	2.30	1.25	9.90	-	-	50.51	-	31	-	Crump *et al.* (1983)
12(M)	250	1.42	1.11	5.43	-	-	46.04	-	-	-	Gonzalez *et al.* (1984)
12(M)	250 q 12 h x 7 doses	1.37	1.00	5.61	-	-	44.56	-	-	-	
12(M)	250 q 12 h x 13 doses	1.35	1.06	5.33	-	-	46.90	-	48	-	
12(M)	500	2.60	1.11	10.60	-	-	47.17	-	-	-	
12(M)	500 q 12 h x 7 doses	2.77	1.11	12.41	-	-	40.29	-	-	-	
12(M)	500 q 12 h x 13 doses	2.89	1.00	13.94	-	-	49.90	-	41	-	
12(M)	750	3.41	1.56	15.03	-	-	49.90	-	-	-	
12(M)	750 q 12 h x 7 doses	4.21	1.00	17.76	-	-	42.29	-	-	-	
12(M)	750 q 12 h x 13 doses	4.15	1.39	22.07	-	-	33.98	-	39	-	
7(M)	100	0.48	0.93	1.49	-	-	67.34	23.54	30	-	Höffler *et al.* (1984)
8(M)	100	0.38	0.81	1.29	-	-	77.58	23.24	23	-	
8(F)	250	1.18	1.19	4.20	-	-	59.59	18.87	27	-	
8(M)	250	0.94	0.88	3.02	-	-	82.78	24.41	24	-	
7(F)	500	1.96	1.14	7.08	-	-	70.58	20.53	27	-	
8(M)	500	2.16	1.00	7.38	-	-	67.72	19.73	27	-	
8(F)	1000	3.76	1.13	14.68	-	-	68.11	18.10	23	-	
7(M)	1000	3.62	1.07	11.61	-	-	86.12	18.51	19	-	
12(M)	200	1.21	0.71	4.80	-	3.54	41.67	17.03	40	-	Drusano *et al.* (1986a)
6(M)	250	0.94	0.81	3.38	-	-	73.98	22.86	27	56	Wingender *et al.* (1984)

Table 1.2 (continued)

No. of subjects (sex)	Dose (mg)	C_{max} (mg/L)	T_{max} (h)	AUC (mg·h/L)	V_{ss}/F (L/kg)	V/F (L/kg)	CL_T/F (L/h)	CL_R/F (L/h)	fu (%)	F (%)	Reference
18(M)	500 (250 mg tab x 2)	2.83	0.99	10.00	5.00	-	50.20	22.20	44	59[a]	Davis *et al.* (1985)
18(M)	500 (500 mg tab x 1)	2.91	1.25	12.70	3.99	-	42.00	20.50	49	75[a]	
18(M)	500 (solution)	3.23	1.00	13.50	3.78	-	38.80	22.30	56	79[a]	
6(M)/6(F)	50	0.28	0.58	1.00	-	3.04	50.00	-	37	77	Höffken *et al.* (1985)
6(M)/6(F)	100	0.49	0.83	1.90	-	3.04	52.63	-	35	63	
6(M)/6(F)	750	2.65	1.16	12.20	-	3.53	61.47	-	33	-	
6(M)/6(F)	500	2.80	1.50	9.60	2.74	-	52.09	-	28	-	Bergan *et al.* (1986)
6(M)/6(F)	500 q 12 h x 10 doses	2.30	1.50	9.60	1.78	-	52.09	-	43	-	
6(M)/6(F)	100	0.73	1.00	2.10	-	-	47.62	-	15	84	Bergan *et al.* (1986)
6(M)/6(F)	250	1.59	1.25	5.28	-	-	47.35	-	30	-	
6(M)/6(F)	500	2.77	1.54	9.61	-	-	52.03	-	28	-	
6(M)/6(F)	1000	5.57	1.75	22.84	-	-	43.78	-	30	-	
6(M)/6(F)	100	0.37	1.17	1.77	-	3.52	56.50	18.06	29	64.0	Borner *et al.* (1986)
5(M)/5(F)	250[b]	1.04	1.01	4.23	-	3.52	59.10	20.40	34	-	
5(M)/5(F)	250[c]	0.83	1.34	3.58	-	3.52	69.83	20.28	28	-	
5(M)/5(F)	500	1.51	1.19	6.78	-	4.65	73.75	18.54	26	52	
5(M)/5(F)	750	1.97	1.26	8.77	-	2.66	85.52	23.04	27	-	

Table 1.2 (continued)

No. of subjects (sex)	Dose (mg)	C_{max} (mg/L)	T_{max} (h)	AUC (mg·h/L)	V_{ss}/F (L/kg)	V/F (L/kg)	CL_T/F (L/h)	CL_R/F (L/h)	fu (%)	F (%)	Reference
6(M)/6(F)	500	2.26	1.33	10.00	3.76	-	54.48	23.76	-	56	LeBel *et al.* (1986)
6(M)/6(F)	500 q 8 h x 12 doses	3.51	1.04	13.93	3.71	-	41.46	21.48	-	56	
8(M)	250	0.76	1.12	3.70	-	-	67.56	23.70	36	-	Tartaglione *et al.* (1986)
11(M)	500	1.60	1.46	7.60	-	-	65.76	28.62	44	-	
11(M)	750	2.54	1.67	12.9	-	-	58.14	21.96	40	-	
11(M)	1000	3.38	1.80	16.6	-	-	60.24	18.96	29	-	
10(M)/10(F)	500	1.80	1.32	8.65	-	-	57.80	-	-	-	Ullmann *et al.* (1986)
10(M)/10(F)	500 q 12 h x 15 doses	2.60	1.13	12.00	-	-	41.67	-	-	-	
8(M)	200	1.18	0.69	4.18	-	3.87	39.10	-	-	69	Plaisance *et al.* (1987)
8(M)	750	2.97	1.38	15.30	-	4.62	42.20	-	-	69	
24(M)	750	3.01	1.33	23.8	-	-	70.50	24.84	-	79	Shah *et al.* (1994)
24(M)	750 q 12 h x 7 doses	3.59	1.44	31.6	-	-	53.76	25.62	-	77	
14(M)	750	3.14	1.5	13.42	-	-	54.27	-	-	-	Gallicano and Sahai (1996)
10(F)	750	3.19	1.5	16.10	-	-	47.33	-	-	-	

[a] Calculated using a dose-corrected AUC from the study of Wise *et al.* (1984).

[b] Drug was administered at fasting.

[c] Drug was administered with food.

Key: C_{max} = maximum concentration, T_{max} = time to reach maximum concentration, AUC = area under the drug concentration-time curve, V_{ss}/F = oral volume of distribution at steady state, V/F = oral volume of distribution, CL_T/F = oral total body drug clearance, CL_R/F = oral renal clearance, fu = fraction unbound of drug in plasma, F = bioavailability, M = male, F = female.

Table 1.3 Pharmacokinetics of ciprofloxacin in healthy subjects after intravenous administration

No. of subjects (sex)	Dose (mg)	Infusion time (min)	C_{max} (mg/L)	AUC (mg·h/L)	V_{ss} (L/kg)	V (L/kg)	CL_T (L/h)	CL_R (L/h)	fu (%)	Reference
6(M)	100	5	-	2.41	1.98	-	43.29	19.89	46	Wingender *et al.* (1984)
6(M)	100	-	-	2.81	2.25	-	34.02	28.74	76	Wise *et al.* (1984)
9(M)	100	30	1.60[a]	3.40	1.95	2.56	30.12	18.84	-	Gonzalez *et al.* (1985a)
9(M)	150	30	2.10[a]	5.14	1.97	2.45	29.82	18.78	-	
9(M)	200	30	3.10[a]	7.70	1.97	2.47	26.88	18.42	-	
12(M)	25	10	0.51	0.70	2.29	-	37.32	21.60	-	Gonzalez *et al.* (1985b)
12(M)	25 q 12 h x 7 doses	10	0.47	0.71	2.19	-	36.60	19.32	-	
12(M)	25 q 12 h x 13 doses	10	0.53	0.71	2.10	-	36.18	20.28	-	
12(M)	50	10	1.04	1.53	1.75	-	32.88	22.20	-	
12(M)	50 q 12 h x 7 doses	10	1.11	1.64	2.02	-	31.32	22.92	-	
12(M)	50 q 12 h x 13 doses	10	1.09	1.74	1.77	-	29.10	20.58	-	
12(M)	75	10	1.56	2.42	1.88	-	31.68	25.80	-	
12(M)	75 q 12 h x 7 doses	10	1.50	2.58	1.90	-	30.12	25.20	-	
12(M)	75 q 12 h x 13 doses	10	1.55	2.53	1.86	-	30.72	23.52	-	
6(M)/6(F)	50	15	1.23	1.20	-	2.66	41.22	25.50	62	Hoffken *et al.* (1985)
6(M)/6(F)	100	15	2.80	3.00	-	2.10	31.80	20.10	62	
6(M)/6(F)	50	15	-	1.23	-	3.10	41.58	23.76	57	Borner *et al.* (1986)
6(M)/6(F)	100	15	-	2.88	-	2.65	36.00	18.90	53	
5(M)/5(F)	200	20	-	5.31	-	2.80	39.12	21.42	54	

Table 1.3 (continued)

No. of subjects (sex)	Dose (mg)	Infusion time (min)	C_{max} (mg/L)	AUC (mg·h/L)	V_{ss} (L/kg)	V (L/kg)	CL_T (L/h)	CL_R (L/h)	fu (%)	Reference
6(M)	100	30	2.28	3.94	1.74	-	24.60	15.12	59	Drusano *et al.* (1986b)
6(M)	200	30	3.80	7.22	1.90	-	25.20	16.50	60	
6(M)	200[b]	-	-	5.84	1.80	-	29.88	17.82	59	
12(M)	200	10	6.48	-	-	2.44	28.50	16.90	60	Drusano *et al.* (1986a)
9(M)	100	30	1.4	2.24	2.17	-	46.94	22.54	48	Dudley *et al.* (1987)
9(M)	150	30	2.0	3.36	2.40	-	46.00	21.52	46	
9(M)	200	30	3.2	5.17	2.00	-	39.85	18.58	46	

[a] derived from graph.

[b] 100 mg loading dose followed by 25 mg/h 4 h infusion.

Key: C_{max} = maximum concentration; AUC = area under the drug concentration-time curve; V_{ss}/F = oral volume of distribution at steady state; V/F = oral volume of distribution; CL_T/F = oral total body drug clearance; CL_R/F = oral renal clearance; fu = fraction unbound of drug in plasma; M = male; F = female.

Table 1.4 Tissue penetration of ciprofloxacin after oral or intravenous administration

Tissue/fluid	No. of subjects (sex)	Dose (mg)	Sampling time (h)	Mean concentration		Mean tissue:serum ratio	Reference
				Tissue (mg/L or mg/kg)	Serum (mg/L)		
Bile	7(M)/5(F)	500 PO	1	1.10	0.69	1.59	Brogard *et al.* (1985)
			4	5.40	0.95	5.68	
			8	5.20	0.83	6.27	
Hepatic tissue	1(M)/9(F)	750 PO	3	6.70	1.64	4.09	Dan *et al.* (1987)
			7	6.00	3.00	2.00	
Kidney	20(M)/3(F)	100 IV	1-2	4.66	0.46	10.13	Daschner *et al.* (1986)
	20(M)/3(F)	100 IV	7-8	0.93	0.13	7.15	
Bone (normal)	6(M)/1(F)	500 PO	3	0.40	1.40	0.29	Fong *et al.* (1986)
	6(M)/1(F)	750 PO	3	0.70	2.60	0.27	
	3(M)/1(F)	1000 PO	3	1.60	2.90	0.55	
Bone (infected)	6(M)	500 PO	3	0.70	2.00	0.35	Fong *et al.* (1986)
	4(M)	750 PO	3	1.40	2.90	0.48	
Bronchial tissue	12(M)/8(F)	200 IV	3-4	2.50	0.60	4.17	Dan *et al.* (1993)
	8(M)/4(F)	200 IV q 12 h x 6 days	2	21.63	1.39	16.90	Fabre *et al.* (1991)
	21(M)/8(F)	500 PO q 12 h x 8 doses	4	4.40	3.01	1.46	Honeybourne *et al.* (1988)
	5(M)/5(F)	200 IV	1	3.94	1.62	2.43	

Table 1.4 (continued)

Tissue/fluid	No. of subjects (sex)	Dose (mg)	Sampling time (h)	Mean concentration		Mean tissue:serum ratio	Reference
				Tissue (mg/L or mg/kg)	Serum (mg/L)		
Bronchial secretion	21	500 PO	2	0.44	2.27	0.19	Bergogne-Bérézin *et al.* (1986)
	21	500 PO	4	0.27	0.89	0.30	
	21	500 PO	6	0.56	0.59	0.95	
Lung parenchyma	12(M)/8(F)	200 IV	3-4	4.70	0.60	7.83	Dan *et al.* (1993)
Pleural tissue	12(M)/8(F)	200 IV	3-4	1.70	0.60	2.83	Dan *et al.* (1993)
Intestinal tissue	8	750 PO x 2 doses then 400 IV x 2 doses	2-3	13.09	3.40	4.3	Brismar *et al.* (1990)
Fat	20(M)/3(F)	100 IV	1-2	0.27	0.46	0.59	Daschner *et al.* (1986)
	20(M)/3(F)	100 IV	7-8	0.04	0.13	0.31	
	3	500 PO	2.75-3.25	0.90	0.58	1.56	Aigner and Dalhoff (1986)
	9	500 PO	5-5.8	0.51	0.52	1.08	
	3	500 PO	6.25-8	0.41	0.49	0.94	
	18	200 IV	1	1.00	2.20	0.45	Silverman *et al.* (1986)
	15	500 PO	12	0.056	0.17	0.33	Dalhoff and Eickenberg (1985)
Skin	20(M)/3(F)	100 IV	1-2	0.23	0.46	0.50	Daschner *et al.* (1986)
	20(M)/3(F)	100 IV	7-8	0.12	0.13	0.92	
	3	500 PO	2.75-3.25	0.89	0.58	1.71	Aigner and Dalhoff (1986)
	9	500 PO	5-5.8	0.98	0.52	2.25	
	3	500 PO	6.25-8	0.62	0.49	1.48	

Table 1.4 (continued)

Tissue/fluid	No. of subjects (sex)	Dose (mg)	Sampling time (h)	Mean concentration		Mean tissue:serum ratio	Reference
				Tissue (mg/L or mg/kg)	Serum (mg/L)		
Muscle	20(M)/3(F)	100 IV	1-2	1.16	0.46	2.52	Daschner *et al.* (1986)
	20(M)/3(F)	100 IV	7-8	0.21	0.13	1.62	
	6(M)/1(F)	500 PO	3	1.10	1.40	0.79	Fong *et al.* (1986)
	6(M)/1(F)	750 PO	3	1.30	2.60	0.81	
	3(M)/1(F)	1000 PO	3	2.60	2.90	0.90	
	15	500 PO	12	0.20	0.17	1.18	Dalhoff and Eickenberg (1985)
	3	500 PO	2.75-3.25	1.23	0.58	2.46	Aigner and Dalhoff (1986)
	9	500 PO	5-5.8	1.90	0.52	4.23	
	3	500 PO	6.25-8	1.74	0.49	3.46	
	18	200 IV	1	1.90	2.20	0.86	Silverman *et al.* (1986)
CSF (non-inflamed)	16(M)/7(F)	200 IV q 12 h x 3 doses	1	0.15	1.30	0.14	Wolff *et al.* (1987)
			2	0.27	1.12	0.23	
			4	0.27	0.84	0.31	
			8	0.15	0.20	0.77	
	25	200 IV q 12 h x 2 doses	4	0.08	0.58	0.15	Gogos *et al.* (1991)
			5	0.07	0.43	0.18	
			6	0.11	0.51	0.24	

Table 1.4 (continued)

Tissue/fluid	No. of subjects (sex)	Dose (mg)	Sampling time (h)	Mean concentration		Mean tissue:serum ratio	Reference
				Tissue (mg/L or mg/kg)	Serum (mg/L)		
CSF (inflamed)	16(M)/7(F)	200 IV q 12 h x 3 doses	1	0.39	1.59	0.26	Wolff *et al.* (1987)
			2	0.56	1.44	0.37	
			4	0.49	1.04	0.57	
			8	0.35	0.24	1.59	
	9	200 IV q 12 h x 2 doses	3	0.10	0.33	0.34	Gogos *et al.* (1991)
			5	0.14	0.43	0.34	

Key: M = male, F = female, PO = oral administration, IV = intravenous administration.

1.4.6 Clinical uses

1.4.6.1 Adults

In adults, ciprofloxacin is currently used to treat several types of infection. The approved indications are as follows (Andriole, 2005):

- Complicated and uncomplicated urinary tract infections
- Acute uncomplicated cystitis in females (oral use only)
- Chronic bacterial prostatitis
- Uncomplicated cervical and urethral gonorrhoea
- Skin and soft-tissue infections
- Bone and joint infections
- Infectious diarrhoea (oral use only)
- Typhoid fever (oral use only)
- Complicated intra-abdominal infections in combination with metronidazole
- Acute sinusitis
- Lower respiratory tract infections
- Nosocomial pneumonia (IV use only)
- Empirical therapy for patients with febrile neutropenia in combination with piperacillin (IV use only)
- Inhalational anthrax (after exposure)

1.4.6.2 Children

Fluoroquinolones, including ciprofloxacin, are not recommended for routine use in children age <18 years old because studies in juvenile animals have demonstrated the development of arthropathy with cartilage erosions in weight-bearing joints (Dagan, 1995). However, based on the absence of arthropathy seen in humans in the past decades, ciprofloxacin has been considered for use in some paediatric populations, particularly in those with cystic fibrosis, immunocompromised patients and those with neutropenia arising from cancer chemotherapy (Gendrel & Moulin, 2001; Paganini *et al.*, 2003; Aquino *et al.*, 2000). It has also been suggested to use ciprofloxacin as a first-line therapy for Gram-negative neonatal meningitis, severe *Salmonella* and *Shigella* spp. infections, chronic otitis media and some cases of complicated acute otitis media that do not response to initial therapy (Edwards &

Freeman, 2006). To date, ciprofloxacin has only been approved for use in children with complicated urinary tract infections and pyelonephritis caused by *P. aeruginosa* or other multidrug-resistant, Gram-negative bacteria (Committee on Infectious Diseases, 2006).

1.4.7 Toxicities

Fluoroquinolones are generally well-tolerated. The most common adverse effects involve the gastrointestinal tract and central nervous system. Other adverse effects include rashes and other allergic reactions, tendonitis and tendon rupture, QT prolongation, hypoglycaemia and hyperglycaemia, and haematologic toxicity *(*Ball *et al.*, 1999; Lipsky & Baker, 1999). The greatest concern regarding the use in children is arthrotoxicity, which is characterised by fluid-filled blisters, fissures and erosions within the joints (Dagan, 1995; Sendzik *et al.*, 2009). Nevertheless, studies in humans have failed to show any significant arthrotoxicity. In 1991, Chyský *et al.* conducted a world-wide surveillance study in 634 children who received ciprofloxacin for treating cystic fibrosis. Mild arthralgias were observed in eight patients (1.3%) and resolved in all children after drug withdrawal. A follow-up of this study, including 1795 children who had received a total of 2030 treatment courses, has reported that mild and moderate arthralgia occurred in 1.5% of patients, mostly in patients with cystic fibrosis (Hampel *et al.*, 1997). A 6-year retrospective study, including more than 6000 children, found that the incidence of joint and tendon toxicities in the fluoroquinolone-treated group was similar to the control group (0.82% vs. 0.78%) (Yee *et al.*, 2002). Among the fluoroquinolones, ciprofloxacin has been considered as drug of choice since it has less arthrotoxicity compared to other agents (Gendrel & Moulin, 2001).

1.4.8 Drug interactions

Ciprofloxacin, as with other fluoroquinolones, can interact with many other drugs. When quinolones are administered concurrently with an aluminium- or magnesium-containing antacid, oral bioavailability is markedly decreased (Wolfson & Hooper, 1989). This is presumably due to the formation of cation–quinolone complexes, which are poorly absorbed (Radandt *et al.*, 1992). Ferrous sulphate, supplements

containing multivalent ions (i.e. iron, zinc, and calcium) and the buffered formulation didanosine have also been reported to decrease quinolone bioavailability (Polk *et al.*, 1989; Knupp & Barbhaiya, 1997). Precipitates have been reported when the intravenous formulation of ciprofloxacin is infused through the same intravenous tube with aminophylline, amoxicillin (with and without clavulanate), or flucloxacillin (Janknegt, 1990). Evidence suggests that fluoroquinolones can decrease the clearance of theophylline and caffeine by inhibiting hepatic cytochrome P450 isozyme 1A2, the main route of metabolism for these drugs. Concurrent administration of ciprofloxacin significantly increases serum levels of theophylline and caffeine by 20-90%; however, the effect on norfloxacin, ofloxacin, levofloxacin, moxifloxacin, and gemifloxacin is small (increase of only 2-11%) (Robson, 1992; Stahlmann & Schwabe, 1997). Ciprofloxacin has been reported to increase the concentration of the R-enantiomer of warfarin but has no effect on the more active S-enantiomer. In a study conducted by Israel *et al*. (1996), prothrombin time was found to increase slightly after 12 days of therapy, but no patient had bleeding. Other possible interactions include nonsteroidal anti-inflammatory drugs (NSIADs) fenbufen, probenecid and cyclosporine (Wolfson & Hooper, 1989).

1.5 MALNUTRITION IN CHILDREN

Malnutrition in children remains a major health problem worldwide. It is estimated that severe acute malnutrition affects approximately 13 million children and accounts for up to two million child deaths annually (Collins, 2007). Although malnutrition may not be the direct cause of death, it is an important contributing factor in up to 50% of deaths in children (Madec *et al.*, 2011). A recent study has demonstrated that malnutrition and its complications, such as dehydration, diarrhoea and infections, are the leading cause of death among children younger than five years of age (O'Reilly *et al.*, 2012). It has been shown that the mortality rate among malnourished children is strongly related to anthropometric indices (Black *et al.*, 2008). The risk of death is ten times higher in children with a weight-for-height Z-score (WHZ) of <-3 compared to that for children with a WHZ ≥-1. The term 'weight-for-height' represents the median reference weight for any given height, and is used for assessment of well-being by comparing the weight of an observed child with that of

the median for his/her height. Weight-for-height is one of the three indices most commonly used in anthropometric assessment of this kind, the other two being weight-for-age and height-for-age.

1.5.1 Definitions, aetiologies and manifestations

The term ‘malnutrition’ is generally used to describe a deficiency in carbohydrate, protein and fat, as well as a deficiency in vitamins, minerals and trace elements. Each type of malnutrition may be classified as ‘acute’ or ‘chronic’, depending upon the duration of nutritional deprivation. Children with acute malnutrition appear wasted, whereas children with chronic malnutrition have stunted growth. The severity of malnutrition may range from mild to severe, with severe forms characterised as ‘kwashiorkor’, ‘marasmus’ or ‘marasmus-kwashiorkor’.

Marasmus is specified by the wasting of muscle mass, depletion of body fat stores and absence of oedema. It is caused by inadequate intake of all nutrients, especially dietary energy sources. Common clinical findings include diminished weight and height-for-age, weakness, dry skin and redundant skin folds caused by loss of subcutaneous fat. Results from simple blood tests often show remarkably decreased albumin and total circulating protein (Gollan, 1948). Children with marasmus are often anaemic due to iron and folic acid deficiencies (Khalil *et al.*, 1969).

Kwashiorkor is characterised by marked muscle atrophy with normal or increased body fat. The main cause is insufficient protein intake in the presence of adequate energy intake. Kwashiorkor is generally used to describe a malnourished child who has pitting oedema of the extremities. Other clinical findings include normal or nearly normal weight- and height-for-age, rounded prominence of the cheeks (‘moon-face’) and hepatomegaly from fatty liver infiltrations.

Marasmus-kwashiorkor is an intermediate condition, that of being markedly underweight but still with oedema. This often occurs in a child who has inadequate dietary intake of all nutrients (marasmus) and is triggered by infections. Clinical signs of children with mixed marasmus-kwashiorkor include anorexia, dermatitis,

neurological abnormalities (e.g. depression) and hepatic steatosis (Jahoor *et al.*, 2008). The mechanisms underlying the transition from marasmus to the mixed marasmus-kwashiorkor remain unclear, but previous studies have suggested that this group of patients has slower rates of protein breakdown, a depressed response to infection and lower concentrations of antioxidants, including glutathione, compared to children with pure marasmus (Jahoor *et al.*, 2008; Reid *et al.*, 2000; Reid *et al.*, 2002; White *et al.*, 2008).

1.5.2 Classification

There is controversy regarding the best and most useful method of nutritional assessment. Gomez and his colleagues (1956) were the first to divide deficits in weight-for-age into three categories of severity, based on the prognosis of malnourished children (Table 1.5). In 1970, the Wellcome Trust working party introduced another simple classification by taking clinical characteristics into consideration. With this method, malnourished children are classified according to two criteria: weight-for-age and the presence or absence of oedema, and thereby giving four categorises of malnutrition as shown in Table 1.6. The drawback of the Gomez and Wellcome classification systems is that they combine two different types of deficit: weight-for-height and height-for-age. Although the children may have the same weight-for-age, clearly one may be tall and thin and the other short and even fat. Thus Waterlow (1973) proposed to describe a child with a deficit in weight-for-height as ‘wasted’ and a child with a deficit in height-for-age as ‘stunted’. This approach is based on the assumption that during periods of nutritional deprivation, weight deficits occur initially, and followed by height or length deficits. Waterlow’s classification can also be used to assess the degree of acute or chronic malnutrition (Table 1.5).

In 1999, the World Health Organization (WHO) developed new criteria for the classification of moderate and severe malnutrition in children (Table 1.7). These are based on the degree of wasting, stunting and the presence of oedema. The measurements of weight and height (or length) are converted to Z-scores, using WHO child growth standards. Z-scores are the values that represent standard

deviations (SD) from the median weight and height values for age. In general, a child whose weight or height falls below 2 SD of the median value is considered to have significant growth abnormalities.

Table 1.5 Gomez and Waterlow classifications of malnutrition

Grade of malnutrition	Gomez classification	Waterlow classification	
	Weight-for-age (%)	Weight-for-height (%)[a]	Height-for-age (%)[b]
Normal	>90	>90	>95
Mild	75-90	80-90	90-95
Moderate	60-75	70-79	85-89
Severe	<60	<70	<85

[a] Decreased weight-for-height suggests acute malnutrition (wasting).
[b] Decreased height-for-age suggests chronic malnutrition (stunting).

Table 1.6 Wellcome Classification of severe malnutrition

%Weight-for-age	Oedema	
	Present	Absent
80-60	Kwashiorkor	Undernutrition
<60	Marasmus-kwashiorkor	Marasmus

Table 1.7 WHO classification of malnutrition

Severity	Symmetrical oedema	Weight-for-height	Height-for-age
Moderate malnutrition	No	-3 ≤ Z-score < -2 (70-79%)	-3 ≤ Z-score < -2 (85-89%)
Severe malnutrition	Yes (oedematous malnutrition)	Z-score <-3 (<70%) (severe wasting)	Z-score <-3 (<85%) (severe stunting)

In some clinical settings in which time and equipment are very limited, the mid upper-arm circumference (MUAC) is sometimes used for screening malnutrition. This measurement can be used to identify children for further evaluation since it is reasonably independent of age and gender between six months and five years of age.

Previously, children with global malnutrition and children with severe wasting were defined as MUAC <12.5 cm and <11 cm, respectively (Myatt *et al.*, 2006). However, a recent study, comparing MUAC screening to the WHO Z-score criteria, has shown that using a MUAC cut-off value of <11.5 cm substantially improves the probability of diagnosing severe wasting, and reduces false-negative results (Fernández *et al.*, 2010). Some investigators suggest that MUAC-for-height and MUAC-for-age Z-scores are better predictors for wasting than a single MUAC (Mei *et al.*, 1997; de Onis *et al.*, 1997).

As described, the severity of malnutrition is defined by comparing weight and height measurements of children to those of a population reference standard. The most regularly updated population standards were developed by the Center for Disease Control (CDC) in 2000, and the WHO in 2006. It has been suggested that compared to WHO standards, the CDC references result in lower estimates of undernutrition, except during the first six months of life, and higher estimates of overweight and obesity (de Onis *et al.*, 2007). Additionally, in most cases, the WHO references are more appropriate because they have been developed based on information obtained from an international multicentre study, using children with diverse ethnic backgrounds (WHO Multicentre Growth Reference Study Group, 2006). However, some studies indicate that WHO growth references will result in a higher measured prevalence of malnutrition when compared to the old US National Center for Health Statistic (NCHS) standards (Seal & Kerac, 2007; Prost *et al.*, 2008).

1.5.3 Bacteraemia in malnourished children

Severely malnourished children are at high risk of infection because of diminished immune defences, and are typically exposed to infections through inadequate sanitation and food preservation. Results from multivariate analyses show that malnutrition is associated with increased rates of bacteraemia in infants and children (Were *et al.*, 2011). Among the 12-17% prevalence of bacteraemia, Gram-negative organisms, including *Salmonella* spp. and *E. coli,* constitute 58-63% of invasive bacterial pathogens (Bachou *et al.*, 2006; Were *et al.*, 2011).

The WHO recommends that all children admitted to hospital with severe malnutrition should routinely receive broad-spectrum antibiotic treatment (WHO, 1999). Choice of medication and dosing regimen depend on whether there is clinical evidence of complications (i.e. septic shock, hypoglycaemia, hypothermia, skin infections and lethargy) as follows:

- If there are no signs of infections and no complications: cotrimoxazole (25 mg of sulfamethoxazole + 5 mg of trimethoprim/kg) orally twice daily for five days.
- If there are symptoms suggesting complications: ampicillin 50 mg/kg IM/IV every six hours for two days, followed by amoxicillin 15 mg/kg orally every eight hours for five days, and gentamicin 7.5 mg/kg once daily for seven days.
- If the child fails to improve within 48 hours: add chloramphenicol 25 mg/kg IM/IV every eight hours for five days.

The duration of treatment depends on the response and nutritional status of the child, but it should be continued for at least five days (WHO, 1999). Blood cultures should also be obtained, but because these children are severely ill, treatment should be initiated while awaiting results.

1.6 FACTORS THAT AFFECT DRUG PHARMACOKINETICS

1.6.1 Age – neonates and children

1.6.1.1 Absorption

The absorption of drugs is altered in neonates and infants. The gastric pH is neutral at birth and gradually declines to reach adult pH values at approximately two years of age. By the age of three years, the secretion of gastric acid per kilogram of body weight is similar to adults (Stewart & Hampton, 1987). As a result, the bioavailability of acid-labile drugs such as ampicillin, amoxicillin and erythromycin is greater in neonates and infants compared to adults. In contrast, such changes are unlikely to affect the absorption of non acid-labile drugs, for which absorption will continue efficiently in the small intestine (Strolin Benedetti & Baltes, 2003). Gastric emptying is slow in neonates and infants and reaches the adult rate by six months of

age (Yokoi, 2009). This may result in delayed absorption of drugs. The intestinal drug-metabolising enzymes and efflux transporters may affect the bioavailability of drugs; however, information on this is very limited. The results of one study showed that age has less influence on the activities of epoxide hydrolase and glutathione peroxidase, whereas the intestinal activity of CYP1A1 appears to increase with age (Ståhlberg *et al.*, 1988). In contrast, Gibbs *et al.* (1999) conducted a biopsy of the distal duodenum and found that the glutathione-S-transferase activity decreases from infancy through early adolescence, as reflected by the reduced oral clearance of busulfan, which is a substrate for this enzyme.

1.6.1.2 Distribution

The distribution of drugs alters throughout life, as demonstrated by Sonnier and Cresteil (1998), who reported a decrease in the volume of distribution of sulfamethoxypyridazine between neonates and infants, and a further decrease from infants to children, followed by a relative stability from children to adults and then a tendency to increase from adults to the elderly. Such changes are mainly due to the alterations in protein binding at different ages, as well as to changes in extracellular fluid volume as a proportion of total body water.

Several studies have reported that the unbound fraction is higher in paediatric populations than in adults (Pacifici *et al.*, 1984; Pacifici *et al.*, 1987; Rane *et al.*, 1971). In general, acidic drugs mainly bind to albumin, whereas basic drugs bind to globulins, α_1-acid glycoprotein and lipoproteins. It was found that the concentrations of binding proteins are low at birth and then slowly increase to reach normal adult values at the first year of life (Strolin Benedetti & Baltes, 2003). Additionally, the binding capacity tends to be lower in neonates than in adults. In the neonatal period, an increase in endogenous substances, such as bilirubin, and free fatty acids capable of displacing a drug from albumin binding sites, may increase the free fraction of highly protein-bound drugs. Results from the study by Silverman *et al.* (1956) showed that the administration of the sulphonamide, sulfisoxazole can be a cause of kernicterus in neonates as a result of the displacement of bilirubin from albumin binding sites.

The total body water is high in very young infants (80-90% of the total body weight). The amount of total body water decreases to 75% for neonates and 50-60% for adults. In neonates, extracellular water accounts for about 40% of the total body weight and then reduces to reach only 20% in adulthood (Yokoi, 2009; Strolin Benedetti & Baltes, 2003). The volume of distribution of hydrophilic drugs is larger in neonates and infants than in adults. For example, the volume of distribution of gentamicin is 0.5-1.2 L/kg in neonates and infants but declines to approximately 0.2-0.3 L/kg in adults (Strolin Benedetti & Baltes, 2003). The volume of distribution of lipophilic drugs, such as flunitrazepam, is smaller in neonates and infants than in adults (Pariente-Khayat *et al.*, 1999).

1.6.1.3 Metabolism

The development of both phase I and phase II drug-metabolising enzymes is age-dependent. The activity of phase I enzymes such as the cytochromes P450 (CYPs) changes markedly during development (Kearns *et al.*, 2003). The total CYP contents in the liver are constant from the foetal period until the age of one year, remaining at 25-50% of the adult level. CYP3A7, the enzyme that protect the foetus from detoxifying dehydroepiandrosterone sulphate, is predominantly expressed in foetal liver. The expression of this enzyme peaks shortly after birth and then reduces rapidly to undetectable levels in most adults. CYP2E1 and CYP2D6 enzymes become detectable within a few hours after birth, requiring a few years to reach adult level, whereas CYP3A and CYP2C subfamilies appear during the first week of life. CYP1A2 is hardly detectable in foetal liver and emerges one to three months after birth to reach the adult expression level within a few years (Strolin Benedetti & Baltes, 2003; Yokoi, 2009). The data for the ontogeny of phase II reactions are scant. Available data indicate that the activity of uridine diphosphate glucuronosyltransferase (UGT) is low in neonates and infants as compared to adults.

Among the UGT isoforms, UGT1A1 and UGT2B7 develop quickly, whereas UGT1A6, UGT1A8 and UGT2B7 develop more slowly (Mirochnick *et al.*, 1999). There are several studies indicating that the metabolism of drugs in the liver is an age-dependent increase in plasma clearance in children aged younger than ten years,

which may require a higher weight-based dose (de Wildt *et al.*, 1999; Kraus *et al.*, 1993; Milavetz *et al.*, 1986; Scott *et al.*, 1999). The greater drug clearance in infants and children may be associated with a disproportionate increase in liver weight as a percentage of total body weight.

1.6.1.4 Excretion

The glomerular filtration rate (GFR) is approximately 2-4 mL/min/1.73 m^2 in full-term neonates, and as low as 0.6-0.8 mL/min/1.73 m^2 in preterm neonates. The GFR increases rapidly during the first two weeks of life and then rise steadily to reach the adult level of 100-120 mL/min/1.73 m^2 at 8-12 months of age (Kearns *et al.*, 2003). Tubular secretion is immature in neonates (20-30% of adult level) and reaches adult capacity during the first year of life (Yokoi, 2009). There is limited data for the renal tubular reabsorption in paediatric populations, but it has been suggested the development of reabsorption is a gradual and continuous process from birth to adolescence, and the key stage of maturation may be at three years of age (Hua *et al.*, 1997).

1.6.2 Malnutrition

1.6.2.1 Absorption

In malnourished patients, the absorption of drugs is affected by the changes in gastrointestinal structure and function. It has been found that in this patient population villi are flattened and broadened (Waterlow, 2006). Gut mucosa is completely flat in patients with kwashiorkor, while the structure of mucosa remains normal but is thinner in marasmus than in kwashiorkor. The production of gastric acid and digestive enzymes is reduced, and greater in kwashiorkor than in marasmus. Since there are several factors that promote bacterial overgrowth – including decreased gastric acidity, reduced gut motility, increased transit time due to diarrhoea and vomiting, and impaired absorption of sugars (which provide a good culture medium) – bacterial colonization of the upper intestine often occurs in malnourished patients (Waterlow, 2006).

Eriksson *et al.* (1983) investigated the pharmacokinetics of chloramphenicol in Ethiopian children with kwashiorkor and found that bioavailability was significantly decreased in kwashiorkor and marasmus-kwashiorkor. In the study by Walker *et al.* (1987), peak plasma concentrations of chloroquine and the mean area under the plasma concentration-time curve (AUC) were markedly decreased in kwashiorkor children as compared to healthy children. A number of studies, however, demonstrated that the AUC is similar or increased (Salako *et al.*, 1989; Akinyinka *et al.*, 2000; Samotra *et al.*, 1985; Lares-Asseff *et al.*, 1992). Oshikoya *et al.* (2010) suggest that this was probably due to the effects of prolonged elimination half-life or decreased clearance.

A few studies have investigated the effect of malnutrition on the rate of absorption (ka). Some studies found that the ka was unaffected by malnutrition (Bolme *et al.*, 1995; Mehta *et al.*, 1985); however, an increased ka (Lares-Asseff *et al.*, 1992) or decreased ka (Bolme *et al.*, 1995; Mehta *et al.*, 1980) have also been reported.

1.6.2.2 Distribution

Hypoproteinaemia often occurs in malnourished patients. The degree of decrease in plasma binding proteins varies according to the type, duration and severity of disease. As a result of this decreased protein binding, the free fraction of drug may be elevated. Buchanan (1977) investigated the binding properties of 18 drugs in kwashiorkor patients and found an increase in the free drug in kwashiorkor serum as compared to normal serum in all drugs. However, a possible clinical significance was only reported for some drugs, viz. cloxacillin, flucloxacillin, streptomycin, sulphamethoxazole, thiopentone and digoxin. Oshikoya and colleagues (2010) performed a systemic review of pharmacokinetic studies in malnourished children and revealed that the volume of distribution of many drugs is not significantly changed (e.g. aspirin, penicillin); however, there are contrasting results for gentamicin, quinine, streptomycin and theophylline.

The alteration in the total body water also affects the distribution of drugs. In malnourished patients, the total body water increases in proportion to the level of

malnutrition, and the greater part of the excess fluid is extracellular water. This is observed particularly in children with oedema. The distribution of lipophilic drugs to adipose tissue may be reduced in malnourished children who have markedly decreased adipose and lean body mass, such as in marasmus and mixed marasmus-kwashiorkor.

1.6.2.3 Metabolism

The biotransformation of drugs is diminished in malnourished patients. Although the liver function tests are reported as normal, hepatomegaly due to fatty infiltration is observed in most cases, particularly in kwashiorkor (Doherty *et al.*, 1992). The effect of malnutrition on the hepatic metabolising enzymes has not been investigated extensively in humans. One study conducted by Mehta *et al.* (1975) reported that the activity of the bilirubin-uridyldiphosphate (UDP) enzyme is markedly reduced in children with severe malnutrition. Akinyinka and colleagues (2000) evaluated the activity of CYP1A2 by measuring plasma paroxanthine, a metabolite of caffeine, and found that the activity of CYP1A2 as well as the hepatic clearance of caffeine decreased significantly in children with kwashiorkor. In an animal study, the total hepatic cytochrome P450 content was reduced by 55% during malnutrition. The levels of CYP1A2, CYP2C11 and CYP2E1 were found to be reduced by 60-90%, 85% and 50-60%, respectively (Cho *et al.*, 1999).

1.6.2.4 Excretion

The GFR and renal blood flow appear to be diminished in malnourished patients, particularly in the presence of dehydration (Alleyne, 1967; Klahr & Tripathy, 1966). The impact of malnutrition on the GFR is more pronounced with those drugs that are mainly excreted via the kidneys, such as penicillin and the aminoglycosides. Several studies have demonstrated that the renal clearance of drugs was significantly reduced in malnourished children as compared to healthy children. This includes the pharmacokinetic studies of amikacin (Hendricks *et al.*, 1995), gentamicin (Bravo *et al.*, 1982; Buchanan *et al.*, 1979) and streptomycin (Bolme *et al.*, 1988).

CHAPTER 2

GENERAL METHODS

INTRODUCTION TO CHAPTER

This chapter provides details of the pharmacokinetic models and statistical methods that are commonly used in subsequent chapters. The first section gives an introduction to these models. Section 2.2 provides information regarding population PK modelling, and primarily focuses on the use of the non-linear mixed effects model. The optimal design methods for population PK study are reviewed in Section 2.3. Details of whole body physiologically based pharmacokinetic (WBPBPK) models are given in the last section. Details of other specific methods are provided within later chapters, as required.

2.1 PHARMACOKINETIC MODELS

The empirical approach, which maps the complex process of drug transport into one or more compartments, is the most common method for developing a PK model. The number of compartments and complexity of the model are dependent on the available concentration-time data. These compartments are imaginary units, representing a group of tissues with similar rates of drug distribution. The simplest model is a 'one-compartment model', which assumes that the body is a single unit in which a drug is instantaneously and homogenously distributed, following administration. Drug concentrations decline over time, as a mono-exponential, or first-order, process. However, some drugs do not distribute instantaneously throughout the body, but they take some time to distribute into tissues. Concentration-time profiles show that concentrations decrease in a bi-exponential, rather than mono-exponential manner, and drop rapidly during the distribution phase. This is a result of both distribution of drug to tissues and the elimination process. After this phase, when pseudo-equilibrium between blood and tissues is reached, concentrations decline more slowly because only the elimination process is affected. Therefore, more complicated models with multiple compartments may be required to describe such concentration profiles. In this thesis, one- and two-compartment models were used to describe the PK of ciprofloxacin.

In a one-compartment model, the entire body is considered as a 'central' compartment. When a drug is administered as an intravenous (IV) bolus, the entire dose immediately enters the systemic circulation, and is rapidly distributed to bodily tissues. However, if a drug is administered extravascularly, for example, via an oral, intramuscular or subcutaneous route, drug concentration is also affected by the rate of drug absorption. A one-compartment model is illustrated in Figure 2.1, where V is the apparent volume of distribution, and ka and k are used to describe the rate of absorption and elimination, respectively.

If X is the amount of drug in the central compartment, the change in amount of drug in the body following an IV bolus dose can be described by the following differential equation:

$$\frac{dX}{dt} = -k \cdot X \tag{2.1}$$

where t is time after injection. Solving the above equation using the Laplace transform method gives:

$$X_t = X_0 \, e^{-k \cdot t} \tag{2.2}$$

where X_0 and X_t are the amount of drug at time 0 and at any time t, respectively. e represents the base of the natural logarithm. Concentrations at any time t can be calculated by dividing the amount of drug by V and therefore yields:

$$C_t = C_0 \, e^{-k \cdot t} \tag{2.3}$$

where C_0 and C_t are the concentration of drug at time 0 and at any time t, respectively.

Following extravascular administration, the rate of drug disappearance from the site of absorption is described as follows:

$$\frac{dX_A}{dt} = - ka \cdot X_A \cdot F \qquad (2.4)$$

where X_A is the amount of drug at the absorption site, which is assumed equal to the administration dose. F is the bioavailability. The rate of drug change in the central compartment is equal to the sum of the rate of drug in and the rate of drug out, as given by the following equation:

$$\frac{dX}{dt} = ka \cdot F \cdot X_A - k \cdot X \qquad (2.5)$$

Solving the above equation, and then dividing by V, respectively, gives:

$$X_t = \frac{ka \cdot F \cdot X_A}{ka - k}(e^{-k \cdot t} - e^{-ka \cdot t}) \qquad (2.6)$$

$$C_t = \frac{ka \cdot F \cdot X_A}{V(ka - k)}(e^{-k \cdot t} - e^{-ka \cdot t}) \qquad (2.7)$$

Figure 2.1 illustrates concentration-time profiles for IV and oral doses, and shows a mono-exponential decline in drug concentration during the terminal phase of elimination. The absorption and elimination half-lives can be calculated by using the following equations:

Absorption half-life = ln 2 / ka (2.8)

Elimination half-life = ln 2 / k (2.9)

Figure 2.1 A one-compartment model with a corresponding concentration-time profile

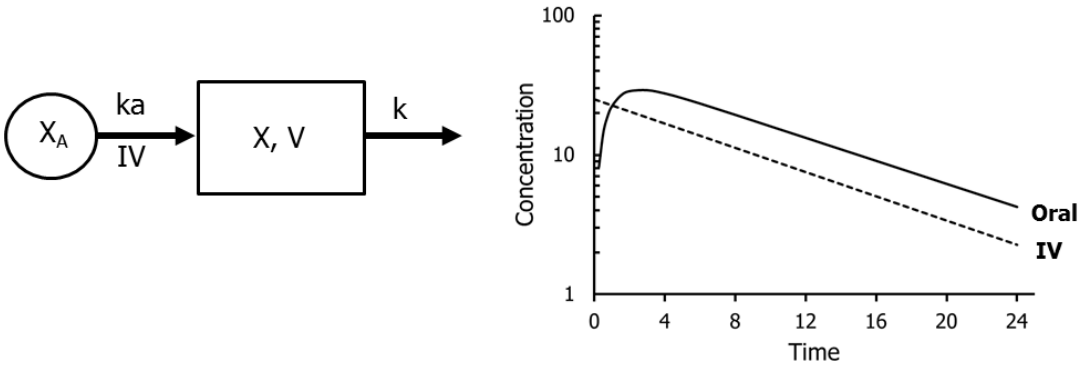

Key: ka is the absorption rate constant, IV is the intravenous administration, X_A is the amount of drug at the absorption site, V is the apparent volume of distribution and k is the elimination rate constant.

When a drug is administered orally, absorption does not begin immediately, rather, it is some time before the drug appears in the systemic circulation This may be due to particular physiological factors, for example, gastric emptying and gut motility, or to delayed release of the drug. The time delay prior to the absorption process is known as 'lag time' (t_{lag}). When the effect of lag time is considered, drug concentrations at any time t can be calculated with equation as follows:

$$C_t = \frac{ka \cdot F \cdot X_A}{V(ka - k)}(e^{-k\cdot(t - t_{lag})} - e^{-ka\cdot(t - t_{lag})}) \qquad (2.10)$$

In a two-compartment model, the body is considered as having a 'central compartment' (compartment 1) and a 'peripheral compartment' (compartment 2). The central compartment represents the blood and extracellular fluid, as well as the highly perfused organs and tissues through which a drug is distributed rapidly. The peripheral compartment represents those tissues through which a drug is distributed more slowly. Drug transfer between the two compartments is assumed to be first-order, and drug elimination is assumed to primarily occur from the central compartment. A two-compartment model is illustrated in Figure 2.2, where V_1 and

V_2 are the volumes of compartment 1 and compartment 2, respectively, k_{12} is the first-order rate of transfer constant of drug from compartment 1 to compartment 2, and k_{21} describes the rate of transfer from compartment 2 to compartment 1. The transfer constants are called 'micro-rate constants'. If X_1 is the amount of drug in compartment 1 and X_2 is the amount of drug in compartment 2, the rate of change of drug in these compartments can be described by the following equations:

$$\frac{dX_1}{dt} = k_{21} \cdot X_2 - k_{12} \cdot X_1 - k \cdot X_1 \quad (2.11)$$

$$\frac{dX_2}{dt} = k_{12} \cdot X_1 - k_{21} \cdot X_2 \quad (2.12)$$

Solving the above equations, and then dividing by V_1, respectively, gives:

$$X_t = X_1 e^{-\alpha \cdot t} + X_2 e^{-\beta \cdot t} \quad (2.13)$$

$$C_t = C_1 e^{-\alpha \cdot t} + C_2 e^{-\beta \cdot t} \quad (2.14)$$

where X_t and C_t are the amount and concentration, respectively, of drug in the central compartment at time t, α is the slope of the distribution phase and β is the slope of the elimination phase. For a two-compartment model with first-order absorption, the changes in amount of drug in the compartment 1 and compartment 2 are described by equations 2.15 and 2.16, respectively. The concentrations of drug in plasma (compartment 1) can be calculated using equation 2.17 (Hacker *et al.*, 2009).

$$\frac{dX_1}{dt} = ka \cdot F \cdot X_A e^{-ka \cdot t} + k_{21} \cdot X_2 - k_{12} \cdot X_1 - ke \cdot X \quad (2.15)$$

$$\frac{dX_2}{dt} = k_{12} \cdot X_1 - k_{21} \cdot X_2 \quad (2.16)$$

$$C_t = C_1e^{-\alpha \cdot t} + C_2e^{-\beta \cdot t} - (C_1 + C_2)e^{-ka \cdot t} \quad (2.17)$$

Figure 2.2 illustrates concentration-time profiles for IV and oral doses, and shows a bi-exponential decline of drug. The distribution and elimination half-lives can be calculated by using the following equations:

Distribution half-life = ln 2 / α (2.18)

Elimination half-life = ln 2 / β (2.19)

Figure 2.2 A two-compartment model with a corresponding concentration-time profile

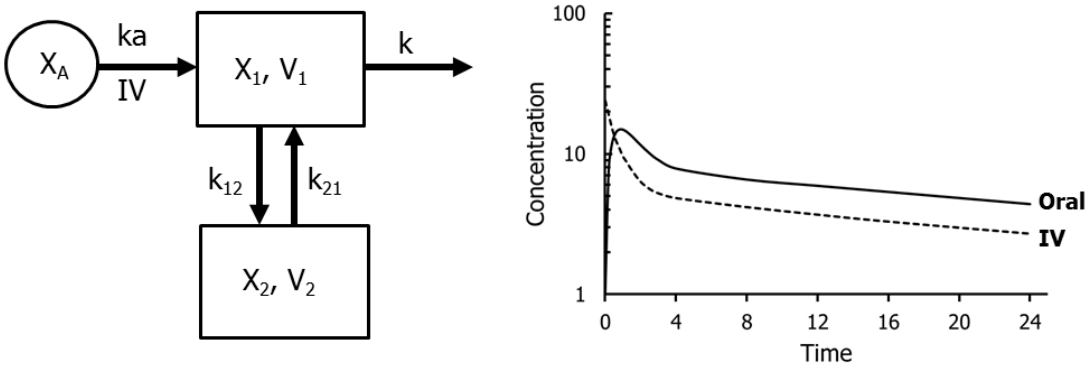

Key: X_A is the amount of drug at the absorption site, X_1 is the amount of drug in compartment 1, X_2 is the amount of drug in compartment 2, V_1 is the volume of compartment 1, V_2 is the volume of compartment 2, k_{12} is the rate constant representing the movement of drug from compartment 1 to compartment 2. k_{21} is the rate constant representing the movement of drug from compartment 2 to compartment 1.

It is sometimes more useful to parameterise the micro-rate constants in terms of clearance. In this thesis, the one-compartment model was parameterised to give clearance (CL) and V and the two-compartment model was parameterised to give CL, V_1, V_2 and Q (inter-compartment clearance). The equations used to relate the micro-rate constants to clearance are shown below.

A one-compartment model:

$$CL = k \cdot V \tag{2.20}$$

A two-compartment model:

$$CL = k \cdot V_1 \tag{2.21}$$

$$Q = k_{12} \cdot V_1 \quad \text{or} \quad Q = k_{21} \cdot V_2 \tag{2.22}$$

The CL value obtained with the above equations can be used to calculate the area under the concentration time curve (AUC). The AUC is the parameter reflecting the overall exposure of the patient to the drug. It depends on dose, bioavailability and CL. In this thesis, the AUC was the PK parameter used to determine the efficiency of the ciprofloxacin dose. The AUC can be calculated by the following equation:

$$AUC = \frac{F \cdot Dose}{CL} \tag{2.23}$$

The unit for AUC is concentration time, for example, $mg \cdot hr/L$.

2.2 POPULATION PHARMACOKINETIC MODELLING

Population PK is a data analysis approach aimed at determining typical PK parameters and their statistical distribution, as well as identifying potential sources of inter- and intra-individual variability. This information can be used to develop dosage regimens that will achieve target drug concentrations. The population PK approach can also identify clinical factors, such as body weight or renal function, which contribute to inter-patient variability in PK. In the simplest case, all data are pooled and analysed as if they come from the same individual. This method is called the ‘naïve pooled data’ (NPD) approach. The drawback of this method is that it is susceptible to bias, as it ignores individual variability and no information can be obtained with regard to PK relationships with patient characteristics. However, NPD can be used if a rich data set is available and the data design is similar across individuals. It may also help to obtain initial PK parameter estimates (Vinks, 2002).

In a second population approach, called the ‘standard two-stage’ method (STS), individual PK parameters are estimated in the first stage, while means and variability are determined in the second stage. The drawback of this method is that it can produce biased and imprecise parameter estimates. Use of the STS method is only recommended if a sufficiently large amount of data can be obtained from all subjects, and the data are balanced across individuals.

In the 1970s, Sheiner *et al.* proposed the use of a non-linear mixed effects model to analyse PK data that have been collected from routine clinical practice or during phase III or phase IV trials. This type of data is very sparse, i.e. only one or two samples per patient can be obtained, and there may be an imbalance in the number of samples taken from each patient. Use of traditional methods may lead to biased parameter estimates if some of the information obtained is significantly far from a typical value, such as data from a patient who has unusual PK. Conversely, the non-linear mixed effects model can handle sparse data because it analyses all data simultaneously, as each individual borrows information from the others. In this thesis, a population analysis was performed with a non-linear mixed effects model. The term ‘mixed effects’ is so-called because it includes two effect types; fixed and random.

2.2.1 Fixed effects modelling

Fixed effects are those factors that can be measured, including (i) independent variables, such as time and dose, and (ii) PK parameters, such as clearance and volume of distribution. These factors are entered in the structural part of the model, which includes the PK model and the regression model. The regression model is used to describe the effect of covariates on PK parameters. For example, equation 2.24 shows a one- compartment model following an IV bolus injection

$$Cp = \frac{D}{V}\exp^{-\frac{CL}{V}\cdot t} \qquad (2.24)$$

where Cp is the predicted plasma concentration at time, t, following a single IV dose, D. CL and V are the clearance and volume of distribution, respectively.

2.2.2 Random effects modelling

Random effects are the difference between the observed concentrations and the predicted concentrations that have been estimated from the structural model. Random effects are primarily divided into two types, according to the sources of variability. These are inter-individual variability and residual variability, which are typically estimated as a variance around the fixed effect parameters assuming a normal distribution. Random effects can be represented graphically, as shown in Figure 2.3A and 2.3B (adapted from Grasela & Sheiner, 1991).

2.2.2.1 Inter-individual variability

Inter-individual variability represents the difference between the parameter of an individual and the typical parameter of the population. If PK parameters are assumed to follow a log-normal distribution, inter-individual variability can be modelled by the following equation:

$$\ln(CL_i) = \ln(TVCL) + \eta_{CLi} \qquad (2.25)$$

where, CL_i is the individual CL value, TVCL is the typical population value of CL and η_{CLi} is the inter-individual error. The η_{CLi} value is assumed to be normally distributed with a mean of zero, and an estimated variance of ω^2, as illustrated in Figure 2.3A.

Equation 2.25 can also be written as follows:

$$CL_i = TVCL \cdot \exp(\eta_{CLi}) \qquad (2.26)$$

2.2.2.2 Residual variability

Although the PK parameters for an individual subject were already known, and were used to predict drug concentrations, these predicted drug concentrations (C_{pred}) may differ from the observed observations (C_{obs}). This discrepancy, called residual error (ε_{ij}), represents model misspecification and experimental errors, as well as other, unknown, errors. Inter-occasional variability (IOV) with respect to the change of PK parameters (e.g. CL and V) over time, may also contribute to residual error (Karlsson & Sheiner, 1993). The ε_{ij} value is assumed to be normally distributed with a mean of zero, and an estimated variance of σ^2, as illustrated in Figure 2.3B. Three types of residual error models were used in this thesis:

1) additive error model

$$C_{obs} = C_{pred} + \varepsilon_{ij} \quad (2.27)$$

with this model, error on each concentration measurement is constant, independent of the concentration value.

2) proportional error model

$$C_{obs} = C_{pred} \cdot (1+ \varepsilon_{ij}) \quad (2.28)$$

with this model, error is proportional to the concentration.

and 3) combined error model

$$C_{obs} = C_{pred} + (C_{pred} \cdot \varepsilon_{ij,prop}) + \varepsilon_{ij,add} \quad (2.29)$$

The combined error model has both an additive and a proportional component. The additive component dominates at low concentrations, while the proportional component dominates at high concentrations.

Figure 2.3A Log-linear parameter distribution, showing the relationship between TVCL, CL and η

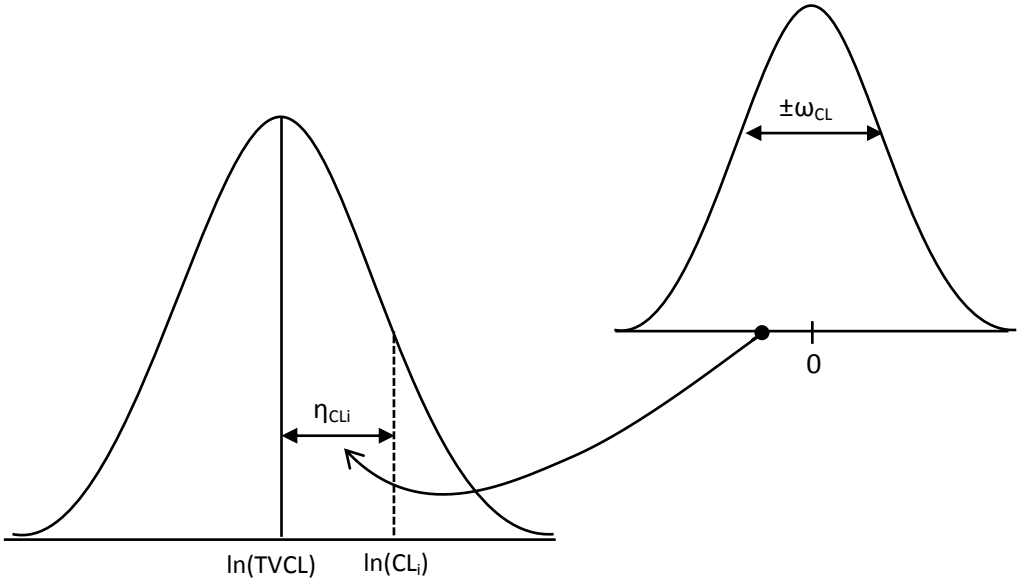

Key: TVCL is the typical value of clearance in the population, CL_i is the estimated CL for an individual, η_{CLi} is the inter-individual error, which is assumed to be normally distributed with mean of zero and variance ω^2.

Figure 2.3B Concentration-time profile showing the relationship between observed concentrations, predicted concentrations and residual error

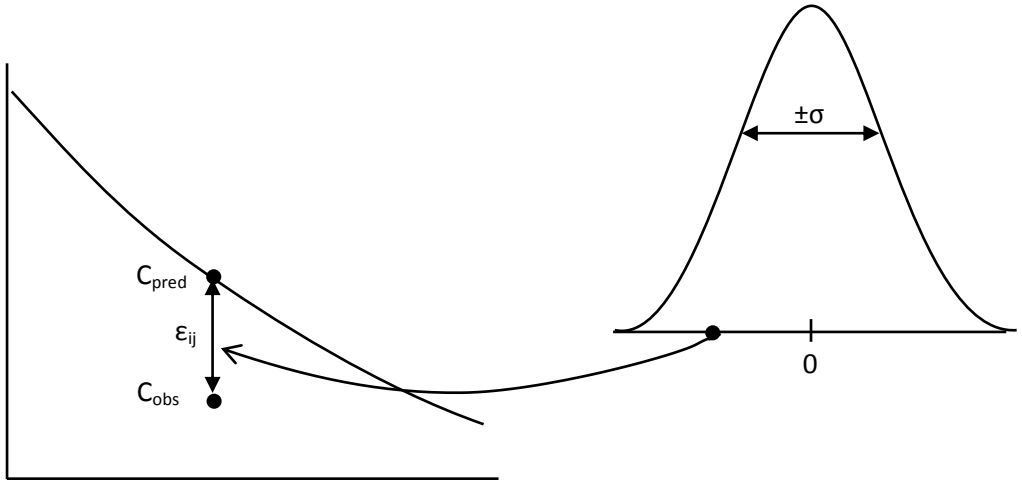

Key: C_{pred} is the predicted concentration, C_{obs} is the observed concentration, ε_{ij} is the residual error which is assumed to be normally distributed with mean of zero and variance σ^2.

2.2.3 Mathematical expression

The general form of the non-linear mixed effects model, assuming time constant parameters and additive residual error, can be written as follows (Beal *et al.*, 1989-2006):

$$y_{ij} = f(\mathrm{P}_i, \mathrm{X}_{ij}) + \varepsilon_{ij} \qquad \varepsilon_{ij} \sim \mathrm{N}(0,\sigma^2) \tag{2.30}$$

where y_{ij} is the *j*th observed concentration from the *i*th individual, *f*(…) is the structural model that relates the vector of the independent variables, X_{ij} (e.g. time and dose) to the response given by the *i*th individuals vector of PK parameters, P_i. ε_{ij} is the residual error.

Each parameter P_i is distributed around the typical population value (θ), and is related to covariates as described in the following equation:

$$\mathrm{P}_i = g(\theta, z_i) + \eta_{ij} \qquad \eta_{ij} \sim \mathrm{N}(0,\omega^2) \tag{2.31}$$

where *g*(…) is a function that describes the relationship between P_i and the vector of the covariates for the *i*th individual, Z_i. The general expression of the non-linear mixed effects model is therefore:

$$y_{ij} = f(g(\theta, z_i) + \eta_{ij}, \mathrm{X}_{ij}) + \varepsilon_{ij} \tag{2.32}$$

2.2.4 Covariate modelling

When adequate structural and error models have been selected, covariates are usually added to the model in order to explain the variability between subjects. Covariates are defined as patient-specific characteristics that are expected to influence the pharmacokinetics or pharmacodynamics of a drug, for example, demographic data (e.g. age, weight and gender) and clinical factors (e.g. renal and liver functions). The relationship between covariates and parameters can be described by using the models as follows:

2.2.4.1 Continuous covariates

Continuous covariates, such as body weight, age and creatinine clearance, can be modelled with the simplest linear function as:

$$P = \theta_1 + \theta_2 \cdot Cov \tag{2.33}$$

where P is the parameter estimate and *Cov* is the covariate. θ_1 is the typical value if the covariate is equal to zero. θ_2 represents the change of parameter estimate per unit change of covariate. Equation 2.33 can be reparameterised to give θ more meaning as:

$$P = \theta_1 \times [1 + \theta_2 \cdot (Cov - \text{median } Cov)] \tag{2.34}$$

with the above equation, θ_1 is the parameter estimate when the covariate is equal to the median value and θ_2 is the fractional change of parameter estimate per unit change of covariate from the median value.

For non-linear relationships, covariates can be modelled by the following equations:

$$P = \theta_1 \cdot \left[\frac{Cov}{\text{median } Cov} \right]^{\theta_2} \tag{2.35}$$

2.2.4.2 Categorical covariates

Categorical covariates can be categorised as binary (e.g. male/female, response/non-response), ordered multiple (e.g. severity and stage of disease) and non-ordered multiple (e.g. genotype, race). In this thesis, a binary covariate was included in the model by coding the covariates as either '0' or '1'; such as '0' for males and '1' for females. The models in equations 2.33 and 2.34 can also be applied to binary data. For multiple category covariates, each category was assigned to different indicator values e.g. '1' for healthy children and '2', '3' and '4' for mild, moderate and severe malnutrition, respectively. The model in equation 2.36 was used for non-ordered

multiple covariates and the model in equation 2.37 was used for ordered multiple covariates.

$$P = \begin{cases} \theta_1 & \text{if } Cov = 1 \\ \theta_2 & \text{if } Cov = 2 \\ \theta_3 & \text{if } Cov = 3 \\ \theta_4 & \text{if } Cov = 4 \end{cases} \quad (2.36)$$

$$P = \begin{cases} \theta_1 & \text{if } Cov = 1 \\ \theta_1 + \theta_2 & \text{if } Cov = 2 \\ \theta_1 + \theta_2 + \theta_3 & \text{if } Cov = 3 \\ \theta_1 + \theta_2 + \theta_3 + \theta_4 & \text{if } Cov = 4 \end{cases} \quad (2.37)$$

2.2.5 NONMEM

2.2.5.1 Program

In this thesis, population PK analysis was performed using the non-linear mixed effects modelling program, NONMEM, Version VI (Beal *et al.*, 1989-2006) with a G77 Fortran compiler, running on a computer with a Microsoft Windows XP operating system. NONMEM is a FORTRAN computer program, and was specially developed to fit non-linear regression models to population PK and pharmacodynamic data. Xpose Version 4.0 (Jonsson & Karlsson, 1999), which is implemented in the R software, Version 2.9.2, was used to process the NONMEM outputs.

A collection of FORTRAN subroutines, including ADVAN, TRANS, PK and ERROR, have been written for use in NONMEM. The ADVAN subroutine is used to describe the structural model, for example, bolus input with mono-exponential decline, first-order input with bi-exponential decline, etc. In this thesis, ADVAN2 was used for a one-compartment model. The parameter k was reparameterised to

give CL and V using the translator subroutine TRANS2. For a two-compartment model, ADVAN4 was used with basic parameters k, k_{12} and k_{21}. This was reparameterised using TRANS4 to provide CL, Q, V_1 and V_2. A PK subroutine was used to estimate the values for the population and individual PK parameters, such as CL, V and ka, as well as to compute the inter-individual variability. An ERROR subroutine is used to describe the differences between observed and predicted dependent variables, for example, drug concentrations.

2.2.5.2 Data file format

In this thesis, a data file for NONMEM analysis was created with Microsoft Excel® 2003 using a 'comma separated values' format. All data were arranged in columns, and the information necessary for inclusion in the data file was identification data number (ID), blood sampling time after the dose (TIME), administration dose (AMT) and dependent variable data, which are drug concentrations (DV). A missing dependent variable (MDV) column was required to specify whether the DV column contained values for observed data. An event identification data (EVID) column was used to identify the types of event described in each data record, for example, '0' for an observation event, '1' for a dose event, '2' for other events, etc. The EVID column was used when using the transit compartment model to describe the absorption process of a drug. Additional columns for covariate data, such as weight, age and gender were subsequently included. An example of the NONMEM data file structure is shown in Figure 2.4

2.2.5.3 Control file format

The control file is an ASCII file that contains a series of statements, each of which begins with an '$' symbol. The first line of the control file states the title of the problem being solved ($PROB), followed by the name of data column ($INPUT), which is the same as that specified in the data file. Some of these column names are reserved and recognised specifically by NONMEM, such as ID, TIME, AMT and DV, whereas others, such as the name of the covariate (e.g. weight, height, age etc.) can be user-defined. $DATA is used to indicate the name and location of the data file. The next part of the file defines the model that will be used to fit the data. Under

$SUBROUTINE, a subroutine that describes a PK model, for example, ADVAN2 and TRANS2, is defined. The parameters to be estimated, THETA (θ) and ETA (η), are assigned in a $PK record. THETAs represent the typical population parameters (e.g. TVCL and TVV) and the relationships between these parameters and covariates. ETAs represent the inter-individual random effects. The scale parameter, S, is also included under the $PK record to convert the amount of drug in the compartment to measured drug concentration. The $ERROR record is used to describe the residual error model (the details of the different approaches used to model the residual error are given in Section 2.2.2.2). Initial estimates for structural parameters, the variance of inter-individual error and the variance of the residual error are specified in the $THETA, $OMEGA and $SIGMA records, respectively. These initial estimates can be fixed by adding the word 'FIXED' after the values, for example, '$OMEGA 0 FIXED'. If the covariance between ETAs is used in the model, the 'BLOCK' command is added to the $OMEGA record. The number specified in the BLOCK command refers to the number of ETAs in the block; for example, 'BLOCK (3)' means that there are three ETA variables and that the covariance between these variables will be estimated. An example of a block variance-covariance matrix coded in the control file is shown below:

	ETA1	ETA2	ETA3
ETA1	ω_{11}		
ETA2	ω_{12}	ω_{22}	
ETA3	ω_{13}	ω_{23}	ω_{33}

where the diagonal values ($\omega_{11,}$ ω_{22} and ω_{33}) are the variances and the off-diagonal values ($\omega_{12,}$ ω_{13} and ω_{23}) are the covariances. An example of a control file is illustrated in Figure 2.5.

The estimation process in NONMEM is controlled by the commands indicated in the $ESTIMATION record, such as 'MAXEVAL' (the maximum number of objective function evaluations allowed during the search), 'METHOD' (the estimation method

e.g. first-order or first-order conditional estimation method) and ‘SIG’ (minimum number of significant figures required for the accuracy). If a $COVARIANCE record is presented, NONMEM will generate the standard error, covariance matrix, correlation matrix and the inverse covariance matrix of parameters. A $TABLE record is used to request NONMEM to create a results table, for example, observed concentrations, individual-predicted concentrations, population-predicted concentrations and other requested data.

Figure 2.4 Excerpt from a NONMEM data file

ID	TIME	AMT	DV	MDV	AGE	SEX	WT	HT	SHOK	EDEM	NA	CLCR
1	0.00	50	0	1	18	0	5.02	66.8	0	0	132	21.24
1	1.07	0	2.01	0	18	0	5.02	66.8	0	0	132	21.24
1	2.93	0	2.62	0	18	0	5.02	66.8	0	0	132	21.24
1	6.07	0	1.18	0	18	0	5.02	66.8	0	0	132	21.24
1	9.90	0	0.46	0	18	0	5.02	66.8	0	0	132	21.24
2	0.00	58	0	1	27	1	5.8	78.5	1	1	129	25.61
2	3.00	0	1.69	0	27	1	5.8	78.5	1	1	129	25.61
2	5.25	0	1.05	0	27	1	5.8	78.5	1	1	129	25.61
2	9.08	0	0.62	0	27	1	5.8	78.5	1	1	129	25.61
2	12.08	58	0	1	27	1	5.8	78.5	1	1	129	25.61
2	0.08	0	0.4	0	27	1	5.8	78.5	1	1	129	25.61
3	0.00	106	0	1	33	1	10.64	88.5	0	1	142	12.12
3	2.00	0	1.77	0	33	1	10.64	88.5	0	1	142	12.12
3	4.05	0	1.47	0	33	1	10.64	88.5	0	1	142	12.12
3	8.05	0	0.73	0	33	1	10.64	88.5	0	1	142	12.12
3	12.00	106	0	1	33	1	10.64	88.5	0	1	142	12.12
3	12.25	0	0.69	0	33	1	10.64	88.5	0	1	142	12.12
4	0.00	61	0	1	14	0	6.7	71	0	0	131	15.00
4	3.02	0	1.82	0	14	0	6.7	71	0	0	131	15.00
4	5.00	0	1.19	0	14	0	6.7	71	0	0	131	15.00
4	9.00	0	0.58	0	14	0	6.7	71	0	0	131	15.00
4	12.00	61	0	1	14	0	6.7	71	0	0	131	15.00
4	0.17	0	0.32	0	14	0	6.7	71	0	0	131	15.00
5	0.00	92	0	1	56	0	9.2	89	1	1	137	22.45
5	2.25	0	1.16	0	56	0	9.2	89	1	1	137	22.45
5	3.92	0	1.84	0	56	0	9.2	89	1	1	137	22.45
5	8.00	0	1.16	0	56	0	9.2	89	1	1	137	22.45
5	12.00	92	0	1	56	0	9.2	89	1	1	137	22.45
5	11.88	0	0.19	0	56	0	9.2	89	1	1	137	22.45
6	0.00	86	0	1	14	0	8.58	70	0	1	125	23.94
6	1.00	0	0.69	0	14	0	8.58	70	0	1	125	23.94
6	3.00	0	2.36	0	14	0	8.58	70	0	1	125	23.94
6	6.00	0	0.89	0	14	0	8.58	70	0	1	125	23.94
6	10.00	0	0.34	0	14	0	8.58	70	0	1	125	23.94

Key: ID = patient identification number, TIME = time after drug administration, AMT = dose, DV = dependent variable (ciprofloxacin concentration), MDV = missing dependent variable, AGE = age, SEX = sex, WT = weight, HT = height, SHOK = shock, EDEM = oedema, NA = sodium concentration, CLCR = creatinine clearance.

Figure 2.5 Example of a control file

```
$PROB CIPROFLOXACIN
$INPUT ID TIME AMT DV MDV AGE SEX WT HT SHOK EDEM NA CLCR
$DATA  DATA2.CSV
$SUBROUTINE ADVAN2 TRANS2
$PK       TVCL=THETA(1)
          TVV=THETA(2)
          TVKA=THETA(3)
          CL=TVCL*EXP(ETA(1))
          V=TVV*EXP(ETA(2))
          KA=TVKA*EXP(ETA(3))
          ALAG1=THETA(4)
          S2=V
$ERROR    IPRED=F
             W=SQRT(THETA(5)**2+THETA(6)**2*F**2)
             IRES=DV-IPRED
             IWRES=IRES/W
Y=F+W*ERR(1)
$THETA    (0,30) (0,120) (0,2.5) (0,0.5) 0.1 0.1
$OMEGA    0.5 0.5 0.5
$SIGMA    1 FIX
$ESTIMATION MAX=1500 METHOD=1 INTERACTION SIG=3 PRINT=2
$COVAR
$TABLE ID TIME AMT DV MDV AGE SEX WT HT SHOK EDEM NA CLCR NOPRINT FILE=RUN1.TAB
```

2.2.5.4 Estimation methods

In the NONMEM program, parameter estimation is based on maximising the likelihood of the data given in the model. An approximation is performed using the extended least squares objective function. If the random effects are assumed to follow a normal distribution, the objective function value (OFV) is equal to -2 times the logarithm of the likelihood (-2LL) of the data (Beal, 1984; Davidian & Giltinan, 1995). The non-linearity of the model precludes the direct calculation of the OFV, with respect to random effects. Therefore, NONMEM addresses this problem by approximating the OFV by a linearisation of the non-linear model.

Several linearisation methods are implemented in NONMEM. The first-order estimation (FO) method linearises the non-linear model around the median of the individual parameters (random effects set to zero) using a first-order Taylor-series expansion. This method gives only the population parameter estimates; it does not provide individual parameters. At the last iteration, the POSTHOC option uses an empirical Bayesian method to estimate η for each individual, by using the population parameters as initial estimates. The first-order conditional estimation (FOCE) method is similar to the FO through linearising the model around the current estimates of the fixed effects but it is conditional on the individual estimates of η, rather than being set to zero. This method estimates the individual value of η at every iteration by maximising the empirical Bayesian posterior density using the current estimates, so it is more time-consuming. FOCE is useful when the number of observations per individual increases and the model has greater non-linearity (Beal *et al.*, 1989-2006). Interactions between η and ε can be accounted for by using the FOCE method with interaction (FOCE-I). When interaction is specified, ε is estimated with the conditional estimates of η_s. If the residual error model contains a proportional component, ε depends on the model prediction, which is in turn a function of the η_s. When the additive error model is used, the model prediction does not affect the parameter estimates.

Several estimation methods, such as stochastic approximation expectation maximisation (SAEM), Monte Carlo importance sampling (IMP) and a full Bayesian

estimation, have become available in the new version of NONMEM. The results from a recent comparative study suggested that, although the computational time of the new methods was much faster, the estimation performance was similar to the traditional FOCE-I method, in terms of parameter estimates and standard errors (Gibiansky *et al.*, 2012). Parameters estimated using the latter method are less biased and more consistent with the actual significance levels, compared to the FO method (Wählby *et al.*, 2001). In addition, the FO method tends to have higher actual significance levels of covariates, which may lead to a covariate selection bias.

2.2.5.5 Individual empirical Bayes estimates and shrinkage

In NONMEM, the individual parameter estimates are generated as empirical Bayes estimates (EBEs). EBEs are highly dependent on the quality of the observed data. If the data are very sparse or lack information for individual parameters, EBEs may tend to shrink towards the population mean value. The phenomenon of reduction in the variability of an EBE is defined as 'η-shrinkage' (Savic & Karlsson, 2009). The consequence of η-shrinkage is that the shape of the true relationship between EBEs and their covariates may become distorted or appear as unimportant or falsely important. The sparseness of data may also lead to ε-shrinkage, which is the phenomenon where the individual weighted residual (IWRES) shrinks towards zero. The power of IPRED and IWRES to diagnose structural and residual error model misspecification may then decrease as a result.

The degree of η- and ε-shrinkage can be calculated using the following equations:

$$\eta\text{-shrinkage} = 1 - \frac{SD(\eta_{EBE})}{\omega} \quad (2.38)$$

$$\varepsilon\text{-shrinkage} = 1 - SD(IWRES) \quad (2.39)$$

where SD is standard deviation.

2.2.6 Model selection

In this thesis, model selection was based on the objective function value (OFV) provided by NONMEM and by graphical assessment. Plausibility and the precision of parameter estimates were also taken into consideration.

2.2.6.1 Objective function value

NONMEM estimates the parameters by an iteration process. It predicts the concentration at all sampling times at each iteration, given the current PK parameter estimates, and then calculates the difference between predictions and observations by using the extended least squares OFV:

$$OFV_{ELS} = \sum_{i=1}^{m}\left[\log(\sigma_i^2) + \frac{(y_i - f(\theta,\eta_i))^2}{\sigma_i^2}\right] \quad (2.40)$$

where y_i is the observation in the *i*th subject, *f*(…) is a function representing the prediction of the observations y_i given the model, σ^2 is the variance of residual errors and *m* is a number of subjects in the data set. The iteration process continues until the minimum value of the OFV is attained. The difference in the OFV (ΔOFV) between two nested models approximately follows a χ^2-distribution, with degrees of freedom (df) corresponding to the difference in the number of parameters between the two models. The likelihood ratio test was used to compare nested models, where ΔOFV of 3.84 and 6.63 corresponded to a significance level of $p<0.05$ and 0.01 (df = 1), respectively.

2.2.6.2 Graphical assessment

1) DV versus PRED and IPRED

Plots of population-predicted concentrations (PRED) and individual-predicted concentrations (IPRED) versus observed concentrations (DV) are commonly used to assess the fit of the model. The data points should ideally be centred along the line of identity. The major drawback of these plots is that, in addition to model misspecification, a skewed distribution may be observed as a result of unexplained variability, adaptive designs (e.g. dose adjustments) and censoring (e.g. omission of

data below the limit of quantification) (Karlsson & Savic, 2007). The solution to this problem is to either use a greater number of assessment tools or to create mirror plots based on the simulations with the final model. If the pattern in the mirror plots for the observed data and the simulated data are similar, there is no evidence of model misspecification. For the plot of IPRED, a perfect fit may occur if ε-shrinkage is high.

2) DV, PRED and IPRED versus time

Data from individual subjects, including DV, PRED and IPRED, created in one plot are used to compare the concentration-time profile of measured concentrations with the population and individual predicted concentrations. These plots are also used to aid assessment of the fit of the model and to identify anomalous values.

3) Residuals versus time

Plots of residuals versus time or any independent variables can be used to detect model misspecification. Residuals based on population predictions (RES = DV – PRED) and individual predictions (IWRES = (DV – IPRED)/σ) have the same limitations as those discussed above; however, IWRES remains useful if ε-shrinkage is sufficiently low. Weighted residuals (WRES) are unaffected by the shortcomings shown with regard to RES and IWRES. However WRES are computed based on the FO method and therefore have a problem with crude first-order linearisations. In the present study, conditional weighted residuals (CWRES) were used. CWRES are the difference between the observations and the predictions weighted with the error magnitude (σ), based on the FOCE approximation. It has been demonstrated that CWRES is more accurate than other residual based diagnostics (Hooker *et al.*, 2007). If the model is adequate, CWRES should be normally distributed, with a mean of zero when plotting against time.

4) IWRES versus IPRED

The IWRES plot is commonly used for assessment of the fit of the residual error model. The general interpretation is that, when the model fit is adequate, IWRES should show a lack of any trends when plotting against the predictions.

2.2.6.3 Identification of potential covariates

Covariate model building can be a difficult and very time-consuming process, particularly if there are a large number of covariates in the data set. Indeed, testing of all existing covariates is unnecessary, as some potential covariates are often correlated, such as weight, age and height. The most important and clinically relevant covariate should be decided on in such circumstances. In this thesis, covariate models were identified using a combination of the following techniques:

1) Graphical inspection

Potential covariates were identified from plots of individual estimates of the parameters versus the covariates. The shape of the relationship, for example, linear and log-linear, may be visible in the plots. The drawbacks of these graphs are that they tend to be biased towards the population values when sparse sampling is used, and the interpretation is somewhat subjective.

2) Generalised additive modelling

Generalised additive modelling (GAM) was also used to identify the important covariates. GAM describes the relationship between individual parameter estimates and the covariates, according to the equation below (Mandema *et al*., 1992):

$$P_i = \alpha + \sum_{j=1}^{n} f_j(X_{ij}) \qquad (2.41)$$

where P_i is the PK parameter estimate for the *i*th individual α is a constant value and $f_j(X_{ij})$ represents either a linear or a spline (non-linear) function of the *j*th covariate.

The influence of covariates on the parameters was tested by a stepwise selection method as follows: a number of hierarchical models were built for each covariate and parameter. These included models with no covariates and models that included the covariates as a linear or spline relationship. The models were evaluated in hierarchical order, based on the Akaike information criterion (AIC). The model which resulted in the largest decrease in AIC was retained. The models at the higher

and lower levels were subsequently evaluated, and again the model that was optimum on the basis of the AIC value was retained. This process continued until the AIC reached a minimum value. The AIC value can be calculated as follows (Akaike, 1978):

$$AIC = N_{obs} \cdot Ln(WRSS) + 2N_{par} \quad (2.42)$$

where N_{obs} is the number of observations, N_{par} is the number of parameters and WRSS is the weighted residual sum of squares.

Several techniques for building covariate models have been developed to date, for example, stepwise covariate modelling (SCM) (Jonsson & Karlsson, 1998), Wald's approximation method (WAM) (Kowalski & Hutmacher, 2001) and the least absolute shrinkage and selection operator (LASSO) (Ribbing *et al*., 2007). These techniques were not applied in the present study.

2.2.6.4 Adding covariates to the model

The candidate covariates identified from the graphical approach and GAM analysis were added to the basic model, one at a time. The most important covariate, as judged by the greatest reduction in the OFV, was retained in the model. Other covariates were then included individually, until no more covariates could reduce the OFV to a level of statistical significance (ΔOFV at least 3.84; $p<0.05$). Scatter plots of inter-individual variability (η) of parameter against the covariate were used to assess the effect of adding covariates. If a relationship between parameter and covariate was shown, the model with the incorporated covariate should lack trends, whereas the model without a covariate may have shown trends. In addition to the graphical inspection, a reduction in inter-individual variability was interpreted by calculating the percentage coefficient of variation (%CV). If inclusion of a covariate failed to decrease variability, as measured by %CV, it was removed from the model. The physiological plausibility was also considered.

2.2.7 Simulation with NONMEM

In this thesis, the NONMEM program was used to perform a Monte Carlo simulation. This approach generates simulated data points using a given model, accounting for inter-individual variability and residual variability. A data file was prepared as a normal data file for estimating parameters (Section 2.2.5.2), having patient identification number, dosage history and blood-sampling time schedule. A value in the DV column was set to zero. In the control file, population parameter estimates (θ), variances of inter-individual error (η) and variances of residual error (ε), obtained from the final population model, were entered into the $THETA, $OMEGA and $SIGMA records, respectively. In NONMEM, simulation can be performed by using the $SIMULATION record instead of $ESTIMATION. This record requires information regarding the number of simulations and a random number. Individual parameter estimates corresponding to the simulated data were computed by adding the command 'ONLYSIMULATION' in the $SIMULATION record. When using this option, the calculation of OFV and WRES is neglected and the predictions are calculated using θ and simulated η.

2.2.8 Model evaluation

There are two general approaches to model evaluation: 'internal' and 'external' evaluation. Internal evaluation involves the use of complex methods, such as data splitting and resampling techniques, whereas external evaluation requires a new data set (called a validation data set) to evaluate the model. There is no consensus as to which method should be used; evaluation methods should be selected on the basis of the objective of the analysis (FDA, 1999). It is possible that in many cases, a model is developed for predictive purposes, so its predictive performance should be assessed. The external evaluation method is considered a method of choice; however, for some populations, for example children and severely ill individuals, a validation data set may be difficult to obtain (Brendel *et al.*, 2007). In addition, the main drawback of this approach is that an unbalanced study design (e.g. number of subjects) and differences in inclusion criteria (e.g. dosage regimen and sampling time) between two data sets may influence the evaluation.

In the present study, a validation data set was not available, the final models were therefore only evaluated using internal evaluation techniques.

2.2.8.1 Bootstrapping

Bootstrapping is a method used to generate a new data set by resampling with replacement from the original dataset (Efron, 1979; Efron & Tibshirani, 1993). The final population model was fitted to each new dataset, then the bias, standard errors and confidence intervals (CIs) of parameter estimates were calculated. If the final model is robust, the parameter estimates calculated from bootstrap datasets should be similar to those obtained from the original dataset, and they should lie within the 95% CI.

2.2.8.2 Visual predictive check

Visual predictive check (VPC) is a simulation-based diagnostic, in which data simulated from the model were compared with the distribution of observed data, which is often grouped within a defined range of an independent variable. The median, 5^{th} and 95^{th} percentiles, with a 95% CI of each percentile derived from the simulations, were graphically compared to the corresponding percentiles of the observed data. If evidence of model misspecification is shown, discrepancies can be observed. In this thesis, a prediction-corrected VPC (pcVPC), which normalises both simulated and observed data to the typical population prediction (Bergstrand *et al.*, 2011), was used for model evaluation.

2.2.8.3 Normalised prediction distribution error

In 2006, Mentré and Escolano proposed a new model-evaluation method called prediction discrepancies (pd); pd is the percentile of each observed piece of data in the simulated predictive distribution for that observed data, under the null hypothesis (H_0). The limitation of pd is that if the subjects have several measurements, pd may lead to an increased type I error, as they are correlated within individuals (Mentré & Escolano, 2006). In the case of repeated measurements, a de-correlated pd, so-called normalised prediction distribution error (npde), should be used. Monte Carlo simulations are performed for the npde to create a posterior predictive distribution.

The percentiles of the observed data in the predictive distribution are then computed, as in pd, but they are normalised with the mean and variance of the simulated data for each subject (Brendel *et al.*, 2006; Brendel *et al.*, 2010). The interpretation of npde is that if the model adequately describes the data, the npde should follow a normal distribution, with a mean of zero and a variance of one. This assumption can be tested statistically by using (i) a Wilcoxon signed rank test to assess whether the mean is significantly different from zero, (ii) a Fisher test for variance to examine whether the variance is significantly different from one and (iii) a Shapiro-Wilks test to test whether the distribution is significant different from a normal distribution (Brendel *et al.*, 2010). The npde can also be interpreted graphically by plotting it against any independent variables. If the assumption above is true, no trend should be observed on these scatter plots.

2.3 OPTIMAL DESIGN FOR POPULATION PHARMACOKINETIC STUDIES

2.3.1 Concepts of the optimal design methods

Optimal study design refers to the selection of design variables that are expected to contain the most information. The ultimate aim of optimal design for population PK studies is to maximise parameter estimate precision (obtain the lowest standard errors and coefficients of variation) while minimising the amount of information required. Optimal design has been studied since Smith (1918) proposed a criterion to obtain optimal designs for polynomial regression models. Now known as ‘G-optimality’ (following Kiefer & Wolfowitz 1959), this criterion minimises the maximum variance of parameters of interest over the design space. Wald (1943) introduced another optimality criterion putting the emphasis on the quality of the parameter estimates, termed ‘D-optimality’ by Kiefer and Wolfowitz (1959), a development subsequently extended by Box and Lucas (1959) to nonlinear regression models.

In this paper, locally D-optimal designs for several chemical kinetic models, including first-order decay and two consecutive first-order reactions, are investigated. For nonlinear models, the specific term ‘locally D-optimal design’ is typically used, since the dependence of such designs will depend on the initial

parameter estimates, which are often obtained from previous studies or by expert guesses. Basing D-optimal design on initial parameter estimates has been justified on the basis that '*in practical problems it will almost invariably be the case that some such information is available, and this will then provide the basis of a first design*' (Box & Lucus 1959: 79).

D'Argenio (1981) was the first to apply the theory of optimal design to a PK study. This led to development of the ADAPT program (D'Argenio & Schumitzky, 1979; D'Argenio *et al*., 2009), which has been used in the optimal design of PK studies in the area of drug development. However, this approach only focused on the optimisation of sampling time schedules and for single subject PK studies.

In 1997, Mentré *et al*. extended the work to population PK studies by proposing an approach to the optimal design of nonlinear regression models that also incorporated random effects. This approach involved first linearising the nonlinear model by using an FO approximation of the model about the mean, and then formulating the Fisher information matrix for linear models and normal distributions. Employing this approach, Mentré and colleagues were able to demonstrate the usefulness of optimal design in a toxicokinetic study of a new compound, using sparse sampling data (six samples taken from 24 rodents) fitted using a one-compartment open model with intravenous infusion input (Mentré *et al*., 1997). The results showed that the optimal (time schedule) design for two samples was 0.5 and 24 hours and for three samples 0.5, 1 and 24 hours, thereby indicating that samples should be taken as early and as late as possible after administration. These results were consistent with an earlier simulation study conducted by Al-Banna *et al*. (1990), which had also found that samples should be taken at the minimum and maximum possible times for a two-sample design. For a three-sample design, a third sample taken anywhere between the extremes led to better estimates of the random effect parameters.

There are two general approaches to developing the optimal design for population PK studies: simulation-based and Fisher information matrix-based (Tod *et al.*, 1998). The former involves the use of simulation techniques to generate concentration-time data, which are subsequently used to estimate population parameters that can be compared with the true values. With this approach, a number of designs are tested and the optimal design is selected based on the precision and bias of the parameter estimates. This approach is time-consuming and suffers also from the drawback that it is difficult to draw general conclusions for the optimal design. The second approach involves the use of statistical and mathematical methods to calculate the Fisher information matrix (FIM). The interesting aspect of this approach is that, from Cramér-Rao inequality, the inverse of the FIM is a lower bound of the covariance matrix of any unbiased estimator of the parameters. The concept of this FIM provides an opportunity to define optimality criteria in order to design optimal population experiments. The FIM-based approach also has an advantage over the simulation-based approach in that it is faster and enables the establishment of general conclusions about optimal designs.

2.3.2 Fisher information matrix

The FIM is a measure of the information contained in the data relative to a particular parameter. It can be calculated by differentiating the negative likelihood twice with respect to the model parameters, as shown in equation 2.43:

$$\mathrm{FIM}(q,\Theta) = -E\left[\frac{\partial^2}{\partial\Theta^2}\log L\right] \tag{2.43}$$

where q are the design variables, Θ represents all population parameters, E is the expectation of score function and L the maximum likelihood estimate.

Equation 2.43 can be expressed in matrix form as follows:

$$\mathrm{FIM}(q,\Theta) = -\begin{bmatrix} E\left[\frac{\delta^2 \log L}{\delta\theta_1^2}\right] & \cdot & \cdot & \cdot & E\left[\frac{\delta^2 \log L}{\delta\theta_1\delta\theta_n}\right] \\ \cdot & \cdot & & & \cdot \\ \cdot & & \cdot & & \cdot \\ \cdot & & & \cdot & \cdot \\ E\left[\frac{\delta^2 \log L}{\delta\theta_n\delta\theta_1}\right] & \cdot & \cdot & \cdot & E\left[\frac{\delta^2 \log L}{\delta\theta_n^2}\right] \end{bmatrix} \quad (2.44)$$

where θ are the model parameters and *n* the number of parameters in the model.

The covariance matrix $Cov(\hat{\Theta})$ in a future study can be calculated by inverting the FIM, shown as equation 2.45, thus:

$$\mathrm{FIM}(q,\Theta)^{-1} \leq Cov(\hat{\Theta}) \quad (2.45)$$

2.3.3 Optimality criteria

The requirements for extracting specific information from study designs are determined by optimality criteria. There are a vast number of optimality criteria, including A, C, D, E and G optimality. The most commonly used of these, D-optimality is used for the population PK study design in this thesis. D-optimality minimises the variability of parameter estimates by minimising the volume of the confidence ellipsoid region of the parameters, thereby maximising the determinant of the information matrix (or, minimising the determinant of the variance-covariance matrix).

2.3.4 PopDes program

There are currently several programs available for designing population PK studies. All programs use the same mathematical derivation of the FIM, but they vary in

terms of their specific features, for example in the algorithm implemented and the function used to calculate sampling windows (Mentré, 2007). In this thesis, both the evaluation and the optimisation of study design were performed with the PopDes program, Version 4.0 (Gueorguieva *et al.*, 2007) and MATLAB Version 7.13 (R2011b) (The MathWorks Inc., Natick, MA, 2011). PopDes is a program for optimal design of uniresponse and multiresponse, individual and population PK and PD experiments. This program has been developed using the FIM-based approach, assuming that a model has been selected at the design stage and the same model will be used to analyse upcoming data (Ogungbenro *et al.*, 2011). PopDes uses D-optimality to minimise the volume of FIM.

2.3.4.1 Design options

The PopDes program has two different functions: PopDes Windows and PopDes script. 'PopDes Windows' is the standard function with a Windows interface. Users need only choose different options from the interface for design evaluation and optimisation. Commonly used PK models can be selected from a list within the model library. 'PopDes script' is a script version of PopDes Windows written in MATLAB. The script version is useful for complex models and study designs. Both functions of the PopDes program were used in this study. Available design options in PopDes are summarised in Table 2.1.

2.3.4.2 Optimisation algorithms

Four algorithms are implemented in PopDes: Simplex, Hybrid, Exchange and First-order algorithm. The Simplex algorithm is very robust and remains the most commonly used for optimising nonlinear models; the main drawback of this algorithm is sensitivity to initial design points, which leads to difficulties in knowing whether it has reached a global minimum. The Hybrid algorithm is a combination of simulated annealing and Simplex algorithms; this algorithm has an advantage over other methods as it can escape local minima through selective uphill moves (Ogungbenro *et al.*, 2011). Simulated annealing first screens the parameter space by moving with large step lengths without getting trapped in local minima, and then decreases the step length for the algorithm to focus only on the most promising area.

Table 2.1 Design options available in the PopDes program

Design options	Description
Individual	Study of a single subject
Population	Study of a group of subjects (population pharmacokinetics)
Uniresponse	Samples collected from only one response in the experiment e.g. drug concentration (PK response)
Multiresponse	Samples collected from more than one response in the experiment e.g. drug and metabolite concentrations or PK and PD responses
Local	Only point estimates of the parameters used during optimisation
Bayesian[a]	Uncertainties of the parameters taken into account during optimisation
Exact	Only optimises sampling times
Continuous	Design variables to be optimised are both sampling times and design structure, which includes number of elementary designs[b], number of subjects per elementary design and number of samples per elementary design
List	Optimal sampling times chosen only from list of admissible times
Interval	Optimal sampling times chosen anywhere between specified lower and upper boundaries (e.g. 0 to 12 hours after dose)

[a] Available for use only with individual uniresponse study.
[b] Groups of subjects with the same number of samples and sampling times.

The modified Fedorov Exchange algorithm (the 'Exchange algorithm' hereafter) was adapted to optimise exact D-optimal designs with respect to the independent variables, i.e. sampling times (Ogungbenro *et al.*, 2005). At each iteration, one of the sampling times is substituted from a list of admissible time points specified as a grid size (e.g. a grid size of 0.25 refers to 15 minutes); this generates a new vector of sampling time points that increase the determinant of the FIM and consequently determine the optimal design. During the optimisation, one of the design points is exchanged with another and the ratio of the determinant of the FIM (the new design compared to the previous design) then computed. The optimal design is selected if

the ratio falls below a tolerance level. Finally, the First-order algorithm has two functions: a forward and backward step. At each forward step, the sensitivity function (used to define the design points containing the most information) is maximised over the design space in order to obtain a new support point, which is the best among candidate support points. In the backward step, the worst support point is removed by minimising the sensitivity function over the design space (Ogungbenro *et al.*, 2011).

2.4 WHOLE BODY PHYSIOLOGICALLY BASED PHARMACOKINETIC MODELS

In contrast to the conventional (e.g. one- or two-compartment) PK models, which are derived from experimental data, physiologically based pharmacokinetic (PBPK) models are based on the anatomical and physiological structure of the studied species. It was three quarters of a century ago that Teorell (1937) first described drug kinetics with mass balance equations using organ volume and organ blood flow. Since that time, PBPK models have become increasingly popular, mainly in the fields of environmental toxicology and risk assessment (Rowland *et al.*, 2011; Thompson *et al.*, 2008). The past decade, however, has seen an extension of PBPK modelling in the pharmaceutical area. This is due to the major advantage that PBPK models offer, with the rich information they include, including physiological parameters (e.g. organ volumes and organ blood flows) and drug specific parameters (e.g. lipophilicity) allowing them to describe and/or predict the pharmacokinetics of drugs, as well as investigate the influence of physiological change on drug kinetics.

PBPK models can be divided into three types, according to their structures (Nestorov, 2003). The most common models are the whole body PBPK (WBPBPK) models, in which, as the name suggests, the entire body is used to create the model. The second type is partial PBPK models, which focus only on isolated body systems (e.g. the gastrointestinal tract). Lastly there are the liver or metabolism models, which describe the hepatic elimination of drugs using physiological and biochemical parameters (Houston & Carlile, 1997). In this thesis, only the first of these, WBPBPK models, are used.

2.4.1 Model development

2.4.1.1 Model structure

Physiological models separate the body into several compartments based on a realistic anatomical structure interconnected by the blood circulation system (Nestorov, 2007) (Figure 2.6). In the first step of model development, it is necessary to make a decision regarding the choice of organs and tissues to be included. Although there is no universal rule for this, the organs and tissues selected should be sufficient for a description of the PK and PD characteristics of the drug being investigated and relevant disease progression, as well as the various potential scenarios of drug usage and administration. Conversely, the complexity of the model should be limited, for practical reasons, such as to limit the quantity of data employed, complexity of mathematical description and computational time involved (Nestorov, 2003). Typically, WBPBPK models use two groups of organs/tissues, referred to as ‘core’ and ‘non-core’ tissues. Core tissues include blood (venous and arterial), sites of major drug elimination (liver, kidney and sometimes intestines and lungs), sites of drug administration (e.g. skin for subcutaneous administration), and potential sites of drug action and/or toxicities (e.g. tumour compartment), along with any other tissues that significantly affect the PK of a drug. The rest of the body is represented as non-core tissue, which is used to maintain the mass balance in the system. Non-core tissues may be further divided, into ‘rapidly equilibrating’ and ‘slowly equilibrating’. Lumping should be performed only with kinetically similar tissues (Nestorov *et al.*, 1998a).

Figure 2.6 General structure of a whole body physiologically based pharmacokinetics (WBPBPK)

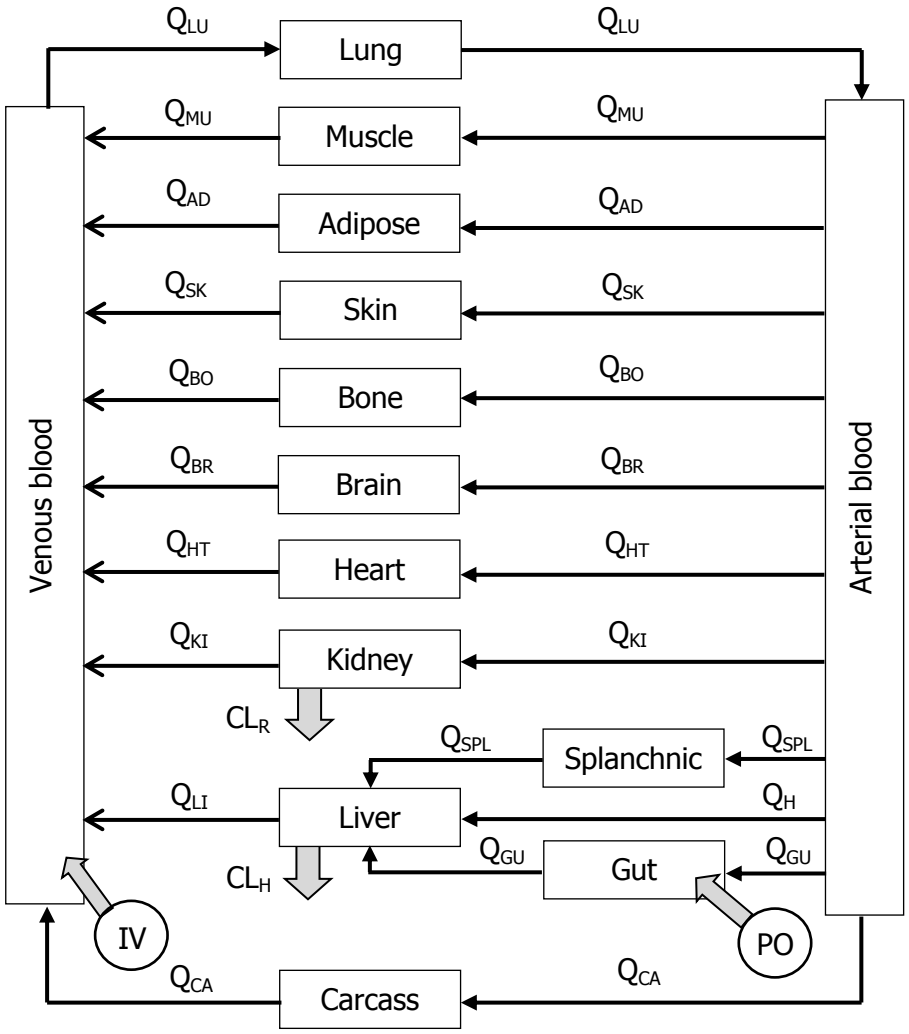

Key: IV = intravenous administration, PO = oral administration, CL_R = renal clearance, CL_H = hepatic clearance, Q = blood flow, LU = lungs, MU = muscle, AD = adipose tissue, SK = skin, BO = bone, BR= brain, HT = heart, KI = kidney, LI = liver, SPL = spleen, H=hepatic, GU = gut and CA= carcass.

2.4.1.2 Tissue model structure

The kinetics of a drug in each particular organ and tissue can be described by tissue models. The general information required for such tissue models include tissue volume, vascular perfusion, drug permeability, binding properties and the drug partition coefficient, and elimination processes. The simplest model is a single well-stirred compartment (perfusion rate-limited) model, in which the drug is freely and

instantly distributed across the membranes without diffusion barriers. This type of model is often applied to small neutral compounds. If diffusion barriers, such as capillary membrane and cellular membrane, are presumed, more complex, permeability rate-limited tissue models (two or more compartments) should be used. Dispersion tissue models are required in cases where diffusion barriers cannot be identified but concentration gradients are known to exist (Nestorov, 2007). More complex tissue models consisting up to six compartments, including red blood cells and vascular, intercellular and cellular spaces, as well as the bound and unbound drugs, have been proposed (Kawai *et al.*, 1998; Tanaka *et al.*, 1999). These models require a large amount of information, which is often difficult to collect.

2.4.1.3 Model equations

The amounts of a drug in different organs are calculated on the basis of the law of mass action, using the mass balance equations. Four different types of mathematical equations for the tissues within PBPK models have been used thus far: algebraic, nonlinear differential, partial differential and linear ordinary differential equations (Nestorov, 2003). Algebraic equations are used when the processes are assumed to equilibrate instantly, such as the PBPK models for inhalation studies; nonlinear differential equations are used to represent nonlinear processes, such as Michaelis-Menten metabolism; partial equations are generally used with dispersion models; and linear ordinary differential equations (LODE) are the mathematical equations most commonly employed to describe the PK processes in WBPBPK models under the well-stirred hypothesis and assumption of linearity. LODE is used in this thesis. The change of drug concentrations in each organ is dependent on the variations in organ volume and organ blood flow, as well as drug elimination (equations 2.46-2.48).

Equation for non-eliminating organs:

$$V_i \cdot \frac{dC_i}{dt} = Q_i \cdot (C_{in} - C_{out}) \qquad (2.46)$$

Equation 2.46 can also be reparameterised as follows:

$$V_i \cdot \frac{dC_i}{dt} = Q_i \cdot (C_{in} - \frac{C_i \cdot R}{fu \cdot Kpu_i}) \quad (2.47)$$

Equation for eliminating organs:

$$V_i \cdot \frac{dC_i}{dt} = Q_i \cdot (C_{in} - \frac{C_i \cdot R}{fu \cdot Kpu_i}) - \frac{C_i \cdot CL_{int,i}}{Kpu_i} \quad (2.48)$$

where

V_i: volume of the organ *i*

Q_i: blood flow to organ *i*

C_i: concentration of the drug in organ *i*

C_{in}: concentration of drug entering the tissue

C_{out}: concentration of drug leaving tissue

R: blood-to-plasma ratio

fu: fraction unbound in plasma

$CL_{int,i}$: intrinsic clearance of organ *i*

Kpu_i: partition coefficient between unbound plasma and organ *i*

2.4.1.4 Model parameters

WBPBPK models have two types of parameters: physiological (organ volume and organ blood flow) and drug-specific (Nestorov, 2007). Collected from various sources, the physiological parameters are assumed to be independent of the study compound. Although there is no official validated reference for these as yet, the most commonly used reference values for healthy populations are those compiled by the International Commission on Radiological Protection (ICRP) in 2003. However, if special populations, such as the obese, infants, elderly and pregnant, are studied, it is essential to take into account any physiological characteristics that may differ from normal. The pharmacological effects of the compound and influence of environmental factors on the physiological parameters should also be considered.

Results from sensitivity analyses have shown that cardiac output and blood flow are the most important parameters for the PBPK model (Nestorov, 1999).

In WBPBPK models specifically, it is very important to have a physiological constraint; that is, all tissue blood flows should sum up to cardiac output and all tissue weights should sum up to body weight. The correlation between physiological parameters should also be included, in order to avoid the generation of physiologically unlikely individuals when doing simulations (e.g. very small heart with excessively high cardiac output). In many cases in which the physiological parameters are not available, allometric equations can be used. There are several excellent review articles of such equations, including Brown *et al.* (1997), Fiserova-Bergerova (1995), Lindstedt and Schaeffer (2002) and Espié *et al.* (2009).

Some drug-specific parameters are available in the literature but these generally still need to be estimated. The best way to obtain these parameters is by estimating from concentration-time data obtained from blood and various tissues (*in vivo* experiments). Some parameters, such as partition coefficients, can be predicted with *in silico* methods, using the physiochemical properties of drugs and tissue composition data of each organ (Poulin *et al.*, 2001; Poulin & Theil, 2000; Poulin & Theil, 2002; Rodgers *et al.*, 2005; Rodgers & Rowland, 2006). *in vitro* experiments are also a good source for this information, for example, those conducted by Ballard *et al.* (2000), Ito and Houston (2005), Johnson *et al.* (2006), Kato *et al.* (2003), and Shibata *et al.* (2002).

2.4.2 Modelling methodology

In general, WBPBPK models are used in two complementary modes: parameter estimation and simulation. For parameter estimation, the equations specified in the model are fitted numerically to the concentration-time data obtained from the experiment, minimising or maximising an objective function. Most frequently, least squares or maximum likelihood optimisation is used (Nestorov, 2003). There are two main approaches for parameter estimation in WBPBPK models: open loop and closed loop. Open loop estimations may result in bias but it has been suggested that

these can be used to generate initial parameter estimates for closed loop estimation (Nestorov, 2007). Otherwise, closed loop estimations tend to present numerical problems due to the large number of parameters fitted simultaneously to the observed data, although the results are less biased (Gueorguieva *et al.*, 2004).

The WBPBPK model equations need to be written with a particular computer software application. Many of these, such as acslX, MATLAB (which graphically interfaces with Simulink), STELLA, ModelMaker and MATHEMATICA, originally come from engineering and mathematics. While they have great flexibility, they also require advanced modelling and programming skills. Software has been developed for general PK modelling, like NONMEM, ADAPT 5 and SAAM II, which offers simplified equation coding but still requires advanced modelling knowledge. There are also tools designed specifically for PBPK modelling and simulation. These usually have a graphical user interface and built-in library for the PBPK model components, which allow the user to more easily create PBPK model structures. Some examples of this type of software are PK-Sim, Simcyp and Gastroplus. An additional, new software, BioDMET, has recently been developed for more complex models (Graf *et al.*, 2012). In addition to drug circulation through organs and tissues at the macroscopic level, this also includes models for biological transport mechanisms and biotransformations within cells and organelles at the molecular scale. The interesting feature of BioDMET is that simulated concentration-time biomarker and imaging agent data can be inputted into an image simulator to generate the expected *in vivo* clinical images.

2.4.3 Model applications

Since WBPBPK models contain large amounts of information, their applications are traditionally for extrapolation proposes. Perhaps the most commonly used is interspecies extrapolation, because the WBPBPK model employs a structure common to all mammalian species (Nestorov, 2007). WBPBPK models can also be applied to predict drug exposure in organs that are inaccessible in practice, such as the brain (Xu *et al.*, 2003) and some tumours (Liu *et al.*, 2005). Other possible uses of WBPBPK models are inter-route (Chiu & White, 2006), inter-drug (Blakey *et al.*,

1997; Nestorov *et al.*, 1998b) and inter-dose extrapolation (Simmons *et al.*, 2005). WBPBPK models have not only been applied to normal subjects, but also to special populations for which little or no relevant information is available, such as patients with altered physiology or in paediatrics.

Edginton and Willmann (2008) developed WBPBPK models for patients with liver cirrhosis by incorporating physiological differences between healthy individuals and patients (e.g. change in hepatic blood flow, reduction in liver function, etc.). The modified models were used to generate concentration-time profiles for four drugs (alfentanil, lidocaine, theophylline and levetiracetam). Comparing the results with the literature data, these researchers found the model to give a reasonable fit, thereby indicating the ability of WBPBPK models to successfully account for altered physiology. WBPBPK models have also been developed to predict drug PK in children (Björkman, 2005; Edginton *et al.*, 2006a; Kersting *et al.*, 2012). In these studies, WBPKPB models were modified for age-related physiological changes such as body weight, organ weights and blood flows, as well as clearance and enzyme ontogeny. The results of these studies showed predicted concentrations to be consistent with the observed values. The effects of ageing, gender difference (Clewell *et al.*, 2004; Yang *et al.*, 2006), pregnancy (Gaohua *et al.*, 2012) and therapeutic interventions (Lagneau *et al.*, 2005) have also been investigated using physiological models.

CHAPTER 3

POPULATION PHARMACOKINETIC ANALYSIS OF CIPROFLOXACIN IN MALNOURISHED CHILDREN

3.1 INTRODUCTION

Malnourished children suffer from numerous associated complications, particularly invasive bacterial infections (Babirekere-Iriso *et al*., 2006; Maitland *et al*., 2006). Therefore, empirical treatment with effective antimicrobials should be given to all children admitted to the hospital with severe malnutrition. The World Health Organization (WHO) recommends treatment with parenteral ampicillin and gentamicin for children who have complications, such as dehydration and shock (WHO, 1999). However, despite adherence to these guidelines, the mortality rate has remained high.

Ciprofloxacin, a fluoroquinolone antibiotic, has been considered as an alternative agent because it is effective against most Gram-negative organisms and has activity against some Gram-positive organisms. Additionally, ciprofloxacin has a high oral bioavailability. However, to date, there is limited information on pharmacokinetics (PK) of oral ciprofloxacin in paediatric patients and none in malnourished children.

This aims of the work in this chapter were:

(i) to estimate population pharmacokinetic parameters of ciprofloxacin following oral administration to paediatric patients with severe malnutrition.
(ii) to identify the influence of clinical and demographic data on these parameters.

3.2 METHODS

3.2.1 Clinical setting

The clinical study was conducted in the Kilifi District Hospital, Kenya by staff from the KEMRI-Wellcome Collaboration Programme, the KEMRI/Wellcome Trust Research Programme and School of Pharmacy, University of Nairobi. Ethical approval for the study was granted by KEMRI/National Ethical Review Committee.

Patients were eligible for inclusion in the study if they met all of the following criteria:

- Age more than 6 months
- Signed informed consent from parent or guardian
- Severe malnutrition as defined by a weight-for-height Z score (WHZ) < -3 or bilateral oedema (kwashiorkor) or mid-upper arm circumference (MUAC) < 11 cm. (if length > 65 cm) (Cogill, 2003; WHO, 1999)
- Able to receive oral treatment

Exclusion criteria were as follows:

- Plasma creatinine concentration > 300 µmol/L and evidence of intrinsic renal disease (hypertension or hyperkalaemia)
- Coexisting chronic bone or joint disease
- Concurrent use of antacids, ketoconazole, theophylline or corticosteroids
- Enrolment in another interventional study

All patients received standard care according to the WHO guidelines for management of severe malnutrition (WHO, 1999) Severe dehydration, shock, hypothermia and hypoglycaemia were initially corrected; empirical antimicrobial therapy with parenteral ampicillin (50 mg/kg every 6 hours) and intramuscular gentamicin (7.5 mg/kg once daily) was given to all children for 7 days. All patients received multi-vitamin, multi-mineral supplement, antihelminths, haematinics and nutrition therapy with special milk-based formula (F-75 and F-100). Malnutrition oral rehydration solution (RESOMAL) was given to children with significant diarrhoea (more than 3 watery stools/day). If children had clinically indicated of infection in cerebrospinal fluid, urine culture or chest X-ray, sampled were also obtained.

3.2.2 Study protocol

Patients were recruited during two study periods. Children who were recruited during the first period received ciprofloxacin 2 hours before or after they had nutritional milks; those during the second period received ciprofloxacin during

nutritional feeding. All patients received an oral ciprofloxacin dose of 10 mg/kg body weight every 12 hours for 48 hours. Individual doses were calculated for each patient then prepared by the pharmacist by grinding ciprofloxacin tablets and suspending the appropriate dose in water. The trial nurse was present and observed this procedure.

The first period included 36 children. The sample size was based upon a previous population pharmacokinetic study of ciprofloxacin in patients with acute infection (Payen *et al.*, 2003) and a previous population pharmacokinetic study from a similar patient population (Seaton *et al*., 2007). An equal number of patients was assigned into one of three categories: low risk; intermediate risk and high risk of mortality. These categories were defined according to the criteria described by Maitland *et al*. (2006). The high risk group included children with any one of the following: depressed conscious state, bradycardia (heart rate <80 beats per minute), hypoglycaemia (blood glucose < 3 mmol/L) or evidence of shock (capillary refill time ≥2 seconds or temperature gradient or weak pulse). Children were categorised to the intermediate risk category if they had deep acidotic breathing, signs of severe dehydration (>3 watery motions/24 hours) plus diarrhoea, lethargy, hyponatraemia (sodium <125 mmol/L) or hypokalaemia (potassium <2.5 mmol/L). Children without any of these features were classified as low risk. The second period included 16 children who were not recruited according to mortality risk.

Each child was randomised to one of following three blood sampling groups using a closed card system. A maximum of 4 blood samples was taken from each patient over a 24 hour period.

- *Group 1*: Samples were obtained at 2, 4, 8, 24 hours (n = 17)
- *Group 2*: Samples were obtained at 3, 5, 9, 12 hours (n = 18)
- *Group 3*: Samples were obtained at 1, 3, 6, 10 hours (n = 17)

In two of the groups, samples were only withdrawn after the first dose but a single trough sample was withdrawn after the second dose in patients who were assigned to group 1. Children in each of the mortality risk categories were allocated across the sampling schedules.

3.2.3 Drug analysis

Ciprofloxacin plasma concentrations were measured by using high performance liquid chromatography (HPLC) with fluorescence detection (Muchohi *et al*., 2011). Briefly, 200 ng of internal standard solution (sarafloxacin) was added to 200 µL of plasma, mixed with 2mL acetonitrile then centrifuged at 4000 rpm for 10 minutes at 4 ^{o}C. The upper organic layer was evaporated under nitrogen gas. The residue was reconstituted in 100 µL mobile phase (aqueous orthophosphoric acid (0.025 M)–methanol–acetonitrile (75:13:12%; v/v/v) adjusted to pH 3.0 with triethylamine). Then, 50 µL was injected onto a *Synergi*® *Max-RP* analytical column (150 mm x 4.6 mm i.d., 4 µm particle size), maintained at 40^{o}C. Calibration curves of ciprofloxacin were linear over the concentration range of 0.02–4 µg/ml. Intra- and inter-assay relative standard deviations were below 8.0%. The limits of detection and quantification were 10 ng/mL and 20 ng/mL, respectively.

3.2.4 Data preparation

A wide range of data were collected for each patient during the study and was collated into a Microsoft Excel® spreadsheet. These included demographic data, drug dose, times of administration and blood sampling times. Vital signs, including respiratory rate, pulse rate, blood pressure and body temperature were recorded. Clinical laboratory tests, including full blood count, electrolytes, blood gases, plasma glucose, plasma creatinine, blood culture, HIV antibody test and blood film for malaria parasites, were collected. The nutritional status was evaluated by measuring mid-upper arm circumference (MUAC) and calculating Z-score for weight-for-height (WHZ). A Z-score describes the deviation of weight and height from the median well-nourished population for specific age and gender. Epi Info software Version 3.5.1 was used to compute the Z-score using the CDC/WHO growth curve as a reference (Dibley *et al*., 1987). The presence of HIV infection, severe dehydration, shock and oedema was also recorded.

To identify any anomalous values in the dataset that could represent data entry errors, each clinical factor was plotted against patient identification number. Ciprofloxacin concentration-time profiles were plotted to check for errors in

concentration. The following additional clinical factors were calculated from demographic and clinical information: creatinine clearance (CLcr); ideal body weight (IBW); body mass index (BMI); lean body weight (LBM) and body surface area (BSA). The equations used for these calculations were as follows:

1) Creatinine clearance (CLcr)

$$\text{CLcr (mL/min/1.73 m}^2\text{)} = \frac{\text{k} \times \text{length (cm)}}{\text{Scr (mg/dL)}} \tag{3.1}$$

where k is defined by age group: infants (1 to 52 weeks old) = 0.45 (Schwartz *et al*., 1984); children (1 to 13 years old) = 0.55 (Schwartz *et al*., 1976); adolescent males (13 to 18 years old) = 0.7 (Schwartz & Gauthier, 1985); and adolescent females (13 to 18 years old) = 0.55 (Schwartz *et al*., 1976). Scr = serum creatinine (mg/L).

2) Ideal body weight (IBW) (Duggan *et al*., 2008)

$$\text{IBW (kg)} = \frac{\text{height (cm)}^2 \times 1.65}{1000} \tag{3.2}$$

3) Body mass index (BMI) (Green & Duffull, 2004)

$$\text{BMI (kg/m}^2\text{)} = \frac{\text{weight (kg)}}{\text{height}^2\text{ (m)}} \tag{3.3}$$

4) Lean body mass index (LBM) (Green & Duffull, 2004)

$$\text{Male LBW} = (1.1 \times \text{weight (kg)}) - 1.28\left[\frac{\text{weight (kg)}}{\text{height (cm)}}\right]^2 \tag{3.4}$$

$$\text{Female LBW} = (1.07 \times \text{weight (kg)}) - 1.48\left[\frac{\text{weight (kg)}}{\text{height (cm)}}\right]^2 \quad (3.5)$$

5) Body surface area (BSA) (Mosteller, 1987)

$$\text{BSA (m}^2\text{)} = \sqrt{\frac{\text{height (cm)} \times \text{weight (kg)}}{3600}} \quad (3.6)$$

3.2.5 Population model development

3.2.5.1 Structural and statistical model development

Population pharmacokinetic modelling was performed with NONMEM Version VI (Beal *et al*., 1989-2006), running under a Windows XP operating system with a G77 Fortran compiler. NONMEM outputs were processed with Xpose Version 4.0 (Jonsson & Karlsson, 1999) which is implemented in R software Version 2.9.2. All models were fitted using the first-order conditional estimation with interaction (FOCE-I) algorithm. Both one- and two-compartment elimination models were fitted to the concentration-time data. Absorption was described using first-order and zero-order models with and without a lag time (ALAG). The pharmacokinetic models, subroutines and pharmacokinetic parameters are shown in Table 3.1.

In addition, absorption was modelled using a transit compartment model proposed by Savic *et al*. (2007). This model describes the absorption process as a multiple-step occurring as the drug travels through a series of hypothetical transit compartments (*n*) with a single transfer rate constant (k_{tr}). Drug is transferred from the last transit compartment to the central compartment via an absorption compartment, from which drug is absorbed with the first-order rate constant (ka). The transit compartment model is shown schematically in Figure 3.1.

Table 3.1 Pharmacokinetic models, subroutines and pharmacokinetic parameters used to fit ciprofloxacin concentration-time data

Pharmacokinetic models	Subroutines	Pharmacokinetic parameters
One-compartment with zero-order absorption	ADVAN1 and TRAN2	D_1, CL/F, V/F
One-compartment with first-order absorption	ADVAN2 and TRAN2	KA, CL/F, V/F
Two-compartment with zero-order absorption	ADVAN3 and TRAN4	D_1, CL/F, Q/F, V1/F, V2/F
Two-compartment with first-order absorption	ADVAN4 and TRAN4	KA, CL/F, Q/F, V2/F*, V3/F*

Key: D_1 = duration of input, CL/F = clearance/bioavailability, V/F = volume of distribution/ bioavailability, KA = absorption rate constant, V1/F = volume of the central compartment/bioavailability, V2/F = volume of the peripheral compartment/bioavailability, Q/F = intercompartment clearance/bioavailability, V2/F* = volume of the central compartment/bioavailability and V3/F* = volume of the peripheral compartment/ bioavailability.

Figure 3.1 Schematic view of drug flow via a number of transit compartments

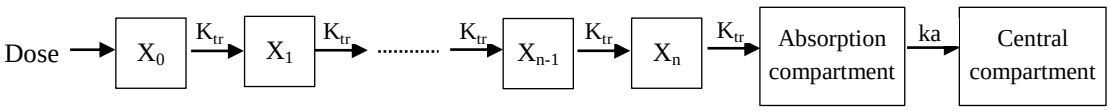

The rate of change of drug amount in the absorption compartment (dX_a/dt) is derived by equation 3.7:

$$\frac{dX_a}{dt} = Dose \cdot F \cdot k_{tr} \cdot \frac{(k_{tr} \cdot t)^n \cdot e^{-k_{tr} \cdot t}}{n!} - ka \cdot X_a \qquad (3.7)$$

where Dose is amount of drug administered, F is bioavailability, k_{tr} is a transit rate constant from *n*th-1 compartment to the *n* compartment, t is time after dose, ka is the first-order absorption rate constant, *n* is the number of transit compartments and *n*! is

the *n* factorial function which is computed by the approximation of Stirling as shown in equation 3.8:

$$n! \approx \sqrt{2\pi} \cdot n^{n+0.5} \cdot e^{-n} \qquad (3.8)$$

To prevent numerical difficulties when *n* is large, the transformation shown in equation 3.9 was used.

$$\frac{dX_a}{dt} = e^{\ln(Dose \cdot F \cdot k_{tr} \cdot \frac{(k_{tr} \cdot t)^n \cdot e^{-k_{tr} \times t}}{\sqrt{2\pi} \cdot n^{n+0.5} \cdot e^{-n}})} - ka \cdot X_a \qquad (3.9)$$

The mean transit time (MTT) represents the average time spent by drug travelling from the first transit compartment to the absorption compartment. The relationship between MTT, *n* and k_{tr} is shown in equation 3.10:

$$k_{tr} = \frac{(n+1)}{MTT} \qquad (3.10)$$

During the analysis, two parameters were estimated while the third parameter was derived by equation 3.10. In this study, *n* and MTT were estimated and were used to calculate k_{tr}. An example of a data file and a control file is given in Figure 3.2 and 3.3, respectively.

The pharmacokinetic parameters were assumed to be log-normally distributed and between subject variability (BSV) was therefore modelled as follows:

CL/F = TVCL x EXP $^{\eta 1}$
V/F = TVV x EXP $^{\eta 2}$
KA = TVKA x EXP $^{\eta 3}$
ALAG1 = θ_4 x EXP $^{\eta 4}$

where η_i are the individual differences between CL/F and TVCL, which are assumed to be normally distributed with a mean of 0 and variance ω^2. NONMEM estimates ω^2. Individual estimates of η are determined at each iteration if the FOCE algorithm is used, are available in the output table file and can be used to determine individual estimates of the parameters (i.e. CL/F, V/F, etc. for each subject). Initial analyses were conducted assuming no covariance between estimates of BSV but as the model was developed, covariances were evaluated using a block covariance matrix.

Three models were applied to describe the residual error in concentration - additive, proportional and combination (additive plus proportional). These models were coded in control files as follows:

1) Additive error model

```
IPRED=F
W=1
Y=F+W*ERR(1)
```

where IPRED and F are the individual predicted concentration, W is a scale factor, Y is the individual observed concentration and ERR is the within subject variability.

2) Proportional error model

```
IPRED=F
W=THETA(5)*F
Y=F+ERR(1)*W
```

3) Combined error model

```
IPRED=F
W=SQRT(THETA(5)**2+THETA(6)**2*F**2)
Y=F+W*ERR(1)
```

Figure 3.2 Excerpt from the data file of the transit compartment model

ID	TIME	AMT	LDV	CMT	MDV	EVID	TYPE	WT
1	0	.	.	2	1	2	2	5.02
1	0	50	.	1	1	1	1	5.02
1	1.07	0	0.698135	2	0	0	1	5.02
1	2.93	0	0.963174	2	0	0	1	5.02
1	6.07	0	0.165514	2	0	0	1	5.02
1	9.9	0	-0.77653	2	0	0	1	5.02
2	0	.	.	2	1	2	2	5.8
2	0	58	.	1	1	1	1	5.8
2	3	0	0.524729	2	0	0	1	5.8
2	5.25	0	0.04879	2	0	0	1	5.8
2	9.08	0	-0.47804	2	0	0	1	5.8
2	12.08	.	.	2	1	2	2	5.8
2	12.08	58	.	1	1	1	1	5.8
2	12.17	0	-0.91629	2	0	0	1	5.8
3	0	.	.	2	1	2	2	10.64
3	0	106	.	1	1	1	1	10.64
3	2	0	0.57098	2	0	0	1	10.64
3	4.08	0	0.385262	2	0	0	1	10.64
3	8.08	0	-0.31471	2	0	0	1	10.64
3	12	.	.	2	1	2	2	10.64
3	12	106	.	1	1	1	1	10.64
3	24.25	0	-0.37106	2	0	0	1	10.64
4	0	.	.	2	1	2	2	6.7
4	0	61	.	1	1	1	1	6.7
4	3.02	0	0.598837	2	0	0	1	6.7
4	5	0	0.173953	2	0	0	1	6.7
4	9	0	-0.54473	2	0	0	1	6.7
4	12	.	.	2	1	2	2	6.7
4	12	61	.	1	1	1	1	6.7
4	12.17	0	-1.13943	2	0	0	1	6.7

Key: ID = patient identification number, AMT = dose (mg), LDV = log-transformed dependent variable (DV), CMT = compartment data item (1 = dosed compartment, 2 = observed compartment), MDV = missing DV (0 = DV is not missing, 1 = DV is missing), EVID = event identification (0 = observation event, 1 = dose event, 2 = other-type event), TYPE = type of data item (1 = real data, 2 = dummy data which is used as a place-holder between real data. NONMEM will not use the data on these record) and WT = patient weight (kg).

Figure 3.3 Example of a control file for the transit compartment model

```
$PROB CIPRO TRANSIT CPT MODEL
$INPUT ID TIME AMT DV CMT MDV EVID TYPE WT
$DATA DATA2_LN_RS.CSV IGNORE=#
$SUBROUTINE ADVAN6 TOL=3 TRANS1
$MODEL COMP=ABS ;ABSORPTION COMPARTMENT (DEFDOSE)
       COMP=CEN ;CENTRAL COMPARTMENT (DEFOBS)
$PK
IF(AMT.GT.0) PODO=AMT
IF(AMT.GT.0) TDOS=TIME
TVCL=THETA(1)*(WT/70)**0.75
CL=TVCL*EXP(ETA(1))
TVV=THETA(2)*(WT/70)**1
V=TVV*EXP(ETA(2))
K=CL/V
S2=V
; absorption model
F1=0
TVKA=THETA(3)          ; absorption rate constant
KA=TVKA*EXP(ETA(3))
TVMTT=THETA(4)         ; mean transit time to the absorption cpt
MTT=TVMTT*EXP(ETA(4))
TVNN=THETA(5)          ; number of transit compartments
NN=TVNN*EXP(ETA(5))
KTR=(NN+1)/MTT         ; transit rate constant
NFAC=SQRT(2*3.1415)*NN**(NN+0.5)*(EXP(-NN))*(1+1/(12*NN))
; Stirling approximation to n!
LNFAC =LOG(2.5066)+(NN+0.5)*LOG(NN)-NN
; logarithm transformation of Stirling approximation

$DES
DEL=1/100000           ; avoid log(0)
;IF(T.GE.TDOS)THEN
;DADT(1)=PODO*KTR*(KTR*(T-TDOS))**NN*EXP(-KTR*(T-TDOS))/NFAC-KA*A(1)
DADT(1)=EXP(LOG(PODO+DEL)+LOG(KTR)+NN*LOG(KTR*(T-TDOS)+DEL)-KTR*(T-
TDOS)-LNFAC)-KA*A(1)
;ELSE
```

```
;DADT(1)=PODO*KTR*(KTR*T)**NN*(EXP(-KTR*T))/NFAC-KA*A(1)
;ENDIF
;DADT(1)=-KA*A(1)
DADT(2)=KA*A(1)-K*A(2)

$ERROR
IPRD=A(2)/S2 +0.00001
IF(IPRD.LE.0) IPRD=0.0001
IPRED=LOG(IPRD)
W=SQRT(THETA(6)**2+THETA(7)**2/IPRD**2)
IRES=DV-IPRED
IWRES=IRES/W
Y=IPRED+W*EPS(1)

$THETA  (0,35) (0,350) (0,3) (0,1) (0,5) (0,0.5) (0,0.1)
$OMEGA 0.1 0.1 0.1 0.1 0.1
$SIGMA 1 FIX

$ESTIMATION MAX=9999 METHOD=1 INTERACTION SIG=3 PRINT=2 NOABORT
$COVAR
$TABLE ID TIME IPRD IPRED IWRES NOPRINT ONEHEADER FILE=SDTAB1
$TABLE ID TVCL TVV TVKA TVMTT TVNN CL V KA MTT NN KTR ETA(1) ETA(2)
ETA(3) ETA(4) ETA(5) NOPRINT ONEHEADER FILE=PATAB1
$TABLE ID TIME TVCL TVV TVKA TVMTT TVNN CL V KA MTT NN KTR ETA(1) ETA(2)
ETA(3) ETA(4) ETA(5) IPRD IPRED IRES IWRES WT NOPRINT ONEHEADER FILE=1.TAB
$SCAT OMIT
```

The objective function value (OFV) was used to aid selection of the structural model that best described the data. The reduction in the OFV indicates the improvement in the structural model. In addition, goodness of fit plots were used to select the best structural model. The goodness of fit was graphically assessed by plotting (i) population predicted concentrations (PRED) and individual predicted concentrations (IPRED) against observed concentrations, (ii) observed concentrations, PRED and IPRED versus time (individual plots) and (iii) conditional weighted residuals (CWRES) (Hooker *et al*., 2007) against population predictions, time and time after dosing.

The best residual error model was selected by plotting CWRES and IWRES versus predicted concentration. The distribution of CWRES was also observed.

3.2.5.2 Covariate model development

The base model was set up assuming an allometric relationship between the pharmacokinetic parameters and weight (Anderson & Holford, 2008; Holford, 1996; Peters, 1986). The typical estimates of CL/F (TVCL) and V/F (TVV) in the population were therefore modelled as:

$$\text{TVCL (L/h)} = \theta_1 \text{ (L/h/70 kg)} \times (\text{WT}/70)^{0.75}$$
$$\text{TVV (L)} = \theta_2 \text{ (L/70 kg)} \times (\text{WT}/70)^{1}$$

where θ_1 represents the standardised clearance estimate (L/h/70 kg) in an adult who weighs 70 kg and θ_2 is the standardised estimate of V (L/70 kg) in an adult who weighs 70 kg. For comparison within the patient population and for ease of dose evaluation, a simple linear model was also applied to the data, i.e.

$$\text{TVCL (L/h)} = \theta_1 \text{ (L/h/kg)} \times \text{WT (kg)}$$
$$\text{TVV (L)} = \theta_2 \text{ (L/kg)} \times \text{WT (kg)}$$

An allometric BSA approach was also investigated (Meibohm *et al*., 2005) and modelled as follows:

$$TVCL\ (L/h) = \theta_1\ (L/h/1.73\ m^2) \times (BSA/1.73)^{0.67}$$
$$TVV\ (L) = \theta_2\ (L/1.73\ m^2) \times (BSA/1.73)^{1}$$

Due to the large number of covariates available in the dataset, an initial screen was conducted by using matrix plots to identify covariates that were highly correlated with each other. Potentially useful covariates were then identified by plotting individual PK parameters against each covariate. Scatter plots with trend lines were produced for continuous variables and box plots for categorical variables. Generalised additive modelling (GAM), implemented in Xpose (Jonsson & Karlsson, 1999), was also used to identify possible covariate relationships.

Covariate models were then built by a forward stepwise procedure. Starting with the base model, each covariate was added individually to the model of CL/F or V/F. During this forward procedure, a reduction in the OFV of at least 3.84 (p<0.05, df=1) was considered to be statistically significant. The most significant covariate was included first and then other covariates were added to the model until there was no further reduction in OFV. In back elimination step, each covariate was removed from the full model unless OFV increased by more than 6.63 (p<0.01, df=1). In addition, the inclusion of each covariate in the model was judged according by goodness of fit plots, physiological plausibility, change in inter-subject variability and the precision of the parameter estimates.

However, these graphical diagnostics are affected by the presence of shrinkage. The parameter correlations and parameter-covariate relationships are affected by η-shrinkage. The power of IPRED and IWRES to diagnose structural and residual error model misspecification is reduced in the presence of ε-shrinkage. A level of 20-30% for both η- and ε-shrinkage is sufficiently high for misleading model interpretation (Savic & Karlsson, 2009; Karlsson & Savic, 2007). Perl-speaks-NONMEM (PsN)

Version 3.1.0 (Lindbom *et al*., 2005; Lindbom *et al*., 2004) was used to calculate the shrinkage. The following example is the command for shrinkage calculation:

execute run1.mod –shrinkage

The commands have the following meaning:

execute	call NONMEM to run one or multiple model files
run1.mod	name of model file
-shrinkage	calculate the shrinkage for the model run

3.3 RESULTS

3.3.1 Patient data

A total of 52 patients were recruited to the study of whom 36 received their first ciprofloxacin dose 2 hours before or after feeding and 16 patients received it during their feed. Demographic and clinical characteristics of the patient group are summarised in Table 3.2. The numbers of male and female patients were similar at 29 (56%) and 23 (44%). The median age of the patients was 23 months and most of the patients (41) were younger than 3 years of age; only 5 patients were more than 5 years old. Positive correlations were observed between age, body weight, height and BSA, between WHZ and MUAC and between sodium concentration, potassium concentration, serum bicarbonate and base excess (Figure 3.4A, 3.4B and 3.4C). Eight (15%) children had HIV infection. Nearly half of the patients (25) had a MUAC below 11 cm, WHZ was less than -3 in 27 patients and bilateral oedema (kwashiorkor) was present in 24 patients (46%). These measurements indicated that the all patients had severe malnutrition.

Table 3.2 Demographic data and clinical characteristics of the patients who received oral ciprofloxacin

Characteristics	Reference Range	Median	Range	*n*
Age (months)		23	8, 102	52
Weight (kg)		6.9	4.1, 14.5	52
Height (cm)		75.4	58.5, 114.4	50
BSA (m^2)		0.39	0.27, 0.62	50
WHZ	<-3	-3.26	-5.69, 0.04	50
MUAC (cm)	<11	11	7.7, 14.3	52
White blood cell count ($x10^6$/L)	6.0, 17.5	13.3	5.5, 84.4	51
Haemoglobin (g/dL)	9, 14	9.0	2.1, 12.8	51
Platelets ($x10^6$/L)	150, 400	309	16, 1369	51
Sodium (mmol/L)	138, 145	136	120, 160	51
Potassium (mmol/L)	3.5, 5	3.1	1.2, 5.1	51
Glucose (mmol/L)	2.8, 5	4.0	0.4, 11.4	47
Bicarbonate (mmol/L)	22, 29	15.4	4.7, 26.0	44
Base excess (mEq/L)	-2, +2	-8.0	-26.9, 2.1	44
Serum creatinine (µmol/L)	44, 88	44	27, 676	47
Creatinine clearance (mL/min/1.73m^2)		86	5, 129	45

Key: BSA = Body Surface Area, WHZ = weight-for-height Z-score, MUAC = mid-upper arm circumference.

Figure 3.4 Matrix plots and scatter plot to assess relationship between covariates

A: Relationship between age, weight, height and BSA

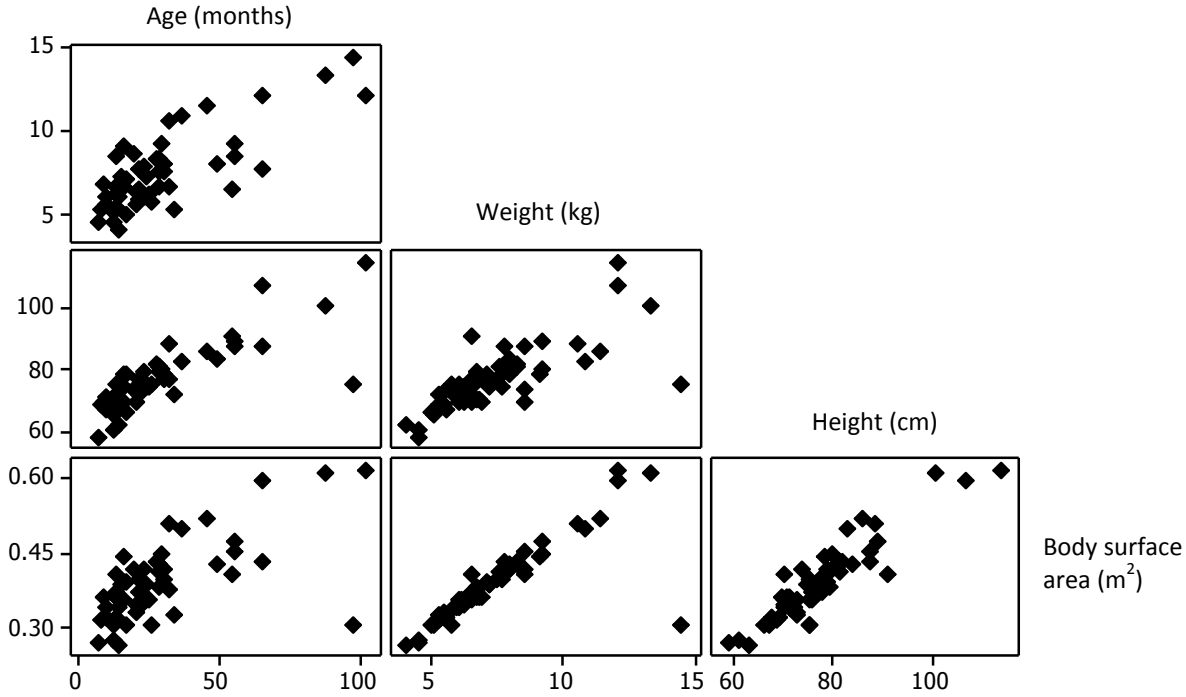

B: Relationship between MUAC and WHZ

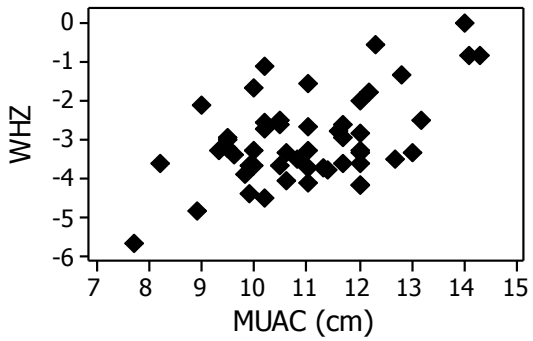

C: Relationship between sodium, potassium, bicarbonate and base excess

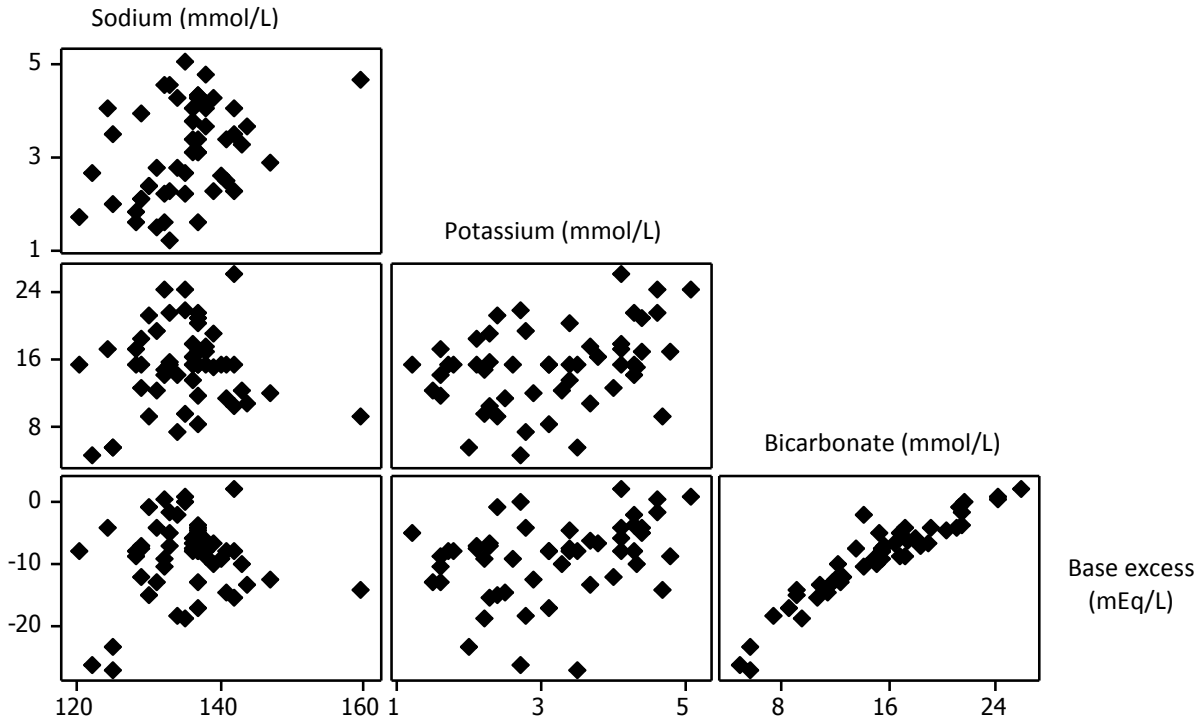

Sixteen patients were included in the high risk group, which included 6 of the 7 patients with shock. Severe dehydration and diarrhoea was observed in 48% and 46% of patients, respectively. All of the patients who were dehydrated also suffered from diarrhoea and/or vomiting. Ten patients had leukocytosis. The serum bicarbonate concentration was below the lower limit of the reference range in nearly all of the patients and base excess values indicated that 37 patients were acidotic. Most of the creatinine concentration measurements were below or within the normal range but 3 patients had values above the normal range and one patient was in renal failure with a serum creatinine concentration of 676 µmol/L.

3.3.2 Ciprofloxacin data

A total of 202 ciprofloxacin concentration measurements were available for analysis. Concentrations ranged from 0.1 to 4.52 mg/L with a median of 0.48 mg/L and the number of samples per patient ranged from 2 to 4 with a median of 4. Figure 3.5 shows a histogram of the times at which blood was sampled after dosing. The most

common sampling times were 3 and 12 hours after the dose but samples were taken throughout the dosage interval. Seventeen samples (8.4%) were taken 12 hours after the second dose (i.e. 24 hours after the start of therapy). Individual ciprofloxacin concentration-time profiles from each of the patients are illustrated in Figure 3.6. Peak concentrations occurred at the first sampling time in 36 patients and were observed at around 1 hour in 7 patients. Overall, the median peak concentration was 1.27 mg/L and ranged from 0.68 to 4.52 mg/L. In most patients (69%) the peak was measured within 1-3 hours after drug administration and ranged from 0.58 to 3.16 mg/L. However, the peak was observed later (3 to 5 hours post dose) in 8 patients and tended to be lower, ranging from 0.84 to 1.96 mg/L.

Figure 3.5 Frequency distribution of the percentages of ciprofloxacin samples taken at different times after the dose

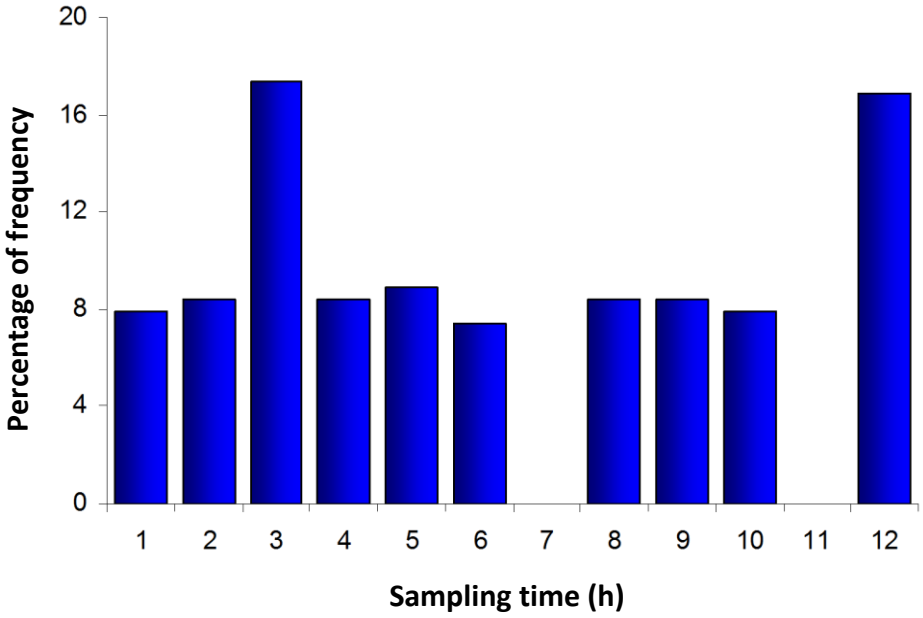

Figure 3.6 Concentration-time profiles of ciprofloxacin following oral administration to 52 malnourished children

A: Concentration data plotted on a linear scale

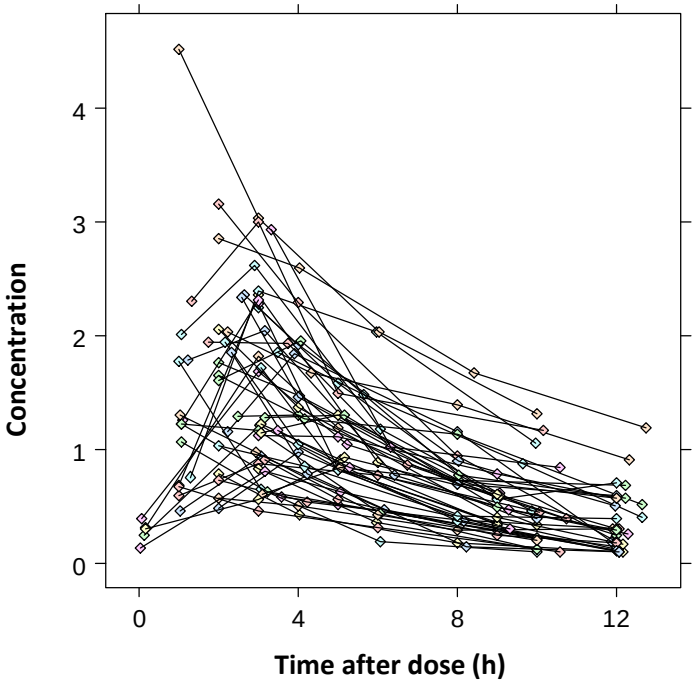

B: Concentration data plotted on a semi-log scale

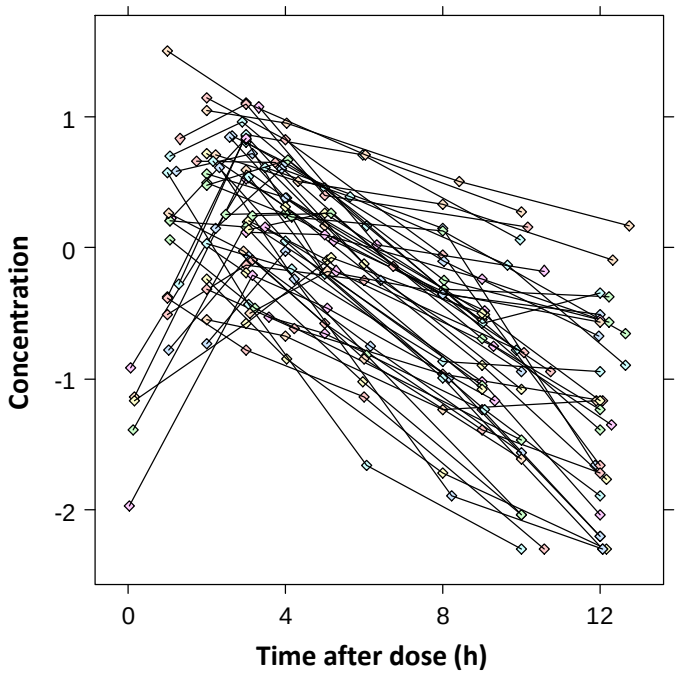

3.3.3 Population model development

3.3.3.1 Structural and statistical model development

Although the two-compartment model achieved a slightly lower OFV compared to the one-compartment model (-240.451 versus -236.047), this difference was not statistically significant. Furthermore, successful convergence could only be achieved with the one-compartment model. There was no indication of a bi-exponential decline in the concentration-time data, as illustrated in Figure 3.6B, and the plots of individual predicted concentrations against measured concentrations and the pattern of CWRES were similar for the two models (Figure 3.7). The one-compartment model was therefore used for model development.

Figure 3.7 Conditional weighted residuals versus time after dose for one- and two-compartment models with combined error

One-compartment model **Two-compartment model**

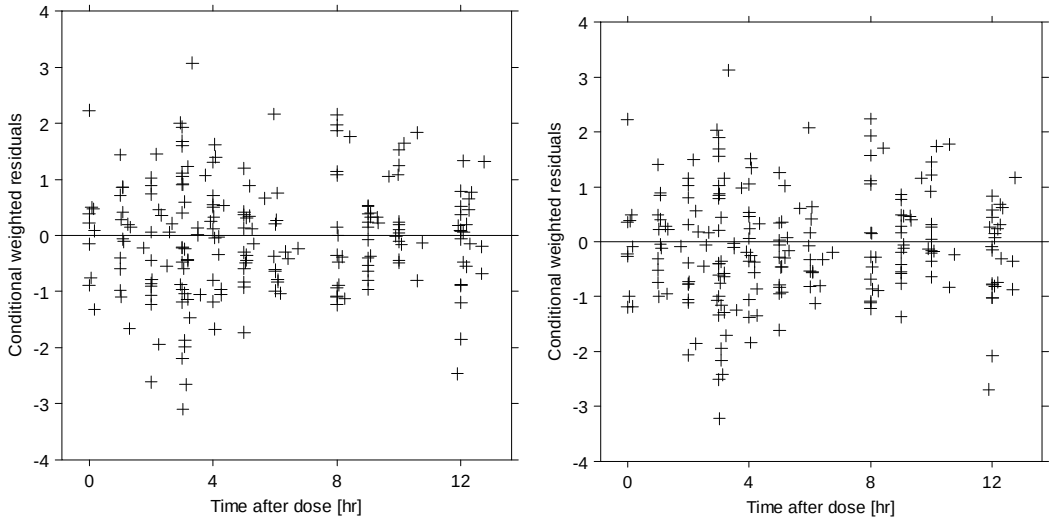

The covariance steps did not converge successfully with zero-order absorption. The transit compartment model had lower OFV compared to the lag model (-145.754 versus -157.427 for the model without allometric weight and -158.754 versus -163.735 for the model using allometric weight). Between subject variability of the parameters (ka, *n* and MTT) for transit compartment model were high and this absorption model slightly improved the fit in some individual plots compared to the

lag model. In addition, the estimation step aborted frequently due to numerical difficulties with the differential equations used in the model. Therefore, the lag model was selected to describe the absorption process. Examples of measured and individual predicted concentration-time profiles, estimated from the lag model and the transit compartment model, are illustrated in Figure 3.8. Table 3.3 compares the parameters estimated from these two models. The parameter estimates (CL/F, V/F and ka) obtained from a transit compartment model were similar to those obtained from a lag model. The estimated MTT and lag time were comparable (~40 min). BSV in MTT were 75.8% and 69.7% for the model without and with allometric WT, respectively.

The additive error model had a higher OFV (-183.533) than both the proportional and combined error models (-231.465 and -236.047) and there was a clear trend in the absolute individual weighted residuals (|iWRES|) with an increase at concentrations less than 1 mg/L and a decrease at concentrations above 1 mg/L, as illustrated in Figure 3.9A. The percentage of ε-shrinkage was high (89%). Plots of absolute individual weighted residuals versus individual predictions were similar for the proportional and combined error models (Figure 3.9B and 3.9C) and the measures of ε-shrinkage were 31% and 32%, respectively. The covariances in BSV were also similar between the two error models. However, since the combined error model achieved a lower OFV (difference 4.58), it was retained for further model development.

Figure 3.8 Measured and individual predicted concentration versus time plots comparing the lag model and the transit compartment model using a one-compartment model with combined error

Patient 8

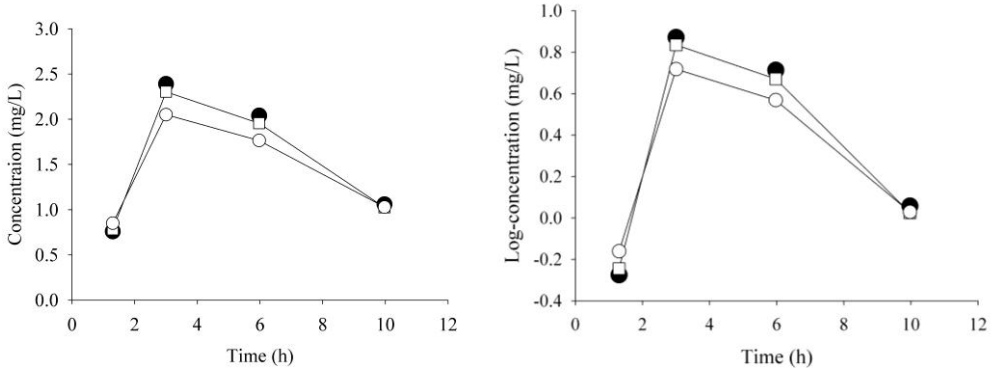

Patient 39

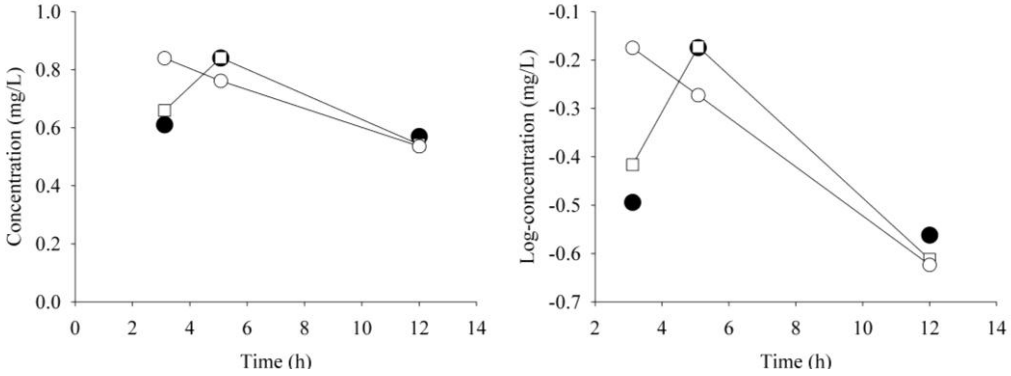

Patient 41

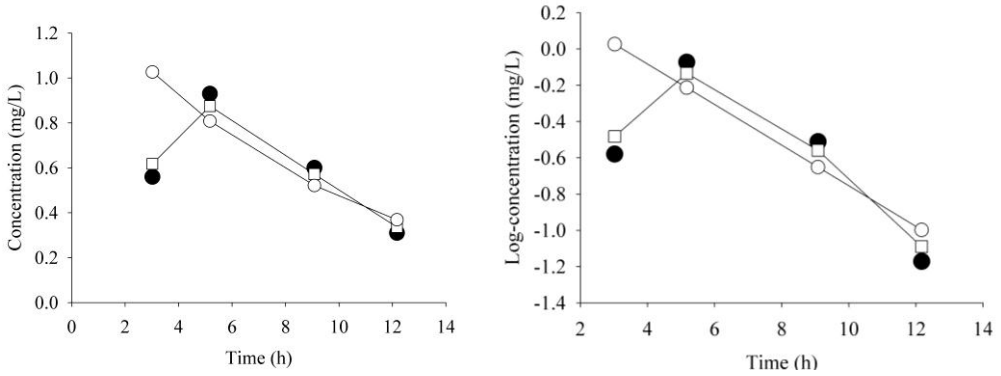

Key: filled circle is the measured concentration, opened square is the individual predicted concentration obtained from the a transit compartment model, opened circle is the individual predicted concentration obtained from a lag model.

Table 3.3 Parameters estimated from lag model and transit model comparing between model with and without allometric weight relationship

Parameters	Without allometric WT		With allometric WT	
	Lag model[a]	Transit model[b]	Lag model[a]	Transit model[b]
CL/F (L/h)	6.49	6.57	35.7	35.8
V/F (L)	36.4	35.9	353	353
ka (h^{-1})	4.11	5.27	3.64	3.02
ALAG (h)	0.784	-	0.763	-
MTT (h)	-	0.675	-	0.537
n	-	1.99	-	2.35
BSV in CL/F (%)	52.2	51.9	49.2	48.2
BSV in V/F (%)	55.0	54.7	48.5	48.7
BSV in ka (%)	117.0	96.7	111.8	83.5
BSV in MTT (%)	-	75.8	-	69.7
Additive error (SD)	0.0258	0.0254	0.0255	0.0255
Proportional (%CV)	19.2	16.9	19.2	18.1

[a] number of parameters = 4

[b] number of parameter = 5

Key: WT = weight (kg), CL/F = clearance/bioavailability, V/F = volume of distribution/bioavailability, BSV = between subject variability, ka = absorption rate constant (h^{-1}), ALAG = lag time (h), MTT = mean transit time (h), *n* = number of transit compartment.

In summary, the model chosen for covariate model development was a one compartment with first-order absorption with a lag time. Weight was included using an allometric model with an exponent of 0.75 for CL/F and 1 for V/F. Measured compared to the predicted and individual predicted concentrations estimated using this base model are illustrated in Figure 3.10. Although the allometric model was used as the base model, a comparison was made with models that used linear weight and allometric BSA relationships. The values of OFV were similar for all three approaches with the allometric weight model having an OFV that was slightly lower than observed with the linear model (1.33) and the BSA model (2.94).

Figure 3.9 The absolute values of individual weighted residuals versus individual predicted concentrations for one-compartment with additive, proportional and combined error models

A: Additive error model

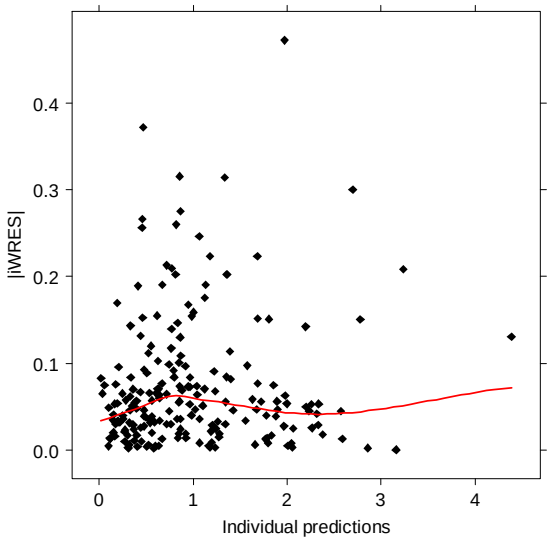

B: proportional error model

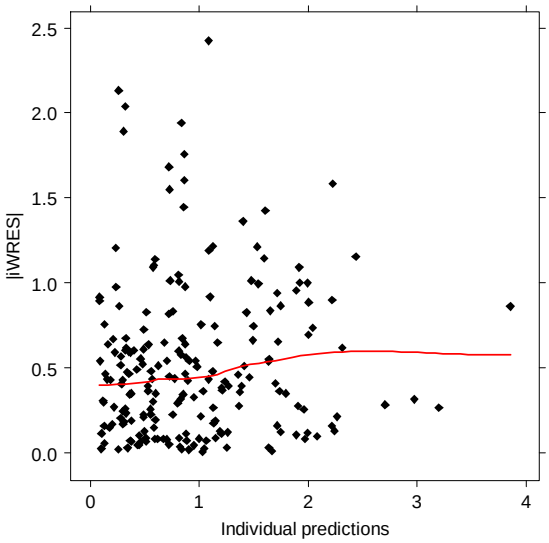

B: combined error model

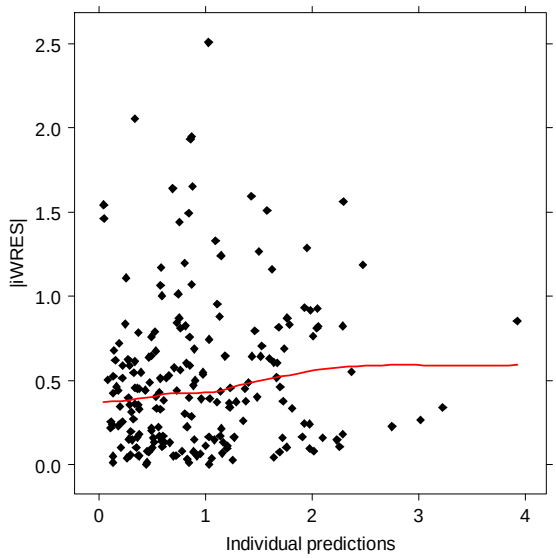

Figure 3.10 Population predicted and individual predicted concentrations versus observed concentrations obtained from a one-compartment model with combined error

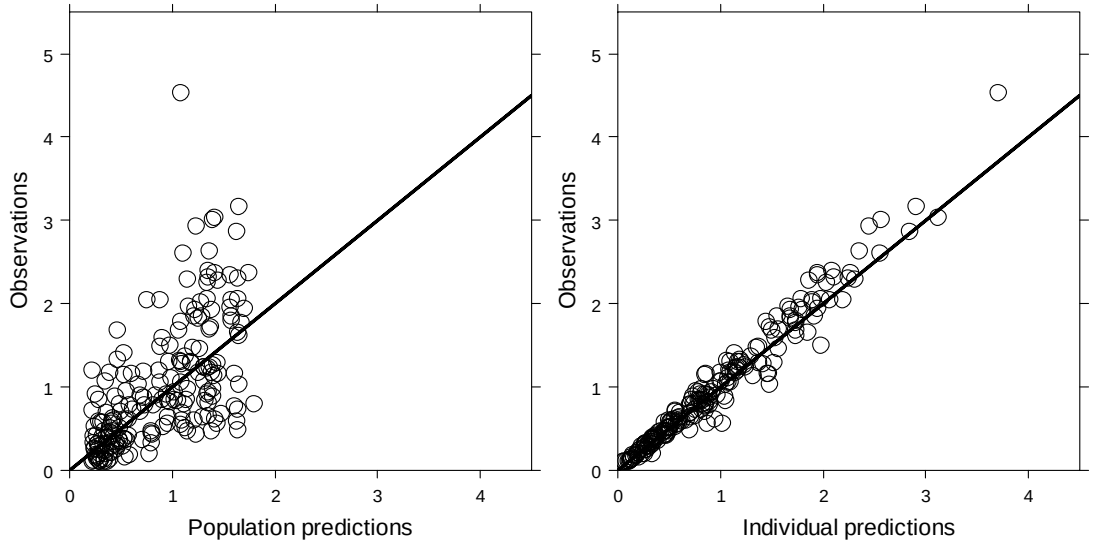

3.3.3.2 Covariate model development

Examination of scatter plots of individual estimates of ciprofloxacin CL/F against clinical factors identified potential relationships with sodium concentration, potassium concentration and estimated creatinine clearance, as illustrated in Figure 3.11. Results for categorical data indicated that CL/F was higher in patients who were given ciprofloxacin with their feed. However, variability was high in both groups. CL/F was lower in patients who had a high mortality risk, dehydration, shock or diarrhoea (Figure 3.12). A potential positive relationship was identified between V/F and serum sodium concentration and serum potassium concentration (Figure 3.13), and lower estimates of V were observed in patients who had shock (Figure 3.14). No relationships between absorption rate constant and any clinical covariate were identified from plots. Shrinkage for η_{CL} and η_V were 3% and 6%, respectively which indicated that these scatter plots have enough power to identify relationships between parameters and covariates.

Figure 3.11 Scatter plots showing potential relationships between individual estimates of clearance/bioavailability (CL/F) and continuous clinical and demographic data

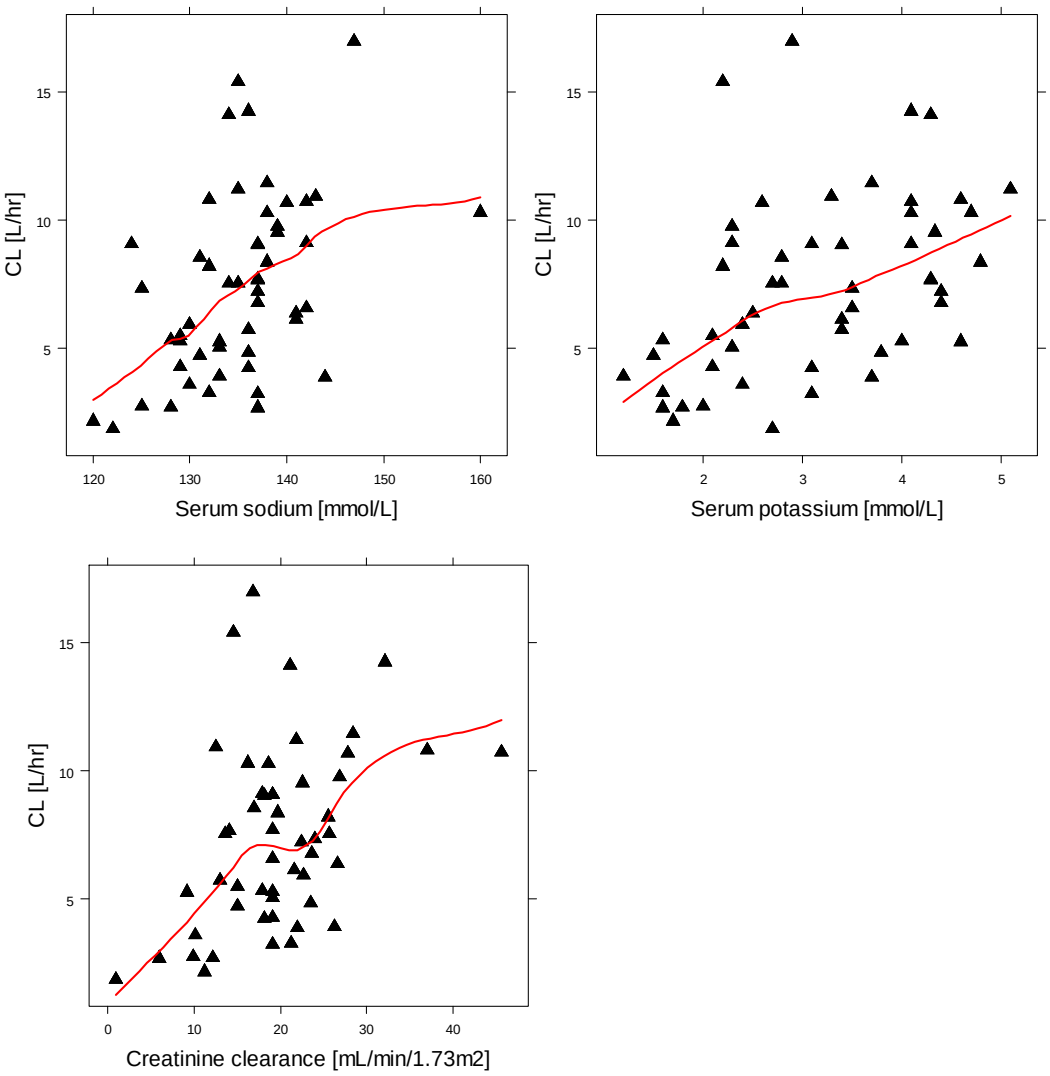

Key: Individual estimates are represented by the solid triangles and the red line represents a regression line.

Figure 3.12 Box plots showing potential relationships between individual estimates of clearance/bioavailability (CL/F) and categorical clinical and demographic data

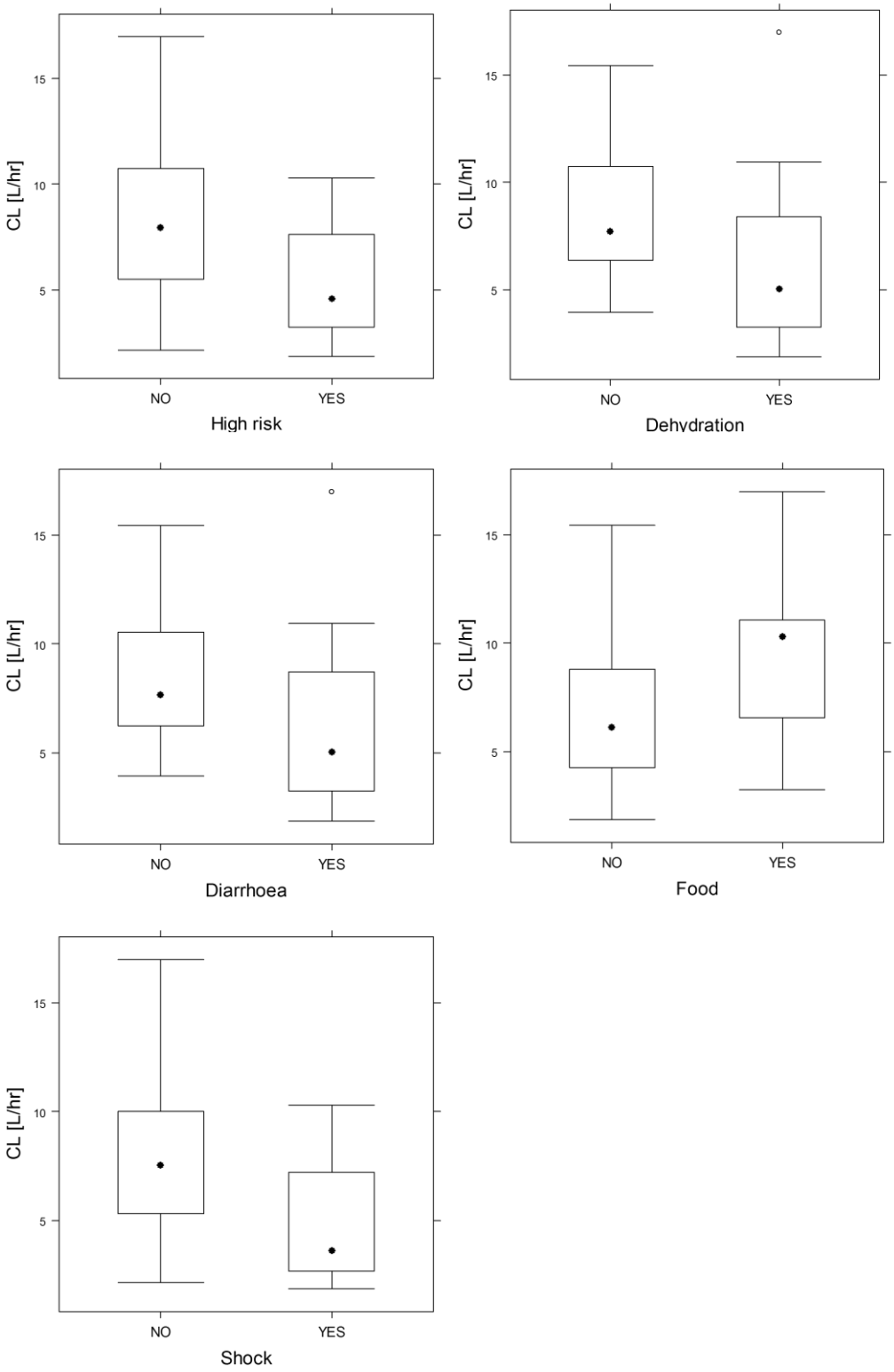

Figure 3.13 Scatter plots illustrating potential relationships between individual estimates of volume of distribution/bioavailability (V/F) and serum sodium and potassium concentrations

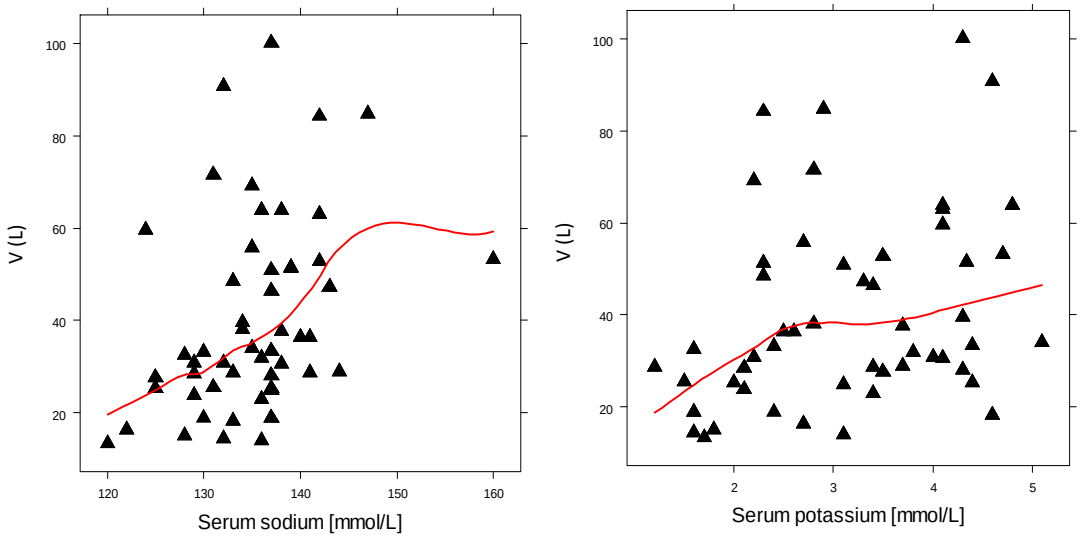

Key: Individual estimates are represented by the solid triangles; the red line represents a regression line.

Figure 3.14 Box plot of individual estimates of volume of distribution/bioavailability (V/F) in patients with and without shock

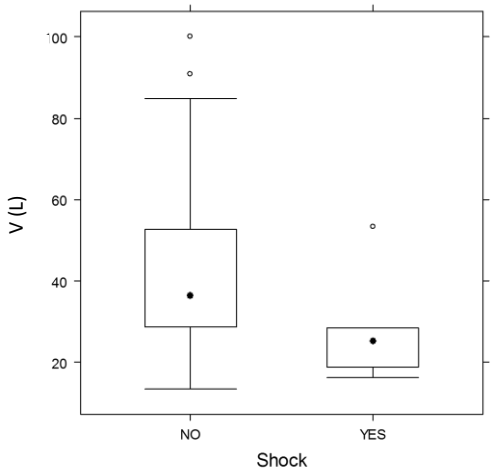

The results of the GAM analysis for CL/F are summarised in the Akaike plot shown in Figure 3.15. The best model, which had the lowest value for the Akaike Information Criterion, identified high risk, serum sodium, serum potassium and creatinine clearance as important factors. The GAM analysis of individual estimates of V/F is summarised in Figure 3.16. Shock, weight and serum sodium were identified as potential covariates.

Figure 3.15 Plot showing the Akaike values resulting from the GAM analysis of factors that might influence clearance/bioavailability (CL/F)

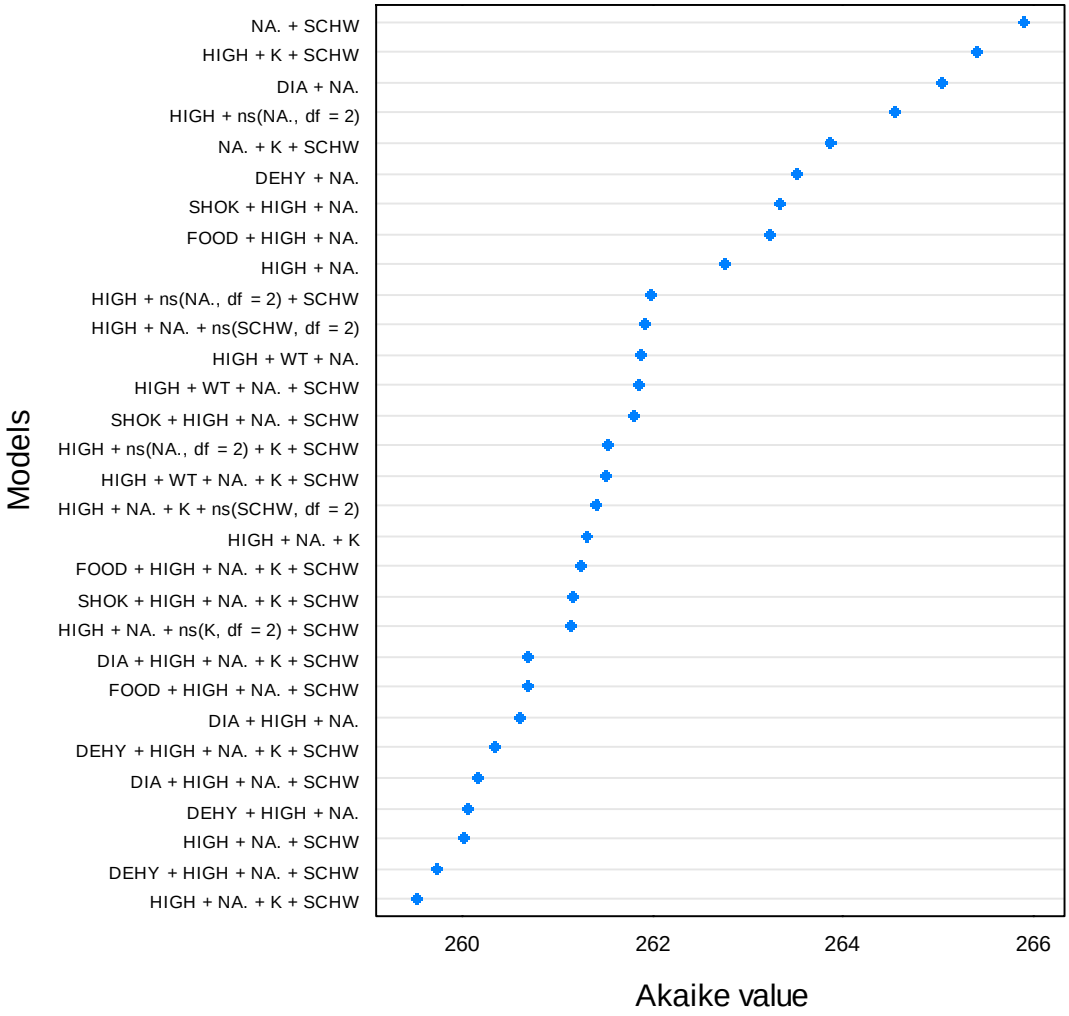

Key: NA = serum sodium, K = serum potassium, DEHY = dehydration, SHOK =shock, HIGH = high mortality risk, SCHW = creatinine clearance calculated by Schwartz equations, WT = weight, DIA = diarrhoea, FOOD = drug administered with feed.

Figure 3.16 Plot showing the Akaike values resulting from the GAM analysis of factors that might influence volume of distribution/bioavailability

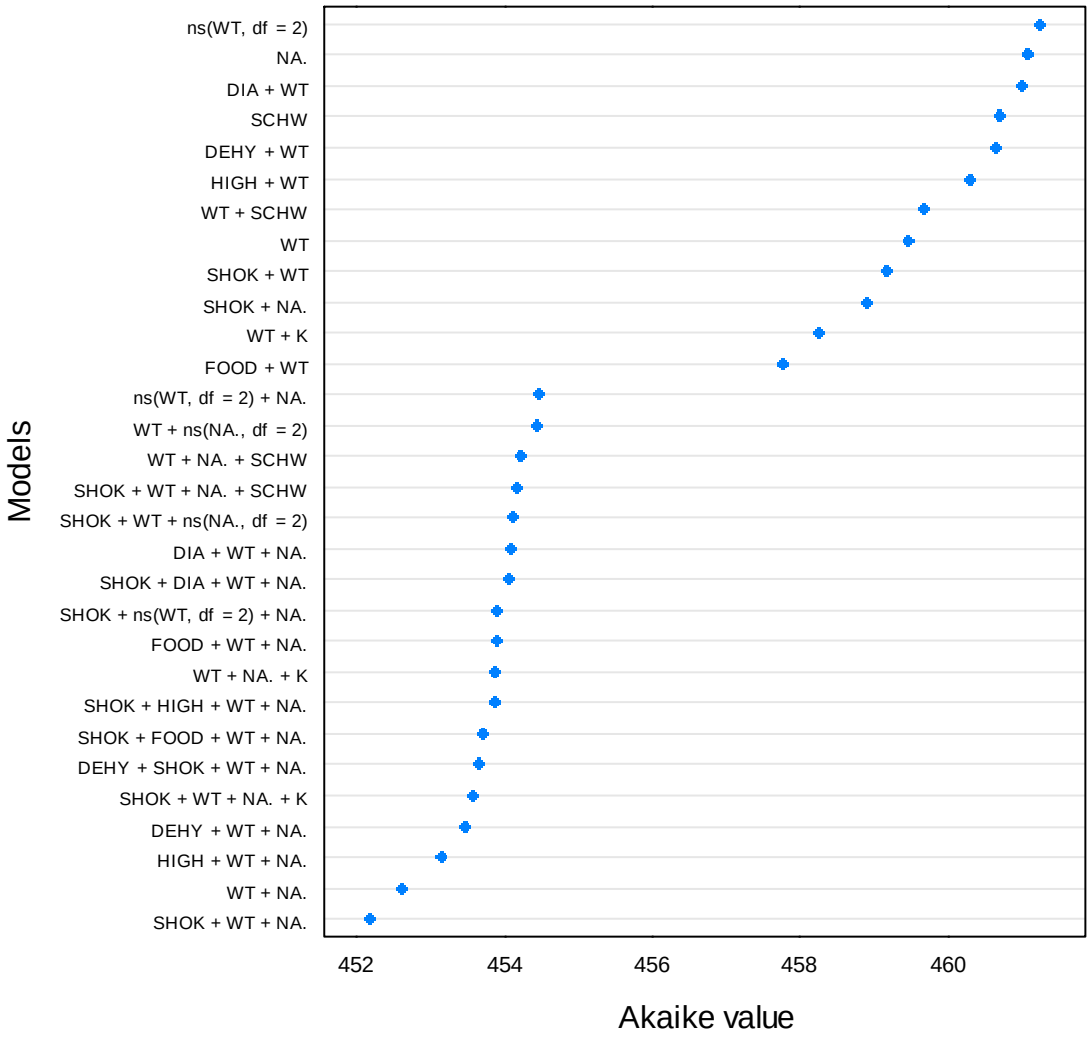

Key: NA = serum sodium; K = serum potassium; DEHY = dehydration; SHOK = shock; HIGH = high mortality risk; SCHW = creatinine clearance calculated by Schwartz equations; WT = weight; DIA = diarrhoea; FOOD = drug administered with feed.

The population analysis that was conducted using NONMEM (Beal *et al*., 1989-2006) examined the influence of the following individual covariates on CL/F: serum sodium; serum potassium; high mortality risk; creatinine clearance; shock; administration with food; diarrhoea and dehydration. The results of these analyses are presented in Table 3.4. All except creatinine clearance produced statistically significant reductions in OFV (p<0.05) but none were significant at p<0.01. Serum

sodium achieved the lowest value of the OFV (reduction of 6.24) followed by serum potassium (6.14) and high risk (6.05). The inclusion of both serum sodium and high risk in the model resulted in a further reduction in OFV of 8.22. The lowest value of OFV was observed with the combination of serum sodium, high risk and dehydration. Adding a fourth covariate had no effect.

The influence of serum sodium, serum potassium, high risk and shock was tested on V/F. A significant reduction in OFV was observed with the inclusion of serum sodium into the model. The full model therefore included the factors serum sodium, high risk and dehydration on CL/F and sodium on V/F. Stepwise back elimination from this model was performed by removing each covariate individually. When dehydration was removed from this model, the increase in OFV was only 5 therefore dehydration was excluded. Removal of all other covariates led to an increase in OFV of more than 6.63. The final model therefore included serum sodium and high risk on CL/F and serum sodium on V/F. This model reduced between subject variability on CL/F from 50% to 38% and on V/F from 49% to 43%. Measured versus population and individual concentrations plots for this model are presented in Figure 3.17 and the parameter estimates from the base and final models are presented in Table 3.5. The final model can be summarised as follows:

$$\text{TVCL (L/h)} = 42.7(\text{L/h/70 kg}) \times (\text{WT}/70)^{0.75} \times (1 + 0.0368 \times (\text{Na}^{+} - 136)) \times (1 - 0.283 \times (\text{High}))$$

$$\text{TVV (L)} = 372\ (\text{L/70 kg}) \times (\text{WT}/70) \times (1 + 0.0291 \times (\text{Na}^{+} - 136))$$

$$\text{TVKA} = 2.97\ \text{h}^{-1}$$

$$\text{ALAG} = 0.742\ \text{h}$$

If the patient has a high mortality risk, High = 1, otherwise High = 0. This model indicates that the typical estimate of CL/F is 42.7 L/h/70 kg and is reduced by 28.3% by high risk and by 3.7% for every 1 mmol/L sodium concentration greater or less than 136 mmol/L. The typical estimate of V/F is 372 L/70 kg (5.3 L/kg) and is changed by 2.9% for every change in 1 mmol/L sodium concentration from 136 mmol/L.

Table 3.6 summarises the individual pharmacokinetic parameter estimates and the derived estimates of the maximum concentration (C_{max}), time to C_{max} (T_{max}), elimination half-life and area under the concentration-time curve from 0 to 24 hours (AUC_{0-24}). Oral CL had a median of 0.98 L/h/kg in patients in the low and intermediate categories and 0.67 L/h/kg in high risk patients. The median half-life was 3.78 hours (ranging from 2 to 9 hours). The median T_{max} predicted from the model was significantly shorter than the observed T_{max} (1.8 versus 3 hours). The median maximum concentration predicted from the model was 1.5 mg/L, which is similar to the observed value of 1.7 mg/L. Individual estimates of AUC_{0-24} ranged from 8 to 61 mg·h/L, indicating high variability. Median estimates of AUC_{0-24} were higher in patients in the high risk group compared to the patients in low and intermediate risk groups (29.7 mg·h/L versus 20.5 mg·h/L).

Figure 3.17 Observed versus population (right) and individual (left) predicted concentrations based on the final population model

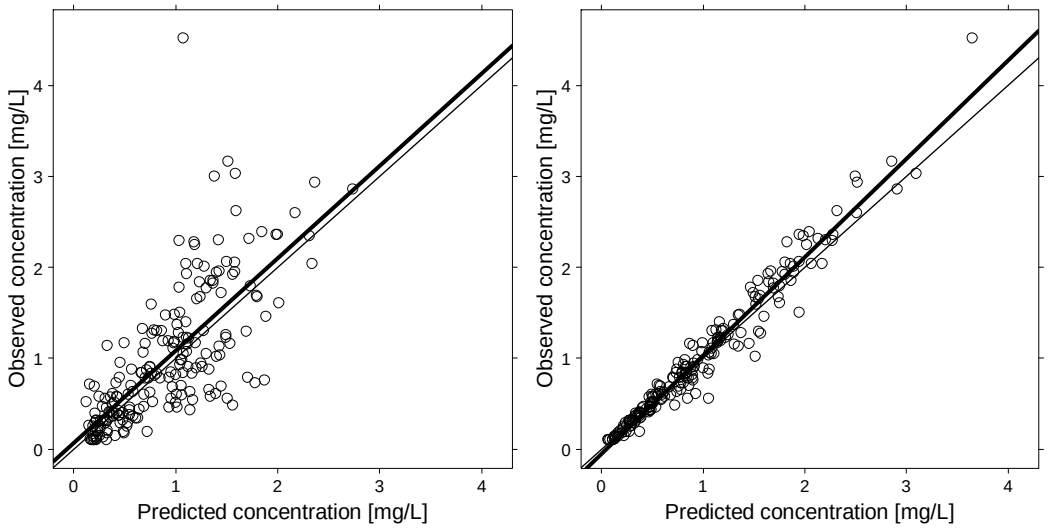

Key: the thin line represents the line of identity and the thick line represents the linear regression line.

Table 3.4 Summary of models of clearance/bioavailability and volume of distribution/bioavailability tested using NONMEM

Model No	Model of CL/F	OFV	Model for comparison	ΔOFV	BSV in CL (%)
0	Base model	-287.711	N/A	-	50
1	**NA**	**-293.953**	0	-6.242	**44**
2	K	-293.851	0	-6.14	45
3	HIGH	-293.76	0	-6.049	46
4	SCHW	-289.609	0	-1.898	48
5	SHOK	-292.415	0	-4.704	47
6	FOOD	-292.201	0	-4.49	47
7	DIA	-293.182	0	-5.471	47
8	DEHY	-292.923	0	5.212	47
9	NA + K	-296.484	1	-2.531	42
10	**NA + HIGH**	**-302.169**	1	-8.216	**40**
11	NA + SHOK	-297.012	1	-3.059	42
12	NA + FOOD	-295.601	1	-1.648	44
13	NA + DIA	-300.359	1	-6.406	42
14	NA + DEHY	-299.806	1	-5.853	42
15	NA + HIGH + K	-306.386	10	-4.217	39
16	NA + HIGH + SHOK	-305.156	10	-2.987	40
17	NA + HIGH + FOOD	-304.759	10	-2.59	40
18	**NA + HIGH + DEHY**	**-307.215**	10	-5.046	**39**
19	NA + HIGH + DIA	-306.5	10	-4.431	39
20	NA + HIGH + DEHY + K	-308.252	18	-1.037	39
21	NA + HIGH + DEHY + SHOK	-307.902	18	-0.687	39
22	NA + HIGH + DEHY + FOOD	-307.533	18	-0.318	39
23	NA + HIGH + DEHY + DIA	-307.461	18	-0.246	39
Model No	**Model of V/F**	**OFV**		**ΔOFV**	**BSV in V (%)**
24	**NA**	**-314.739**	18	-7.524	**43**
25	K	-307.429	18	-0.214	47
26	HIGH	-307.969	18	-0.754	47
27	SHOCK	-306.352	18	0.863	48

Key: NA = serum sodium; K = serum potassium; DEHY = dehydration; SHOK = shock; HIGH = high mortality risk; SCHW = creatinine clearance calculated by Schwartz equations; DIA = diarrhoea; FOOD = drug was administered with feed, CL/F = clearance/ bioavailability, V/F = volume of distribution/bioavailability.

Table 3.5 Population parameters estimates of ciprofloxacin following oral administration to malnourished children obtained using the base and final models

Parameters		Base model		Full model		Final model	
		Estimate	RSE (%)	Estimate	RSE (%)	Estimate	RSE (%)
CL/F (L/h)	θ_1	36.1	7.1	45.2	7.6	42.7	7.3
V/F (L)	θ_2	353	7.1	371	7.1	372	7.2
ka (h^{-1})	θ_3	4.04	24.5	3.05	42.3	2.97	44.4
ALAG (h)	θ_4	0.794	9.4	0.749	17.4	0.742	18.7
NA (CL/F)	θ_5			0.0357	12.7	0.0368	12.6
HIGH (CL/F)	θ_6			-0.239	33.1	-0.283	23.0
DEHY (CL/F)	θ_7			-0.149	57.7		
NA (V/F)	θ_8			0.0286	18.0	0.0291	17.6
BSV (CL/F)		49.8	17.7	37.0	19.8	38.1	20.3
BSV (V/F)		48.6	20.0	43.1	23.8	43.0	24.4
BSV (ka)		117.0	34.9	104.9	53.5	102	57.1
Additive error (SD)		0.0284	35.0	0.0282		0.0273	51.6
Proportional (%CV)		18.1	11.4	18.5		18.6	15.0

Key: BSV = between subject variability (%CV), CL/F = oral clearance, V/F = oral volume of distribution, ka = absorption rate constant (h^{-1}), ALAG = absorption lag time (h), NA = serum sodium (mmol/L), HIGH = high mortality risk, DEHY = dehydration, RSE=relative standard error (%).

Table 3.6 Summary of individual ciprofloxacin pharmacokinetic parameter estimates obtained in 52 children with severe malnutrition

Parameter estimates	N	Mean	SD	Median	Minimum	Maximum
CL (L/h)	52	7.43	3.54	7.19	1.83	17.1
CL (L/h/kg)	52	1.02	0.52	0.87	0.32	2.54
CL (L/h/kg) Low/intermediate risk	36	1.14	0.53	0.98	0.46	2.54
CL (L/h/kg) High risk	16	0.77	0.41	0.67	0.32	1.53
V (L/kg)	52	5.47	2.69	4.49	2.14	14.2
$T_{1/2}$ (h)	52	3.97	1.38	3.78	2.01	9.04
Observed T_{max} (h)	52	2.77	1.08	3.00	1.00	5.17
Model predicted T_{max} (h)	52	1.91	0.58	1.79	1.09	3.85
Observed C_{max} (mg/L)	52	1.68	0.79	1.71	0.58	4.52
Model predicted C_{max} (mg/L)	52	1.51	0.60	1.50	0.61	3.56
AUC_{0-24} (mg·h/L)	52	24.8	12.4	22.4	7.9	61.3
AUC_{0-24} (mg·h/L) low/intermediate risk	36	21.1	8.8	20. 5	7.9	43.4
AUC_{0-24} (mg·h/L) high risk	16	32.9	15. 5	29.7	13.1	61.3

Key: CL= oral clearance; V= oral volume of distribution; $T_{1/2}$= elimination half-life; T_{max}= time of the maximum concentration; AUC_{0-24}= the steady state 24 hour area under the concentration-time curve.

3.4 DISCUSSION

This work is the first population pharmacokinetic analysis of oral ciprofloxacin in paediatric patients with severe malnutrition. The study included 52 patients with an age range of 8 to 102 months. Body weight, sodium concentration and presence of high mortality risk were found to influence the pharmacokinetics of ciprofloxacin in this patient population. Since the oral suspension form of ciprofloxacin was not available in the research setting, the tablet was ground and individual doses were measured according to body weight and reconstituted with water. This preparation method was successfully used in a previous pharmacokinetic study in a paediatric population (Peltola *et al*., 1992).

In the present study, all the children received oral ciprofloxacin 10 mg/kg every 12 hours for 48 hours and a series of blood samples were collected at various times during the first 24 hours after the drug was administered. This dose produced a median observed C_{max} of 1.7 mg/L (ranging from 0.6 to 4.5 mg/L) at a median of 3 hours (ranging from 1 to 5.2 hours) after dosing. The C_{max} values that were predicted from the final model were similar with a median of 1.5 mg/L but the estimated time to peak concentration was earlier, at a median of 1.8 hours after the dose. The final model predicted the peak concentration to occur earlier in 85% of patients.

Prior to this study, there have been a few studies that examined the pharmacokinetics of ciprofloxacin in paediatric patients. Peltola *et al*. (1992) gave oral ciprofloxacin 15 mg/kg to infants and children aged 5 weeks to 5 years and up to 11 blood samples were collected during the first 12 hours (7 of these were drawn within 3 hours after the dose). A median C_{max} of 2.2 mg/L (range 0.5 to 5.3 mg/L) was observed at a median of 1 hour after the dose. The same authors also investigated the pharmacokinetics of an oral suspension formulation by giving ciprofloxacin 10 mg/kg three times daily to children with ages ranging from 0.3 to 7.1 years (Peltola *et al*., 1998). Nine blood samples were collected during the first 24 hours. With this dosage regimen, mean C_{max} values varying from 2 to 2.7 mg/L, which were reached within 1 hour after dosing, were reported. Rubio *et al*. (1997) reported that the C_{max} was 3.7 mg/L at 2.5 hours after oral dosing of ciprofloxacin 20 mg/kg twice daily.

Another study, conducted by Schaefer *et al.* (1996), showed that the mean C_{max} was around 8.4 mg/L after giving ciprofloxacin 15 mg/kg intravenously every 12 hours to paediatric patients with cystic fibrosis. However, a mean C_{max} of 3.5 mg/L was reported with an oral dose of 15 mg/kg twice daily. The variability in C_{max} and T_{max} observed in the present study may have been due to the difference between patient populations. The patients included in this study had severe malnutrition, which can alter intestinal transit time. Malnutrition is also associated with villous atrophy in the jejunal mucosa and may impair drug absorption (Oshikoya & Senbanjo, 2009; Brewster, 2006). Additionally, the transit time through the bowel may change due to diarrhoea and vomiting. There are several pieces of evidence illustrating that the oral absorption of several drugs decreases significantly in children with malnutrition compared to normal healthy children (Bolme *et al*., 1995; Bravo *et al*., 1984; Eriksson *et al*., 1983; Mehta *et al*., 1980; Salako *et al*., 1989; Walker *et al*., 1987). Another explanation for this variability was the limited sampling strategy used in this study. For ethical and practical reasons, a maximum of only four blood samples per patient were collected and each patient was assigned to one of three blood sampling schedules. Although these sampling times covered most of the dosage interval, only one sample was withdrawn from each patient during the first 3 hours. Most samples (35) were collected at least 2 hours after the dose and therefore the C_{max} may have already been achieved. Previous studies have reported an observed C_{max} of around 1-2 hours. A delayed T_{max} of 3 hours observed in this study may be a reflection of the available sampling times, because the majority of the patients (35) had samples taken at around 3 hours after the dose.

A one-compartment model with first-order absorption with a lag adequately described the concentration-time data. Several previous studies have identified that a two-compartment model best describes the ciprofloxacin data, but the sparse sampling schedule used in this study limited the identification of a distribution phase. The population model indicated that oral ciprofloxacin was rapidly absorbed with an estimated half-life of 14 minutes after a lag of around 45 minutes. Previous population studies conducted in paediatric patients have reported slower rates of absorption with half-lives of 30-96 minutes after a lag time of 21-45 minutes (Payen

et al., 2003; Rajagopalan & Gastonguay, 2003; Schaefer *et al.*, 1996). The between subject variability in absorption rates was around 50 to 55%.

The initial population model for clearance assumed an allometric relationship between oral clearance, oral volume of distribution and body weight. Several studies have demonstrated that the use of allometric weight can improve the fit of the model, especially in paediatric populations (Anderson *et al.*, 1997; Anderson & Holford, 2009; Holford, 1996). In this study, the OFV after incorporating allometric weight, linear weight and allometric BSA were -252.364, -251.020 and -249.402, respectively. Although the findings suggested that an allometric weight has no additional benefit over other models, an allometric approach allows comparison of pharmacokinetic parameters (CL and V) in children with adult data and hence it was used in this study.

Rajagopalan and Gastonguay (2003) conducted a pharmacokinetic study in paediatric patients aged 14 weeks to 17 years and found that a standardised clearance was 30.3 L/h/70 kg. Correcting with their bioavailability of 61% gives an oral clearance of 49.7 L/h/70 kg, which is similar to the value of 42.7 L/h/kg reported in this study. These values are consistent with adult values of around 40 – 70 L/h (Forrest *et al*., 1988; Gasser *et al*., 1987; Plaisance *et al*., 1987). After correcting individual oral clearance estimates for weight, a median of 0.9 L/h/kg (range 0.3 – 2.5 L/h/kg) was obtained and is consistent with oral clearances of 0.2 – 1.5 L/h/kg observed previously (Lipman *et al.*, 2002; Peltola *et al.*, 1998; Rajagopalan & Gastonguay, 2003).

Renal clearance accounts for approximately two-thirds of total ciprofloxacin clearance (Drusano *et al*., 1986a; Drusano *et al.*, 1986b; Forrest *et al*., 1988); therefore the pharmacokinetics of ciprofloxacin are altered in patients with renal impairment. However, during the covariate model building, the inclusion of creatinine clearance did not affect ciprofloxacin clearance. This was due to the pre-specified criteria that excluded patients with severe renal impairment. In the present study, only one patient had a high creatinine concentration (676 μmol/L) and was

also categorised in the high risk group. This patient had the lowest estimates of oral clearance at 1.8 L/h (0.33 L/h/kg). Hence, the final model cannot be used to predict ciprofloxacin concentrations in patients with severe renal impairment. The results suggested that a dosage adjustment is not necessary in patients with mild to moderate renal impairment. The median elimination half-life observed in this study was 3.8 hours (ranging from 2 to 9 hours), which is similar to those reported previously in adults with normal renal function and in paediatric patients (Forrest *et al*., 1988; Gasser *et al*., 1987; Plaisance *et al*., 1987). Dehydration, diarrhoea and shock also have an influence on oral clearance, but these factors have already been accounted for in 'high risk' patients. Of the 16 patients in the high risk group, 12 had dehydration (of whom 11 had diarrhoea) and 6 had shock. Therefore, adding these clinical factors to the model, after including high risk, provided a little additional benefit. Interestingly, serum sodium concentration was found to be an important clinical factor that influences oral clearance. Hyponatraemia is frequently observed in patients with severe malnutrition, due to impairment of Na/K pumps. This leads to increased extracellular fluid and consequently low sodium (Alleyne, 1967; Costa-Silva *et al*., 2009; Klahr & Alleyne, 1973). There are currently no physiological explanations for the correlation between sodium concentration and the clearance. Additionally, despite sodium concentration decreasing OFV more than other covariates, it reduced subject variability in oral clearance by only 6% and in oral volume of distribution by 4%. Therefore, sodium concentration may be a spurious finding.

Several studies have reported that the oral bioavailability of ciprofloxacin decreases when given simultaneously with milk, yogurt or divalent cations such as iron or zinc supplements (Frost *et al*., 1989a; Kara *et al*., 1991; Neuvonen *et al*., 1991; Polk *et al*., 1989). The effect of food feeding is one of interest. Since most children are in a poorly resourced healthcare setting with a limited number of healthcare professionals, it is impractical and impossible to ensure that feeding times are synchronised around the times of drug administration. Subsequently, a significant proportion of children are likely to receive ciprofloxacin with food and the bioavailability may reduce. Although the initial analysis found that the oral clearance

increased when patients were given ciprofloxacin, the OFV dropped by only 4.5 units, which indicated a weak effect. In the final model, no influence of food was identified. This may be due to the fact that 13 of the 16 patients (81%) who received ciprofloxacin with food were in the low or intermediate risk categories, and they had a high oral clearance (0.98 L/h) and low AUC estimates (20.5 mg·h/L) compared to the patients in the high risk group (0.67 L/h and 29.7 mg·h/L). The influence of high mortality risk may be a confounding factor masking the effect of food on oral clearance. In addition, if food was important, it may have enhanced the apparent influence of risk in the model.

The standardised estimate of oral V in the present study was 372 L/70 kg, which was similar to that reported by Forrest *et al*. (1988) in adult patients with normal renal function (321 L/1.73 m^2) but higher than that reported previously by Rajagopalan and Gastonguay (2003) (V_{ss} was 240 L/kg after correction for bioavailability). Individual estimates of oral V ranged from 2 to 14 L/kg with a median of 4.5 L/kg, which was considerably higher than the values of around 1.5 – 3.8 L/kg reported previously (LeBel *et al*., 1986; Lipman *et al*., 2002; Payen *et al*., 2003; Schaefer *et al*., 1996). These results indicated that children with malnutrition have an increase in oral V, which is consistent with the observed oral V in gentamicin in malnourished children (Seaton *et al*., 2007). Septicaemia, oedema and electrolyte imbalance, which are common complications, may contribute. In a similar way to the case with oral clearance, sodium concentration was found to influence the oral V. Higher sodium concentration is associated with larger estimates of oral V.

CHAPTER 4

VALIDATION OF THE POPULATION MODEL FOR CIPROFLOXACIN

4.1 INTRODUCTION

Population pharmacokinetic (PK) and pharmacodynamic (PD) modelling is a useful tool for analysing the relationship between drug dose and its concentration, and between the drug concentration and its effects/toxicities. PK-PD modelling can also be used to identify variability among population subgroups, which may be utilised to support decisions in drug therapy and to select the optimal dosage regimens. The choice of the population model is dependent on the quality of data and modeller decisions taken during the model building process, which are often subjective e.g. graphical assessments. Therefore, the final population model should be tested for validity.

There is currently no consensus as to which is the most appropriate approach to validate population models. Importantly, the need for model validation may vary depending on the objective of the analysis. If the final model is to be used for prediction, clinical trial simulation or incorporation into a drug label, the predictive performance of the model should be tested. However, if the model is developed to explain variability with no dosage adjustment recommendation, a simpler validation method for testing the stability can be used (Brendel *et al.*, 2007). The current European Agency of Evaluation of Medicinal Products (EMEA) guideline on the reporting of results of population PK analyses recommends that model evaluation be performed to demonstrate that the final model is robust and functions as a sufficiently good description of the data to enable the objective(s) of the analysis to be met (EMEA, 2006). The guidance for industry on population PK published by the Food and Drugs Administration (FDA) also suggests the need for model evaluation during the drug development process (FDA, 1999).

The predictive performance of a population model is generally assessed by comparing the measured concentrations in a validation dataset to those values predicted by the population model. Although external validation (using a new dataset from another study) is the most stringent method to validate the model (FDA, 1999; Sun *et al.*, 1999), an internal validation is more practical and can be used to identify an invalid model. Among all of the internal validation techniques, data splitting is

one of the most often recommended (Ette, 1997). The drawback with this method, however, is that its predictive accuracy is a function of the sample size resulting from the data splitting, which means that it is not suitable for studies with a small sample size (e.g. paediatric studies). In order to maximise predictive accuracy while retaining a reliable estimate of the parameters in such a situation, the use of all data for model development and validation is recommended (Ette, 1997).

Bootstrapping was used to validate the population model in the present study. This method has the advantage that it employs the entire available dataset during model building. It is also useful for testing model stability in terms of covariate selection and for model performance evaluation (Ette, 1997). A major drawback of this approach is the extensive computation time required to validate hundreds of datasets, especially when the original dataset is large and the model complex. However, this has become less problematic as improved computer systems and automated model building software have become available (Jonsson & Karlsson, 1998). It has been suggested that a minimum of 200 bootstrap replicates is adequate for this method (FDA, 1999). In addition to the bootstrapping, the final population model in this study was also validated with the visual predictive check (VPC) and normalised prediction distribution error (npde) as described in Chapter 2.

Modelling generally should be performed with caution because the parameter estimates may depend on only one or two unusual individuals in the dataset. Case deletion diagnostics such as jackknife analysis can be used to identify influential individuals. The jackknife is a non-parametric method, which involves repeated population parameter estimates following consecutive deletion of data from individuals.

The aim of the analysis in this chapter is to assess the performance of the final population model with respect to both stability and predictability, using internal validation techniques.

4.2 METHODS

4.2.1 Bootstrap estimates

A bootstrap was performed using Perl-speaks-NONMEM (PsN) Version 3.1.0 (Lindbom *et al.*, 2005; Lindbom *et al.*, 2004). One thousand datasets were generated and used to calculate confidence intervals of parameter estimates. The following is an example of the bootstrap commands used in this study:

bootstrap run1.mod –samples=1000 –seed=1234 –threads=8 –dir=bootstrap1

The meaning of each command is shown below:

bootstrap	Call the PsN to run bootstrap
run1.mod	Name of model file
-samples	Number of bootstrap datasets to generate
-seed	A seed to generate a random number
-threads	Number of parallel processes
-dir	Name of directory in which the output will be stored

4.2.2 Jackknife analysis

The jackknife analysis was performed using the PsN Version 3.4.4. From the original dataset, 52 new datasets were created so that each excluded the data from one patient. Each dataset (so-called ‘jackknife sample’) was analysed with NONMEM using the final population model. The following is an example of the case deletion diagnostic command used in this study:

cdd run1.mod -case_column=ID -dir=cdd_run1

The following is the meaning of arguments:

cdd	Call the PsN to run case deletion diagnostic
run1.mod	Name of model file
-case_column	Name of the column on which the case deletion is performed
-dir	Name of directory in which the output will be stored

The jackknife standard error (*se*) for the population parameter was calculated using equations 4.1-4.3 (Bonate, 2011).

$$P_i = n\theta - (n - 1)\theta_i \quad (4.1)$$

where P_i are pseudovalues, θ the population parameter estimated from all subjects, θ_i the population parameter estimated from a jackknife sample, and *n* the total number of subjects in the dataset. With

$$\bar{P} = \frac{\sum_{i=1}^{n} P_i}{n} \quad (4.2)$$

where $\bar{P}$ is the average of the pseudovalues, and

$$se = \sqrt{\frac{1}{n(n-1)} \sum_{i=1}^{n} (Pi - \bar{P})^2} \quad (4.3)$$

those individuals with a high impact on the population parameter estimates were identified by comparing population parameter estimates from the jackknife samples with the population values determined using the final model.

4.2.3 Visual predictive check (VPC)

A visual predictive check (VPC) was performed using the PsN Version 3.1.0. The example command used to run VPC is shown below:

vpc run1.mod –lst=run1.lst –samples=1000 –seed=1234 –bin_by_count=1
–no_of_bins=5 –idv=tad –predcorr –dir=run1_tad

The command line parameters are listed below:

vpc	Call the PsN to run VPC
run1.mod	Name of model file

-lst	Name of result file
-samples	Number of simulated datasets to generate
-seed	A seed to generate random number
-bin_by_count	Request data binning (0 = each bin has an equal width based on the independent variable, 1 = each bin has an equal counts of observations)
-no_of_bins	Number of bins
-idv	Name of the independent variable
-predcorr	Perform prediction correction of dependent variable values
-dir	Name of directory in which the output will be stored

In this study, the *–predcorr* option was used for all analyses and time after dose (TAD) was set as an independent variable. Initial analysis was performed without binning the data. The data were subsequently binned both by width (each bin has similar width of independent variable) and by count (each bin has similar amount of data). Different numbers of bins, ranging from four to ten bins, were compared. Since the PsN program itself does not produce graphical outputs, VPC results were then processed with Xpose Version 4.0 (Jonsson & Karlsson, 1999), which is implemented in R software Version 2.9.2. Xpose reads two files, 'vpctab', which contains the original observed data and 'vpc_results.csv', which contains the VPC results. To create VPC plots, the Xpose library was loaded within R by typing the following script:

library(xpose4)

and then a basic VPC plot was created with the following script:

xpose.VPC()

There are several ways to construct more informative VPCs (by altering the appearance). The R script used in this study is shown below:

xpose.VPC(PI.real=T, PI.limits=c(0.1,0.9), PI.ci="area", PI.ci.up.arcol="blue", PI.ci.down.arcol="blue", PI.ci.med.arcol="red", PI.real.up.col="red", PI.real.down.col="red", PI.real.med.col="red", PI=NULL)

The following is the meaning of arguments:

PI.real	Plot the median/percentile of the real data in various bins (can be selected either 'NULL' or 'TRUE')
PI.limits	A vector of two values that describe the limits of the prediction interval displayed (the limit values can be found in vpc_results.csv file).
PI.ci	Plot the confidence interval for the percentiles of the simulated data for each bin. For each simulated dataset, percentiles for each bin are computed, then all percentiles from all of the simulated datasets were used to compute the CI of these percentiles (can be selected either 'area', 'lines' or 'both')
PI.ci.up.arcol	The colour of the upper PI.ci
PI.ci.down.arcol	The colour of the lower PI.ci
PI.ci.med.arcol	The colour of the median PI.ci
PI.real.up.col	The colour of the upper PI.real
PI.real.down.col	The colour of the lower PI.real
PI.real.med.col	The colour of the median PI.real
PI	Whether prediction intervals should be added to the plot (can be selected either 'area', 'lines' or 'both'. In this study, the 'NULL' option was used to plot confidence intervals for the percentiles instead of the prediction interval)

4.2.4 Normalised prediction distribution error (npde)

The add-on package npde Version 1.2 (Brendel *et al.*, 2006; Comets *et al.*, 2008) for the R software was used to compute npde. This package requires two files: the one containing the original dataset (named 'observed data') and the one containing the simulations (named 'simulated data'). The following outlines the way these two files were prepared before running the npde package.

1) Observed data

The final model was run again. The table file was generated as a tab format without a header. This file has to contain at least the following three columns:

1) ID Patient identification
2) xobs Independent variable (time, and time after the dose was investigated in this study)
3) yobs Dependent variable (concentration)

An additional column was added in the present study, that of missing dependent variable (MDV). This column indicates missing data (with '0' representing missing data and '1' observed data). During the computation of npde, the missing observations (MDV value of 0) were removed from the observed dataset reported in the graphical output. It should be noted that excluding the MDV column may lead to misleading results. Further columns are optional, depending on the final model developed. In the present study, body weight, sodium concentration, and high mortality risk were included in the final model and were therefore added to the dataset use for the simulations.

2) *Simulated data*

This file contains simulated datasets stacked one after the other. The simulated data file must contain at least three columns, in the following order: ID, xobs (TIME or TAD, depending on which independent variable is to be used for analysis), yobs (DV). In this study, one thousand simulated datasets without header were generated in tab format using NONMEM Version VI (Beal *et al*., 1989-2006).

After preparing two input data files containing observed and simulated data, npde were computed by typing the following command on R command window. Initially, the npde library was loaded by:

library("npde")

then the function *autonpde()* was called. The minimum input includes the name of the observed data file and the name of the simulated data file, but a number of options can be used as arguments. The following example is of the command used to run the npde package in this study:

autonpde<-function(manobs="CIPRO.TAB", namsim="CIPROSIM.TAB", iid=1, ix=3, iy=4, imdv=5, namsav="output.eps", boolsave=T, type.graph="jpeg", output=T, verbose=T, calc.npde=T, cal.pd=T)

The following is the meaning of arguments:

manobs	Name of the observed data file
namsim	Name of the simulated data file
iid	Number of the column in which ID is located in the observed data file
ix	Number of the column in which xobs is located in the observed data file
iy	Number of the column in which yobs is located in the observed data file
imdv	Number of the column in which MDV is located in the observed data file
namsav	Name of the files in which results are saved
boolsave	Whether graphs should be saved to a file
type.graph	Graph format (can be selected either 'JPEG', 'PNG', or 'PDF')
output	Whether the function returns the results
verbose	Whether a message should be printed as the computation of npde begins in a new subject
calc.npde	Whether npde should be computed
calc.pd	Whether pd should be computed

The advantages of the computation for npde are that a statistical test can be applied to test adequacy of the final model. Under the null hypothesis (H_0) that the final model adequately describes the data, the npde should have a mean of zero and a variance of one. Three statistical tests implemented in npde package were used to test this assumption: Wilcoxon signed rank test, Fisher variance test, and Shapiro-Wilks test. These three tests were combined with a Bonferroni correction and were reported as a global test. If the final model describes the data adequately, these statistical tests

are expected to be non-significant. In addition, the central moments of the npde distribution (mean, variance, skewness and kurtosis) were examined. The expected values of these variables are 0, 1, 0 and 0, respectively.

4.3 RESULTS

4.3.1 Bootstrap estimates

The results from the bootstrap are presented in Table 4.1. The median value of absorption rate constant (ka) estimated from the final model was 2.97 h^{-1}, which was lower than the median estimate from the bootstrap (3.44 h^{-1}). Furthermore, the 95% confidence interval was also wide, ranging from 1.32 to 8.86. This indicated poor precision. For the ALAG, the bootstrap estimate of 0.792 hours was almost identical to the value obtained from the final model (0.742) but a wide range of confidence interval was again observed (0.168-0.924). The 95% confidence interval for the additive error was also wide, ranging from 0.0041 to 0.0438, with a median value of 0.0278 which was similar to the value estimated from the final model (0.0273). Apart from ka, ALAG and additive error, the other population parameter estimates obtained from the bootstrap were generally comparable with the estimates from the final model, and the 95% confidence intervals were narrow, indicating good precision of these parameters.

Table 4.1 Parameter estimates obtained from the bootstrap and the final model

Parameters	Population estimate	Bootstrap estimate	Bootstrap 95% CI
CL/F (L/h/70 kg)	42.7	42.5	(37.0, 49.3)
V/F (L/70 kg)	372	367	(316, 429)
ka (h^{-1})	2.97	3.44	(1.32, 8.86)
ALAG (h)	0.742	0.792	(0.168, 0.924)
NA^+ CL/F	0.0368	0.0361	(0.0217, 0.0446)
HIGH CL	-0.283	-0.285	(-0.412, -0.118)
NA^+ V/F	0.0291	0.0282	(0.0155, 0.0388)
BSV CL/F	38.1	37.8	(28.7, 45.8)
BSV V/F	43.0	42.9	(32.4, 51.8)
BSV ka	102	110	(56, 159)
Additive error (SD)	0.0273	0.0278	(0.0041, 0.0438)
Proportional error (%CV)	18.6	17.8	(14.0, 22.6)

Key: CL/F = oral clearance, V/F = oral volume of distribution, ka = absorption rate constant, ALAG = absorption lag time, BSV = between subject variability expressed as a percentage coefficient of variation (%CV), NA^+ = sodium concentration, HIGH = high risk of mortality.

4.3.2 Jackknife analysis

The jackknife standard errors were similar to those values estimated with NONMEM (Table 4.2). The mean population parameters for ka (θ_3), ALAG (θ_4) and inter-individual variability of ka (η_3) derived from the jackknife sample were higher than those estimated with NONMEM, while other mean population parameters were almost identical.

The estimates of the population parameters from the jackknife samples are shown in Figure 4.1. There was little variability in population parameter estimates between jackknife samples for CL (θ_1) and V (θ_2) with most estimates being within 5% of the final population estimate. However, CL was 5.3% higher when Patient 38 was removed. Patient 18 had the greatest impact on the V estimate, which dropped 10.3% after this patient was removed from the dataset. For θ_5 and θ_7, most jackknife samples were within 5% of the final population estimates with only four or five jackknife samples varying more than that (by approximately 10%). Removal of any single individual had little effect on the θ_6. The population estimates of ka and ALAG were found to be the most sensitive to removal of individuals with maximum variations of +76% and -43%, respectively. For inter-individual variability of CL (η_1) and V (η_2), only a few jackknife samples varied by more than 5% from the final estimates. It was found that the inter-individual variability of ka (η_3) varied with a maximum variation of 226% when patient 15 was removed. The jackknife estimates of the additive error varied by more than 5% in 28 jackknife samples (more than 10% in 15 samples), and the proportional error varied by more than 5% in 12 jackknife samples.

Table 4.2 Population parameter estimates and standard error obtained from NONMEM and jackknife analysis

Parameters	Estimated from NONMEM		Estimated from jackknife analysis	
	Population estimate	***se***	**Mean population estimate**	***se***
θ_1	42.7	3.23	42.7	3.16
θ_2	372	27.1	371	27.1
θ_3	2.97	1.29	3.39	1.50
θ_4	0.742	0.138	0.760	0.163
θ_5	0.0368	0.00467	0.0370	0.00471
θ_6	-0.283	0.066	-0.285	0.066
θ_7	0.0291	0.00512	0.0288	0.00524
η_1	0.145	0.0295	0.148	0.0300
η_2	0.185	0.0452	0.186	0.0468
η_3	1.05	0.595	1.21	0.717
σ_1	0.0273	0.0143	0.0266	0.0155
σ_2	0.186	0.028	0.186	0.032

se = standard error

$TVCL\ (L/h) = \theta_1 \times (WT/70)^{0.75} \times (1+ \theta_5*(Na^+ -136)) \times (1+ \theta_6 *(High))$

$TVV\ (L) = \theta_2 \times (WT/70) \times (1+ \theta_7*(Na^+ -136))$

$TVKA\ (h^{-1}) = \theta_3$

$ALAG\ (h) = \theta_4$

$CL = TVCL*EXP(\eta_1)$

$V = TVV*EXP(\eta_2)$

$KA = TVKA*EXP(\eta_3)$

$C_{obs} = IPRED+SQRT(\sigma_1^2+ \sigma_2^2*IPRED^2)$

Figure 4.1 Population parameter estimates from jackknife samples

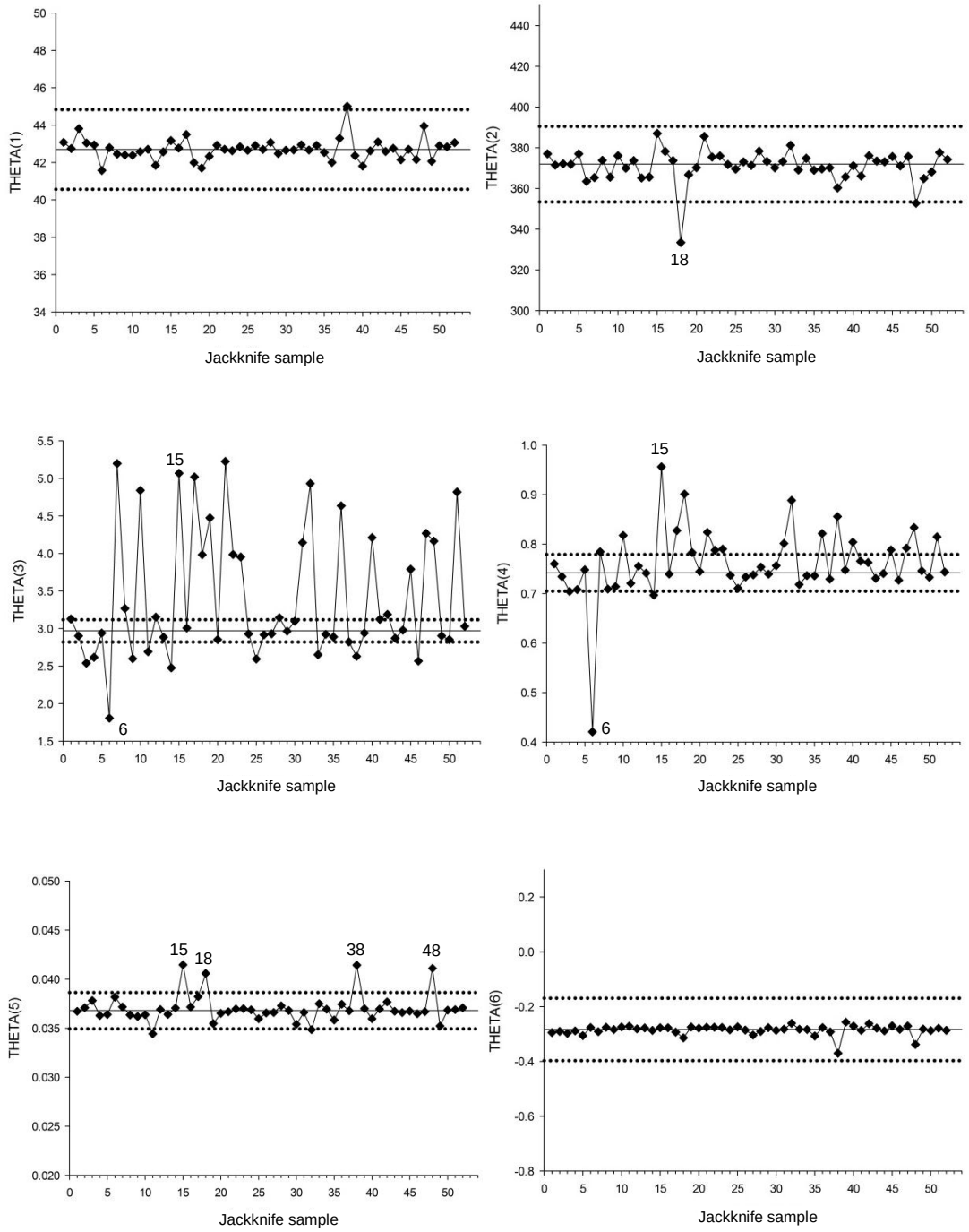

NB Jackknife sample 1 was the dataset excluding Patient 1, etc.
The solid line represents the population estimate from final model.
The dotted line represents ±5% from the final population estimate.

Figure 4.1 (continued)

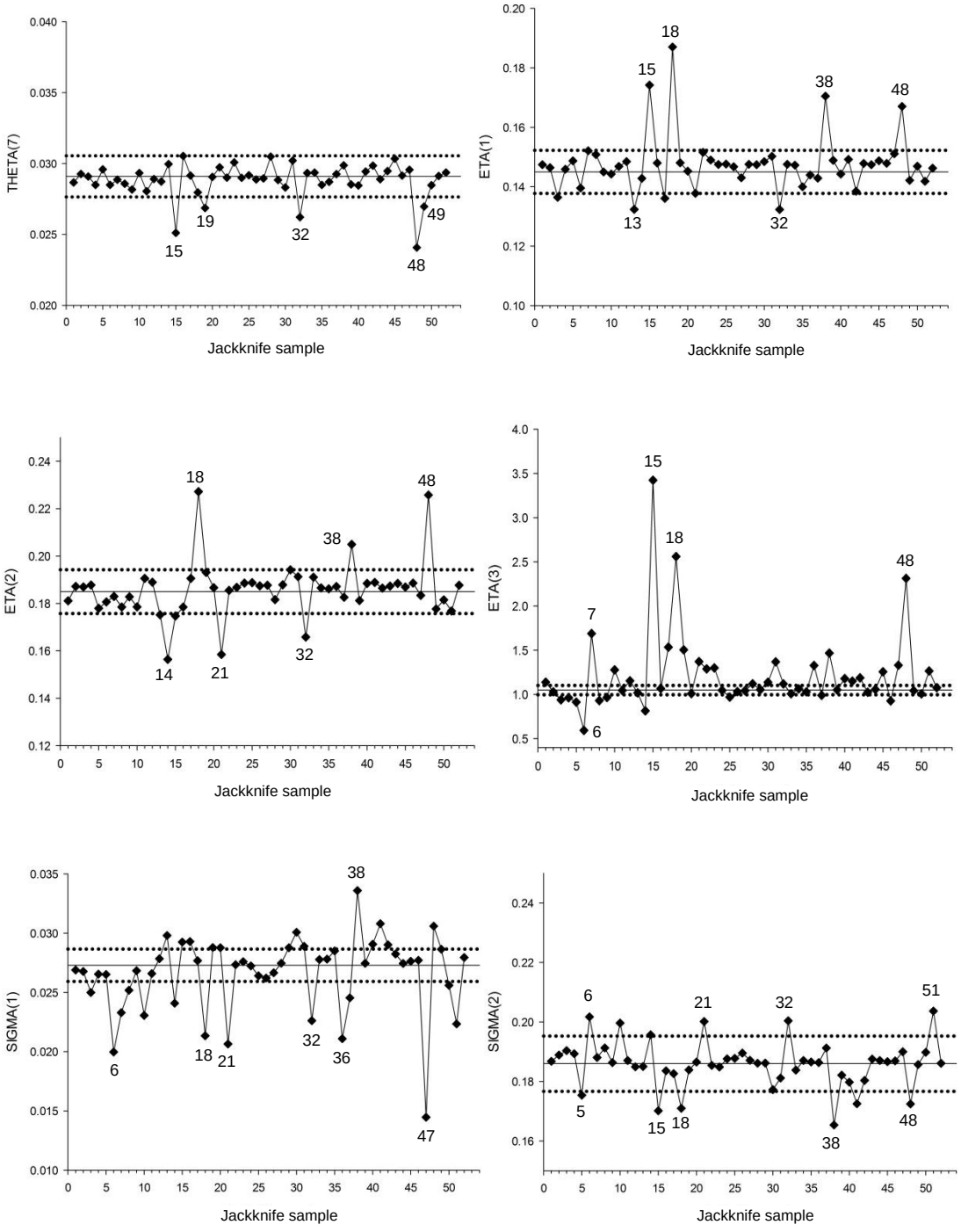

NB Jackknife sample 1 was the dataset excluding Patient 1, etc.
The solid line represents the population estimate from final model.
The dotted line represents ±5% from the final population estimate.

4.3.3 Visual predictive check (VPC)

Figure 4.2A and 4.2B show the results of VPCs performed for the medians (solid red line), and 10% and 90% percentiles (dashed red lines) for the observed data; the 95% confidence intervals (based on 1000 simulations) for the median (red field), and 10% and 90% percentiles (blue field) were also constructed. Figure 4.2A shows the results after binning the data to have a similar number of dependent variables (drug concentrations) into 4 bins, and Figure 4.2B 5 bins. These plots indicate that the model predicts the data adequately. Binning the data to have similar widths of independent variable values also indicates that there is no model misspecification (Figure 4.3A and 4.3B).

4.3.4 Normalised prediction distribution error (npde)

Table 4.3 shows the statistical results of the npde. Using the different independent variables of time and time after dose gave the same result. The mean, variance and skewness were close to the expected values of 0, 1 and 0. However, a slightly positive kurtosis was observed (0.3294). The results from statistical tests suggest that the distribution of npde followed a normal distribution. The shape of the distribution of the npde is presented in Figure 4.4. There were no trends observed (H_0 is true), meaning that the final model described the data adequately.

Figure 4.2 Graphical output from visual predictive check after binning the data by count

A: 4 binning intervals **B: 5 binning intervals**

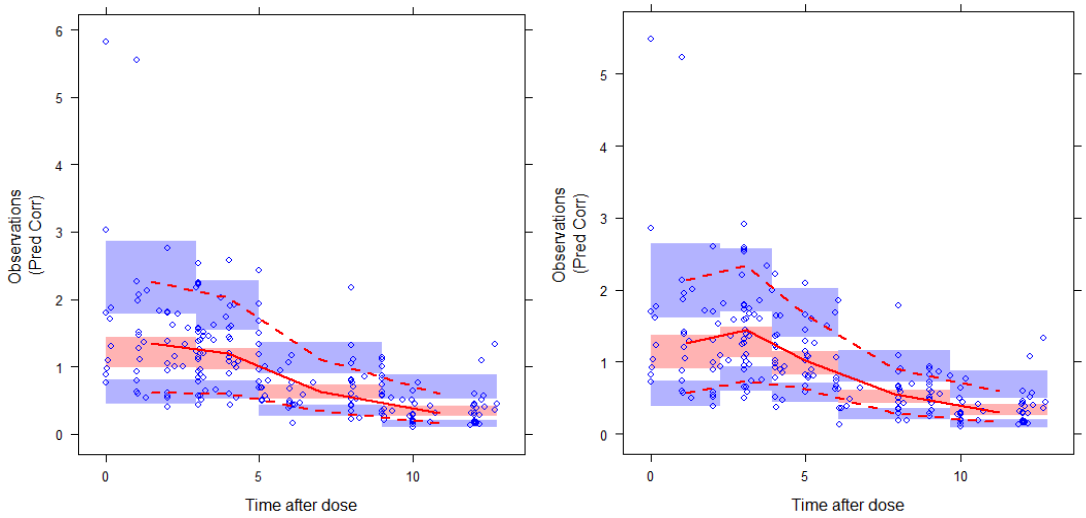

Figure 4.3 Graphical output from Visual Predictive Check after binning the data by width

A: 4 binning intervals **B: 5 binning intervals**

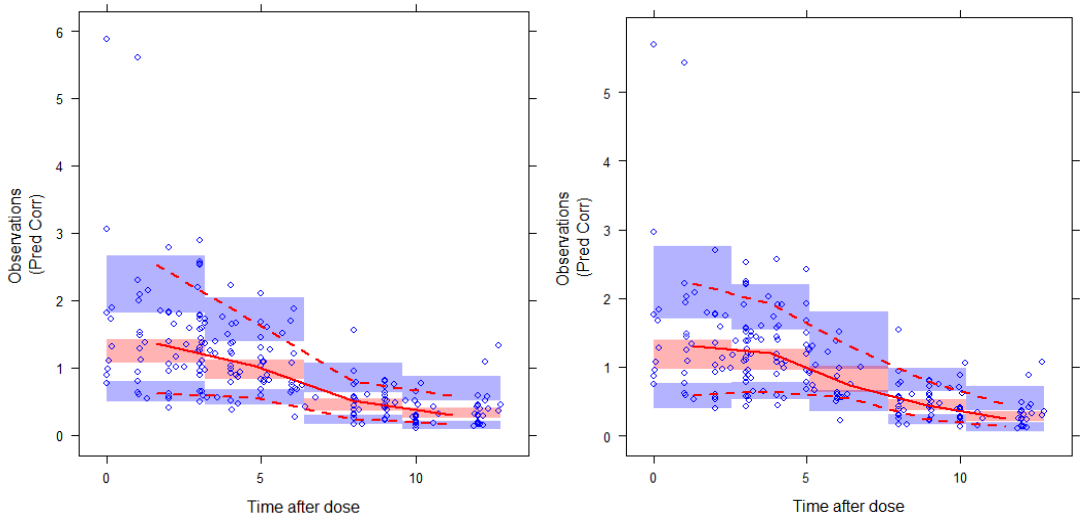

Table 4.3 Results for the distribution of npde and statistical tests used to evaluate the null hypothesis (H_0)

npde tests	Independent variable	
	Time	**Time after dose**
Distribution of npde		
Mean	0.0474	0.0474
Variance	1.074	1.074
Skewness	-0.07766	-0.07766
Kurtosis	0.3294	0.3294
Statistical tests		
Wilcoxon signed rank test	$p = 0.403$	$p = 0.403$
Fisher variance test	$p = 0.447$	$p = 0.447$
Shapiro-Wilks test	$p = 0.359$	$p = 0.359$
Global test	$p = 1$	$p = 1$

Figure 4.4 Graphical output from npde analysis: Quantile-quantile plot of npde versus expected standard normal distribution (upper left); Histogram of npde with density of overlaid standard normal distribution (upper right); Scatter plot of npde versus independent variable X or time after dose (lower left); Scatter plot of npde versus predicted Y or concentration (lower right)

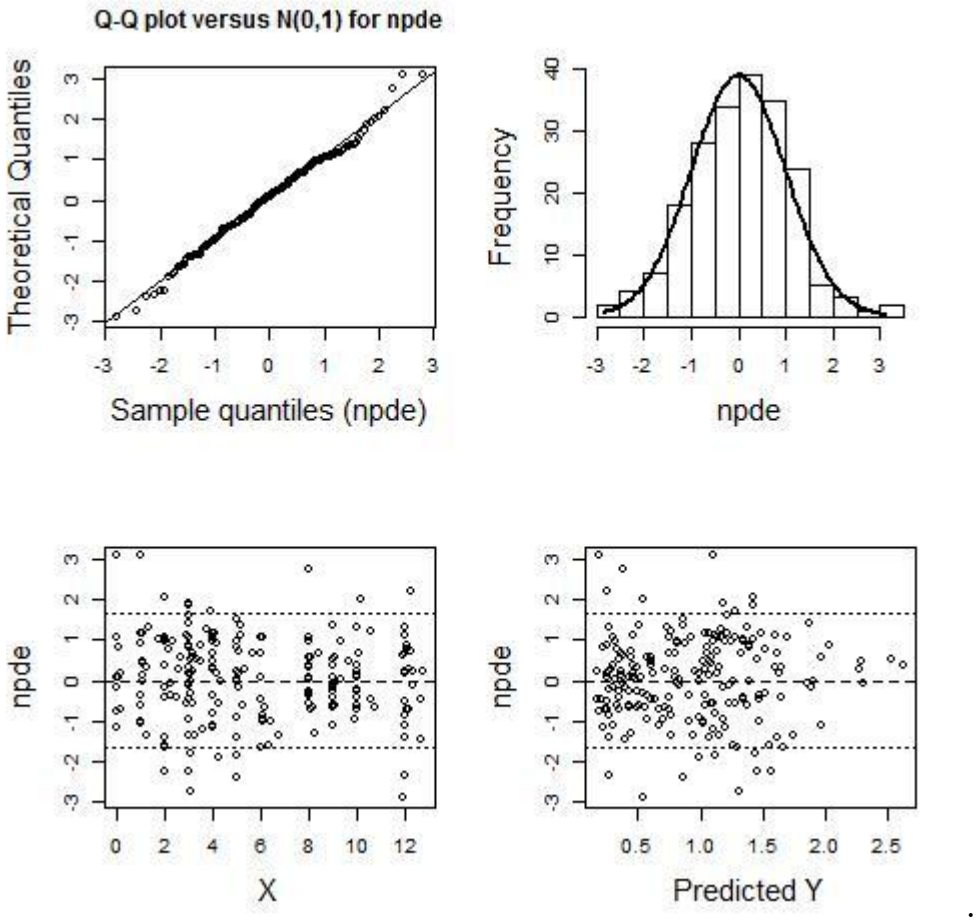

:

4.4 DISCUSSION

The population PK model for oral ciprofloxacin developed in the previous chapter is aimed for use in determining the optimal dosage guideline for children with severe malnutrition. Therefore, the predictive performance of the final model needs to be validated. Since a new validation dataset was not available in the present study, internal validation techniques only were applied.

Although data splitting is often recommended (Ette, 1997), the number of patients recruited in the present study was rather small (n = 52) to split the data into a learning and a validation dataset. Bootstrapping was used to test the performance of a population model for its predictive accuracy. The poor precision results observed for ka and ALAG, as judged by the wide confidence interval range, may have been due to the insufficient information with which to estimate these parameters. The wide confidence interval of the additive error model could have been the result of a poor fit of early time-points data to the absorption model. Likewise, the results from the jackknife analysis showed that estimations of ka and ALAG were highly influenced by certain individuals.

In contrast, the estimations of CL and V were more precise and accurate, as indicated by narrow bootstrap confidence intervals. The results from the jackknife analysis also revealed that removal of individuals did not result in any major changes to these parameters. It was noticed that the population estimate for V decreased with a maximum of 10.5% when Patient 18 was removed. This patient was identified as having the largest individual parameter estimates, of 14.2 L/kg compared to the mean population value of 5.47 L/kg. Removal of this patient would probably have resulted in a significantly decreased population value.

Standard errors calculated from the jackknife samples were comparable to those estimated with NONMEM. This is consistent with the previous study by Gibiansky *et al.* (2001), which demonstrated that standard error estimated by NONMEM was in most cases reliable and rarely improved by more computer intensive methods such as bootstrap, jackknife and likelihood profile techniques.

The graphical results from the VPC suggest that the model is relatively robust and able to reproduce the variability in the observed data. It should be noted that the interpretation of VPC is somewhat subjective, depending on the appearance of the plots. In this study, a number of plots were produced using different number of bins and variables for binning, and no evidence of model misspecification was observed in any plots. The robustness of the model was also confirmed statistically using an npde test.

The various internal validation techniques used in this study found that the models for CL and V are robust and have favourable predictive performance, whereas the models for ka and ALAG are influenced by individuals. The efficacy of ciprofloxacin is the determined by the AUC, which can be calculated using the CL (Dose/CL), so a conclusion of the usefulness of the model with respect to its ability to predict CL is warranted.

CHAPTER 5

DEVELOPMENT OF NEW DOSAGE REGIMENS OF ORAL CIPROFLOXACIN FOR MALNOURISHED CHILDREN

5.1 INTRODUCTION

The aim of this chapter was to (i) develop new dosage regimens of oral ciprofloxacin for severely malnourished children by using the final population PK model derived in Chapter 3, (ii) determine PK-PD susceptibility breakpoints of ciprofloxacin, and (iii) compare the PK-PD breakpoints with the values reported by international organisations, including the Clinical and Laboratory Standards Institute (CLSI) and the European Committee on Antimicrobial Susceptibility Testing (EUCAST).

5.2 METHODS

5.2.1 Microbiological data

Five pathogenic bacteria that commonly cause bacteraemia in malnourished children, including Gram-negative organisms i.e. *Salmonella* spp., *P. aeruginosa*, *K. pneumoniae*, *E. coli*, and Gram-positive organisms i.e. *S. pneumoniae*, were selected. The MIC distribution data of their clinical isolates were derived from the database of the EUCAST (2011). The CLSI and EUCAST susceptibility breakpoints for ciprofloxacin are consistent for all Gram-negative organisms investigated in this study (CLSI, 1 mg/L; EUCAST, 0.5 mg/L) (CLSI, 2012; EUCAST, 2011). The CLSI does not have a breakpoint for *S. pneumoniae* whereas the EUCAST reported a breakpoint value of 0.125 mg/L for this organism.

5.2.2 Probability of target attainment

The final parameters of the population PK model obtained in Chapter 3 were used to perform a 10,000 subject Monte Carlo Simulation using NONMEM Version VI (Beal *et al*., 1989-2006). The control file for simulation is presented in Figure 5.1. The clinical characteristics included in the model, i.e. body weight and sodium concentration, were sampled from a log-normal distributions with outer limits set to the values observed in the raw data (weight 4.1-14.5 kg; sodium concentration 120-160 mmol/L). The incidence of high risk of mortality in the simulated dataset was set equal to 31%. Simulations were conducted for three dosage regimens: 20 mg/kg/day (current daily dosage regimen); 30 mg/kg/day; and 45 mg/kg/day. AUC_{0-24} estimates

were calculated for each simulated patient by using daily dose and oral clearance ($AUC_{0\text{-}24}$ = Dose/CL/F).

The probability of target attainment (PTA), which was defined as the probability that the pharmacodynamic target of the drug was achieved, was estimated at each MIC. In the present study, target $AUC_{0\text{-}24}$/MIC ratios of ≥125 and ≥35 were used for Gram-negative (Forrest *et al.*, 1993) and Gram-positive organisms (Lacy *et al.*, 1999, Lister & Sanders, 1999), respectively. For each ciprofloxacin regimen, the highest MIC at which the PTA achieved ≥90% was defined as the PK-PD susceptibility breakpoint.

5.2.3 Susceptibility interpretations

Cumulative MIC distributions for five organisms were extracted from the EUCAST database. Consequently, PK-PD, CLSI, and EUCAST breakpoints were applied to these distributions in order to evaluate the impact of breakpoint discrepancies on the interpretation of global organism susceptibilities.

Figure 5.1 NONMEM control file for simulation of patient data

```
$PROB SIMULATION
$INPUT ID TIME DV MDV EVID AMT CMT TYPE WT NA HIGH
$DATA  DATA.CSV IGNORE=#
$SUBROUTINE ADVAN2 TRANS2

$PK
WT2=WT*EXP(ETA(4))
IF(WT2.LT.4.1)WT2=WT
IF(WT2.GT.14.5)WT2=WT

NA2=NA*EXP(ETA(5))
IF(NA2.LT.120)NA2=NA
IF(NA2.GT.160)NA2=NA

IF(ICALL.EQ.4) THEN
RISK=0
CALL RANDOM(2,R)
HRSK=R
IF(HRSK.LT.0.31) THEN
RISK=1
ENDIF
ENDIF

TVCL=THETA(1)*(WT2/70)**0.75*(1+THETA(7)*(NA2-136))*(1+THETA(8)*RISK)
TVV=THETA(2)*(WT2/70)**1*(1+THETA(9)*(NA2-136))
TVKA=THETA(3)
CL=TVCL*EXP(ETA(1))
V=TVV*EXP(ETA(2))
KA=TVKA*EXP(ETA(3))
ALAG1=THETA(4)
S2=V

$ERROR
IPRED=F
W=SQRT(THETA(5)**2+THETA(6)**2*F**2)
IRES=DV-IPRED
IWRES=IRES/W
Y=F+W*ERR(1)
$THETA (42.7) (372) (2.97) (0.742) (0.0273) (0.186) (0.0368) (-0.283) (0.0291)
$OMEGA BLOCK(3)
0.145
0.105 0.185
0.0643 0.193 1.05
$OMEGA 0.0783 0.0024
$SIGMA 1 FIX
$SIMULATION (399069982) (1503701723 UNIFORM) ONLYSIM SUBPROBLEMS=10000
$TABLE ID TVCL CL WT2 NA2 NOPRINT NOAPPEND NOHEADER FILE=SIM1.TAB
```

5.2.4 Cumulative fraction of response

Since the MIC values may be located primarily at one end or the other of the range of MICs, the calculated PTA for each MIC requires to be integrated with the MIC distribution data for each organism in order to properly interpret the likelihood of response by dose. The cumulative fraction of response (CFR) was used to determine the expected overall response of each pathogen to ciprofloxacin with each of the three dosage regimens. This estimate takes into account the variability of the drug exposure in the population, as embodied in the Monte Carlo simulation. It also takes into consideration the variability in the MIC of the drug for clinically appropriate pathogens, as embodied in the measured distribution of MICs for the pathogens. For each MIC value, the fraction of simulated patients who met the pharmacodynamic target ($AUC_{0\text{-}24}$/MIC $\geq$125 or $\geq$35) was multiplied by the fraction of the distribution of microorganisms for which the MIC was at that MIC value. The CFR was calculated as the sum of fraction products over all MICs (Drusano *et al*., 2001). Table 5.1 shows the method for calculating CFR by using the MIC distribution of *E. coli* and a dosage regimen of 20 mg/kg/day.

Table 5.1 Example of data used to calculate CFR

MIC (mg/L)	Number of isolates	Percentage of distribution at the indicated MIC	Fraction target attainment (AUC_{0-24}/MIC≥125) at the MIC	Percentage products
0.002	14	0.078	1	0.078
0.004	189	1.057	1	1.057
0.008	4433	24.797	1	24.797
0.016	7543	42.194	1	42.194
0.032	1684	9.420	1	9.420
0.064	693	3.876	0.991	3.842
0.125	623	3.485	0.762	2.654
0.25	624	3.491	0.239	0.835
0.5	241	1.348	0.019	0.026
1	121	0.677	0.0001	0.0000677
2	63	0.352	0	0
4	157	0.878	0	0
8	292	1.633	0	0
16	257	1.438	0	0
32	584	3.267	0	0
64	201	1.124	0	0
128	89	0.498	0	0
256	62	0.347	0	0
512	7	0.039	0	0
Sum	**17877**	**100**	**-**	**85**

5.3 RESULTS

5.3.1 Microbiological data

The MIC distributions extracted from the EUCAST database are displayed in Figure 5.2 as cumulative percentage plots and frequency distribution plots. The MICs at which 50% of isolates were inhibited were 0.032 mg/L for *Salmonella* spp. and *K. pneumoniae*; 0.25 mg/L for *P. aeruginosa*; 0.016 mg/L for *E. coli*; and 1 mg/L for *S. pneumoniae*. The MICs at which 90% of isolates were inhibited were 0.064 mg/L for *Salmonella* spp.; 2 mg/L for *K. pneumoniae* and *S. pneumoniae*; 8 mg/L for *P. aeruginosa*; and 1 mg/L for *E. coli*.

Figure 5.2 Cumulative percentage (left) and frequency distribution (right) of *Salmonella* spp., *P. aeruginosa, K. pneumoniae, E. coli,* and *S. pneumoniae*

A: *Salmonella* spp.

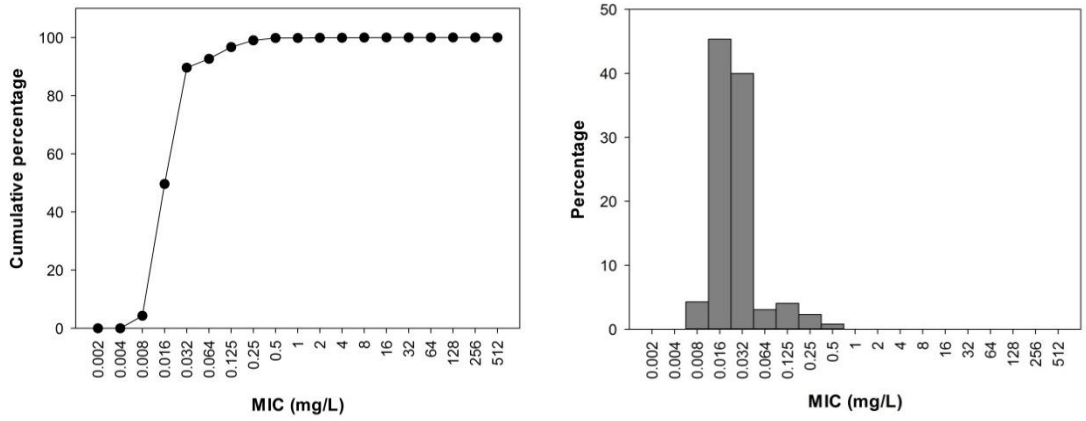

B: *P. aeruginosa*

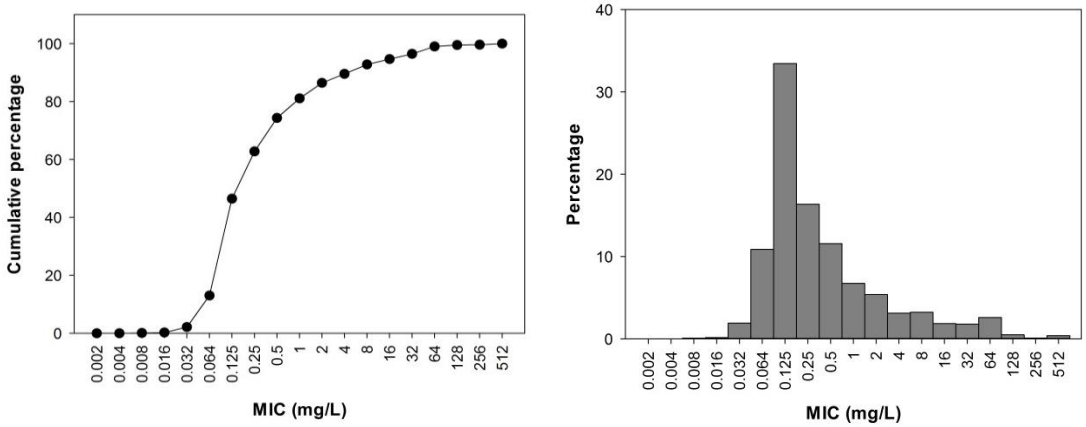

C: *K. pneumoniae*

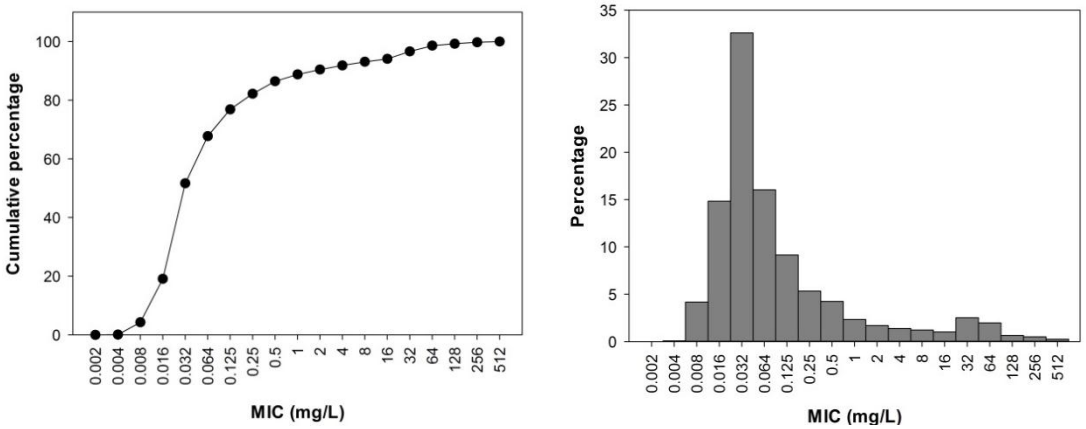

Figure 5.2 (continued)

D: *E. coli*

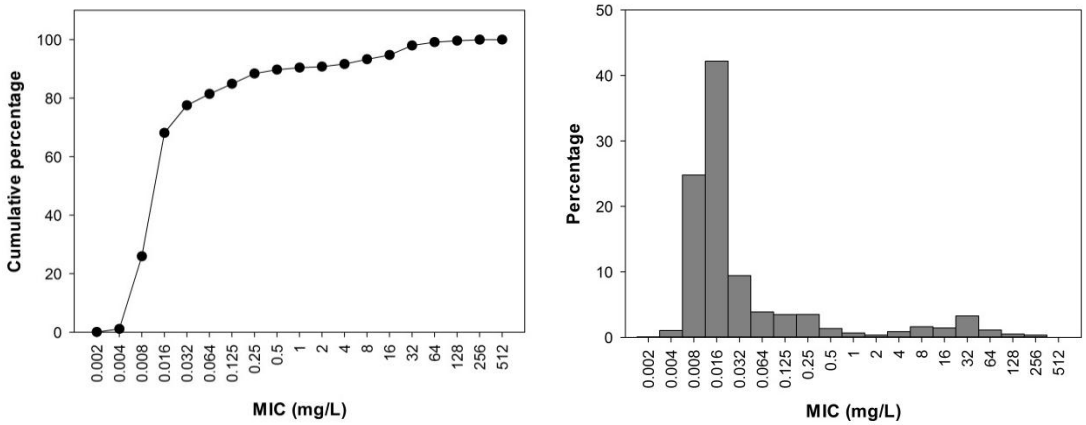

F: *S. pneumoniae*

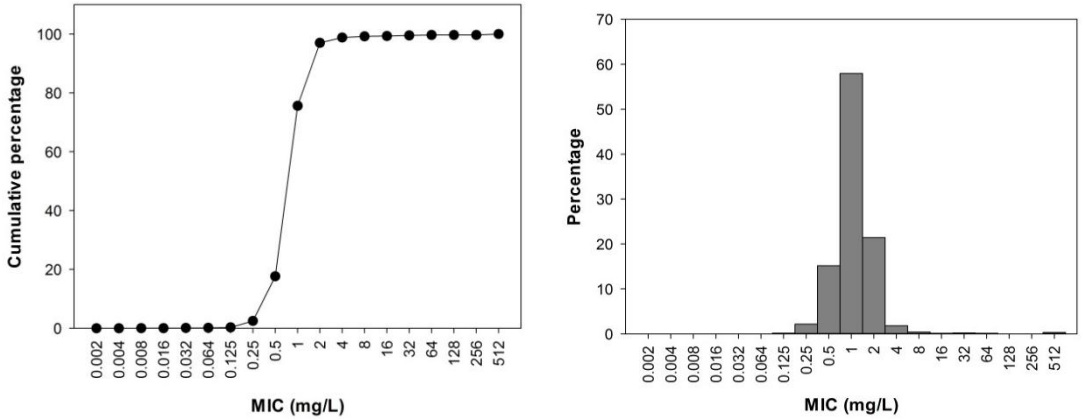

5.3.2 Probability of target attainment

The percentage of simulated patients who achieved an $AUC_{0\text{-}24}$/MIC ratio of ≥125 at each MIC value with three ciprofloxacin daily dosage regimens is illustrated in Figure 5.3A. With a dose of 20 mg/kg/day, only 76% of patients would be expected to achieve the therapeutic target if the MIC of the organism was 0.125 mg/L. However, with the higher doses of 30 and 45 mg/kg/day, the percentages increased to 95% and 99%, respectively. Therefore, the PK-PD susceptibility breakpoints for Gram-negative organisms were <0.06 mg/L for the current dose of 20 mg/kg/day and <0.125 mg/L for doses of 30 and 45 mg/kg/day. If the MIC was >1 mg/L, it was found that the target $AUC_{0\text{-}24}$/MIC ratio was attained in <5% of patients with all dosage regimens. For Gram-positive organisms, the PK-PD breakpoint was <0.25 mg/L for 20 mg/kg/day and <0.5 mg/L for 30 and 45 mg/kg/day (Figure 5.3B).

5.3.3 Susceptibility interpretations

Table 5.2 depicts the species-specific cumulative frequency distributions for ciprofloxacin. For *Salmonella* spp. and *E. coli*, breakpoint discrepancies resulted in lowest differences (<10%) in the percentage susceptibility. *S. pneumoniae* and *K. pneumoniae* had modest differences of 17.3% and 21.1%, respectively. In contrast, larger discrepancies were observed for *P. aeruginosa* with a difference of 68.1%. This indicates that the percentage of susceptible organisms varies greatly depending on which breakpoint is applied.

Figure 5.3 Percentage probability of achieving a target AUC_{0-24}/MIC ratio ≥125 (A) and ≥35 (B) with three daily doses of ciprofloxacin and a range of MIC values

A:

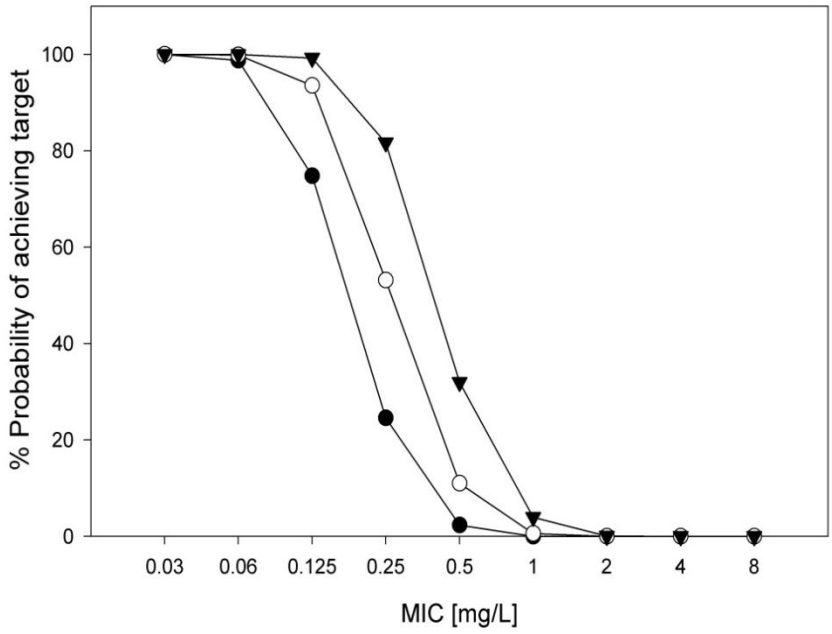

B:

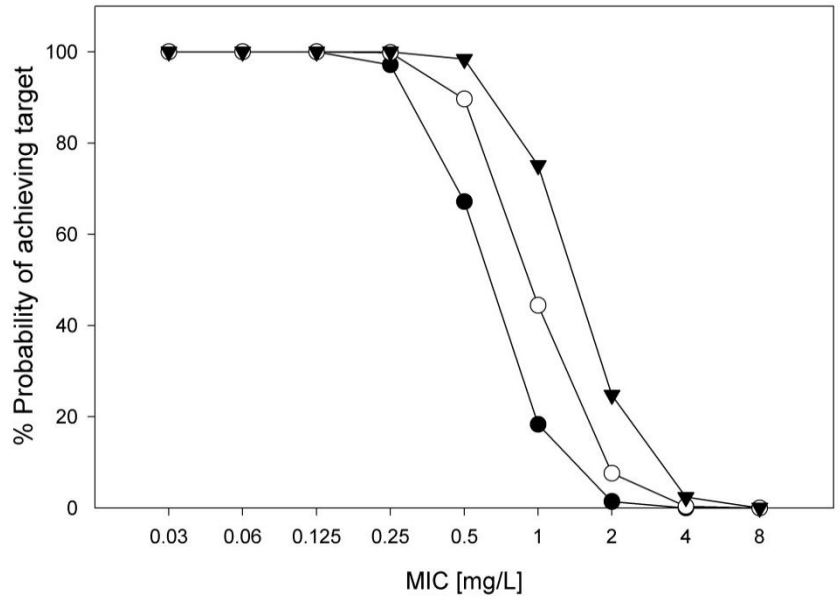

Key: Solid circles represent 20 mg/kg/day, open circles represent 30 mg/kg/day and solid triangles represent 45 mg/kg/day.

Table 5.2 Cumulative frequency distribution for *Salmonella* spp., *P. aeruginosa, K. pneumoniae, E. coli,* and *S. pneumoniae* isolates extracted from the EUCAST database with corresponding percentage susceptibility using PK-PD (P1 and P2), CLSI (C) and EUCAST (E) breakpoints

Organisms	No of isolates	Cumulative MIC (mg/L) distribution																		Divergence in %susceptibility[a]
		0.002	0.004	0.008	0.016	0.03	0.06	0.125	0.25	0.5	1	2	4	8	16	32	64	128	256	512	
Salmonella spp.	1733	0	0	4.3	49.6	89.6	92.7^{P1}	96.7^{P2}	99.0	99.8^{E}	99.8^{C}	99.9	99.9	99.9	100	100	100	100	100	100	7.1
P. aeruginosa	27855	0	0	0.1	0.2	2.1	13.0^{P1}	46.4^{P2}	62.8	74.3^{E}	81.1^{C}	86.5	89.6	92.8	94.6	96.4	99.0	99.5	99.6	100	68.1
K. pneumoniae	5898	0	0.1	4.3	19.1	51.7	67.7^{P1}	76.9^{P2}	82.2	86.4^{E}	88.8^{C}	90.5	91.9	93.1	94.1	96.6	98.6	99.2	99.7	100	21.1
E. coli	17877	0.1	1.1	25.9	68.1	77.5	81.4^{P1}	84.9^{P2}	88.4	89.7^{E}	90.4^{C}	90.8	91.7	93.3	94.7	98.0	99.1	99.6	100	100	9
S. pneumoniae	73840	0	0	0	0	0.1	0.1	0.3^{E}	2.5^{P1}	17.6^{P2}	75.6	97.0	98.8	99.2	99.3	99.5	99.7	99.7	99.7	100	17.3

[a] This column reflects the difference in percentage susceptibility among the three different breakpoints (PK-PD, CLSI and EUCAST). Large discrepancies indicate that percentage susceptible varies greatly depending upon which breakpoint is applied.
Key: P1 = PK-PD breakpoints for the dose of 20 mg/kg/day, P2 = PK-PD breakpoints for the dose of 30 and 45 mg/kg/day.

5.3.4 Cumulative fraction of response

Table 5.3 shows the CFR for each pathogen at the specific doses. It was found that more than 80% of patients would be expected to achieve the target AUC_{0-24}/MIC ratio of 125 with all three daily dosage regimens for *salmonella* spp. and *E. coli.* The predicted response was 80% for *K. pneumoniae* with a dose of 30 mg/kg/day. With the current dosage regimen of 20 mg/kg/day, CFR values were only 43% and 23% for *P. aeruginosa* and *S. pneumoniae*, respectively. CFR values for these organisms remained below 70% even if the dose was increased to 45 mg/kg/day.

Table 5.3 Cumulative fraction of predicted response to achieve the target AUC_{0-24}/MIC ratio for three dosage regimens of ciprofloxacin against *Salmonella* spp., *P. aeruginosa, K. pneumoniae, E. coli,* and *S. pneumoniae*

Organisms	Target AUC_{0-24} /MIC ratio	Cumulative Fraction of Predicted Response (%)		
		20 mg/kg/day	30 mg/kg/day	45 mg/kg/day
Salmonella spp.	125	96	98	99
P. aeruginosa	125	43	55	64
K. pneumoniae	125	76	80	83
E. coli	125	85	87	88
S. pneumoniae	35	23	44	67

5.4 DISCUSSION

In this chapter, the final population PK model was used to perform a simulation to estimate the PTA for different doses of ciprofloxacin. The results suggest that a dose of at least 30 mg/kg/day would be required to achieve an AUC_{0-24}/MIC ratio of 125 in >90% of patients if the MIC was 0.125 mg/L and that an MIC of <0.6 mg/L was necessary to achieve target AUC_{0-24}/MIC ratio with the current dose of 20 mg/kg/day. The current dose should be effective for Gram-positive organisms with an MIC <0.25 mg/L but higher doses would be required to achieve an AUC_{0-24}/MIC ratio of at least 35 in >90% of patients if the MIC was 0.5 mg/L. Using internationally derived distributions of the MICs of a range of organisms, including

the most common isolates in children with severe malnutrition complicated by invasive bacterial disease, a dose of 20 mg/kg/day was sufficient for most isolates of *Salmonella* spp. and *E. coli* but 30 mg/kg/day would be necessary to treat *K. pneumoniae* infections.

The results of this study were similar to previous reports that an oral daily dose of ciprofloxacin of 30 mg/kg/day would be more appropriate for children (Lipman *et al*., 2002; Peltola *et al*., 1998; Peltola *et al.*, 1992; Schaefer *et al*., 1995). Similar problems of underdosing have also been identified in adults. Standard intravenous doses of 400 mg twice daily yielded inadequate $AUC_{0\text{-}24}$/MIC and C_{max}/MIC ratios in critically ill patients unless the MIC was less than 0.25 mg/L (van Zanten *et al*., 2008). Montgomery *et al.* (2001) demonstrated that for an MIC of 0.5 mg/L, 400 mg 12 hourly would achieve an $AUC_{0\text{-}24}$/MIC >125 in only15% of adults with cystic fibrosis and that an increase to 600 mg 8 hourly would be required to achieve >90% success.

If the dose of ciprofloxacin used in the present study was increased to 15 mg/kg three times daily and assuming no change in bioavailability, the probability of achieving an $AUC_{0\text{-}24}$/MIC ratio above 125 would increase to 83% for an MIC of 0.25 mg/L and 32% for an MIC of 0.5 mg/L. However, 37% of patients would then reach daily AUCs above 60 mg·h/L. These values are higher than the mean daily AUCs reported following the administration of intravenous high dose ciprofloxacin (400 mg 8 hourly) to critically ill adults (Lipman *et al.*, 1998) and it is possible that such high exposure would increase the risk of toxicity. Recently, Khachman *et al.* (2011) investigated the PK of ciprofloxacin in intensive care unit patients and reported similar results. They found that the standard intravenous dose of 400 mg two or three times daily should achieve the target $AUC_{0\text{-}24}$/MIC ratio for the Gram-negative organisms *K. pneumoniae, P. mirabilis, E. cloacae* and *E. coli,* but not for *P. aeruginosa.*

DeRyke *et al*. (2007) also evaluated susceptibility breakpoints for Gram-negative organisms. Similar to the present study, they conducted PK-PD simulations to develop susceptibility breakpoints and then compared the percentage of susceptible organisms achieved using PK-PD and CLSI values. They found that PK-PD and CLSI breakpoints resulted in similar susceptibilities for some organisms, such as *Enterobacteriaceae*, but not *P. aeruginosa* and *Acinetobacter baumannii*. In the present study, it was found that the PK-PD breakpoints were generally lower than the CLSI and the EUCAST breakpoints. This was probably due to differences in the methods, the PK model and the PK parameters used for determining the susceptibility breakpoint. It should be noted that when PK-PD simulations are used to establish antimicrobial breakpoints, the following assumptions are made. Firstly, the therapeutic targets, such as $AUC_{0\text{-}24}$/MIC and C_{max}/MIC ratios, were derived from prior studies which have identified correlations between these parameters and clinical outcomes. In addition, these relationships have typically been obtained from immunocompromised murine models, although some have been validated in clinical populations (Ambrose *et al*., 2001). Secondly, breakpoints determined by using PK-PD simulation are dependent on PK models and PK parameters. Generally, the PK information is obtained from healthy adult data instead of patients with specific disease states. Since the elimination of antimicrobials in patient populations may be reduced, the use of healthy adult data may predict lower drug exposures, yielding lower PK-PD breakpoints. The results from the present study suggested that the discrepancies of susceptibility breakpoints between reference sources may have a significant impact on some organisms, i.e. *P. aeruginosa, K. pneumoniae,* and *S. pneumoniae*, but not on others, such as *Salmonella* spp. and *E. coli*. Frei *et al.* (2008) reported a slightly lower percentage susceptible to ciprofloxacin for *Enterobacteriaceae* (10%) and *P. aeruginosa* (24%). This could due to the fact that the PK model and PK parameters utilised in this study were derived from different populations. Moreover, they used a different database for extracting the MIC distributions.

In conclusion, oral treatment with a dose of 10 mg/kg twice daily should be effective against *Salmonella* spp. and *E. coli* but a higher dose of 10 mg/kg three times a day

would be recommended for *K. pneumoniae*. Oral ciprofloxacin is likely to be inadequate for treating *P. aeruginosa* and *S. pneumoniae.* In cases where these organisms are suspected, other effective antimicrobial agents should be considered. Discrepancies in susceptibility breakpoints exist between reference sources and wider differences occur for some organisms.

CHAPTER 6

OPTIMAL DESIGN OF POPULATION PHARMACOKINETIC STUDIES

6.1 INTRODUCTION

In the study of pharmacokinetics (PK), the population approach allows the use of sparsely sampled data from individual patients to estimate typical PK parameters (e.g. clearance and volume of distribution), inter-individual variability and residual variability. However, the design of population PK studies is not straightforward, and raises several questions that must be addressed before a study is conducted, including the following:

- How many subjects should be recruited?
- How many elementary designs or subgroups are required?
- How many subjects should be assigned to each elementary design?
- How many samples should be taken from each subject?
- What are the sampling times?

In order to identify the optimal design for such PK studies, prior information must be made available and then specified and implemented in the optimal design program. The required information is: a structural PK model (e.g. a one-compartment model with first-order absorption); typical PK parameter estimates (e.g. clearance, volume of distribution, absorption rate constant); and estimates of inter-individual variability and residual variability. In addition, information on the dosage regimen is used to characterise the drug concentration-time profile and must therefore be provided as an input variable.

Problems arise when previous studies and models used are very complex, such as models that contain covariate relationships. One important aim of population PK studies is to identify the influence of clinical factors on the PK parameters. Therefore, the majority of studies include at least one covariate (e.g. weight) in the population model under investigation. However, currently there are no optimal design programs that contain a standard function to account for covariates. This is due to the difficulty that program developers face in envisaging the kind of covariate model that researchers might incorporate into their population models. Furthermore, it is also impossible to account for all types of models. Therefore, individual adjustments to the optimal design model script for each population model are

required. Although a user-friendly features, such as a graphical user interface, is available in all optimal design programs, many investigators examining optimal design have modified or created their own script in order to implement models of greater complexity, as shown in the studies conducted by Green and Duffull (2003), Waterhouse *et al.* (2005), Roos *et al*. (2008), Ogungbenro *et al*. (2009), Hennig *et al*. (2012), and Sherwin *et al*. (2011). However, this is not a feasible option for researchers who do not have the relevant programming skills.

Furthermore, the drug PK are known to vary between patient populations; therefore, it is difficult to know whether the optimal study designs obtained from one population are appropriate to use in other populations. Prior information used to design a new population PK study should be considered when using optimal design techniques. It should be noted that the influence that discrepancies in prior information exert on the optimal design results has not been investigated to date.

The aims of the work in this chapter were:

(i) to develop optimal study designs and sampling windows for future PK studies of oral ciprofloxacin in malnourished children.
(ii) to compare different techniques for implementing study design and models.
(iii) to investigate the influence of a variety of prior information on the optimal study design.

6.2 METHODS

6.2.1 Programs for optimal design of population PK studies

Several programs are currently available for designing population PK studies. All of these use the same mathematical derivation of the Fisher information matrix (FIM), but vary in terms of their specific features; for example, they differ in the algorithm implemented and the function used to calculate sampling windows (Mentré *et al*., 2007). In this thesis, both the evaluation and the optimisation of study design were performed with the PopDes program, Version 4.0 (Gueorguieva *et al*., 2007) and MATLAB Version 7.13 (R2011b) (The MathWorks Inc., Natick, MA, 2011).

6.2.2 Overview of the basic features of PopDes

6.2.2.1 PopDes Windows

The PopDes Windows interface is initiated by opening MATLAB, changing to the PopDes program directory and typing 'PopDes' at the command line prompt. This opens the selection window shown in Figure 6.1. Several design options are available in this program (the details are given in Chapter 2). When the required design option has been selected, an input file called 'required_param.dat' is created by pressing 'Select'. This file contains a list of required input variables, such as dose, number of subjects, number of samples, etc. that are relevant to the selected design option. The 'Model' section of the interface provides two options: 'Model Library', which contains a range of PK models and 'External File', which allows a model to be created by the user. Two options are available for computing the FIM in the PopDes program: Block FIM, which computes the FIM as a block diagonal matrix; and Full FIM, which computes the full matrix. In the present study, the Full FIM option was selected for both design evaluation and optimisation. The 'Task' option was set at 'evaluation', when evaluating the original or pre-specified designs and 'optimisation' when developing optimal study designs. Four algorithms are available: Simplex; Hybrid; Exchange; and First-order.

6.2.2.2 PopDes script

PopDes scripts were written in MATLAB language and saved as MATLAB files. In order to evaluate and optimise the design with PopDes script, two PopDes files: 'ext_model.m' and 'PopDes.m' were developed. The first of these contained the PK model with lag time and covariate models, which were written in analytical form. The second file was used to specify design options and input variables.

Figure 6.1 Windows interface of the PopDes program

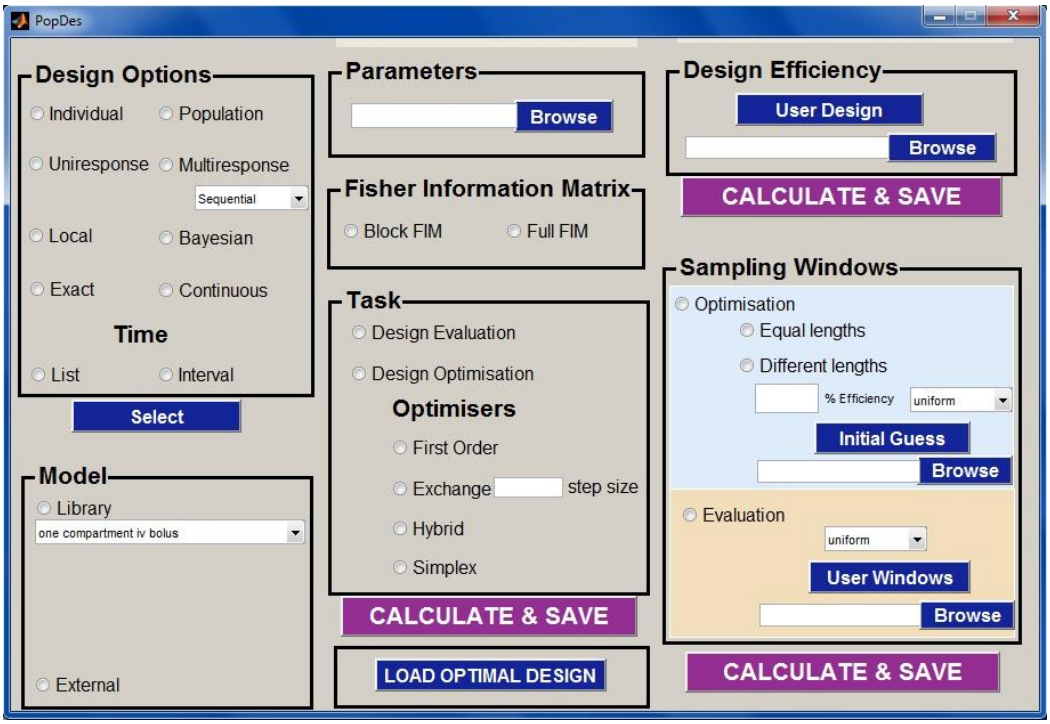

6.2.3 Original study design and results

The population PK study of oral ciprofloxacin in severely malnourished children was described in Chapter 3. In summary, a total of 52 malnourished children were administered 10 mg/kg oral ciprofloxacin every 12 hours. The population design was composed of three elementary designs, which had similar numbers of subjects. The number of sampling times was constrained at a maximum of four samples per individual. The allocations of sampling times and the number of subjects in each subgroup were as follows:

- *Group A* (n = 17): 2, 4, 8 and 24 hours after the first dose (a 24-hour sample was taken 12 hours after the second dose)
- *Group B* (n = 18): 3, 5, 9, and 12 hours after the dose
- *Group C* (n = 17): 1, 3, 6 and 10 hours after the dose

A total of 202 concentration measurements were fitted using non-linear mixed effects modelling. A one-compartment model with first-order absorption with a lag time adequately described the concentration data. The final model parameters were as follows:

$$\text{TVCL (L/h)} = 42.7\ (\text{L/h/70 kg}) \times (\text{WT}/70)^{0.75} \times (1 + 0.0368 \times (\text{Na}^{+} - 136)) \times (1 - 0.283 \times (\text{HIGH}))$$

$$\text{TVV (L)} = 372\ (\text{L/70 kg}) \times (\text{WT}/70) \times (1 + 0.0291 \times (\text{Na}^{+} - 136))$$

$$\text{TVKA} = 2.97\ \text{h}^{-1}$$

$$\text{ALAG} = 0.75\ \text{hours}$$

where TVCL is typical value of clearance (L/h), TVV is the typical value of volume of distribution (L), TVKA is typical value of absorption rate constant (h^{-1}), ALAG is an absorption lag time (hours), WT is weight (kg), Na^{+} is sodium concentration (mmol/L) and HIGH is high risk of mortality (if the patient had a high risk of mortality, HIGH=1 otherwise HIGH=0). The inter-individual random effects were assumed to be exponential for all PK parameters and a full variance-covariance matrix of random effects was estimated. A combined proportional and additive error was used for the residual model.

This original design and the final model were relatively complex and their direct implementation in the program was not possible without prior modifications. The major problems are listed below:

- Ciprofloxacin was administered as a weight-based dose.
- The study design combined patients who received a single dose (n = 35) and patients who received multiple doses (n = 17).
- Weight, sodium concentration and high risk of mortality were included in the final model as covariates.
- The structural model included an absorption lag time of 0.75 hours.

6.2.4 Design options and variables

Several design options are available for selection in the PopDes program. In the present study, the population uniresponse and local design options were used to both evaluate and optimise study design via the employment of both functions of PopDes (Windows and script). However, when optimising designs, both exact and continuous design options were investigated, as were both time list and time interval options. The details of these variables are given below.

6.2.4.1 The exact design

This option allows the group structure to be constrained. In this study, the maximum number of subjects that it was possible to include in the future study was assumed to be equal to the original study at 52, and different numbers of subgroups, ranging from one to three, were investigated. The same proportion was assumed for three elementary designs (17, 18 and 17), but different proportions including 0.5/0.5 (26 patients in each group), 0.65/0.35 (34 and 18 patients), 0.75/0.25 (39 and 13 patients) and 0.8/0.2 (42 and 10 patients) were compared when the number of elementary designs was fixed at two. The number of blood samples that were permitted to be taken from each patient was constrained to be three, four or five. These constraints provided a total of 18 possible design structures.

If the time interval was used, each design was optimised using the Simplex algorithm (SM), the Hybrid algorithm (HB) and the Exchange algorithm (EX). A grid size of 0.25 was used when optimising with the EX. The admissible sampling times were limited to between 0 to 12 hours after the first dose. However, if the designs were optimised with the time list option, two types of time lists, ‘rich’ and ‘sparse’, were applied. The rich list consisted of 46 possible sampling times from 0.75 hours until 12 hours after the dose. It was permitted for samples to be taken every 15 minutes during this period. The gap of 0.75 hours refers to the absorption lag time during which a drug concentration should not be measured. The possible sampling times in the sparse list were constrained to every 15 minutes during the first 3 hours and then hourly until 12 hours after the dose. To avoid the absorption lag, the first sampling time was again fixed to 0.75 hours after the dose. The 19 possible sampling times

included in the sparse list were 0.75, 1, 1.25, 1.5, 1.75, 2, 2.25, 2.5, 2.75, 3, 4, 5, 6, 7, 8, 9, 10, 11 and 12 hours. The two types of time list were used to identify the importance of sampling times during drug elimination. For the exact design optimisation, the time list option can only be used with the EX.

If the SM or the HB was used, the optimisation was repeated five or six times to ensure that the global minimal had been achieved. This was conducted by substituting the initial sampling times with the obtained optimal sampling times.

6.2.4.2 The continuous design

For this option, the group structures, i.e. the number of elementary designs, number of samples per elementary design, and number of subjects allocated to each elementary design, were determined in addition to the sampling times. Other variables, including total number of subjects in the study and the number of samples to be taken from each of them, were constrained in a similar manner as described for the exact design option. Only the First-order algorithm (FO) and the time list option can be used for the continuous design. When using the FO, it was again necessary to repeat the optimisation five or six times to ensure that the global minimal had been achieved. This was done by substituting the initial sampling times with the obtained optimal sampling times. Both types of time lists were tested with the continuous design.

6.2.5 Evaluation of the original study design

6.2.5.1 Evaluation of the original design using PopDes Windows

The use of PopDes Windows to evaluate the original design was limited by the complexities of its structure and the final model. As a result, the following assumptions were made when using PopDes Windows:

- All patients were given the same dose of ciprofloxacin. The median dose of 68.5 mg was used as the input variable.
- Median estimates of the typical values of clearance (TVCL) and volume of distribution (TVV) were used, as shown in Table 6.1, and these median values had already accounted for the variability of covariates in the model.

The typical value of absorption rate constant (TVKA) was used as an input variable without modification because there was no covariate in the model.

- The samples taken at 12 hours after the second dose provided the same information as those taken at 12 hours after the first dose, thereby simplifying the design. Therefore, the 24 hour sampling time from the 17 patients in Group A was converted to 12 hours, and all patients in the study were administered ciprofloxacin as a single dose.
- There was no lag time but the optimal sampling times were delayed by the lag time.

Population uniresponse and local design options were chosen when evaluating the study design. A one-compartment model with first-order absorption was selected from the model library. The input file created for specifying design variables contained several lines of variables, as shown in Figure 6.2.

Table 6.1 Population parameter values used with PopDes Windows to evaluate and optimise study designs

Parameters	Fixed effects (β)	Inter-subject variability (ω^2)
CL[a] (L/h)	6.82	0.145
V[b] (L)	37.2	0.185
ka (h^{-1})	2.97	1.05
$COV_{(CL,V)}$	-	0.105
$COV_{(CL,ka)}$	-	0.0694
$COV_{(V,ka)}$	-	0.193
Lag time[c] (h)	0.75	-
Additive[d] (SD)/SD^2	0.0273/0.0007	-
Proportional[d] (CV)/CV^2	0.186/0.035	-

[a] Median estimate of the typical value of clearance (TVCL).
[b] Median estimate of the typical value of volume of distribution (TVV).
[c] The lag time of 0.742 h obtained in previous chapter may not be applicable in practice. Thus, the lag time used in this study was rounded to be 0.75 h (45 min).
[d] In PopDes, the variance (SD^2) and the square of the coefficient of variation (CV^2) were used for the additive part and the proportional part, respectively.

Figure 6.2 Parameter estimates and design variables specified in the required_param.dat file

```
DOSE FOR EACH ELEMENTARY DESIGN
68.5
DOSE INTERVAL FOR EACH ELEMENTARY DESIGN
12
INITIAL FIXED EFFECT PARAMETER VALUES
2.97 6.8 37.2
VALUE OF THE FIXED EFFECT PARAMETERS CAN BE FIXED, INDICATE POSITION
(ENTER 0 FOR NONE)
0
OMEGA MATRIX ELEMENTS: DIAGONAL ELEMENTS ONLY OR FULL MATRIX (ROW-by-
ROW)
1.05 0.0694 0.193 0.0694 0.145 0.105 0.193 0.105 0.185
FIXING VALUES OF THE OMEGA MATRIX (DIAGONAL OR FULL) INDICATE: 1=NOT
FIXED 0=FIXED (ROW-by-ROW)
1 1 1 1 1 1 1 1 1
INDEPENDENT RANDOM EFFECTS MODELS: ENTER 1=EXPONENTIAL, 0=ADDITIVE
1
RESIDUAL ERRORS - PROPORTIONAL (CV^2) AND ADDITIVE (VARIANCE)
0.035 0.0007
NUMBER OF ELEMENTARY DESIGNS (GROUPS) IN THE DESIGN
3
NUMBER OF SUBJECTS IN EACH ELEMENTARY DESIGN
17 18 17
NUMBER OF DESIGN POINTS IN EACH ELEMENTARY DESIGN
4 4 4
INITIAL DESIGN POINTS FOR EACH ELEMENTARY DESIGN
1.25 3.25 7.25 11.25 2.25 4.25 8.25 11.25 0.25 2.25 5.25 9.25
LOWER BOUNDS OF TIME POINTS
0
UPPER BOUNDS OF TIME POINTS
12
```

The descriptions of each input variables are as follows:

1) DOSE FOR EACH ELEMENTARY DESIGN

In the present study, ciprofloxacin was orally administered to subjects as an individual dose, which was calculated based on the actual body weight of the patient. It was assumed that all the patients received the same dose by using the median value of 68.5 mg.

2) DOSE INTERVAL FOR EACH ELEMENTARY DESIGN

PopDes ignores dose interval for a single-dose study. However, the variables in the input file cannot be left empty, so this variable was fixed to the last sampling time at 12 hours.

3) INITIAL FIXED EFFECT PARAMETER VALUES

This was used to specify the estimates for the fixed-effect parameters. For a one-compartment model with first-order absorption, three parameters, including absorption rate constant (ka), clearance (CL) and volume of distribution (V), were listed, in that order, to ensure consistency with the order of parameters specified in the model that had been selected from the model library.

4) VALUE OF THE FIXED EFFECT PARAMETERS CAN BE FIXED, INDICATE POSITION (ENTER 0 FOR NONE)

The precision of any parameters can be computed by their inclusion in the FIM. The fixed-effect parameters (ka, CL and V) were the parameters of interest, and ‘0’ was entered for this variable. This indicated that these parameters were not fixed.

5) OMEGA MATRIX ELEMENTS: DIAGONAL ELEMENTS ONLY OR FULL MATRIX (ROW-by-ROW)

Since there was a correlation between the inter-individual variabilities of the parameters in this study, the full omega matrix was used. Each element of this matrix was listed row-by-row, beginning with ka, CL and V, respectively. The length of this variable was nine, which was equal to the square of the number of parameters.

6) FIXING VALUES OF THE OMEGA MATRIX (DIAGONAL OR FULL) INDICATE: 1=NOT FIXED 0=FIXED (ROW-by-ROW)

The number '1' was specified for this variable, indicating that each element of the omega matrix was not fixed. The length of this variable was nine, which was equal to the number of elements of the omega matrix defined for variable 5.

7) INDEPENDENT RANDOM EFFECTS MODELS: ENTER 1=EXPONENTIAL, 0=ADDITIVE

For this variable, '1' was entered. This indicated that the inter-individual variability in ka, CL and V was described by the exponential error model.

8) RESIDUAL ERRORS - PROPORTIONAL (CV^2) AND ADDITIVE (VARIANCE)

This variable was used for specifying the parameters for residual errors. In this study, the residual error was best described by the combined proportional and additive error model. The square of the coefficient of variation (CV^2) of 0.035 and the variance (SD^2) of 0.0007 were specified for proportional and additive elements, respectively.

9) NUMBER OF ELEMENTARY DESIGNS (GROUPS) IN THE DESIGN

This variable was used to specify number of subgroups, and '3' was entered. This indicated that the original design consisted of three subgroups of subjects.

10) NUMBER OF SUBJECTS IN EACH ELEMENTARY DESIGN

This variable was used to specify the number of subjects included in each subgroup. There were 17, 18 and 17 individuals in each subgroup, respectively, therefore the order was specified as '17 18 17'.

11) NUMBER OF DESIGN POINTS IN EACH ELEMENTARY DESIGN

The number of design points refers to the number of blood samples taken from each subject. In the study, four samples were collected from each individual in the three subgroups, so this variable was specified as '4 4 4'.

12) INITIAL DESIGN POINTS FOR EACH ELEMENTARY DESIGN

This variable was used for specifying the sampling times to be evaluated. The four sampling times used in the original study were entered in the order of each of the three subgroups. Since the PK model available in PopDes Windows gave no lag time option, and it was necessary to add an absorption lag of 0.75 hours to the sampling times after evaluation, the sampling times used in the original study were modified by subtracting 0.75 from each time point prior to specification in the input file. For example, the actual sampling times that had been used for the patients in group A were 2, 4, 8 and 12 hours after the dose, respectively. To account for the effect of the lag time, these actual sampling times were corrected to 1.25, 3.25, 7.25 and 11.25 hours when the original study design was evaluated.

13) LOWER BOUNDS OF TIME POINTS and UPPER BOUNDS OF TIME POINTS

The PopDes program ignores these two variables when evaluating study design. However, they cannot be left empty, so the lower bound and the upper bound were set as being equal to 0 and 12, respectively.

When the PK parameters and group structure of the original design had been specified in the input file (required_param.dat), this file was saved in the PopDes directory and then uploaded to the program by using the 'Parameters' option of the interface. The original design was evaluated by selecting evaluation mode under the 'task' option of the interface and then pressing 'CALCULATE & SAVE'.

6.2.5.2 Evaluation of the original design using PopDes script

The flexibility offered by the PopDes script allowed for the inclusion of additional factors from the original study design and population model in the evaluation. Two files had to be modified when using the PopDes script: 'ext_model' and 'PopDes.m'. In the first file, used to specify the PK model, a one-compartment model with first-order absorption with a lag was written, and the script for the multiple-dose model was added in order to investigate the importance of the sample taken after the second dose in Group A. In addition, the script was modified to account for each individual

dose administered to subjects by incorporating the body weight of each patient in the dosing regimen. The covariates that influenced the PK parameters, including body weight, sodium concentration and high risk of mortality, were also included in the model. The second file contained several variable lines that were similar to the input file (required_param.dat) of PopDes Windows. The PK parameters and design structures of the original design were entered in this file, as previously described for PopDes Windows. However, since the lag model had already been included when using the script option, the original sampling times were used immediately with no subtraction of the 0.75 hour lag time.

The expressions for the population FIM written in the PopDes.m file were also modified to account for the covariates in the model. Examples of modified scripts for ext_model.m and PopDes.m files are provided in Appendix I.

In the present study, two approaches were applied for evaluation of the original design with PopDes script. In the first of these, the FIM for each subject was initially computed, after which the population FIM was calculated from the individual FIM. The covariates and sampling times for each subject were listed in a separate text file and were added to the program during design evaluation. In the second approach, the population FIM was approximated by a Monte Carlo integration of the latter over the covariates. A Latin hypercube sampling technique was applied to efficiently sample from the covariate distribution.

6.2.6 Optimisation of the study design

6.2.6.1 Optimisation of the study design using PopDes Windows

In a similar manner to design evaluation, when PopDes Windows was used for optimisation, the input file (required_param.dat), which contained several input variable lines, was created and the PK parameter estimates and design variables were then specified. Drug dose and dosing interval, as well as PK parameter estimates, were entered as was described for design evaluation. However, when optimising designs with the exact design option, the sampling times specified in this file were used as initial values for the optimisation. These values may be changed after

optimisation, while the group structures of the design were constrained as described in Section 6.2.4. However, for the continuous design, both the sampling times and the group structures that were specified in the input file were used as initial values and may be changed after optimisation. The input file for continuous design optimisation contained some additional variable lines that were completed as follows:

1) WEIGHT/PROPORTIONS OF SUBJECTS FOR THE INITIAL DESIGN (FOR EACH ELEMENTARY DESIGN)

This variable was used to specify initial values of the proportion of study subjects in each of the elementary designs. It was entered as '0.5 0.5', which indicated that the initial predictions for group structures were two elementary designs with the same number of subjects being allocated to each group.

2) TOTAL NUMBER OF SUBJECTS IN THE STUDY IF KNOWN (IF UNKNOWN ENTER 1)

For this variable, '52' was entered. This indicated that the total number of subjects it was permitted to recruit for future study was constrained at 52.

3) MINIMUM NUMBER OF TIME POINTS ALLOWS IN EACH ELEMENTARY DESIGN and MAXIMUM NUMBER OF TIME POINTS ALLOWS IN EACH ELEMENTARY DESIGN

These two variables were used to specify the minimum and maximum number of sampling times for each elementary design. In this study, three, four or five sampling times were examined.

6.2.6.2 Optimisation of the study design using PopDes script

The optimisation methods were similar to those described for PopDes Windows. The exception was that all design variables had to be entered in the PopDes.m file, which was modified to account for the covariates in the model, instead of using the required_param.dat file. The ext_model.m file, which implemented the PK models, was also needed to perform the optimisation.

6.2.7 The influence of uncertainty in the prior information

The optimal designs are dependent on the prior model and parameters. To explore the influence that uncertainty in prior information exerted on the optimal design results, optimal designs for administering ciprofloxacin to children with severe malnutrition were also determined by using population models and PK parameters obtained from two other studies. Since these studies had covariates in the model, PopDes script was used. Table 6.2 summarises the final model and population parameter estimates for Study 1 and Study 2, which were implemented in the program.

6.2.7.1 Study 1: Rajagopalan and Gastonguay (2003)

In a study by Rajagopalan and Gastonguay (2003), oral and/or intravenous ciprofloxacin was administered to 150 individuals aged between 0.27 and 16.9 years (median 2.5 years). Their weight range was 4.2 to 63.2 kg, with a median value of 13.15 kg, and 28 patients had cystic fibrosis. A two-compartment model with first-order absorption and absorption lag adequately described the concentration-time profiles. PK parameters were influenced by age, weight and the presence of cystic fibrosis, and the exponential error model was used to describe inter-individual variability of the parameters. A preliminary analysis found that the inclusion of a full omega matrix led to numerical difficulty during the optimisation. Therefore, to avoid this problem, only the diagonal elements were included in the FIM. The residual error was described by a combination of proportional and additive error models. The standard error for the additive model was small (0.0131) and imprecise (77.5%), so it was fixed during the optimisation.

6.2.7.2 Study 2: Schaefer et al. (1996)

Schaefer *et al.* (1996) conducted a study in 10 paediatric patients with cystic fibrosis aged 6 to 16 years (mean 10.1 years) and with a weight range of between 14.9 and 42 kg (mean 27.5 kg). Each patient received ciprofloxacin 10 mg/kg by infusion over 30 minutes, followed by oral ciprofloxacin at a dose of 15 mg/kg. The structural model was a two-compartment model with first-order absorption. Body weight was incorporated in the clearance (CL), central volume of distribution (V_1) and peripheral

volume of distribution (V_2) models. The mean renal clearance was 11.4 L/h. Inter-individual variability terms were added to the CL, V_1 and V_2 models using the exponential model. Residual variability was adequately described by the proportional error model.

6.2.8 Investigation of additional sampling times after the second dose

The upper boundary of sampling times was initially limited to 12 hours after the first dose. The need for sampling times after the second dose was investigated by extending the sampling region to 12 hours after the second dose (or 24 hours after the first dose). This was only performed by using optimal designs derived from the PopDes script.

6.2.9 Calculation of sampling windows for optimal designs

There are two options to choose from for computing sampling windows: equal lengths and different lengths. The equal lengths option computes the same duration of sampling window for all sampling time points, while the different lengths option calculates an individual sampling window for each sampling time. The sampling windows can be computed by using either PopDes Windows or PopDes script. The optimisation of sampling windows is time-consuming, so in this study it was performed only for the optimal designs derived from PopDes script. The different lengths option was used with a minimum efficiency of 80%. The distribution of samples within sampling windows was assumed to be uniform.

Table 6.2 Final model and population parameters from previous studies of ciprofloxacin and used for optimising a study design for malnourished children

Parameters	Study 1	Study 2
TVCL (L/h)	30.3(L/h/70 kg) x $(WT/70)^{0.75}$ x (1+ 0.045 x (AGE -2.5))	8.8 + (0.396 x WT)
TVV1 (L)	56.7 (L/70 kg) x (WT/70)	0.698 x WT
TVV2 (L)	89.8 (L/70 kg) x (WT/70)	1.3 x WT
TVQ (L/h)	37.5(L/h/70 kg) x $(WT/70)^{0.75}$	21.0
TVKA (h^{-1})	1.27 x (1+ 0.045 x CF)	0.644
ALAG (h)	0.353	-
F1	0.611	0.618
CL_R (L/h)	-	11.4
ω^2_{CL}	0.0901	0.006
ω^2_{V1}	0.120	0.051
ω^2_{V2}	0.0963	0.022
ω^2_{Q}	0.165	-
ω^2_{ka}	0.248	-
ω^2_{F}	0.0509	-
Proportional error (%CV)	40	31.9
Additive error (SD)	0.04	-

TVCL is typical value of clearance (L/h), TVV1 is the typical value of central volume of distribution (L), TVV2 is the typical value of peripheral volume of distribution (L), TVQ is the typical value of inter-compartment clearance (L/h), TVKA is typical value of absorption rate constant (h^{-1}), ALAG is a lag time (h), F is oral bioavailability fraction, WT is weight (kg), AGE is age (years) and CF is cystic fibrosis (if the patient has cystic fibrosis, CF=1 otherwise CF=0), ω^2 is inter-individual variability, %CV is the percentage coefficient of variation and SD is the standard deviation.

6.2.10 Optimisation of the total number of subjects

The optimal designs obtained after optimisation were subsequently used to investigate the optimal number of subjects. This number does not affect the optimal sampling times, but it can influence the precision of the parameter estimates. A variety of numbers of subjects between five and 100 were tested. A similar proportion of subjects was assumed from studies that involved two and three subgroups. Coefficients of variation (CV) of ka, CL and V were set to have cut-off points of 10 and 20%. The minimal number of subjects to provide an estimated CV of under 10% for ka, CL and V was considered to be optimum in the present study.

6.2.11 Interpretation of the design results

After performing design evaluation or optimisation, PopDes reports the results as the standard errors and coefficients of variation, as well as the determinant of the FIM. The determinant is a measure of the volume of a matrix and was used to evaluate the amount of information given by the design. When comparing designs, the highest value of the determinant was considered to be the optimum. In this study, the determinant was also converted to the criterion, which is the determinant raised to the power of one over the number of parameters to be estimated in the model. This value was used to compare any designs with different numbers of parameters in the model. However, the determinant and the criterion values cannot themselves be interpreted individually. It is more meaningful to compare these values between two study designs and interpret them as the design efficiency. The efficiency of any design was defined as the ratio of any two criteria (e.g. criteria of the optimal design compared to the original design) and was expressed as a percentage.

In this study, the determinant and the criterion were used to identify a rough estimate of the potential optimal design; however, the primary criterion for selecting the optimal design was the coefficients of variation of the parameters.

6.3 RESULTS AND DISCUSSION

6.3.1 Evaluation of the original design

6.3.1.1 Evaluation of the original design using PopDes Windows

The original design was composed of three subgroups containing similar numbers of subjects. Four blood samples were collected from each patient at various times from 1 to 12 hours after the dose. In order to evaluate the original design with PopDes Windows, several assumptions were applied to the design and parameters. The concentration-time profile generated using the median dose, median typical parameter estimates and a one-compartment model with first-order absorption without a lag is illustrated in Figure 6.3A. The sampling times, which are marked on the profile, were obtained after subtracting the 0.75 hour absorption lag. The profile clearly showed that the majority of samples (191 of 208; 92%) were collected during the elimination phase. Only 17 samples, taken from the subjects in Group C, were collected during the absorption phase. The estimated coefficient of variation (CV) for ka was 19.7%, which was considerably lower than the value reported by NONMEM (44.4%). For the additive error, the CV was 274.6%, compared to the 103.3% obtained by NONMEM. With the exception of these two parameters, the CVs of the remaining parameters, which were derived from PopDes Windows, were comparable with those estimated by NONMEM (Table 6.3).

6.3.1.2 Evaluation of the original design using PopDes script

When evaluating the original design with PopDes script, no assumptions were used. The PK models were modified to include covariates and a lag time, as well as to account for the sampling time after the second dose. The concentration-time profile generated by using these models is shown in Figure 6.3B. It was observed that the shape of the concentration-time profile and the position of sampling times on the profile were similar to those obtained with PopDes Windows, i.e. the majority of samples were collected during the elimination phase, and the first samples taken at 1 hour were available from 17 patients in Group C.

The CVs for additive error were 206.9% and 158.7% when evaluating the original design by using the individual value of covariates and the distribution of covariates,

respectively. With the exception of the additive error, the determinant, criterion and CVs of the parameters obtained from the two methods used to account for covariates in the model were similar, and they were also consistent with the results estimated using NONMEM (Table 6.3).

The CVs of ka were close to the value estimated by NONMEM when a lag time was considered, which was probably because there was a correlation between the two parameters (ka and lag time). A variation in CV of the additive error may be explained by the small value of the additive error (CV = 0.0007), which may have led to an inaccurate estimation of the CV. Further investigation found that when the additive error was fixed at 0, the values of each criterion did not considerably change.

Figure 6.3 The concentration-time profile of oral ciprofloxacin generated using the PK models and parameters specified in PopDes Windows (A) and PopDes script (B)

Key: A, B and C characters marked on the profile refer to the sampling times for Groups A, B and C, respectively.

A: The profile generated using a one-compartment model with first-order absorption, without a lag and median typical parameters.

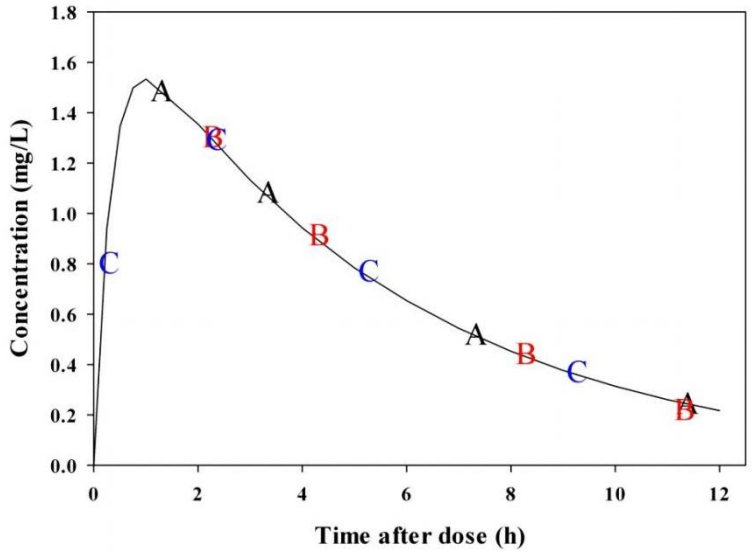

B: The profile generated using a one-compartment model with first-order absorption and a lag (the solid line is the profile for patients who had a high mortality risk. The dotted line is the profile for patients who had a low or intermediate mortality risk. Median weights and concentrations were used).

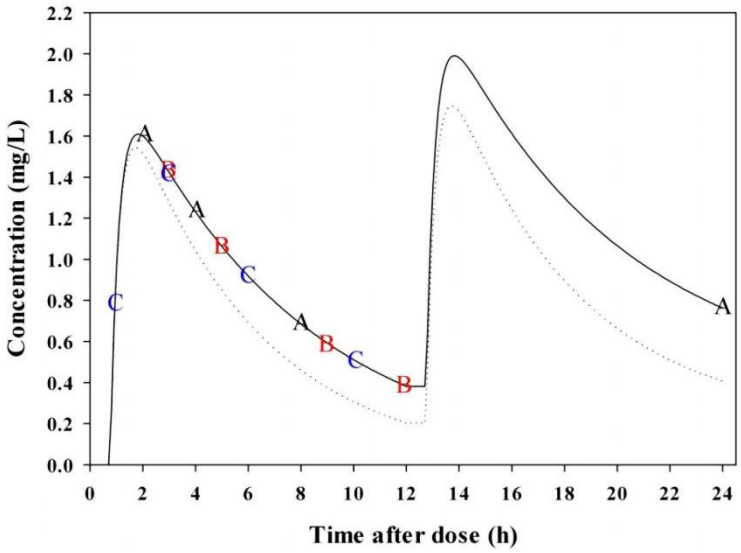

Table 6.3 Determinant, criterion and percentage coefficient of variation of parameters computed by PopDes Windows and PopDes script and the results estimated by NONMEM

Methods	Determinant	Criterion	%CV								
			ka	CL	V	Lag	ω^2_{ka}	ω^2_{CL}	ω^2_{V}	Prop	Add
Original study (estimated by NONMEM)	-	-	44.4	7.3	7.2	18.7	57.1	20.3	24.4	30.0	103.3
PopDes Windows	4.6e+25	215	19.7	5.5	6.4	-	39.5	24.0	26.3	27.9	274.6
PopDes script using individual covariates	9.9e+35	251	36.9	6.5	6.1	16.1	40.0	24.0	26.2	25.0	206.9
PopDes script using the distribution of covariates	1.5e+36	258	37.7	6.3	7.1	16.3	40.0	24.1	26.3	24.6	158.7

Prop: proportional error, Add: additive error

6.3.2 Optimisation of the study design

6.3.2.1 Optimisation of the study design using PopDes Windows

1) The exact design

Table 6.4 shows the determinant and criterion values derived from the optimisation with time interval option. It was found that the determinant and criterion values computed by the EX were comparable to those calculated by the HB. A major difference was observed with design four, in which the criterion was 266 when optimising with the EX, compared to 188 when optimising with the HB. The results estimated using the EX and the HB were generally higher than those obtained by the SM. This can be explained by the fact that estimation of the SM is very sensitive to the initial design values; the SM moves only from the initial point to the next local maximum or minimum and then stops, so it may be unable to reach the global maximum or minimum.

The five-sample design had higher determinant and criterion values compared to the four- and three-sample designs. This was observed for all group structures tested. This can be explained as the determinant and criterion being the values that represented the amount of information contained in each design, and to the fact that the amount of information is normally related to the number of samples that it is permissible to take from each subject. Therefore, five sample designs can provide more information than four- and three-sample designs.

The number of elementary designs, or subgroups, was related to the number of samples. For three- and four-sample designs, the results were comparable when using either two or three subgroups. However, it was revealed that each criterion of the five-sample design was very similar to the others when using either one, two or three subgroups. For example, when optimising five-sample design with the HB, the criterion was 581, 580 and 571 for one, two (26/26) and three elementary designs, respectively, and when optimising a five-sample design with the EX, the criterion was 546, 546 and 549 for one, two (26/26) and three elementary designs, respectively. This suggested that more complex design structures had only slight advantages when a greater number of samples were permitted.

The different proportions of subjects were examined when optimising two elementary designs. The results suggested that this design variable had minor effects and the number of subjects in each subgroup could vary. For example, the criterion obtained with three samples optimising with the EX were 266, 291, 298 and 298 for the different numbers of proportions of subjects of 26/26, 34/18, 39/13 and 42/10, respectively.

The results using the time list option are shown in Table 6.5. When comparing the rich and sparse time lists, it was found that the determinant and criterion values were almost identical; for example, the criterion was 545 for the rich list and 547 for the sparse list when the design was constrained to three subgroups with five samples taken from each subject. This indicated that the optimal sampling times lay primarily in the drug absorption phase, and frequent sampling points are required during this period. The importance of group structure was similar to what was found with the time interval option, i.e. five samples gave more information than four and three samples, meaning that a complex design structure may not be required if up to five samples can be obtained from each patient.

2) The continuous design

The continuous design option was used to determine both optimal sampling times and optimal design structures, i.e. number of samples, number of elementary designs and number of subjects in each elementary design. In this study, numbers of samples were fixed at three, four and five samples per subject, while other design structures were optimised. Table 6.6 shows the optimal designs determined from the continuous design option in PopDes Windows. The results obtained by using different types of time list were very similar. The group structure for three samples that were optimised with the rich time list was three elementary designs with 3, 14 and 35 subjects allocated, respectively, while 3, 15 and 34 subjects were allocated, respectively, when optimising with the sparse time list. Two elementary designs with a large number of subjects in one group were suggested for four- and five-sample designs (Table 6.6). It was found that the optimal sampling times for the small group were intense in the absorption phase (between 0 and 3 hours after the dose).

6.3.2.2 Optimisation of the study design using PopDes script

1) The exact design

When the designs were optimised using the time interval option, the determinant and criterion values computed with different optimisers were comparable across almost all designs (Table 6.4). Discrepancies were generally observed between the SM and two remaining algorithms; for example, the criterion values were 842 and 501 for design five and 826 and 496 for design eight when optimising with the HB and the SM, respectively. The results of the time list option were in accordance with those found when optimising with PopDes Windows, that is, the criterion values derived from the different types of time lists were almost identical (Table 6.5). This confirmed that the optimal sampling times lay primarily during the drug absorption phase.

The optimal group structures were consistent with the results obtained from the time interval or time list options. It was shown that two subgroups were required for three and four samples, while a single subgroup was sufficient for five samples.

2) The continuous design

The results obtained from the continuous design are shown in Table 6.6. It was found that two subgroups, with a similar number of subjects allocated to each, were needed for a three-sample design. For four samples, two subgroups were suggested, consisting of 46 to 48 subjects in one group and four to six subjects in the other. The design structures could be simplified by using only one group if it was possible to collect up to five samples from each patient.

Table 6.4 Determinant and criterion of optimal designs obtained from the exact design and time interval option

Design	No. of groups	No. of subjects	No. of samples	Algorithm	PopDes windows		PopDes script	
					Determinant	Criterion	Determinant	Criterion
1	1	52	3	EX	1.9e-05	0	8.3e+36	289
				HB	6.6e-05	0	2.1e+35	227
				SM	4.6e-07	0	1.8e+35	224
2	1	52	4	EX	9.8e+26	284	3.7e+42	689
				HB	1.3e+28	361	3.5e+42	686
				SM	1.8e+27	301	3.7e+42	668
3	1	52	5	EX	1.3e+30	546	3.2e+44	927
				HB	2.6e+30	581	1.0e+45	1000
				SM	1.8e+29	456	3.8e+44	938
4	2	26/26	3	EX	4.7e+26	266	1.1e+40	466
				HB	1.1e+25	188	1.8e+40	483
				SM	1.0e+25	188	8.8e+39	460
5	2	26/26	4	EX	1.7e+29	454	1.7e+43	762
				HB	3.1e+29	480	7.6e+43	842
				SM	6.6e+26	274	3.2e+40	501
6	2	26/26	5	EX	1.3e+30	546	3.2e+44	927
				HB	2.5e+30	580	6.5e+44	972
				SM	6.3e+28	415	3.2e+44	926
7	2	34/18	3	EX	1.3e+27	291	7.8e+39	457
				HB	4.5e+26	265	6.2e+39	449
				SM	4.8e+24	175	5.6e+38	383
8	2	34/18	4	EX	1.2e+29	439	1.4e+43	751
				HB	2.0e+29	462	5.7e+43	826
				SM	5.7e+26	270	2.7e+40	496
9	2	34/18	5	EX	1.4e+30	548	2.7e+44	916
				HB	2.7e+30	584	1.1e+45	1007
				SM	1.2e+30	544	3.8e+44	938
10	2	39/13	3	EX	1.7e+27	298	8.4e+39	459
				HB	2.2e+27	307	1.1e+41	544
				SM	1.9e+24	161	2.3e+38	361
11	2	39/13	4	EX	7.8e+28	423	1.2e+43	744
				HB	3.5e+29	485	4.7e+43	815
				SM	1.9e+26	245	8.8e+41	626
12	2	39/13	5	EX	1.4e+30	549	2.8e+44	918
				HB	2.8e+30	586	1.2e+45	1013
				SM	1.7e+29	454	1.4e+44	879
13	2	42/10	3	EX	1.6e+27	298	9.7e+39	463
				HB	2.1e+27	305	5.9e+40	522
				SM	2.1e+26	248	8.1e+37	337

Table 6.4 (continued)

Design	No. of groups	No. of subjects	No. of samples	Algorithm	PopDes windows		PopDes script	
					Determinant	Criterion	Determinant	Criterion
14	2	42/10	4	EX	5.6e+28	411	1.4e+43	752
				HB	3.1e+29	480	5.3e+43	822
				SM	2.0e+26	246	1.2e+42	638
15	2	42/10	5	EX	1.4e+30	549	3.8e+44	938
				HB	1.9e+30	566	1.2e+45	1010
				SM	1.1e+30	537	2.6e+44	914
16	3	17/18/17	3	EX	1.5e+27	296	2.9e+40	498
				HB	3.4e+27	318	1.1e+41	545
				SM	4.4e+22	114	2.9e+40	498
17	3	17/18/17	4	EX	1.9e+29	459	1.3e+43	750
				HB	3.7e+29	487	5.6e+43	825
				SM	4.3e+23	141	9.6e+41	629
18	3	17/18/17	5	EX	1.4e+30	549	2.7e+44	916
				HB	2.1e+30	571	1.3e+45	1016
				SM	2.8e+27	312	9.4e+43	854

EX: Exchange algorithm
HB: Hybrid algorithm
SM: Simplex algorithm

Table 6.5 Determinant and criterion of optimal designs obtained from the exact design with time list option using the Exchange algorithm

Design	No. of groups	No. of subjects	No. of samples	Time list options	PopDes windows		PopDes script	
					Determinant	Criterion	Determinant	Criterion
1	1	52	3	Rich	8.7e-06	0	8.3e+36	289
				Sparse	4.4e-06	0	6.7e+36	285
2	1	52	4	Rich	4.1e+26	263	3.7e+42	689
				Sparse	9.6e+26	284	4.6e+42	699
3	1	52	5	Rich	1.0e+30	535	3.2e+44	927
				Sparse	1.2e+30	544	3.7e+44	936
4	2	26/26	3	Rich	2.1e+26	247	8.7e+39	460
				Sparse	4.6e+26	265	1.3e+40	471
5	2	26/26	4	Rich	1.5e+29	449	1.4e+43	753
				Sparse	1.6e+29	453	2.2e+43	770
6	2	26/26	5	Rich	1.1e+30	540	2.7e+44	916
				Sparse	1.2e+30	544	3.7e+44	936
7	2	34/18	3	Rich	1.3e+27	291	8.1e+39	458
				Sparse	1.2e+27	290	1.1e+40	467
8	2	34/18	4	Rich	1.1e+29	435	1.4e+43	753
				Sparse	1.1e+29	438	1.9e+43	768
9	2	34/18	5	Rich	1.3e+30	545	2.8e+44	918
				Sparse	1.3e+30	547	3.7e+44	936
10	2	39/13	3	Rich	1.7e+27	298	1.1e+40	468
				Sparse	1.7e+27	298	9.9e+39	464
11	2	39/13	4	Rich	7.4e+28	421	1.4e+43	752
				Sparse	7.6e+28	422	1.6e+43	759
12	2	39/13	5	Rich	1.3e+30	547	2.8e+44	918
				Sparse	1.3e+30	548	3.7e+44	936
13	2	42/10	3	Rich	1.6e+27	298	9.4e+39	462
				Sparse	1.6e+27	298	7.0e+39	453
14	2	42/10	4	Rich	5.6e+28	411	1.4e+43	752
				Sparse	5.5e+28	410	1.1e+43	742
15	2	42/10	5	Rich	1.3e+30	547	4.3e+44	945
				Sparse	1.3e+30	548	3.2e+44	926
16	3	17/18/17	3	Rich	1.5e+27	296	4.1e+40	510
				Sparse	1.5e+27	295	4.1e+40	510
17	3	17/18/17	4	Rich	1.8e+29	456	1.6e+43	759
				Sparse	1.9e+29	458	1.9e+43	767
18	3	17/18/17	5	Rich	1.3e+30	545	2.8e+44	918
				Sparse	1.3e+30	547	2.7e+44	917

Table 6.6 Optimal designs obtained from the continuous design with time list option using the First-order algorithm

Design	No. of samples	Time list option	Optimal No. of groups	Optimal No. of subjects	Determinant	Criterion
PopDes windows						
1	3	Rich	3	3/14/35	1.4e+27	293
		Sparse	3	3/15/34	1.4e+27	294
2	4	Rich	2	6/46	3.6e+28	395
		Sparse	2	7/45	4.0e+28	398
3	5	Rich	2	5/47	3.5e+29	485
		Sparse	2	4/48	2.6e+29	472
PopDes script						
4	3	Rich	2	20/32	4.3e+39	439
		Sparse	2	25/27	4.0e+39	436
5	4	Rich	2	6/46	3.6e+42	687
		Sparse	2	4/48	4.5e+42	698
6	5	Rich	1	52	4.0e+44	941
		Sparse	1	52	3.7e+44	936

6.3.3 Selection of the candidate designs

In this study, several design options and design variables were examined using different design options and constrained variables. In the majority of cases, the optimal sampling times obtained by using different algorithms were very close; however, the designs optimised using the EX were selected as the candidate designs because they can be determined using a grid size to give sampling times, which is more practical than other algorithms. For example, when using the EX, the optimal sampling times for one group with four samples were 0.75, 1.25, 3 and 12 hours, while the results were 0.751, 1.233, 2.948 and 11.789 hours when using the SM. Furthermore, the computation time of the EX was faster. Since the use of different proportions of subjects in each elementary design was not of importance, an equal number (26 in each group) was used for two elementary designs. A total of nine candidate designs were obtained from each optimisation method, PopDes Windows and PopDes script according to these restrictions, as presented in Table 6.7. The optimal design for three-, four- and five-sample designs was selected from a list of

candidates, and the primary selection criterion used was the coefficient of variation (CV) of the parameters.

6.3.3.1 Optimal designs obtained from the PopDes Windows

The CVs for inter-individual and residual variability could not be estimated for a study with one elementary design and three samples. When the maximum number of samples was fixed at three per subject, the results were similar with either two or three subgroups. Therefore, two elementary designs were selected as being optimum for a three-sample design. Disregarding the additive error, the CVs of the parameters were comparable when using one, two and three elementary designs with four samples. The CV of additive error when one subgroup of subjects was used was very high (477.7%), compared to 27.7% and 33.3%, respectively, when two and three subgroups were used. Two subgroups were selected as the optimal design structure in this case. It was observed that the CVs of all parameters were very similar when using one, two and three subgroups with five samples, so the simplest design structure with one group of subjects was chosen as the optimal design.

6.3.3.2 Optimal designs obtained from the PopDes script

Many parameters had a high CV when one elementary design was used with a fixed number of three samples per subject. The CVs for ω^2_{ka}, ω^2_{V}, proportional error part and additive error part were 122.2%, 139.2%, 187.8% and 86.2%, respectively (Table 6.7). The results were almost the same when using two and three elementary designs. However, the proportional error was estimated more precisely with three subgroups (44.1%) compared to two subgroups (92.7%). Therefore, the optimal number of groups for a three-sample design was three. When the number of samples was increased to four, it was observed that the CVs of the parameters were almost the same for one, two and three subgroups, with the exception of the proportional error. The proportional errors were 62.2%, 29.7% and 22.3% for one, two and three subgroups of subjects, respectively. As a result, the optimal design was two subgroups, with four samples being taken from each subject. This was consistent with the results of PopDes Windows, in that the study design was simplified by using

only one group of subjects if it was not possible to collect five samples from each of them, so it was therefore chosen as the optimal design in this case.

6.3.3.3 Comparison of the optimal designs obtained from PopDes Windows and PopDes script

Table 6.7 shows all candidate designs derived from PopDes Windows and PopDes script. The optimal designs for three, four and five samples optimising with PopDes Windows were the design numbers four, five and three, respectively, while the design numbers seven, five and three were selected on the basis of the results obtained from PopDes script. Both optimisation methods suggested identical optimal designs for four and five samples.

For four samples, design number five, in which a similar number of subjects was allocated to each subgroup, was chosen. The optimal sampling times obtained from PopDes Windows and PopDes script were identical, as it was suggested that the optimal sampling times for the first subgroup were 0.75, 1.00, 2.75 and 12.00 hours and for the second subgroup were 1.00, 1.50, 3.25 and 12.00 hours (Table 6.8).

The results indicated that design number three, in which there was only one subgroup of subjects, was optimum for five samples. The CVs estimated by PopDes Windows and PopDes script were very similar with both designs, for example, the CVs of ka for design number three (five-sample design) were 6.5% and 6.8% when optimising with PopDes Windows and PopDes script, respectively. The optimal sampling times obtained from both methods were identical at 0.75, 1.00, 1.50, 3.25 and 12.00 hours after the dose (Table 6.8).

A discrepancy in the results was observed with regard to three samples. The CVs of design number seven, which was selected by PopDes script, were similar to those estimated by PopDes Windows. However, the discrepancies were observed in design number four, which had been selected as the optimal design using PopDes Windows. When optimising this design with PopDes script, the CVs for ω^2_{ka}, proportional error, and additive error were 51.2%, 92.7% and 46.2%, respectively, which were higher

than those values estimated by PopDes Windows (35.9%, 39.5% and 27.7%, respectively). A higher degree of variation suggested by PopDes script was probably the result of the inclusion of a lag time in the model. The optimal sampling times of designs four and seven are presented in Table 6.8.

Table 6.7 Coefficient of variation of the parameters of interest obtained from the exact design and time interval option using the Exchange algorithm

Design	No. of groups	No. of subjects	No. of samples	%CV (PopDes script/PopDes windows)								
				ka	CL	V	Lag[a]	ω^2_{ka}	ω^2_{CL}	ω^2_{V}	Proportional	Additive
1	1	52	3	86.5/23.2	9.7/7.0	23.6/13.7	0.7	122.2/na	37.2/na	139.2/na	187.8/na	86.2/na
2	1	52	4	11.8/9.4	7.4/5.4	6.2/6.2	0.1	29.7/27.0	25.0/23.8	28.3/27.5	62.2/36.3	44.2/477.7
3	1	52	5	6.5/6.8	7.4/5.4	5.8/5.9	0.1	25.2/25.5	24.5/24.3	25.7/25.8	22.3/22.5	25.8/19.6
4	2	26/26	3	18.0/18.1	8.0/6.5	8.8/6.6	0.1	51.2/35.9	28.6/31.0	38.9/28.2	92.7/39.5	46.2/27.7
5	2	26/26	4	8.5/8.6	7.4/5.5	6.0/6.1	0.1	25.6/25.8	24.8/24.5	26.7/26.9	29.7/30.1	36.6/27.7
6	2	26/26	5	6.5/6.8	7.4/5.4	5.8/5.9	0.1	25.2/25.5	24.5/24.3	25.7/25.8	22.3/22.5	25.8/19.6
7	3	17/18/17	3	17.4/15.6	7.5/6.2	7.7/6.6	0.2	37.3/32.3	26.8/28.9	31.8/30.1	44.1/36.2	49.1/34.3
8	3	17/18/17	4	6.4/7.8	7.2/5.5	5.8/6.0	0.1	25.2/25.7	24.5/24.4	25.6/26.5	22.3/26.8	25.8/33.3
9	3	17/18/17	5	6.4/6.4	7.2/5.4	5.8/5.8	0.1	25.2/25.4	24.5/24.2	25.6/25.5	22.3/20.2	25.8/23.9

[a] Estimated by PopDes script.
CV = Coefficient of variation expressed as a percentage
na: not available

Table 6.8 Optimal designs for oral ciprofloxacin in paediatric patients obtained from the different prior information and extending the upper sampling limit to 24 hours

Design	No. of groups	No. of subjects	Sampling times	Determinant	Criterion	Efficiency[a]	CV (%)								
							ka	CL	V	Lag	ω^2_{ka}	ω^2_{CL}	ω^2_{V}	Prop	Add
3 samples															
PopDes script	3	17	0.75 1.00 12.00	2.9e+40	498	198[b]	17.4	7.5	7.7	0.2	37.3	26.8	31.8	44.1	49.1
		18	1.00 2.25 12.00												
		17	2.00 3.25 12.00												
PopDes windows	2	26	0.75 1.75 1.75	1.5e+27	296	137	15.6	6.2	6.6	-	32.3	28.9	30.1	36.2	34.3
		26	1.00 3.25 12.00												
			1.00 1.75 12.00												
Rajagopalan and Gastonguay	3	17	0.50 1.25 12.00	3.5e+20	74	15[c]	30.4	8.1	39.3	7.3	86.8	49.6	216.0	27.3	-
		18	0.50 3.25 12.00												
		17	0.50 1.00 12.00												
Schaefer *et al.*	3	17	0.25 12.00 12.00	1.4e+19	541	109[c]	16.6	15.5	22.5	-	-	94.9	77.5	17.7	-
		18	0.25 0.25 12.00												
		17	0.25 1.00 12.00												
Extend sampling time to 24 hour	3	17	0.75 1.00 24.00	5.2e+40	518	104[c]	17.4	7.7	7.3	0.2	37.2	27.1	31.6	44.9	49.4
		18	1.00 2.25 24.00												
		17	2.00 3.50 24.00												
4 samples															
PopDes script	2	26	0.75 1.00 2.75 12.00	1.7e+43	762	304[b]	8.5	7.4	6.0	0.1	25.6	24.8	26.7	29.7	36.6
		26	1.00 1.50 3.25 12.00												
PopDes windows	2	26	0.75 1.00 2.75 12.00	1.7e+29	454	211	8.6	5.5	6.1	0.1	25.8	24.5	26.9	30.1	27.7
		26	1.00 1.50 3.25 12.00												
Rajagopalan and Gastonguay	2	26	0.50 1.00 3.50 12.00	1.0e+22	100	13[c]	22.2	7.5	29.0	5.5	73.1	44.7	189.3	21.2	-
		26	0.50 1.00 3.50 12.00												

Table 6.8 (Continued)

Design	No. of groups	No. of subjects	Sampling times					Determinant	Criterion	Efficiency[a]	CV (%)								
											ka	CL	V	Lag	ω^2_{ka}	ω^2_{CL}	ω^2_{V}	Prop	Add
Schaefer *et al.*	2	26	0.25	0.25	7.75	12.00		1.1e+20	734	96 [c]	15.3	13.6	19.9	-	-	74.3	64.5	14.3	-
		26	0.25	1.25	12.00	12.00													
Extend sampling time to 24 hour	2	26	0.75	1.00	2.75	24.00		2.6e+43	785	103 [c]	8.4	6.0	7.0	0.1	25.5	24.7	26.5	29.8	36.6
		26	1.00	1.50	3.50	24.00													
5 samples																			
PopDes script	1	52	0.75	1.00	1.50	3.25	12.00	3.2e+44	927	369 [b]	6.5	7.4	5.8	0.1	25.2	24.5	25.7	22.3	25.8
PopDes windows	1	52	0.75	1.00	1.50	3.25	12.00	1.3e+30	546	253	6.8	5.4	5.9	0.1	25.5	24.3	25.8	22.5	19.6
Rajagopalan and Gastonguay	1	52	0.50	1.00	3.50	12.00	12.00	7.9e+22	121	13 [c]	20.5	6.7	25.7	5.2	69.1	38.5	177.9	18.2	-
Schaefer *et al.*	1	52	0.25	1.25	1.25	12.00	12.00	5.6e+20	920	99 [c]	12.8	12.9	16.8	-	-	68.7	52.5	12.2	-
Extend sampling time to 24 hour	1	52	0.75	1.00	1.50	3.50	24.00	6.9e+44	975	105 [c]	6.3	5.8	7.0	0.1	25.1	24.3	25.5	22.3	25.9

[a] relative comparison of criterion of any designs to criterion of original design and expressed as a percentage.

[b] compared to the original design evaluated by incorporating the individual covariate.

[c] compared to the results of optimal design estimated by PopDes script.

CV: coefficient of variation expressed as a percentage

Prop: proportional error

Add: additive error

6.3.4 The influence of uncertainty in the prior information

Table 6.8 shows the optimal designs for three, four and five samples, derived by using prior information obtained from different patient populations. When using PK models and parameters from Study 1 (Rajagopalan & Gastonguay, 2003), the optimal sampling times were 0.5 hours and 12 hours for the first and the last samples, and it was suggested that the other samples be taken between 1 and 3.5 hours after the dose. These results were similar to those found by Al-Banna *et al*. (1990), who demonstrated that the optimum sampling time points of a two-sample design are as early and as late as possible, and the addition of the third sample anywhere between those two points can improve the estimation of the population parameters. It was observed that the first sampling time at 0.5 hours was slightly earlier than the first optimal sampling time obtained by using the information from the study of a malnourished population. This was because Study 1 reported a lag time of 0.353 hours (21 minutes); therefore the earliest possible time that the first sample can be taken is 0.5 hours when optimising with the EX with a fixed grid size of 0.25.

The CVs of the parameters estimated using the information from Study 1 were generally higher than those estimated using the information obtained from the study of malnourished patients. For example, the CVs of V were 39.3%, 29.0% and 25.7% for three-, four- and five-sample designs, respectively, when using the information from Study 1, compared to the values of 7.7%, 6.0% and 5.8%, respectively, when using the information obtained from malnourished patients. A high variation was obtained when using the information from Study 1, which was probably because this study included a wide range of paediatric populations, i.e. children aged from 0.27 to 16.9 years (median 2.5 years) and weighing from 4.2 to 63.2 kg (median 13.5 kg). If the population model accounted for these covariates, the PK parameter estimates resulted in a high variation.

The designs optimised with the information from Study 2 (Schaefer *et al*., 1996) had first and last sampling times at 0.25 hours and 12 hours. The remainder of the sampling points were at 1, 1.25 and 7.5 hours (Table 6.8). Although the criterion and design efficiencies were higher than those obtained by using the information from

malnourished patients; the CVs of the parameters were generally higher. The precisions of inter-individual variability in CL and V were particularly high; over 50%, even with the five-sample study. This was probably due to the final population models reported in Study 2 being developed from a small number of individuals (10 children) and the parameter estimates being imprecise, i.e. the inter-individual variabilities for CL and V were 7.8% and 22.6%, with standard errors reported as 70.7% and 57.8%, respectively.

6.3.5 Investigation of additional sampling times after the second dose

The designs obtained previously were optimised by fixing the upper limit of the sampling region to 12 hours after the first dose. The importance of sampling times after the second dose was investigated by extending the upper limit to 24 hours or 12 hours after the second dose. The results are given in Table 6.8. It was found that most sampling time points remained the same; only the final sampling time at 12 hours was changed to 24 hours. Nevertheless, the determinants, criterion values and design efficiencies, as well as the CVs of the parameters, were almost identical to the results estimated by fixing the last sampling point to 12 hours.

6.3.6 Sampling windows

The sampling windows of each optimal sampling time are presented in Table 6.9. The results showed that the lengths of sampling windows for the fixed sampling times of 0.75 and 1 hour were very short (0.04 and 0.1 hours, respectively), while they were more flexible for other sampling points. For the sampling times of 1.5 to 3.25 hours, the sampling windows were for 15 minutes around the fixed sampling times. The sampling windows for the last samples at 12 hours were 1 hour. The efficiencies of the sampling window designs were 82%, 81% and 82% for three-, four- and five-sample study designs, respectively.

It was observed that the efficiencies of the sampling window designs were sensitive to their length, especially with regard to the first sampling window. This was due to

the steepness of the profile during the absorption phase of ciprofloxacin. Sampling windows of 0.04 hours or 2.4 minutes and 0.1 hours or 6 minutes around the fixed sampling times during drug absorption may not be practical. In a further investigation, the length of the sampling windows was gradually extended, while the decrease of design efficiency was simultaneously monitored. It was found that when the sampling windows were extended from 2.4 minutes to 5 minutes and from 6 minutes to 10 minutes, the efficiencies of the designs decreased slightly to approximately 70%.

6.3.7 Optimisation of the total number of subjects

Figure 6.4 presents the plots of percentage coefficient of variation (CV) against the total number of study subjects. The final criterion to select the optimal sample size was based on the 10% precision limit on ka, CL and V. On the basis of this criterion, a sample size of 25 (one group) was chosen for a five-sample design (Figure 6.4A). If four samples per subject were permitted, a sample size of 20 was selected for each subgroup (a total of 40 individuals) (Figure 6.4B). For three groups in which three samples had been taken from each subject, the CV of ka remained above the precision limit, even if the sample size was increased to 100. To determine the optimal number of individuals in this design, the higher precision limit of 20% was used for ka. It was found that a total of 40 subjects, divided into three subgroups (e.g. 13, 14 and 13 subjects in each subgroup), would be appropriate (Figure 6.4C). If the CL and V were the parameters of interest, the results suggested a total of 25, 30 and 35 subjects for the five-, four- and three-sample designs, respectively.

Table 6.9 Sampling times and sampling windows for three different optimal designs based on the number of samples per subject

Properties	3 samples			4 samples		5 samples
Group number	1	2	3	1	2	1
Optimal sampling times (h)	0.75 1.00 12.00	1.00 2.25 12.00	2.00 3.25 12.00	0.75 1.00 2.75 12.00	1.00 1.50 3.25 12.00	0.75 1.00 1.50 3.25 12.00
Determinant Criterion	2.9e+40 498			1.7e+43 762		3.2e+44 927
Sampling windows (h)	0.75-0.79 0.90-1.10 11.00-12.00	0.90-1.10 2.00-2.50 11.00-12.00	1.50-2.50 3.00-3.50 11.00-12.00	0.75-0.79 0.90-1.10 2.50-3.00 11.00-12.00	0.90-1.10 1.25-1.75 3.00-3.50 11.00-12.00	0.75-0.79 0.90-1.10 1.25-1.75 3.00-3.50 11.00-12.00
Determinant Criterion	3.8e+39 408			2.0e+42 616		3.9e+43 758
Efficiency (%)	82			81		82

Figure 6.4 Plots of percentage coefficient of variation versus total number of study subjects, using the optimal designs obtained from different numbers of samples (filled circles = ka, open circles = CL and filled solid triangles = V)

A: One-subject subgroup (five samples)

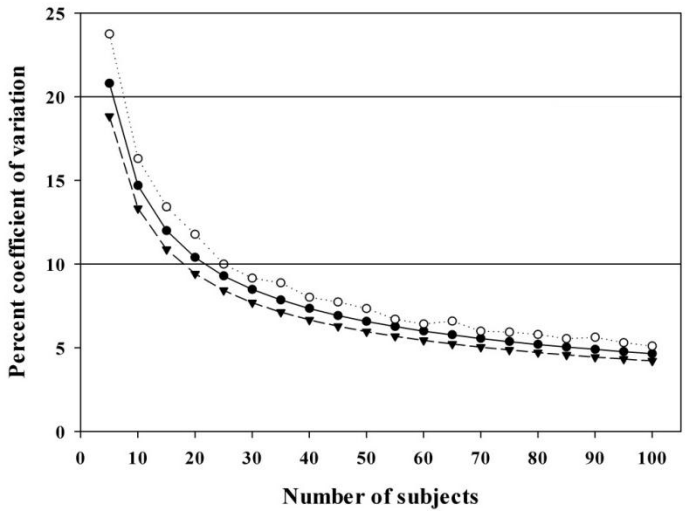

B: Two-subject subgroups (four samples)

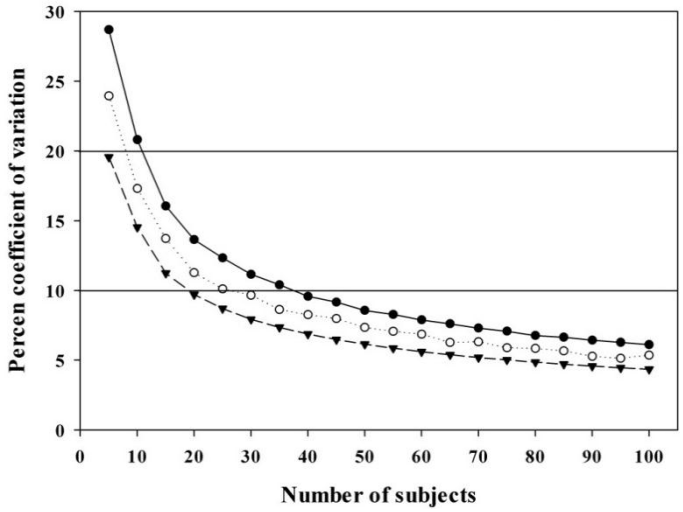

C: Three-subject subgroups (three samples)

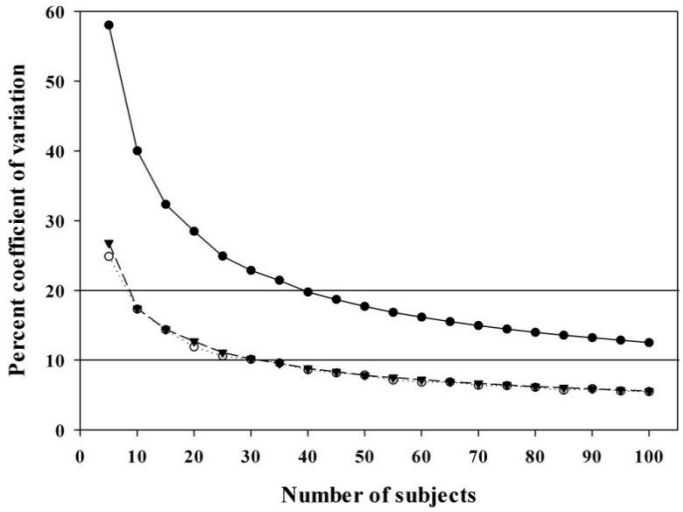

6.4 CONCLUSIONS

In the present study, a number of design options and design variables were used with different optimisers. The results suggested that the total number of subjects and the optimal number of elementary designs is related to the number of samples. In addition, the number of subjects in each elementary design could be varied, but was related to the allocation of sampling times.

In future population PK studies of oral ciprofloxacin, the original study which is a four-sample design containing a total of 52 subjects assigned into three groups of subjects (n = 17, 18 and 17) can be simplified by using two groups with a minimum of 20 subjects in each group. The number of samples used in the original study may reduce to three samples per subject while remaining the design efficiency However, if up to five samples are allowed to be taken from each patient at the appropriate sampling times, it would be expected that one group with a minimum of 25 subjects would give precise parameter estimates. In addition, it was revealed that the samples taken after the first dose contains sufficient information and the sampling time after the second dose may not be needed in the future studies.

It is of note that although the optimal design methods are useful in providing guidance around the optimal sampling times and sampling windows, as well as the optimal group structure, the results of the optimal design methods were greatly influenced by the information gained previously. Therefore, drug concentration-profile knowledge should be considered when designing population PK studies.

CHAPTER 7

DEVELOPMENT OF WHOLE BODY PHYSIOLOGICALLY BASED PHARMACOKINETIC MODELS OF CIPROFLOXACIN

7 INTRODUCTION TO CHAPTER

Physiologically based pharmacokinetic (PBPK) models have been more widely used in pharmaceutical research during the past decade, as shown by a large increase in the number of related publications (Rowland *et al*., 2011). PBPK models are composed of several compartments, each of which reflects the actual organs and tissues in the body. Unlike conventional models, a PBPK model mathematically describes and/or predicts drug absorption, distribution and elimination processes by using the relevant physiological, physicochemical and biochemical parameters. Two types of input data are required for a PBPK model; physiological (or species-specific) data and drug-specific data. The former refers to tissue volumes and tissue blood flows, which are derived from the species of interest, while the latter includes the tissue-to-plasma partition coefficient (Kp), clearance (CL), free fraction unbound (fu) and blood:plasma ratio (R).

A whole body PBPK (WBPBPK) model is developed by the incorporation of information from different sources, e.g. *in vitro* and *in vivo* experiments, so that it more easily allows altered physiological conditions to be considered. The WBPBPK model is an ideal technique for the prediction of pharmacokinetics in special populations; for example, WBPBPK simulations have been successfully performed for a paediatric population (Björkman, 2005; Edginton *et al*., 2006a), individuals with liver cirrhosis (Edginton & Willmann, 2008) and people undergoing orthopaedic surgery who have sustained substantial blood loss and blood dilution (Björkman *et al*., 2001).

This chapter is divided into four sections. Section 7A describes the general methods used for developing the WBPBPK models. The aims of Section 7B were to (i) develop a WBPBPK model of ciprofloxacin for healthy adults, and (ii) to investigate the impact of different methods for predicting Kp. In Section 7C, a WBPBPK model for healthy children in different age groups was created. In the final section, the parameters for healthy children were then scaled to malnourished children, in order to predict the PK of ciprofloxacin in this specific population.

7A GENERAL METHODS

7A.1 Model development

7A.1.1 Structural model

In the present study, a WBPBPK model for ciprofloxacin, composed of 11 tissue compartments and two blood compartments (venous and arterial), was developed, as illustrated in Figure 7.1. For the oral model, ciprofloxacin was administered to gut lumen and was then absorbed into gut tissue. For the intravenous (IV) model (both IV bolus and IV infusion), ciprofloxacin was administered directly to the venous compartment. Blood flow to the liver was the sum of the flows from the hepatic artery, gut and spleen. The lung compartment was used to close the circulation loop, and received blood at a flow rate equal to that of the cardiac output.

Ciprofloxacin is rapidly absorbed and distributed in the body (Drusano *et al*., 1986a), so it was assumed that this compound faces minimal hindrance in its systemic transport. Therefore, all tissues were considered to represent perfusion-rate limited, well-stirred compartments. Approximately two-thirds of an administered dose of ciprofloxacin is renally eliminated (Davis *et al*., 1996). It has been found that the renal clearance of ciprofloxacin greatly exceeds creatinine clearance, indicating that, in addition to glomerular filtration, tubular secretion makes a significant contribution (Drusano *et al*., 1987; Wingender *et al*., 1984). The metabolites of ciprofloxacin have been detected in both urine and faeces, indicating that there is also hepatic clearance (Hoffken *et a*l., 1985; Rohwedder *et al*., 1990). Moreover, as a small amount of unchanged drug (7.3%) can be detected in faeces after ciprofloxacin was infused intravenously (Rohwedder *et al*., 1990), transintestinal elimination is considered to be an additional elimination route for ciprofloxacin. A ‘rest of the body’ compartment was also included in the model in order to compensate for the mass of drug that is unaccounted for in the closed loop system and for model misspecification.

Figure 7.1 A WBPBPK model for ciprofloxacin

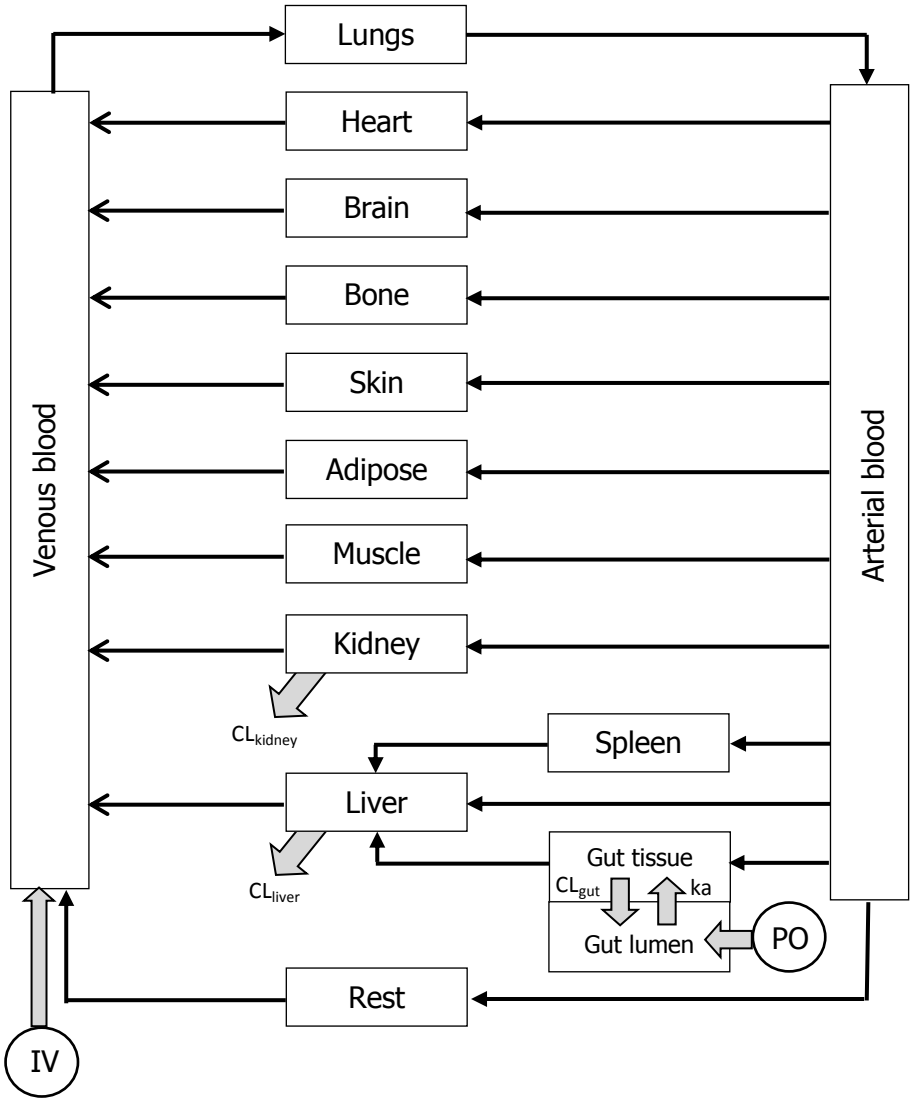

Key: IV = intravenous administration, PO = oral administration, ka = absorption rate constant and CL=clearance.

7A.1.2 Statistical models

A normal distribution was assumed for bioavailability (F) and fu, while other drug-specific parameters, including Kp, CL and absorption rate constant (ka), were assumed to be log-normally distributed. R was fixed in this study. Physiological variability was incorporated in the model via the use of the multivariate Dirichlet distribution (Gisbert *et al*., 2002; Peters, 2012). This type of distribution allows the physiological parameters to be constrained as follows:

(i) Inter-relationships between physiological parameters are considered

(ii) Organ volumes are represented as proportions of body weight

(iii) Organ blood flows are represented as proportions of the cardiac output

(iv) Parameters are sampled with upper and lower limits

The mean value for each organ volume, as well as the variance and covariance, was calculated by using the Dirichlet distribution formula (equations 7.1-7.3), as suggested by Krewski *et al*. (1995).

$$\mathrm{E_D}[V_j] = \frac{\mathrm{E}[Bw](\eta_j b_j + (\Omega - \eta_j)a_j)}{\Omega} \tag{7.1}$$

$$\mathrm{Var_D}(V_j) = \frac{\mathrm{E}[Bw^2](b_j - a_j)^2 \eta_j (\Omega - \eta_j)}{\Omega^2(1+\Omega)} + \mathrm{Var}(Bw)\frac{\left(\eta_j b_j + (\Omega - \eta_j)a_j\right)^2}{\Omega^2} \tag{7.2}$$

$$\mathrm{Cov_D}(V_i, V_j) = \frac{\mathrm{E}[Bw^2](b_i - a_i)(b_j - a_j)\eta_i \eta_j}{\Omega^2(1+\Omega)} + \mathrm{Var}(Bw)\frac{\left(n_i b_i + (\Omega - \eta_i)a_i\right)\left(n_j b_j + (\Omega - \eta_j)a_j\right)}{\Omega^2} \tag{7.3}$$

where:

$\mathrm{E_D}[V_j]$: Dirichlet mean value for the volume of the organ *j*

E[*Bw*]: mean value of the body weight

η_i, η_j: mean value for the volume of the organs *i* and *j*

Ω: sum of all the organ volumes

b_i, b_j: upper bound value for the volume of the organs *i* and *j* expressed as a fraction of Ω. The upper bound value was calculated by assuming equality to η+2SD, where η is mean of the organ volume and SD is standard deviation, respectively.

a_i, a_j: lower bound value for the volume of the organs *i* and *j* expressed as a fraction of Ω. The lower bound value was calculated by assuming equality to η-2SD.

$\mathrm{Var_D}(V_j)$: Dirichlet variance for the volume of the organ *j*

Var[*Bw*]: variance of the body weight

$\mathrm{Cov_D}(V_i, V_j)$: Dirichlet covariance between the volume of the organs *i* and *j*

The mean values of the organ volumes calculated using equation 7.1 were different from the mean physiological values obtained from the literature, so the variance and covariance calculated with equations 7.2 and 7.3 were adjusted as follows:

$$\mathrm{Var}[V_j] = \left(\frac{\mathrm{E_L}[V_j]\sqrt{\mathrm{Var_D}[V_j]}}{\mathrm{E_D}[V_j]} \right)^2 \tag{7.4}$$

$$\mathrm{Cov}(V_i, V_j) = \frac{\mathrm{Cov_D}(V_i, V_j)}{\sqrt{\mathrm{Var_D}[V_i]\mathrm{Var_D}[V_j]}} \sqrt{\mathrm{Var}[V_i]\mathrm{Var}[V_j]} \tag{7.5}$$

where

$\mathrm{Var}[V_i]$: variance of the volume of the organ *i*

$\mathrm{Var}[V_j]$: variance of the volume of the organ *j*

$\mathrm{E_L}[V_j]$: mean value for the volume of the organ *j* obtained from the literature

$\mathrm{Cov}(V_i,V_j)$: covariance between the volumes of the organs *i* and *j*

The variance-covariance matrix calculated with equations 7.4 and 7.5 was subsequently used to sample from a multivariate normal distribution, which can give similar results to those sampled directly from a Dirichlet multivariate distribution.

In this study, the mean values for tissue volumes and blood flows were obtained from the literature. The volume of the rest of the body compartment was calculated as being the difference between the total body weight and the sum of the volumes of the remaining 13 organs. The blood flow of the rest of the body compartment was calculated as being the difference between the cardiac output and the sum of blood flows to the remaining eight organs. The organ volumes sampled from a Dirichlet distribution were used to calculate organ blood flows by using the following equation (Farrar *et al*., 1989):

$$\mathrm{Q}_i = \frac{V_{\mathrm{D},i} \cdot \mathrm{Q}_{\mathrm{P},i} \cdot \mathrm{CO}}{\eta_i} \tag{7.6}$$

where

Q_i: blood flow to the organ *i*

$V_{D,i}$: volume of the organ *i* sampled from a Dirichlet distribution

$Q_{P,i}$: preferred proportion of organ blood flow to the cardiac output of the organ *i*

CO: cardiac output

η_i: mean volume of the organ volume *i*

7A.2 Mechanistic model for Kp prediction

7A.2.1 Poulin model

Poulin and colleagues have developed mechanistic-based equations to predict Kp values, using tissue composition data, physicochemical properties and plasma protein binding of the compound (Poulin *et al*., 2001; Poulin & Theil, 2000; Poulin & Theil, 2002). These equations are based on the assumption that the drug is distributed homogeneously in each tissue (and plasma), primarily by passive diffusion. The drug then divides between lipids and water, and also reversibly binds to common proteins present in plasma and tissue interstitial space. In 2004, Berezhkovskiy corrected some of the errors related to protein binding in these equations, and this yielded equations 7.7 and 7.8, as follows:

Kp values for lean tissues:

$$Kp = \frac{\left[P_{O:W}(V_{nl} + 0.3V_{ph}) + V_{wt}/fu_t + 0.7V_{ph}\right]_{\text{-tissue}}}{\left[P_{O:W}(V_{nl} + 0.3V_{ph}) + V_{wt}/fu_p + 0.7V_{ph}\right]_{\text{-plasma}}} \quad (7.7)$$

Kp values for adipose tissues:

$$Kp = \frac{\left[D_{VO:W}(V_{nl} + 0.3V_{ph}) + V_{wt}/fu_t + 0.7V_{ph}\right]_{\text{-tissue}}}{\left[D_{VO:W}(V_{nl} + 0.3V_{ph}) + V_{wt}/fu_p + 0.7V_{ph}\right]_{\text{-plasma}}} \quad (7.8)$$

where

$P_{O:W}$: *n*-octanol:buffer partition coefficient (PC) of the non-ionised form at pH 7.4

$D_{VO:W}$: olive oil:buffer PC of both non-ionised and ionised forms at pH 7.4

V: fraction of volume for neutral lipids (nl), phospholipids (ph) and water (wt)

fu_p: fraction unbound in plasma

fu_t: fraction unbound in tissue

$P_{O:W}$ and $D_{VO:W}$ were used as input information of drug lipophilicity for lean tissues and adipose tissues, respectively. In this thesis, $P_{O:W}$ was taken from the literature and was used to calculate $D_{VO:W}$ as follows. The ionised form is generally only soluble in the buffer phase, but the non-ionised species is soluble in both the aqueous and the lipophilic phases. $P_{O:W}$ that accounted only for the non-ionised form was changed to $K_{OV:W}$, which is the olive oil:buffer PC of the non-ionised form, by using linear regression, as shown in equation 7.9 (Leo *et al*., 1971).

$$\text{Log}K_{OV:W} = 1.115 \times \text{Log}P_{O:W} - 1.34 \qquad (7.9)$$

The $K_{OV:W}$ was then used to estimate $D_{VO:W}$ using classical Henderson-Hasselbalch equations, assuming that $D_{VO:W}$ and $K_{OV:W}$ differ by a factor corresponding to the ionised form in the aqueous phase. Since ciprofloxacin is an amphoteric compound, the following equation was used:

$$\text{Log}D_{OV:W} = \text{Log}K_{OV:W} - \text{Log}(1 + 10^{pH - pKa1}) - \text{Log}(1 + 10^{pKa2 - pH}) \qquad (7.10)$$

where pKa1 < pKa2

fu_t can be calculated by using fu_p and r, where r is the average value of the tissue interstitial fluid:plasma ratio of albumin and lipoproteins (r = 0.5 for lean tissue and r = 0.15 for adipose tissue) (Poulin *et al*., 2011).

$$fu_t = \frac{1}{1 + \left((1 - fu_p) / fu_p\right) \times r} \qquad (7.11)$$

In the present study, $P_{O:W}$, fu_p, pKa1 and pKa2 values obtained from the literature were used to calculate Kp values using the specific tissue composition data of each organ, as presented in Table 7.1.

7A.2.2 Rodgers model

The Poulin model was further expanded by Rodgers and colleagues by the incorporation of electrostatic interactions between compound and tissue acidic phospholipids, where the affinity of this interaction can be estimated using blood cell binding data (Rodgers *et al*., 2005; Rodgers & Rowland, 2006). Using these equations, it has been found that Kp values are more accurately predicted when 89% of the predicted Kp values lie within a factor of three, compared to experimental values (Rodgers & Rowland, 2006). The unbound tissue:plasma partition coefficient (Kpu) can be calculated by the following equations:

Kpu values for lean tissues:

$$Kpu = \frac{(1+X \cdot f_{IW})+(Ka_{AP} \cdot C_{AP} \cdot X)+(P_{O:W} \cdot V_{nl})+(0.3P_{O:W}+0.7)V_{ph}}{1 + Y} + f_{EW} \qquad (7.12)$$

Kpu values for adipose tissues:

$$Kpu = \frac{(1+X \cdot f_{IW})+(Ka_{AP} \cdot C_{AP} \cdot X)+(K_{O:W} \cdot V_{nl})+(0.3P_{O:W}+0.7)V_{ph}}{1 + Y} + f_{EW} \qquad (7.13)$$

where f_{IW} and f_{EW} represent the volume fraction of intracellular water and extracellular water, respectively. C_{AP} is the concentration of acidic phospholipids. This input information is shown in Table 7.1. Ka_{AP} is the affinity constant for the acidic phospholipids, which can be obtained by the equation derived from red blood cell partitioning data (equation 7.14). The estimated Ka_{AP} value can be negative if the affinity is very low. In these circumstances, Ka_{AP} was set to zero.

$$Ka_{AP} = \frac{[Kpu_{BC} - (1 + Z \cdot f_{IW}) - (P_{O:W} \cdot V_{nl}) + (0.3P_{O:W} + 0.7)V_{ph}]}{1 + Y} \times \frac{1 + Y}{C_{AP} \cdot Z} \quad (7.14)$$

where Kpu_{BC} is the red blood cell:plasma water concentration ratio, which can be determined *in vitro* from R, fu_p and haematocrit (Hct) (equation 7.15) (Rowland & Tozer, 1995). X, Y and Z are parameters used to consider drug ionisation in intracellular tissue water, plasma and red blood cells, and can be calculated by equations 7.16-7.18 (Rodger & Rowland, 2007), respectively.

$$Kpu_{BC} = \frac{[R - (1 - Hct)]}{fu_p \cdot Hct} \quad (7.15)$$

$$X = 10^{pKa_{BASE} - pH_{IW}} + 10^{pH_{IW} - pKa_{ACID}} \quad (7.16)$$

$$Y = 10^{pKa_{BASE} - pH_{P}} + 10^{pH_{P} - pKa_{ACID}} \quad (7.17)$$

$$Z = 10^{pKa_{BASE} - pH_{BC}} + 10^{pH_{BC} - pKa_{ACID}} \quad (7.18)$$

where the $pH_{p,}$ which is the pH of plasma, is equal to 7.4, $pH_{IW,}$ which is the pH of intracellular tissue water, is equal to 7, and pH_{BC} ,which is the pH of red blood cells, is equal to 7.22.

Table 7.1 Input parameters used for prediction of Kp values by Poulin model and Rodgers model

Tissues	Tissue composition data for humans (fraction of tissue wet weight)						Tissue volume (L/kg)
	Water	Neutral phospholipids	Neutral lipids	Extracellular water	Intracellular water	Acid phospholipids	
Plasma	0.95	0.0032	0.0021	-	-	-	0.0450
Adipose	0.15	0.79	0.002	0.135	0.017	0.40	0.1490
Bone	0.45	0.074	0.0011	0.10	0.346	0.67	0.0976
Brain	0.78	0.051	0.0565	0.162	0.62	0.40	0.0213
Gut	0.76	0.0487	0.0163	0.282	0.475	2.41	0.0264
Heart	0.78	0.0115	0.0166	0.32	0.456	2.25	0.0044
Kidney	0.76	0.0207	0.0162	0.273	0.483	5.03	0.0044
Liver	0.73	0.0348	0.0252	0.161	0.573	4.56	0.0360
Lungs	0.78	0.003	0.009	0.336	0.446	3.91	0.0131
Muscle	0.71	0.022	0.0072	0.079	0.63	1.53	0.4841
Skin	0.67	0.0284	0.0111	0.382	0.291	1.32	0.0804
Spleen	0.79	0.0201	0.0198	0.207	0.579	3.18	0.0029
Blood cells	0.63	0.0012	0.0033	-	0.603	0.50	0.0347

Data were obtained from Poulin and Theil (2009) and Rodgers *et al.* (2005).

7A.2.3 Empirical method

The empirical method was proposed by Jansson and colleagues (2008). This method was developed on the basis of the previous finding that a correlation between Kp_{muscle} and Kp values of other tissues exists. Therefore, if the Kp of muscle is known, it can be used as a predictor for other tissues (Björkman, 2002; Poulin & Theil, 2000). The correlation between Kp_{muscle} and other tissues can be described by log-transformation of linear regression, as follows:

$$Kp_{tissue} = 10^{a_{tissue,i} \times \log Kp_{muscle} + b_{tissue,i} \times \log X_{drug} + intercept_{tissue,i}} \quad (7.19)$$

where a_{tissue} is a slope factor for tissue *i* and b_{tissue} is a slope factor for the drug-specific lipophilicity parameter, $LogX_{drug}$.

The volume of distribution at steady-state (V_{ss}) can be calculated using the plasma volume and the sum of apparent volumes of each tissue, as shown in the following equation:

$$V_{ss} = V_{plasma} + \sum_{i=1}^{n} V_{tissue,i} \times Kp_{tissue,i} \quad (7.20)$$

where V_{plasma} is plasma volume and $V_{tissue,i}$ is the apparent volume of tissue *i*.

By insertion of equations 7.19 and 7.20, the V_{ss} can be explained by:

$$V_{ss} = V_{plasma} + \sum_{i=1}^{n} V_{tissue,i} \times 10^{a_{tissue,i} \times \log Kp_{muscle} + b_{tissue,i} \times \log X_{drug} + intercept_{tissue,i}} \quad (7.21)$$

Kp_{muscle} was calculated by inserting the slope factors, intercepts and a lipophilicity descriptor, as shown in Table 7.2, together with the specific values for tissue volumes, into equation 7.21. The value of Kp_{muscle} was then iteratively changed by using the 'Solver' function, which was implemented in Microsoft Excel®, until the calculated V_{ss} was in accordance with the experimental data. The Kp of other tissues was consequently estimated by inserting the iteratively obtained Kp_{muscle} value into equation 7.19. Data to determine the correlation of Kp between muscle and spleen were limited, so the Kp value for spleen was assumed to be identical to that of muscle.

Table 7.2 Slope factors, intercepts and lipophilicity descriptors for zwitterion compounds

Tissues	$a_{tissue,i}$	$b_{tissue,i}$	Intercept	X_{drug}
Adipose	0.897	0.265	0.084	$K_{OV:W}$
Bone	0.817	0	-0.042	-
Brain	0.620	0.255	-0.442	$P_{O:W}$[a]
Gut	0.520	0	0.206	-
Heart	0.845	0.033	0.140	$P_{O:W}$[a]
Kidney	0.337	-0.070	0.524	$P_{O:W}$[a]
Liver	0.484	0.074	0.382	$P_{O:W}$[a]
Lungs	0.790	0	0.166	-
Skin	0.663	0	0.165	-

[a] adjusted for ionisation at physiological pH 7.4 using the Henderson-Hasselbalch equations for zwitterion compounds (equation 7.10).

7A.3 WBPBPK modelling

In this study, all WBPBPK models were developed using the MATLAB program Version 7.11 (MathWorks, Natick, MA, USA) on a personal computer with a Microsoft Windows 7 operating system and an Intel Core i7 processor. The model was composed of the arterial and venous blood, lungs, brain, bone, skin, adipose, kidneys, liver, muscle, heart, gut, spleen and rest of the body compartments (as presented in Figure 7.1). This model was used to generate a concentration-time profile for a population of 1000 virtual subjects that had an equal proportion of males (n = 500) and females (n = 500).

7A.4 Model assessment

The predictive performance of the model was assessed by comparing the simulated concentration-time data with corresponding measured concentrations obtained from the literature. Studies were selected if the measured concentration data were presented numerically or as graphs. If the data were provided as a graph, they were extracted by using the GetData Graph Digitizer program, Version 2.24.

Accuracy and precision were calculated using the methods described by Sheiner and Beal (1981). Prediction error (pe_i), which is the difference between the prediction and observation ($C_{pred} - C_{obs}$), was used to calculate the mean squared prediction error (*mse*) and the root mean squared prediction error (*rmse*) as follows:

$$mse = \frac{1}{N}\sum_{i=1}^{N} pe_i^2 \qquad rmse = \sqrt{mse} \tag{7.22}$$

The smaller the *mse* and *rmse*, the greater the precision of the prediction. Bias is a measure of the amount by which the predictions are systemically too high or too low. The mean prediction error (*me*) that was used to describe the bias of the prediction was calculated as follows:

$$me = \frac{1}{N}\sum_{i=1}^{N} pe_i \tag{7.23}$$

The standard error of the *mse* and *me* were calculated by the following equation:

$$se_{\overline{X}} = \left[\frac{1}{N(N-1)} \sum_{i=1}^{N} (X_i - \overline{X})^2 \right]^{1/2} \tag{7.24}$$

where for *mse*, X_i and $\overline{X}$ are the individual squared pe_i values and the mean of squared pe_i values (*mse*), respectively. For *me*, X_i and $\overline{X}$ are pe_i values and the mean of pe_i values (*me*), respectively. Confidence intervals (95% CI) were also calculated for *mse* and *me*, using the following formula:

$$95\%\ \text{CI} = \overline{X} \pm t_{0.975}(N-1) se_{\overline{X}} \tag{7.25}$$

where $t_{0.975}(N\text{-}1)$ is the 97.5th percentile of the *t*-distribution with *N*-1 degrees of freedom.

7B WBPBPK MODEL FOR HEALTHY ADULTS

7B.1 METHODS

7B.1.1 Input parameters

7B.1.1.1 Physiological parameters

The physiological parameters used for adults in this study are given in Table 7.3. The reference values of a total body weight of 73 kg for males and 60 kg for females were taken from the International Committee on Radiological Protection (ICRP, 2003). The body weight was sampled from a log-normal distribution, assuming that the coefficient of variation (CV) was 20% (14.6 kg for males and 12 kg for females). Body weight was subsequently used to estimate the cardiac output by using the following formula (Fiserova-Bergerova, 1995):

$$\text{Cardiac output (L/h)} = 11.22 \times [\text{body weight (kg)}]^{0.81} \quad (7.26)$$

Mean values for organ weights and organ blood flows were also taken from the ICRP (2003). WBPBPK model compartments are defined by their volume, rather than their mass, so the density of each organ was used to convert weight to volume. The densities of the majority of organs were obtained from the ICRP (2003), with the few exceptions being the arterial, venous, liver and rest of the body compartments, for which there were no available data in the literature. The densities of these organs were therefore assumed to be equal to 1. Bone density varies depending on the type of bone tissue, i.e. cortical or trabecular. In the present study, the cortical bone density of 2 g/cm^3 was chosen because it accounts for 80% of total bone mass (Brown *et al*., 1997; ICRP, 2003). Several different organs located in the gastrointestinal tract (stomach, small intestine and large intestine) were included in a gut compartment. It has been reported that such organs have very similar densities, ranging from 1.041-1.052 g/cm^3; therefore, the value of 1.042 g/cm^3, which represents the density of both small intestine and large intestine, was used. The density of total body weight was also assumed equal to 1 g/cm^3. All organ volumes were assumed to have a CV of 20%.

Table 7.3 Physiological parameters for healthy adults

Organs	Density (g/cm^3)	Weight (kg) (M/F)	Volume (L) (M/F)	Blood flow (L/h) (M/F)
Adipose	0.916	14.5/19	15.83/20.74	19.50/30.09
Bone	2	5.5/4	2.75/2	19.50/17.70
Brain	1.04	1.45/1.3	1.39/1.25	46.80/42.48
Gut	1.042	1.24/1.15	1.19/1.10	62.40/63.72
Heart	1.03	0.33/0.25	0.32/0.24	15.60/17.70
Kidney	1.05	0.31/0.275	0.30/0.26	74.10/60.18
Liver	1	1.8/1.4	1.8/1.4	25.35/23.01
Muscle	1.041	29/17.5	27.86/16.81	66.30/42.48
Skin	1.1	3.3/2.3	3.0/2.09	19.50/17.70
Spleen	1.06	0.15/0.13	0.14/0.12	11.70/10.62
Lungs	1.05	0.5/0.42	0.48/0.40	Predicted[a]
Arterial	1	1.8/1.8	1.8/1.8	Predicted[a]
Venous	1	3.6/3.6	3.6/3.6	Predicted[a]
Rest of the body	1	9.52/6.88	12.54/8.18	Calculated[b]
Total	1	73/60	73/60	Predicted[a]

[a] predicted from the sampled total body weight using equation 7.26.
[b] calculated as the difference between predicted cardiac output and the sum of organ blood flows.
M = male, F = female.

7B.1.1.2 Drug-specific parameters

Ciprofloxacin is an amphoteric compound with pKa1 of 6.09 and pKa2 of 8.74 (Ross *et al*., 1992). For $LogP_{O:W}$, the experimental value of 0.28 was used, as reported in the studies of Takács-Novák *et al*. (1992) and Singh (2005). The values of 0.70 (SD = 0.07) and 1 were used for fu_p and R, respectively (Chen *et al*., 2008; Poulin & Theil, 2002; Uchimura *et al*., 2010). In the initial step of model development, different methods for Kp prediction were compared; however, the empirical method was further used for predicting Kp values in subsequent models. All Kp values were assumed to have a CV of 10%

A renal clearance (CL_R) of 0.27 L/h/kg (SD = 0.0549) and non-renal clearance (CL_{NR}) of 0.2417 L/h/kg (SD = 0.09) were selected (Borner *et al*., 1986). The CL_R was assumed to account for both the glomerular filtration and tubular secretion processes of CL_R. The relative contributions that the clearance of each elimination pathway made to the total CL_{NR} were obtained from a study by Rohwedder *et al*. (1990), which suggested that hepatic metabolism and transintestinal secretion account for 63% and 37% of total CL_{NR}, respectively. Unbound intrinsic hepatic clearance ($CLu_{int,H}$) can also be determined by using hepatic drug clearance (CL_H), hepatic blood flow ($Q_{H,B}$), fu and R as shown in the following equation:

$$CLu_{int,H} = \frac{Q_{H,B} \cdot CL_H}{fu \cdot (Q_{H,B} - CL_H/R)} \qquad (7.27)$$

For the oral model, drug absorption was predicted using the first-order absorption model and a lag time; the model requires the estimates of ka and lag time. A value of 2.03 h^{-1} with an SD of 1.07 h^{-1}, which was obtained from the literature, was used for ka (Borner *et al*., 1986). The lag time was fixed at 0.35 hours (Ullmann *et al*., 1986). A value of 0.837, taken from the study by Bergan *et al*. (1986) was used for F, with the variability assumed equal to 10%.

7B.1.2 Simulation and comparison with experimental data

7B.1.2.1 Comparison of different methods for Kp prediction

The impact that the different methods for Kp prediction, including the Poulin model, the Rodgers model and the empirical method, had on the Kp values, as well as on the concentration-time profiles, were investigated using an IV bolus model. When using the empirical method, the impact of the discrepancy in V_{ss} values on the predictions was also tested. This was performed by using a variety of V_{ss} values reported in the literature, including a minimum value of 1.74 L/kg, a maximum value of 2.40 L/kg and a median value of 2 L/kg (as shown in Table 1.3 of Chapter 1).

7B.1.2.2 IV bolus model

Concentration-time data were generated for a dose of 100 mg by IV bolus injection. The predicted concentrations in the venous compartment and the lung compartment were compared with the experimental data obtained from the studies conducted by Wise *et al.* (1984) and Schlenkhoff *et al.* (1986), respectively.

7B.1.2.3 IV infusion model

This model was used to simulate concentration-time profiles for three dosing regimens, including a 100 mg 30-minute infusion, a 200 mg 10-minute infusion and a 200 mg 30-minute infusion. There were no available data regarding the tissue concentrations in the literature, so the model was evaluated by only comparing the predicted concentrations in the venous compartment with the values given in the literature. The experimental data for this model were obtained from the studies of Gonzalez *et al.* (1985a), Drusano *et al.* (1986a), and Drusano *et al.* (1986b).

7B.1.2.4 Oral model

Several dosing regimens, including 100 mg, 250 mg, 500 mg, 750 mg and 1000 mg, were tested for this model. The predicted concentrations in the venous compartment were compared with the experimental data obtained from the studies of Crump *et al.* (1983), Gonzalez *et al.* (1984) and Bergan *et al.* (1986), and the predicted concentrations in adipose, muscle and skin were validated with the data provided in a study conducted by Aigner and Dalhoff (1986).

7B.2 Results

7B.2.1 Comparison of different methods for Kp prediction

The Kp values predicted using the different methods are presented in Table 7.4. The Kp values obtained by using Poulin model were considerably lower than those obtained using other methods. The V_{ss} estimated from the Kp values of the Poulin model was 0.57 L/kg, which was significantly lower than the values given in the literature (1.74-2.40 L/kg). The Kp values obtained from the Rodgers model and the empirical method were comparable with regard to the majority of organs; however, significant discrepancies were observed with the brain and liver. The Kp_{brain}

predicted from the Rodgers model was 1.27, compared to the values of between 0.18-0.26 that were obtained from the empirical method. The Kp_{liver} predicted from the Rodgers model was 6.52, which was higher than the values estimated using the empirical method (2.79-3.70). The V_{ss} calculated from the results of the Rodgers model was 2.78 L/kg, which was in accordance with the value in the literature. As expected, when using the empirical method, the Kp value of each organ was dependent on the V_{ss} value given in the literature, which had been defined initially. The use of a higher V_{ss} resulted in higher Kp estimates.

The concentration-time profiles that were generated from different sets of predicted Kp values are illustrated in Figure 7.2. The profiles produced by using the Kp values of the Poulin model were significantly different from the profiles obtained with the other methods used. With the exception of the brain and liver, the predicted concentrations obtained from the Kp values of the Rodgers model and the empirical method were very similar. For the brain, the predicted concentrations derived from the Rodgers model were higher than those derived from the empirical method. A similar trend was also observed for the liver compartment. In addition, it was found that the predictions regarding the venous compartment and the lung compartment fitted very well with the observed data.

7B.2.2 IV bolus model

Figure 7.3 shows the predicted concentration-time profiles in the venous and lung compartments after a 100 mg IV bolus administration of ciprofloxacin to a healthy adult. The venous compartment predictions fit perfectly to the observed data; almost all observed data were within the 95% prediction interval. The small values of *rmse* (0.200; 95% CI 0.055, 0.277) and *me* (-0.037; 95% CI -0.333, 0.260) indicated that the model is precise and unbiased. Variability of the observed data in the lung compartment was higher than in the venous compartment; however, the model was reasonably precise (*rmse* 0.506; 95% CI 0.462, 0.547) although there was a small bias resulting in under prediction (*me* -0.386; 95% CI -0.426, -0.345).

Table 7.4 Kp values predicted from Poulin model, Rodgers model and the empirical method

Organs	Poulin model	Rodgers model	Empirical method		
			V_{ss}= 1.74 L/kg (M/F)	V_{ss}= 2.0 L/kg (M/F)	V_{ss}= 2.4 L/kg (M/F)
Adipose	0.12	0.64	0.35/0.43	0.40/0.49	0.48/0.59
Bone	0.50	1.29	1.33/1.79	1.65/2.17	2.13/2.75
Brain	0.82	1.27	0.18/0.21	0.20/0.23	0.22/0.26
Gut	0.76	3.77	2.93/3.28	3.18/3.56	3.53/3.96
Heart	0.72	3.57	3.05/3.66	3.48/4.19	4.13/4.99
Kidney	0.72	7.10	7.27/7.83	7.66/8.26	8.21/8.85
Liver	0.72	6.52	2.79/3.11	3.01/3.35	3.32/3.70
Muscle	0.67	3.79	3.17/3.94	3.71/4.62	4.54/5.68
Skin	0.65	2.26	3.14/3.63	3.48/4.03	3.99/4.62
Spleen	0.75	4.80	3.17/3.94	3.71/4.62	4.54/5.68
Lungs	0.71	5.68	3.65/4.33	4.13/4.91	4.84/5.78

V_{ss} = volume of distribution at steady-state, M = male, F = female.

Figure 7.2 Concentration-time profiles generated using different sets of Kp values predicted by the Poulin model, the Rodgers model and the empirical method

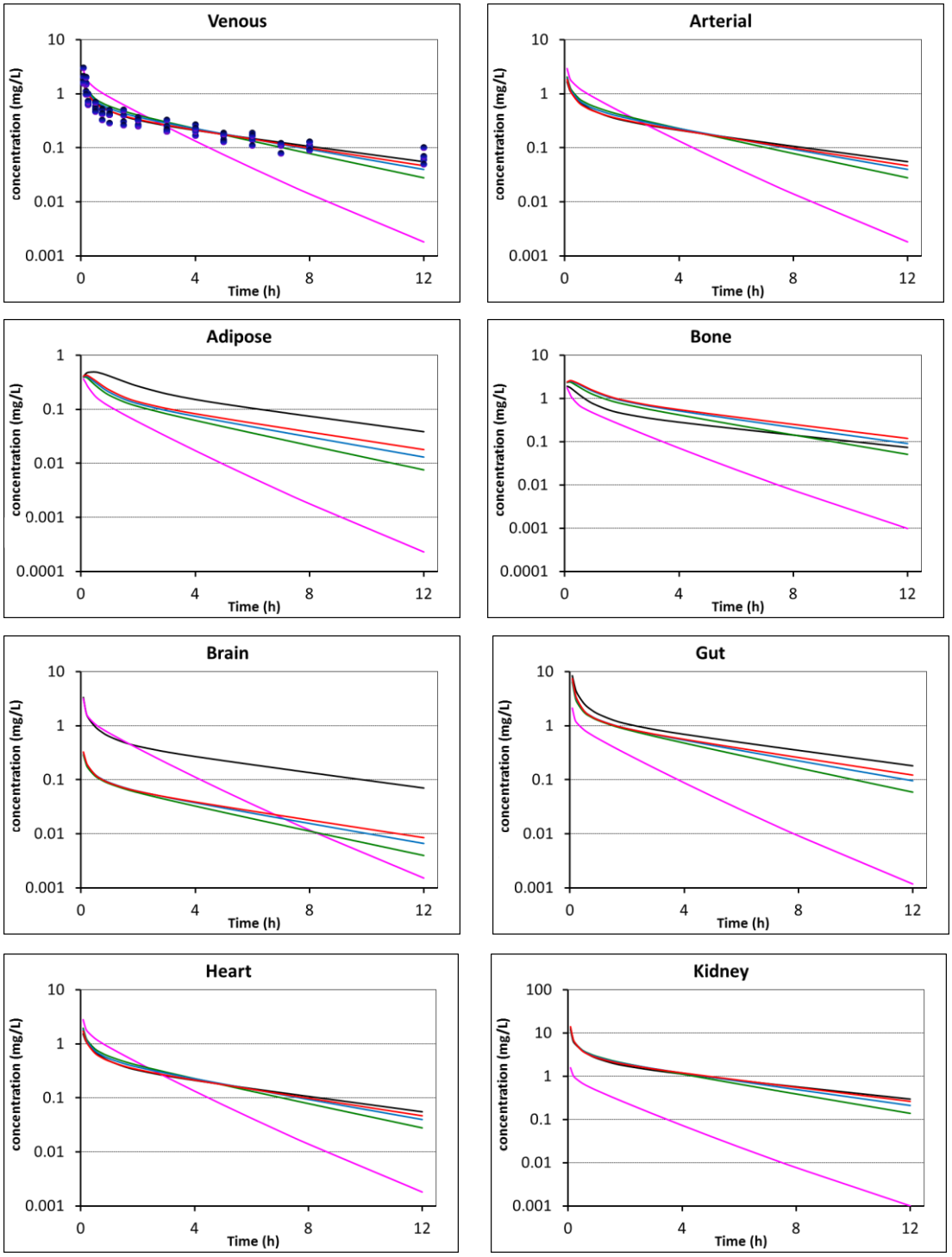

Figure 7.2 (continued)

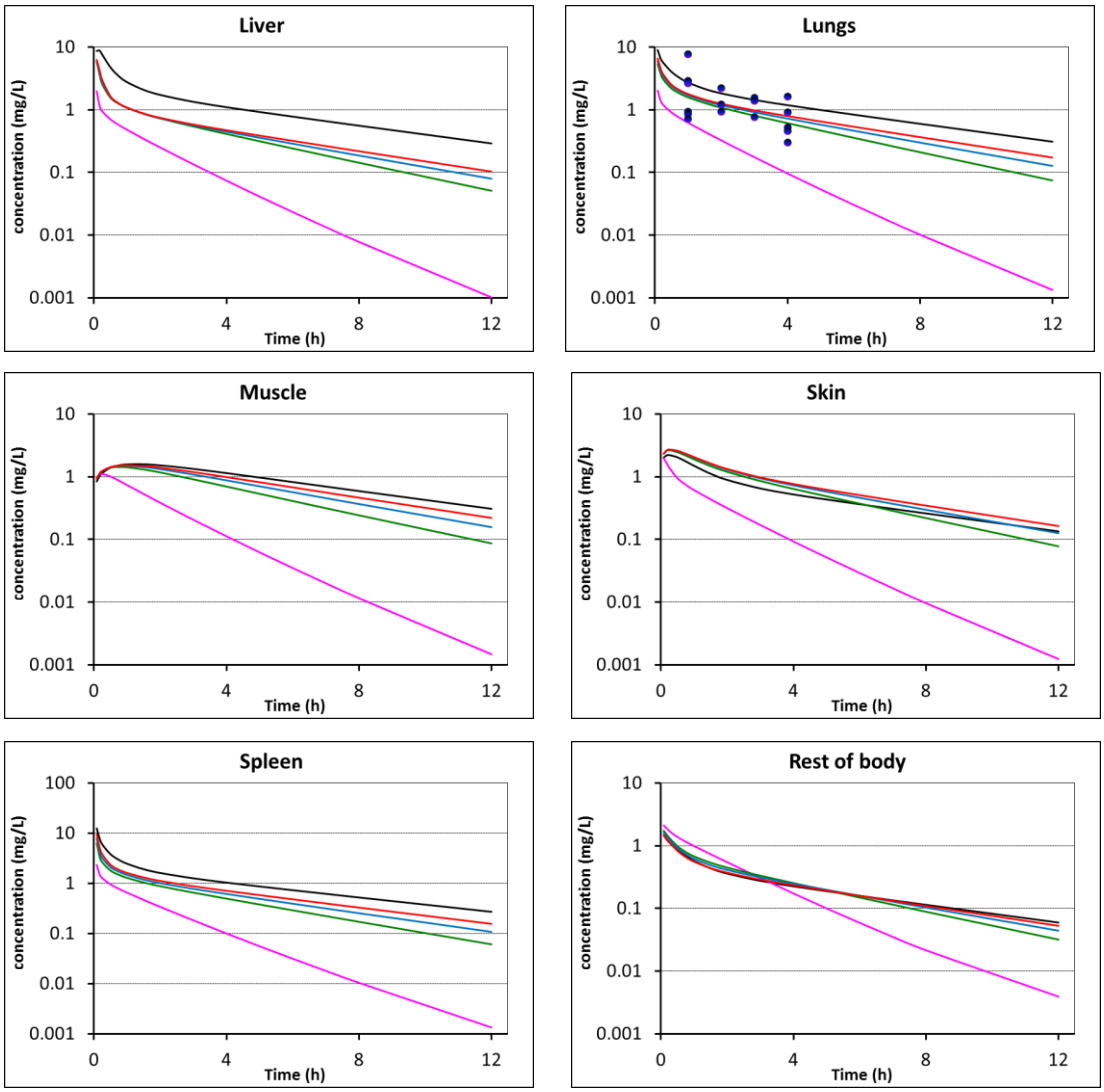

Key: pink line = the Poulin model, black line = the Rodgers model, green line = the empirical method (V_{ss}= 1.24 L/kg), blue line = the empirical method (V_{ss}= 2 Lkg) and red line = the empirical method (V_{ss}= 2.4 L/kg).

Figure 7.3 Concentration-time profiles of ciprofloxacin in plasma and tissue predicted using the IV bolus model.

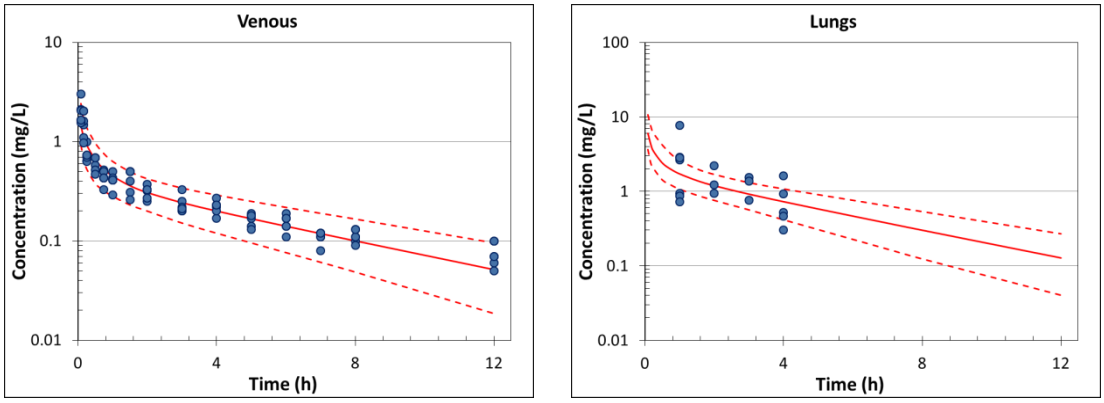

Key: the blue symbols are the observed data (venous = Wise *et al.*, 1984; lungs = Schlenkhoff *et al.*, 1986), the red solid line is the mean prediction and the red dashed lines are the 2.5th (lower) and 97.5th (upper) percentiles of prediction.

7B.2.3 IV infusion model

Figure 7.4 shows the predicted concentration-time profiles when ciprofloxacin was administered by IV infusion. It was found that the predictions and the observed outcomes were very well matched, although the models were tested with different doses (100 mg and 200 mg) and different infusion times (10 minutes and 30 minutes). With a 100 mg 30-minute infusion dosing regimen, *rmse* and *me* were 0.040 (95% CI 0.020, 0.053) and -0.003 (95% CI -0.029, 0.022), and 0.114 (95% CI 0.055, 0.152) and -0.023 (95% CI -0.125, 0.079), when compared with the experimental data obtained from the studies of Gonzalez *et al.* (1985a) and Drusano *et al.* (1986b), respectively. The results obtained using a 200 mg 30- minute infusion dosing regimen were also precise and unbiased, with a *rmse* value of 0.141 (95% CI 0.057, 0.192) and a *me* value of -0.075 (95% CI -0.197, 0.046). When the model was tested using a 200 mg dose with a shorter infusion time (10 minutes), the mean predicted concentrations were slightly overestimated; however, all observed data remained within the prediction interval. The *rmse* and *me* were 0.200 (95% CI 0.088, 0.269) and -0.043 (95% CI -0.269, 0.183), respectively.

Figure 7.4 Concentration-time profiles of ciprofloxacin in plasma, predicted using an IV infusion model

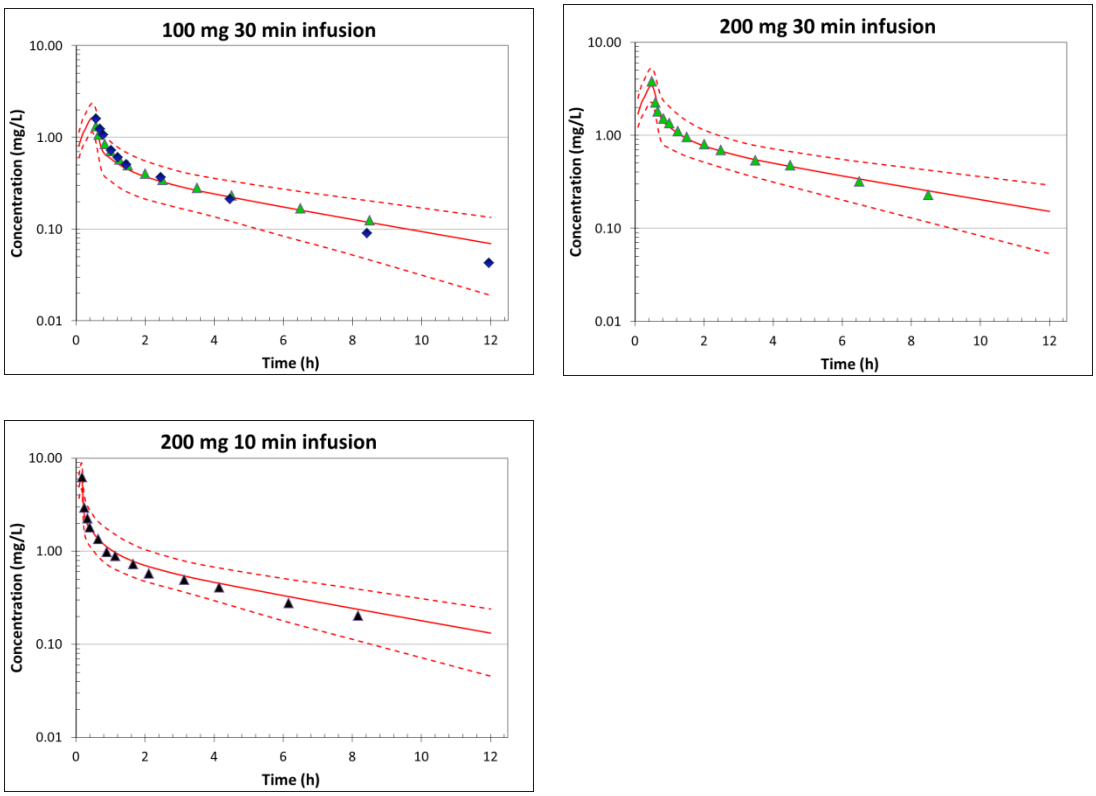

Key: The symbols are the observed data obtained from the literature (blue = Gonzalez *et al.*, 1985a; green = Drusano *et al.*, 1986b; black = Drusano *et al.*, 1986a), the red solid line is the mean prediction and the red dashed lines are the 2.5th (lower) and 97.5th (upper) percentiles of prediction.

7B.2.4 Oral model

Figure 7.5 shows the concentration-time profiles across a wide range of doses generated with an oral model. The concentrations predicted from the model were a reasonable fit with the real-life data obtained from the literature, although there was evidence of model misspecification during the drug absorption phase. With a dose of 100 mg, the peak concentration predicted from the model was slightly lower than the observed data, and the predicted peak concentrations were reached more rapidly than in the observed data when a dose of over 500 mg was applied in the model. The *rmse* results also indicated that the higher-dose models were more imprecise (*rmse* 0.245-0.701 for a dose ≥500 mg) than the smaller-dose models (*rmse* 0.055-0.154 for a dose of 100-250 mg; Table 7.5).

Figure 7.5 Concentration-time profiles of ciprofloxacin in plasma predicted using the oral model

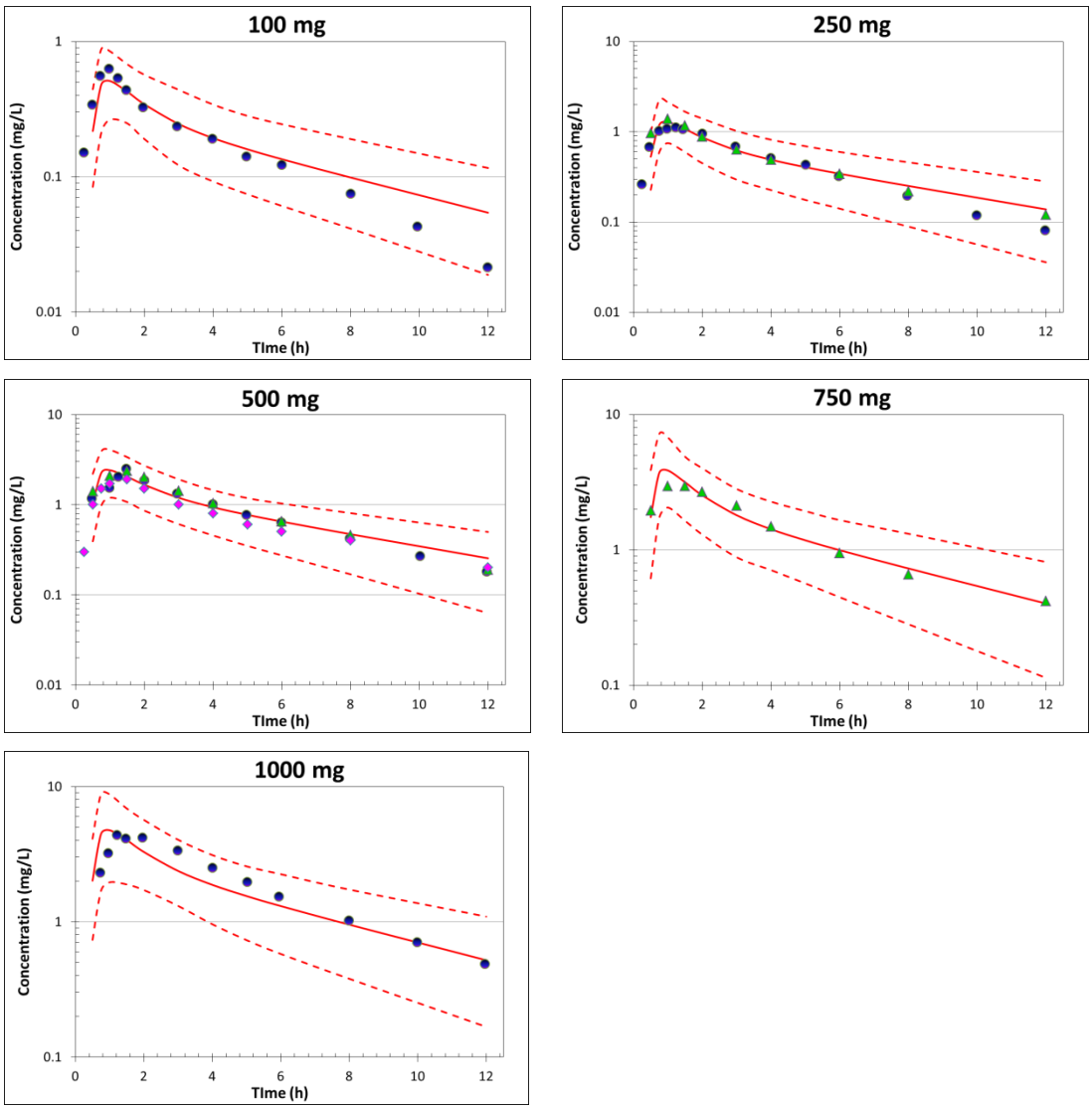

Key: The symbols are observed data obtained from the literature (blue = Bergan *et al.*, 1986; green = Gonzalez *et al.*, 1984; pink = Crump *et al.*, 1983), the red solid line is the mean prediction and red dashed lines are the 2.5th (lower) and 97.5th (upper) percentiles of prediction.

Figure 7.6 shows the concentration-time profiles in skin, muscle and adipose tissue after oral administration of ciprofloxacin 500 mg. It was found that the predicted concentrations were generally consistent with the experimental data; with a few data points being lower or higher than the prediction interval. The *rmse* and *me* of predicted plasma concentrations obtained from the oral model are summarised in Table 7.5.

Figure 7.6 Predicted concentration-time profiles of ciprofloxacin in skin, muscle and adipose predicted using the oral model

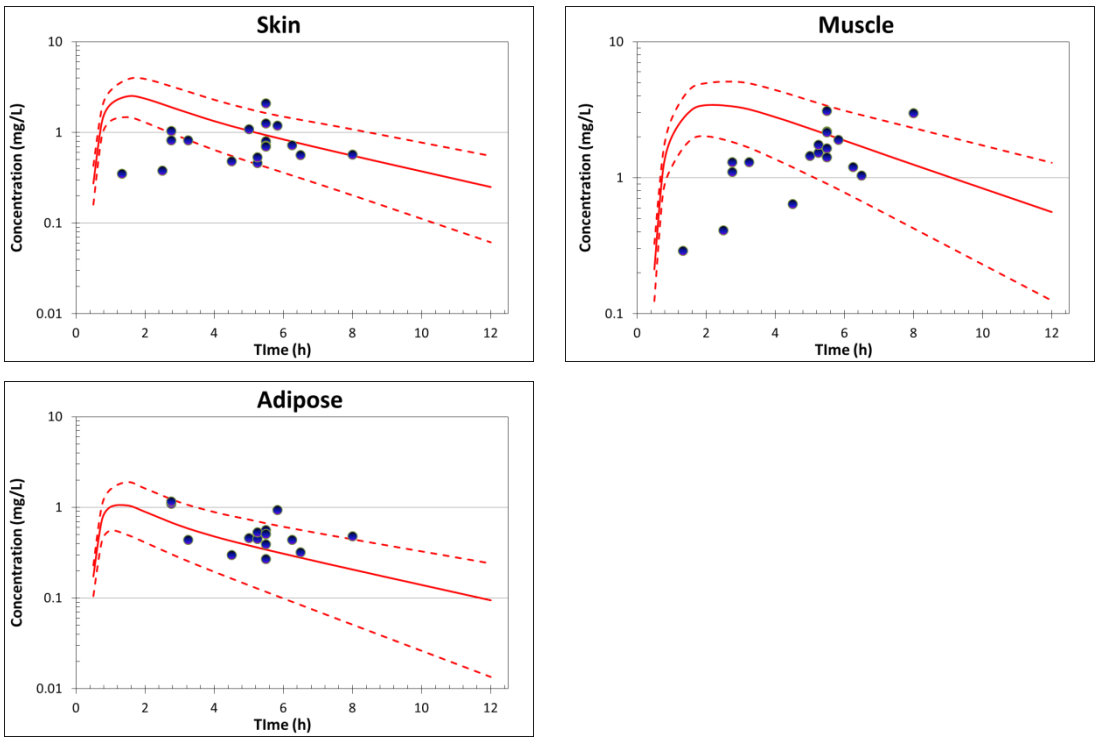

Key: The blue symbols are the observed data (Aigner & Dalhoff, 1986), the red solid line is the mean prediction and the red dashed lines are the 2.5th (lower) and 97.5th (upper) percentiles of prediction.

Table 7.5 The *rmse* and *me* of predicted plasma concentrations from different doses, obtained from the oral model

Doses	*rmse* (95% CI)[a]	*me* (95% CI)[a]	Sources of experimental data
100	0.055 (0.041, 0.095)	-0.019 (-0.076, 0.037)	Bergan *et al.* (1986)
250	0.100 (0.078, 0.118)	0.013 (-0.089, 0.115)	Bergan *et al.* (1986)
250	0.154 (0.110, 0.190)	-0.069 (-0.176, 0.039)	Gonzalez *et al.* (1984)
500	0.327 (0.313, 0.341)	0.001 (-0.293, 0.295)	Bergan *et al.* (1986)
500	0.245 (0.018, 0.103)	-0.110 (-0.279, 0.059)	Gonzalez *et al.* (1984)
500	0.345 (0.134, 0.439)	-0.294 (-0.434, -0.155)	Crump *et al.* (1983)
750	0.344 (0.279, 0.397)	0.050 (-0.212, 0.312)	Gonzalez *et al.* (1984)
1000	0.701 (0.381, 0.915)	-0.211 (-0.812, 0.390)	Bergan *et al.* (1986)

[a] Data points during the lag time were excluded from the calculation.

7B.3 Discussion

The aim of this section was to develop a WBPBPK of ciprofloxacin for healthy adults and also to investigate the usefulness of different methods for Kp prediction with regard to predicted Kp values and concentration-time profiles. The three most commonly used Kp prediction methods were compared; the Poulin model, the Rodgers model and the empirical method. The Poulin model and the Rodgers model predict the Kp values based on tissue composition data, physicochemical properties and protein binding data, while the empirical method predicts the Kp by using the value of V_{ss} given in the literature, the correlation between the Kp of muscle and the Kp of other tissues and drug lipophilicity data.

The results of the comparison suggested that the Kp values for ciprofloxacin obtained from the Poulin model were lower than the values obtained using the other two methods, and it was observed that V_{ss} was under-predicted when calculated using the Kp values of the Poulin model. These findings were in accordance with the results reported by the investigators who originally developed this method of prediction (Poulin & Theil, 2002). They found that the V_{ss} predicted using this model was 0.47 L/kg, which is considerably lower than the experimental value of approximately 1.7-2.4 L/kg, and argued that this was probably the result of different degrees of drug accumulation in the intestinal lumen, as well as error in V_{ss} determination, due to species variation. However, the results of the present study revealed that the V_{ss} value predicted by the Rodgers model was comparable to the experimental values. This may be because the Poulin model was developed only for structurally unrelated acidic, basic and neutral compounds, and therefore may not be applicable for use with ciprofloxacin, which is an amphoteric compound. In contrast, the Rodgers model is developed by incorporating the electrostatic interactions, so it offers greater predictability when used with moderate-to-strong basic compounds; those with at least one pKa value ≥7 (Rodgers *et al.*, 2005; Rodgers & Rowland, 2006).

The Kp values predicted by the Rodgers model and the empirical method were comparable, with the exception of those obtained for the brain and liver. The Kp_{brain}

obtained from the Rodgers model was 1.27, compared to approximately 0.20 from the empirical method. Wolff *et a*l. (1987) administered 200 mg IV ciprofloxacin every 12 hours to patients with bacterial meningitis and then measured drug concentrations in plasma and cerebrospinal fluid (CSF) at 1, 2, 4 and 8 hours after the third infusion. They found that the mean drug concentrations in inflamed CSF: and non-inflamed CSF:serum ratio were 0.26-1.59 and 0.14-0.77, respectively. In another study, the CSF penetration of ciprofloxacin was assessed in individuals with and without inflamed meningitis (Gogos *et al.*, 1991). It was found that the mean drug concentration in CSF:serum was 0.34 for inflamed CSF and 0.43-0.58 for non-inflamed CSF. The results from both studies have demonstrated that ciprofloxacin concentrations are likely to be lower in CSF than in plasma, therefore the Kp_{brain} predicted by the empirical method may be more accurate in this instance. Dan and colleagues (1987) measured ciprofloxacin concentrations in serum and hepatic tissue after administration of a single oral 750 mg dose prior to cholecystectomy. They found that the mean hepatic tissue:serum ratio was approximately 2 – 4, which was consistent with the result of the empirical method (2.79 - 3.70). However, the tissue:serum ratio reported in this study may be different to the Kp_{liver}; since the Kp value should be determined by using steady-state concentrations. In this context, it is difficult to draw a conclusion as to whether the Rodgers model or the empirical method is more accurate when used with amphoteric compounds, because the tissue concentration data were not sufficient nor accurate enough to validate the Kp values of those models.

In this study, ciprofloxacin concentrations obtained from the literature, with regard to lungs, skin, muscle and adipose tissue, were also used to validate the models. The results showed that the model reasonably predicted concentration-time data in those tissues; however, some data points lay outside the prediction interval. This was probably due to these experimental data being very sparse and to high inter-individual variation, as each data point was individually obtained from different subjects. In addition, it is noteworthy that the experimental data of tissue concentrations may vary depending on certain factors, e.g. techniques used to measure drug concentration and the site of measurement. A single intravenous dose

of 200 mg demonstrated that the mean (SD) ciprofloxacin concentrations were 1.8 (0.9) mg/kg in bronchial mucosa, 3.4 (2.5) mg/kg in lung parenchyma and 1.7 (1.7) mg/kg in plural tissue (Dan *et al*., 1993). Concentrations in bronchial secretion were approximately 0.5-0.8 mg/L after oral administration of 500 mg ciprofloxacin (Bergogne-Bérézin *et al*., 1986).

The results obtained from the oral model showed that the time to peak concentration is slightly shorter when using doses over 500 mg. This is probably due to a fixed ka value of 2.03 h^{-1}, as well as a fixed lag time of 0.35 hours, which were applied for all dose regimens used in the present study. Bergan *et al*. (1986) investigated the PK of ciprofloxacin when increasing oral doses and found that, as the doses increased, there was an apparent drop from a mean ka of 3.6 h^{-1} after 100 mg to a mean ka of 2.4 h^{-1} after 1000 mg. There was also a small parallel increase in the apparent time lag from 0.34 hours after the lowest dose to 0.53 hours after the highest dose. The findings of Plaisance *et al*. (1987) were similar, reporting a decrease in mean ka from 8.58 h^{-1} after a 200 mg dose to a mean ka of 1.48 h^{-1} after a 750 mg dose. Lag time also increased from 0.22 hours after a 200 mg dose to 0.30 hours after a 750 mg dose. In addition, the discrepancies between the predictions and the observed data that arose in the absorption phase may be due to the use of a relatively simple absorption model (a first-order absorption model with a lag time), meaning that this model delivers inadequate predictions for processes as complex as drug absorption. To date, several advanced absorption models, including the compartmental absorption and transit (CAT) model (Yu & Amidon, 1999) and the advanced dissolution, absorption and metabolism (ADAM) model (Jamei *et al*., 2009), have been developed and it has been demonstrated that these models have improved predictability for oral drug absorption. However, their primary drawback is that they require a large amount of input information, which is often difficult to obtain from the literature. In the present study, the simple first-order absorption model with a lag time was selected because the aim was to develop a WBPBPK model for severely malnourished children and the use of advanced models is limited by the scarcity of available information for this patient population.

In summary, a WBPBPK model for ciprofloxacin was successfully developed for healthy adults, as described in this section. In the next section, the oral model will be scaled to children, in order to predict the influence of age on the PK of ciprofloxacin.

7C WBPBPK MODEL FOR HEALTHY CHILDREN

7C.1 METHODS

7C.1.1 Input parameters

7C.1.1.1 Physiological parameters

A WBPBPK model was created to encompass children aged 0.5, 1, 2, 5 and 10 years. Total body weight and height measurements for those aged 1, 5 and 10 years were obtained from the ICRP (2003), while body weight and height measurements for the remaining children were obtained from results compiled by the National Health and Nutrition Examination Surveys (NHANES) (2008). All organ weights for children aged 1, 5 and 10 years were obtained from the ICRP report. In order to predict organ weights for the remaining children, i.e., those aged 0.5 and 2 years, the following methods were applied:

1) Brain, heart, kidney, liver and spleen

Brain, heart, kidney, liver and spleen weights were predicted using a polynomial equation (Young *et al.*, 2009), as follows:

$$Y = X^0 + (X^1 \cdot WT) + (X^2 \cdot WT^2) + (X^3 \cdot WT^3) + (X^4 \cdot WT^4) + (X^5 \cdot WT^5) \qquad (7.28)$$

where Y is organ weight expressed as a fraction of total body weight, WT is body weight (g) and X^0, X^1, X^2,X^3, X^4 and X^5 are the constant coefficients for each organ, as shown in Table 7.6.

2) Gut

Gut weight was calculated as the sum of the weights of the intestinal tract (small and large intestines) and stomach, without their contents. In order to predict the weight of these organs, the following equations derived from Haddad *et al.* (2001) were used:

$$Y = X^0 + (X^1 \cdot a) + (X^2 \cdot a^2) + (X^3 \cdot a^3) + (X^4 \cdot a^4) + (X^5 \cdot a^5) \quad (7.29)$$

where Y is organ weight (g), *a* is age (year). The coefficients for intestinal tract and stomach are given in Table 7.6.

3) Adipose tissue

Adipose tissue weights with regard to children aged 0.5 and 2 years were estimated from measurements of body composition, i.e., as total weight of body fat divided by percentage fat in adipose tissue (ICRP, 2003). The data for weight of body fat were obtained from Fomon *et al.* (1982), and the percentages of fat in adipose tissue for children aged 0.5 and 2 years were estimated with linear interpolations between neonate and 1 year, and 1 and 5 years, respectively.

Table 7.6 Coefficients for predicting organ weights

Organs	X^0	X^1	X^2	X^3	X^4	X^5
Male						
Brain	1.41E-01	-5.54E-06	9.30E-11	-6.83E-16	1.80E-21	0
Heart	6.32E-03	-1.67E-08	0	0	0	0
Kidney	7.26E-03	-6.69E-08	3.33E-13	0	0	0
Liver	4.25E-02	-1.01E-06	1.99E-11	-1.66E-16	4.83E-22	0
Spleen	3.12E-03	-5.57E-09	0	0	0	0
Intestinal tract	51.125	107.09	-22.382	1.925	-4.7817E-2	0
Female						
Brain	1.12E-01	-3.33E-01	4.30E-11	-2.45E-16	5.03E-22	0
Heart	5.40E-03	-1.07E-01	0	0	0	0
Kidney	7.56E-03	-5.58E-01	1.54E-13	0	0	0
Liver	3.34E-02	-1.89E-01	5.34E-13	0	0	0
Spleen	2.96E-03	-7.72E-01	0	0	0	0
Intestinal tract	49.229	110.61	-23.478	2.0352	-0.0513	0
Male and female						
Stomach	7.54	17.888	-4.0437	0.5823	-0.0356	0.0008

Data were obtained from Young *et al.* (2009), and Haddad *et al.* (2001).

4) Bone

Bone weight was calculated from bone mineral weights obtained in measurements of chemical body composition, as described in the ICRP (2003). Bone mineral weights for children ages 0.5 and 2 years were derived from Butte *et al.* (2000), assuming the same ratio of bone-to-mineral weight as found in a 1-year-old.

5) Skin

Skin weight was estimated as BSA multiplied by epidermal plus dermal skin mass thickness ($mg \cdot cm^{-2}$) (ICRP, 2003). According to the ICRP, which indicated that skin thickness remains constant between the ages of 0 and 10 years, the values of skin thickness (5 $mg \cdot cm^{-2}$ for epidermal and 68 $mg \cdot cm^{-2}$ for dermal) that were used to calculate the skin weights of children aged 1, 5 and 10 years were identical to those that were used in the calculations of the skin weights of children aged 0.5 and 2 years. BSA was calculated using the formula developed by Mosteller (1987).

6) Muscle and lungs

Muscle and lung weights for children aged 0.5 and 2 years were calculated by linear interpolations between neonate and 1 year, and 1 and 5 years, respectively.

In the present study, venous and arterial blood compartment weights for children of all ages were scaled from adult data using equation 7.30, assuming that these organ weights are proportional to the BSA:

$$WT_{i,child} = \left(\frac{BSA_{child}}{BSA_{adult}} \right) \times WT_{i,adult} \qquad (7.30)$$

where $WT_{i,child}$ and $WT_{i,adult}$ are organ weight i (venous and arterial) of children and adult, respectively.

The weight of each organ was converted to volume by using the same organ density as found in adults (shown in Table 7.3). In this study, total body weight and all organ

volumes were assumed to have a variability of 20%. Cardiac output for each age group was estimated using an equation derived by Young *et al.* (2009), as follows:

$$\text{Cardiac output (L/h)} = \left[f \cdot \exp\left(a + b \cdot \text{WT} + c \cdot \text{WT}^2 + d \cdot \text{WT}^3\right) \right] \times \frac{60}{1000} \qquad (7.31)$$

where WT is body weight (kg), f = 9119, a = 9.164, b = -2.91E-0.2, c = 3.91E-04, and d = -1.91E-06.

Blood flow to adipose tissue, bone, heart and skin was calculated from adult data, assuming that the flow rate per organ weight (L/h/kg) in children is similar to that observed in adults. Data for blood flow to the brain were obtained from Chiron *et al.* (1992), who reported mean cerebral blood flows (CBF) of 55, 60, 65, and 62 mL/min/100 g of brain tissue for children aged 0.5, 1, 2 and 10 years, respectively. For 5-year-old children, CBF was estimated by using equation 7.32 (Wintermark *et al.*, 2004):

$$\text{CBF (mL/min/100 g tissue)} = (-26.6+(90.2 \times \text{AGE})) \cdot \exp^{(-0.140 \times \text{AGE}^2)} + (138.4-(10.3 \times \text{AGE})) \cdot \exp^{(-0.213 \times (\text{AGE}-13.97)^2)} + 47 \qquad (7.32)$$

On the basis of the findings of Hayton (2000), blood flow to the kidney can be calculated as a function of age and weight, using the maturation-growth model as follows:

$$\text{RBF (mL/min)} = 10.2(\text{WT})^{0.916} e^{-0.178 \cdot a} + 19.8(\text{WT})^{0.916} (1 - e^{-0.178 \cdot a}) \qquad (7.33)$$

where RBF is renal blood flow, WT is body weight (kg), and a is age (month).

Total hepatic blood flow (Q_H) in children was assumed to be proportional to BSA, which was estimated as follows (Björkman, 2005):

$$Q_{H,child} = \left(\frac{BSA_{child}}{BSA_{adult}} \right) \times Q_{H,adult} \quad (7.34)$$

Blood flow to the liver and prehepatic organs was calculated in relation to total liver blood flow, retaining the adult proportions between hepatic arterial flow and the respective blood flows through the gut and spleen. The muscle blood flow rates for children, which were required for the present study, were calculated from the average blood flow rate to lower limbs; 3.2 mL/min/100 g tissue (Price *et al.*, 2003). This value was multiplied by the muscle weight of the children in each age group.

7C.1.1.2 Drug-specific parameters

1) Fraction unbound (fu)

The change in binding protein concentrations as a function of age was calculated on the basis of the equation proposed by McNamara and Alcorn (2002):

$$fu_{child} = \frac{1}{1 + \frac{(1 - fu_{adult}) \times [P]_{child}}{[P]_{adult} \times fu_{adult}}} \quad (7.35)$$

where [P] is albumin concentration. The data for albumin concentration in children and adults were taken from Knapp and Routh (1949), and Josephson and Gyllensward (1957), respectively.

2) Blood-to-plasma ratio (R)

Since R is a function of fu, haematocrit (Hct) and the affinity of blood cells (Kpu_{BC}), the drug- and age-related changes in R were determined by modification equation 7.15, yielding equation 7.36. This equation assumed that Kpu_{BC} in children is similar to that in adults:

$$R_{child} = \frac{(R_{adult} + Hct_{adult} - 1)(fu_{child} \cdot Hct_{child})}{fu_{adult} \cdot Hct_{adult}} + 1 - Hct_{child} \quad (7.36)$$

where R and fu for adults were those values used in Section 7B (1 for R and 0.70 for fu). The fu values of children for each age group were estimated using equation 7.35, as previously described. The Hct data in adults (42.3%) was taken from Rosenson *et al.* (1996) and the Hct values for children were those cited in Wintrobe's Clinical Hematology textbook (Greer *et al.,* 2009).

3) Tissue:plasma partition coefficient (Kp)

The Kp values for children were predicted with the empirical method, using specific plasma volume and organ volume values for children in different age groups. The plasma volume data were derived from Russell (1949). Experimental data for the V_{ss} of ciprofloxacin in healthy children were not available in the literature, therefore, in the present study, V_{ss} was calculated as being the sum of the volume of the central compartment (V_1) and the volume of the peripheral compartment (V_2). A V_1 of 56.7 L/70 kg and a V_2 of 89.8 L/70 kg were taken from the population PK study conducted by Rajagopalan and Gastonguay (2003) and then corrected for the body weight, yielding a V_{ss} value of 2.09 L/kg to be used for children of all age groups.

4) Clearance

The adult clearance (CL) values were scaled to children using the method suggested by Edginton *et al.* (2006b). This method requires prior information as follows:

- Adult CL value
- Elimination pathways and the relative contribution of each pathway to total CL
- Plasma fraction unbound (fu_p) in adults
- Physiological information regarding age-dependent changes in body weight, liver weight, hepatic blood flow, and gut weight

Adult CL information was in the form of values obtained from Borner *et al.* (1986), in which CL_R and CL_{NR} were reported as being 18.9 L/h and 16.92 L/h, respectively. The CL_R of ciprofloxacin has two processes: (i) the CL due to glomerular filtration (CL_{GFR}), and (ii) the CL due to tubular secretion (CL_{TS}). It has been found that CL_{GFR} accounts for 36% (6.8 L/h) of CL_R, while the remainder is the result of CL_{TS}

(64%; 12.1 L/h) (Jaehde *et al.*, 1995). The CL_{NR} of ciprofloxacin was composed of hepatic CL (CL_H) and gut CL (CL_{GUT}), which have been reported to account for 63% and 37% of CL_{NR}, respectively (Rohwedder *et al.*, 1990).

Renal CL

In order to estimate renal CL (CL_R) for children, the GFR (GFR_{child}) and tubular secretion (TS_{child}) values were initially predicted by using the equations proposed by Hayton (2000) as follows:

$$GFR_{child}\ (mL/min) = 2.6(WT)^{0.662}e^{-0.0822 \cdot a} + 8.14(WT)^{0.662}(1 - e^{-0.0822 \cdot a}) \quad (7.37)$$

$$TS_{child}\ (mg/min) = 1.08(WT)^{1.04}e^{-0.185 \cdot a} + 1.83(WT)^{1.04}(1 - e^{-0.185 \cdot a}) \quad (7.38)$$

where WT is body weight (kg), and *a* is age (month).

Using the GFR and TS rate obtained from the above equations with the information of fu in adults (fu_{adult}) and children (fu_{child}), and the values of CL_{GFR} and CL_{TS} of adults, the ciprofloxacin CLs in children, due to GFR ($CL_{GFR,child}$) and tubular secretion ($CL_{TS,child}$), can be calculated by using equations 7.39 and 7.40, respectively:

$$CL_{GFR,child} = \frac{GFR_{child}}{GFR_{adult}} \times \frac{fu_{child}}{fu_{adult}} \times CL_{GFR,adult} \quad (7.39)$$

$$CL_{TS,child} = \frac{TS_{child}}{TS_{adult}} \times \frac{fu_{child}}{fu_{adult}} \times CL_{TS,adult} \quad (7.40)$$

where GFR_{adult} is the GFR in adults (125 mL/min), and TS_{adult} is the tubular secretion rate in adults, which is estimated on the basis of para-aminohippuric acid CL (80 mg/min). The reference values were taken from a study by DeWoskin and Thompson

(2008). The total CL_R in children was then calculated as the sum of $CL_{GFR,child}$ and $CL_{TS,child}$.

Hepatic CL

To estimate hepatic CL (CL_H) for children, the CL_H of adults was initially converted to $CLu_{int,H}$, using equation 7.27. The $CLu_{int,H}$ value was then divided by the liver weight of adults, which yields the $CLu_{int,H}$, to give a unit of mL/min/kg of liver tissue. The scaling step was then performed by multiplying the $CLu_{int,H}$ of adults by age scaling factors, which are an age-dependent, enzyme-specific percentages of adult activity (% of adult activity). The scaling factors of CYP1A2, the primary metabolizing enzyme of ciprofloxacin, for each age group were obtained from Björkman (2005), who used the demethylation reaction of imipramine as a probe of CYP1A2 activity. These data were fitted with a bi-exponential growth function to estimate age scaling factors, as follows: 0.5 years, 51%; 1 year, 63%; 2 years, 81%; and 5 years, 107%. It was assumed that the activity of CYP1A2 is the same in 10-year-old children as it is in adults.

The $CLu_{int,H}$ value for children (in a unit of mL/min/kg liver tissue) was consequently multiplied by the liver weight of children and then converted back to CL_H by using the following equation (Yang *et al.*, 2007):

$$CL_H = \frac{Q_{H,B} \cdot fu \cdot CLu_{int,H}}{Q_{H,B} + fu \cdot CLu_{int,H}/R} \quad (7.41)$$

Gut CL

No data were available for age-dependent changes in the transintestinal elimination process. Therefore, in the present study, gut CL (CL_{GUT}) was scaled to children using the three-quarter power allometric size model, scaled by weight of gut (WT_{GUT}) as follows:

$$CL_{GUT,child} = CL_{GUT,adult} \left(\frac{WT_{GUT,child}}{WT_{GUT,adult}} \right)^{0.75} \quad (7.42)$$

5) F, ka, and lag time

In the present study, F was set equal to 0.837 (CV = 10%). The data for ka and lag time of ciprofloxacin in children were the values that were reported by Rajagopalan and Gastonguay (2003) (ka = 1.27 h^{-1} and lag time = 0.35 hours), and were applied to children of all ages.

7C.1.2 Simulation and comparison with experimental data

A total of 1000 concentration-time profiles for an oral dose of 10 mg/kg were generated for the children of each age group, and the predictions were then compared with the experimental data. Due to the lack of information on the disposition of ciprofloxacin in healthy children, the data used for comparison in the present study were generated by using a PK model and PK parameters from studies by Rajagopalan and Gastonguay (2003) and Peltola *et al.* (1998). Both of these studies were conducted in children with minor infections, e.g., urinary tract infections and otitis media, and it was therefore assumed that the PK of ciprofloxacin is not significantly altered in this patient population.

1) Rajagopalan and Gastonguay (2003)

The final population models obtained from this study were used to generate concentration-time data for all age groups of children, as shown:

$$\text{CL (L/h)} = 30.3 \times (\text{WT}/70)^{0.75} \times (1+0.045(\text{AGE}-2.5))$$

$$V_1 \text{ (L)} = 56.7 \times (\text{WT}/70)^{1.0}$$

$$V_2 \text{ (L)} = 89.8 \times (\text{WT}/70)^{1.0}$$

$$\text{Q (L/h)} = 37.5 \times (\text{WT}/70)^{0.75}$$

$$\text{ka } (h^{-1}) = 1.27 \times (1 - (0.611 \times \text{CF}))$$

$$\text{lag time} = 0.35 \text{ hours}$$

where WT is the body weight of the children in each age group, AGE is the age of the children (year), and CF is cystic fibrosis, which was set to zero in this study.

2) Peltola (1998)

In this study, the following PK parameters were determined using the non-compartmental method: C_{max}, T_{max}, $T_{1/2}$ and CL/F (Table 7.7). Elimination rate constant (k) was calculated from $T_{1/2}$ ($k = \ln 2/T_{1/2}$). The ka for each age group can be estimated using estimations of k and T_{max} by equation 7.43, using the 'Solver' function in Microsoft Excel®. The estimated ka and k were used, together with the reported T_{max} and C_{max} values, to estimate V/F by equation 7.44, using the 'Solver' function in Microsoft Excel®:

$$T_{max} = \frac{\ln(ka) - \ln(ke)}{ka - ke} \tag{7.43}$$

$$C_{max} = \frac{Dose \cdot ka}{V/F(ka-ke)}(e^{-ke \cdot T_{max}} - e^{-ka \cdot T_{max}}) \tag{7.44}$$

The parameters obtained from these studies were used to generate concentration-time data for healthy children using the MATLAB program, Version 7.11 (MathWorks, Natick, MA, USA). These are referred to as 'observed data' hereafter in this section.

Table 7.7 PK parameters used for generating experimental data

PK parameters	Age groups				
	6 months	**1 year**	**2 years**	**5 years**	**10 years**
C_{max} (SD) (mg/L)	1.99 (1.30)	2.43 (1.07)	2.67 (1.12)		2.08 (1.53)
T_{max} (range) (h)	2 (1-4)	1 (1-2)	1 (1-2)		1 (1-2)
$T_{1/2}$ (SD) (h)	4.7 (1.10)	4.2 (1.11)	5.1 (1.12)		4.9 (1.07)
CL/F (SD)[a] (L/h/kg)	0.98 (0.20)	1.10 (0.22)	1.04 (0.21		1.46 (0.29)
V/F (SD)[a] (L/kg)	3.74 (0.75)	3.49 (0.70)	3.27 (0.65)		3.29 (0.83)
ka (SD)[a] (h^{-1})	1.19 (0.24)	3.10 (0.62)	3.34 (0.67)		3.29 (0.66)

[a] assumed equal to 20%.

7C.2 RESULTS

Organ volume, total body weight, and height, as well as BSA, are presented in Table 7.8. The 'rest of the body' compartment ranged from 4 to 20% (6-20% in males and 4-16% in females). Table 7.9 shows the estimated blood flow parameters and cardiac output for the children of each age group. The predicted Kp values, albumin, Hct, fu, and R, as well as the CL values for each of the elimination pathways, are provided in Table 7.10. The Kp values tended to decrease with age, with the exception being children aged 1 and 2 years, for whom the Kp values estimated for 2-year-old children were minimally higher than those estimated for children aged 1 year. It was also observed that the Kp values were similar between males and females. The CL per body weight values were generally comparable between age groups, and were very similar between males and females. The fu and R values were identical for males and females, and there was little variation in these values across age groups (fu 0.72-0.74; R 1.011-1.022).

Figure 7.7A illustrates the concentration-time data that were generated for children of each age group with the PK model and PK parameters from Rajagopalan and Gastonguay (2003). It was observed that the profiles of each group were similar, with C_{max} of around 3.1 to 3.5 mg/L being reached approximately 1 hour after drug administration. The trough concentrations at 12 hours were also similar between age groups (~0.2-0.25 mg/L). Figure 7.7B illustrates the concentration-time data generated from the results of Peltola *et al.* (1998). Discrepancies between profiles are clearly shown. Children aged 2 and 5 years had the highest C_{max}, approximately 3 mg/L, compared to the children of the remaining age groups (~2.8 mg/L for the group aged 1 year, ~2.3 mg/L for the groups aged 6 months and aged 10 years). The results show that C_{max} was achieved at approximately 2 hours for children aged 6 months, while it was attained at around 1 hour for the children in the remaining age groups. The trough concentrations were minimally different between age groups, being 0.2 mg/L for children aged 6 months, 0.06 mg/L for those aged 10 years, and approximately 0.12 mg/L for those aged 1, 2, and 5 years.

Plasma concentration curves of ciprofloxacin predicted from the WBPBPK model are shown in Figure 7.8, which demonstrates a good fit between the model-predicted concentrations and the observed data. When the predictions were compared with the observed data of Peltola *et al.* (1998), significant discrepancies were observed with regard to the 6 month age group and the group of those aged 10 years. For the 6 month age group, the peak concentration predicted from the model was considerably higher than the observed data. The model-predicted concentrations for the 10-year-old children tended to be higher compared to the observed data, especially at the terminal phase of drug elimination, in which the observed data were lower than the prediction interval.

Table 7.8 Organ volumes, body weight, height and BSA in the different age groups used in a WBPBPK model of healthy children

Organs	6 months (M/F)	1 year (M/F)	2 years (M/F)	5 years (M/F)	10 years (M/F)
Adipose	3.08/2.89	3.93/3.93	3.93/3.90	5.46/5.46	8.19/8.19
Bone	0.20/0.19	0.30/0.30	0.43/0.41	0.63/0.63	1.15/1.15
Brain	0.81/0.68	0.91/0.91	1.08/0.96	1.26/1.13	1.35/1.17
Gut	0.11/0.11	0.16/0.16	0.21/0.21	0.39/0.39	0.66/0.66
Heart	0.05/0.04	0.05/0.05	0.08/0.07	0.08/0.08	0.15/0.15
Kidney	0.05/0.05	0.07/0.07	0.09/0.09	0.10/0.10	0.17/0.17
Liver	0.30/0.26	0.33/0.33	0.45/0.41	0.57/0.57	0.83/0.83
Muscle	1.30/1.30	1.83/1.83	2.72/2.72	5.38/5.38	10.57/10.57
Skin	0.27/0.26	0.32/0.32	0.40/0.38	0.52/0.52	0.74/0.74
Spleen	0.02/0.02	0.03/0.03	0.04/0.04	0.05/0.05	0.08/0.08
Lungs	0.10/0.10	0.15/0.15	0.17/0.17	0.24/0.24	0.40/0.40
Arterial	0.38/0.42	0.45/0.52	0.57/0.63	0.74/0.85	1.06/1.21
Venous	0.76/0.85	0.91/1.04	1.14/1.26	1.48/1.69	2.12/2.43
Rest of the body	0.97/0.92	0.57/0.37	2.8/2.15	2.11/1.91	4.54/4.25
Total body weight (kg)	8.40/8.10	10/10	14.10/13.40	19/19	32/32
Height (cm)	88/89	94/96	80/84	89/90	86/87
BSA (m^2)	0.40/0.39	0.48/0.48	0.60/0.58	0.78/0.78	1.12/1.12

M=male, F=female

Table 7.9 Organ blood flows (L/h) and cardiac output (L/h) used in a WBPBPK model of healthy children of different age groups

Organs	6 months (M/F)	1 year (M/F)	2 years (M/F)	5 years (M/F)	10 years (M/F)
Adipose	3.79/4.19	4.84/5.70	4.84/5.65	6.72/7.92	10.09/11.88
Bone	1.42/1.68	2.09/2.61	3.01/3.63	4.47/5.58	8.15/10.18
Brain	27.89/23.45	34.20/34.20	43.73/38.95	47.02/42.35	52.08/45.38
Gut	13.20/14.99	15.76/18.43	19.70/22.24	25.62/29.94	36.78/42.99
Heart	2.45/3.04	2.36/3.54	4.06/4.98	4.02/6.02	7.47/11.19
Kidney	6.79/6.57	8.97/8.97	12.92/12.33	17.09/17.09	27.55/27.55
Liver	5.36/5.41	6.40/6.65	8.00/8.03	10.41/10.81	14.94/15.52
Muscle	2.59/2.59	3.65/3.65	5.43/5.43	10.75/10.75	21.12/21.12
Skin	1.73/2.19	2.07/2.70	2.59/3.26	3.36/4.38	4.83/6.29
Spleen	2.47/2.50	2.96/3.07	3.69/3.71	4.80/4.99	6.90/7.17
CO (lungs, arterial and venous)[a]	86.50/83.31	102.72/102.72	138.57/132.98	172.58/172.58	230.68/230.68
Rest of the body	18.80/16.69	19.41/13.20	30.58/24.76	38.32/32.75	40.77/31.41

[a] blood flows to lungs, arterial and venous compartments were equal to cardiac output (CO).
M=male, F=female

Table 7.10 Tissue:plasma partition coefficient (Kp), albumin, haematocrit, fu, R, and clearance used in a WBPBPK model of healthy children of different age groups

Organs	6 months (M/F)	1 year (M/F)	2 years (M/F)	5 years (M/F)	10 years (M/F)
Kp					
Adipose	0.71/0.71	0.63/0.63	0.65/0.62	0.51/0.51	0.47/0.47
Bone	4.43/4.40	3.97/3.97	4.07/3.93	3.25/3.25	3.01/3.01
Brain	0.29/0.29	0.27/0.27	0.27/0.27	0.23/0.23	0.22/0.22
Gut	4.41/4.39	4.11/4.11	4.17/4.08	3.62/3.62	3.45/3.45
Heart	5.93/5.88	5.29/5.29	5.42/5.23	4.29/4.29	3.97/3.97
Kidney	9.48/9.45	9.06/9.06	9.15/9.02	8.34/8.34	8.08/8.08
Liver	4.09/4.07	3.83/3.83	3.89/3.81	3.40/3.40	3.25/3.25
Muscle	6.97/6.90	6.09/6.09	6.27/6.01	4.76/4.76	4.34/4.34
Skin	5.30/5.26	4.84/4.84	4.94/4.80	4.11/4.11	3.87/3.87
Spleen	6.97/6.90	6.09/6.09	6.27/6.01	4.76/4.76	4.34/4.34
Lungs	6.79/6.74	6.11/6.11	6.25/6.05	5.03/5.03	4.67/4.67
Albumin[1] (g/dL)	3.92	4.37	4.37	4.23	4.23
Haematocrit[1] (%)	35	36	36	37	40
fu[a]	0.74	0.72	0.72	0.73	0.73
R[a]	1.022	1.011	1.011	1.015	1.016
CL_R[b] (L/h)	3.38/3.27	4.51/4.51	6.76/6.46	9.24/9.24	14.92/14.92
CL_{GFR} (L/h)	1.10/1.08	1.55/1.55	2.36/2.28	3.18/3.18	4.50/4.50
CL_{TS}	2.28/2.19	2.96/2.96	4.40/4.18	6.06/6.06	10.42/10.42
CL_{NR}[c] (L/h)	2.31/2.57	3.02/3.56	4.32/4.90	6.71/7.80	9.59/11.14
CL_H (L/h)	1.27/1.46	1.64/2.10	2.60/3.07	4.03/4.96	5.59/6.91
CL_{GUT} (L/h)	1.05/1.11	1.38/1.46	1.72/1.83	2.69/2.84	4.00/4.23

[a] the results were similar between males and females.
[b] calculated as the sum of CL_{GFR} and CL_{TS}.
[c] calculated as the sum of CL_H and CL_{GUT}.
M=male, F=female

Figure 7.7 Mean simulated concentration-time data in the different age groups used for comparison with the predictions from a WBPBPK model

A: Study of Rajagopalan and Gastonguay (2003)

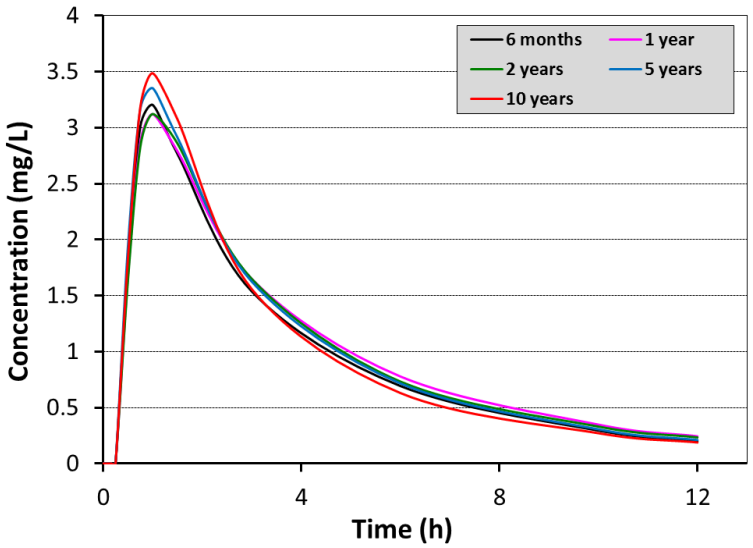

B: Study of Peltola *et al.* (1998)

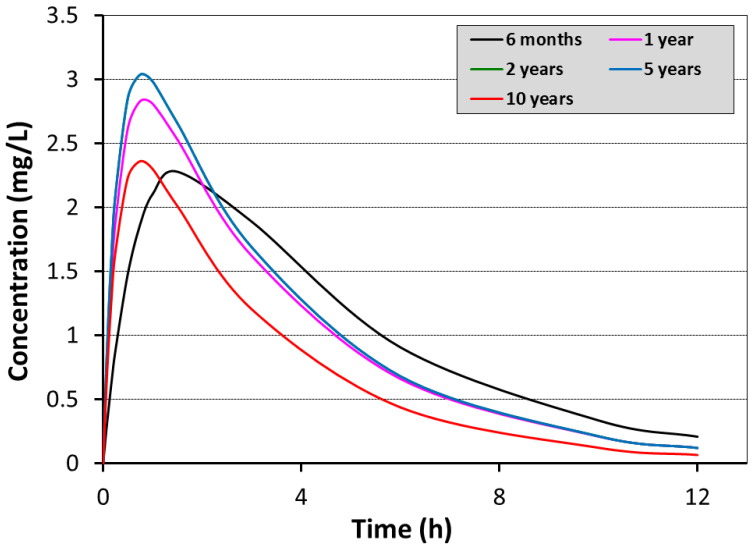

Figure 7.8 Plasma concentration-time profiles of oral ciprofloxacin in the different age groups predicted using a WBPBPK model of healthy children

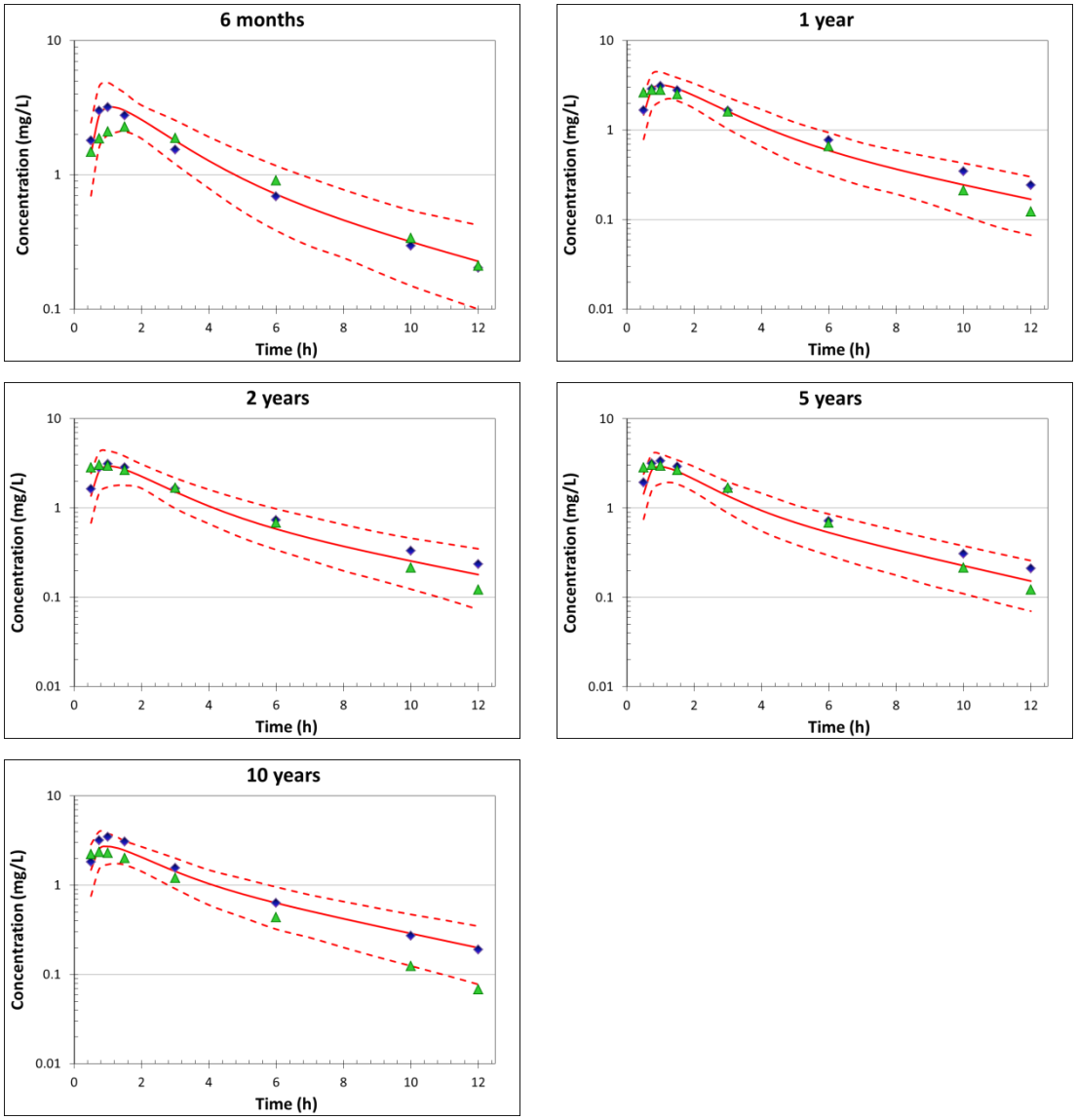

Key: The symbols are the observed data obtained from the simulation using a PK model and PK parameters from the literature (blue = Rajagopalan & Gastonguay, 2003; green = Peltola *et al.*, 1998), the red solid line is the mean prediction and the red dashed lines are the 2.5th (lower) and 97.5th (upper) percentiles of prediction.

7C.3 Discussion

A WBPBPK model was created for the prediction of drug disposition in children whose ages ranged from 6 months to 10 years. The comprehensive tables of organ volume and organ blood flow required the compilation of data of varying quality from a variety of sources. Physiological data for children aged 1, 5, and 10 years were available in the ICRP report; however, for the remaining children, several techniques were used to estimate these data. It was found that the 'rest of the body compartment' constituted between 4 and 20% of total body weight, with the minimum value of 4% being observed in a group of 1-year-old females. This was because the model did not account for some organs, such as gonads, thyroid, and adrenals. These results were consistent with those obtained by Björkman (2005), who reported a carcass compartment of 8 to 16% of total body weight. Edginton *et al.* (2006a) found that the sum of the weights of all organs included in the model amounted to 91 to 93% of the total body weight. This was probably because the model they developed included a greater number of organs, i.e., it included the pancreas and gonads.

The sum of the regional blood flows accounted for approximately 80 to 87% of the cardiac output, which may be due to the model's lack of inclusion of some organs . In the present study, CO was predicted from the equation of Young *et al.* (2009), using body weight as a predictor. The results obtained with this equation corresponded fairly well to those values reported by Björkman (2005), and Sholler *et al.* (1987). In addition, it was suggested that CO is closely related to metabolic rate, and it is also reasonable to assume that resting CO relates allometrically to body weight (Björkman, 2005). If this is so, and the allometric exponent is close to that of BSA, then cardiac index (CI), i.e., the CO normalized to BSA (CI = CO/BSA), should be fairly constant over age. The CIs reported in this study are in agreement with this assumption, being approximately 205 to 230 L/h/m^2 for ages ranging between 6 months and 10 years.

There was a small discrepancy in Kp values between age groups. When using the empirical method, Kp values are predicted by using V_{ss}, as well as organ volumes.

V_{ss} was fixed at 2.09 L/kg for children of all ages in the present study, so the minimal difference in Kp values between age groups was therefore considered to be the result of a difference in organ volumes.

The CL of ciprofloxacin for children was scaled from adult data in the present study. The CL_T of children was approximately 6 L/h for 0.5 years; 8 L/h for 1 year; 11 L/h for 2 years; 16-17 L/h for 5 years; and 25-26 L/h for 10 years. These results were consistent with the findings of Payen *et al.* (2003), who reported mean CLs of 2.93 L/h (range 0.29-8.79 L/h) and 17.7 L/h (range 0.58-37.4) for children aged 0.5-1 year, and 2-11 years, respectively. Peltola *et al.* (1998) also reported CLs (when corrected for an F of 0.837) of 6.3 L/h for children aged <1 year; 10.1 L/h for those aged 1 year; 13.8 L/h for children aged 2-5 years; and 27.5 L/h for those aged ≥ 6 years, which were comparable to those found in the present study.

The primary limitation for the development of a model of healthy children was the lack of existing experimental data for use in validating the model. The solution applied in the present study was to use PK models, and their corresponding parameters, from previous PK studies conducted in children with mild infections to generate the observed data. It was found that the concentration-time profiles generated from two studies were very different. When using the data of Rajagopalan and Gastonguay (2003), the profiles for each group of children were similar. This could be because these profiles were generated using the same population PK model, and therefore the PK parameters for each age group were identical (F, ka, lag time) or somewhat similar (CL, V_1, and V_2). For example, the typical values of CL, V_1, and V_2 for children aged 6 months were respectively 5.5 L/h, 6.8 L, and 10.8 L, compared to the values of 6.5 L/h, 8.1 L, and 12.8 L, respectively, estimated for 1-year-old children. In the Peltola *et al.* (1998) study, CL/F and $T_{1/2}$ values were given. These parameters were used in combination with the observed C_{max} and T_{max} to estimate other parameters, i.e., ka and V/F. It was found that CL/F and $T_{1/2}$ were determined more precisely compared to C_{max} and T_{max} values. This was due to the C_{max} and T_{max} results being highly dependent on the sampling schedule that was implemented in the study. In this same study, ciprofloxacin was administered three

times daily and the samples were collected at 0, 0.5, 1, 2, 4, 6, 8, 12, and 24 hours after dosing. Therefore, the C_{max} and T_{max} results were constrained to being one of these sampling time points. A T_{max} of 1 hour was reported for all age groups, apart from for the children aged 6 months, corresponding to ka values of approximately 3.3-3.5 h^{-1}, while a T_{max} of 2 hours observed for 6-month-old children gave a lower ka estimate (1.19 h^{-1}). V/F values estimated from Peltola *et al.* (1998) were approximately 3.3-3.7 L/kg, which were higher than those results obtained by Rajagopalan and Gastonguay (2003) (~2 L/kg). This could explain why the predicted C_{max} of Peltola *et al.* (1998) was generally lower than that of Rajagopalan and Gastonguay (2003). In this circumstance, it can be judged that the observed data generated from the latter study may be of greater accuracy and of superior use for comparative proposes. The results of the present study showed a good fit between the predicted concentrations and the observed data generated by Rajagopalan and Gastonguay (2003), and, with the exception of the children aged 6 months and those aged 10 years, they were also a reasonable fit to the observed data of Peltola *et al.* (1998). This indicated that the model possessed reliable predictability.

In summary, a WBPBPK model of healthy children was successfully developed, as described. The following section will describe how this model was scaled to malnourished children for the prediction of drug disposition in this patient population.

7D WBPBPK MODEL FOR MALNOURISHED CHILDREN

7D.1 Methods

7D.1.1 Input parameters

7D.1.1.1 Physiological parameters

In contrast with healthy adults and children, the body weight of malnourished children is more difficult to generate. This is because there is not a fixed mean value, rather, the value varies depending on the severity of the disease. In children, malnutrition severity is commonly represented as a Z-score, which is defined as the SD from the median weight, as compared to a reference population with the same

height or age. Therefore, body weights for malnourished children should be sampled together with their reference values, i.e., other anthropometric data (height or age). In addition, a child's body weight should be constrained in the defined range of Z-score values.

In the present study, anthropometric data, including body weight and height of children of differing ages and gender, as well as different Z-score values (-4 to 4) were taken from the WHO Global Database on Child Growth and Malnutrition (2012). These data were used to create the following equations with a forward stepwise linear regression, using the SigmaPlot program, Version 12.0.

Children aged <2 years:

$$BW = -8.555 + (0.243 \cdot HT) + (0.883 \cdot SD) - (0.104 \cdot SEX) \quad (7.45)$$

Children aged 2-5 years:

$$BW = \exp(0.773 + (0.0197 \cdot HT) + (0.0880 \cdot SD) - (0.0123 \cdot SEX)) \quad (7.46)$$

Children aged >5 years:

$$BW = \exp(2.335 + (0.00969 \cdot AGE) + (0.153 \cdot SD) - (0.00102 \cdot SEX)) \quad (7.47)$$

where BW is body weight (kg), HT is height (cm), SD is Z-score value, SEX is gender (0 = male, 1 = female), and AGE is the age of the child (month). HT was assumed to correspond to a log-normal distribution, with the mean values of each age group as presented in Table 7.8, and a CV of 10%. SD and SEX were sampled from a uniform distribution. In order to predict body weight for severely malnourished children, SD values were constrained between -3 and -4. The body weight for healthy children was obtained by fixing SD equal to zero. Since height was not given for children aged > 5 years in this database, the equation for predicting body weight in this age group was developed by using age as a reference (equation 7.47). In the

present study, this equation was applied only to 10-year-old children, therefore AGE was fixed at 120 months. The body weights of healthy and malnourished children of each age group, as estimated with the above equations, were used to calculate the BW fraction (*f*BW) as follows:

$$fBW = \frac{BW_M}{BW_H} \tag{7.48}$$

where BW_M and BM_H are the body weight of malnourished children and healthy children, respectively. The *f*BW estimated for each child was subsequently used to calculate the organ weight fraction (*f*OW) with the equations given in Table 7.11. These equations were developed by using data from humans and represent the correlation between the change of body weight and the change of organ weight in malnourished children. After the *f*OW of each organ was obtained, the weight of each organ of malnourished children was estimated by using equation 7.49:

$$OW_{M,i} = fOW \times OW_{H,i} \tag{7.49}$$

where $OW_{M,i}$ and $OW_{H,i}$ are weight of organ *i* for malnourished children and healthy children, respectively. $OW_{H,i}$ were those values sampled from a multivariate Dirichlet distribution using the parameters of healthy children as described in Section 7C.

There was no information with regard to the gut, venous, and arterial blood compartment, so the changes of weight for these organs were assumed to decrease in proportion to body weight. With regard to the brain, the evidence suggests that, in children with malnutrition, a weight decrease occurs more slowly compared to a decrease in body weight (Waterlow, 2006); when body weight had decreased to 50% of its normal value, brain weight had decreased by only 10%. On the basis of this evidence, brain weight was fixed as decreasing by 10% for all age groups in the present study, independent of the severity of malnutrition.

Table 7.11 Equations for predicting *f*OW of each organ

Organs	Equations	*n*	r^2
Adipose	*f*OW=(1.9**f*BW)-0.9	2	1
Bone	*f*OW=(0.2**f*BW)+0.8	2	1
Heart	*f*OW=(0.5384**f*BW)+0.3824	5	0.4665
Kidney	*f*OW=(0.5368**f*BW)+0.4092	3	0.4356
Liver	*f*OW=(0.7436**f*BW)+0.2254	8	0.4974
Muscle	*f*OW=(1.3571**f*BW)-0.3401	3	0.9804
Skin	*f*OW=(1.5945**f*BW)-0.5945	2	1
Spleen	*f*OW=(0.8942**f*BW)+0.0269	4	0.7757
Lungs	*f*OW=(0.7027**f*BW)+0.2836	3	0.9574

n = number of experimental data used to generate the equations
*f*OW = organ weight fraction
*f*BW = body weight fraction
Data were compiled from Waterlow, 2006; Bosy-Westphal *et al.*, 2004; Garrow *et al.*, 1965; and Metcoff, 1967.

According to the results of Öcal *et al.* (2001), which indicated that the CI between healthy and malnourished individuals is similar, the CO for malnourished children can be estimated by using the CO of healthy children, which is obtained from equation 7.31 and BSA, as follows:

$$CO_M = \frac{CO_H \times BSA_M}{BSA_H} \tag{7.50}$$

where subscripts M and H refer to malnourished and healthy children, respectively. Organ blood flows were calculated from data obtained from healthy children by assuming that the flow rate per organ weight (L/h/kg tissue) was similar between healthy and malnourished children (equation 7.51):

$$BF_{M,i} = \frac{BF_{H,i} \times OW_{M,i}}{OW_{H,i}} \quad (7.51)$$

where $BF_{M,i}$ and $BF_{N,i}$ are blood flow to organ *i* in malnourished and healthy children, respectively.

7D.1.1.2 Drug-specific parameters

The fu values for malnourished children (fu_M) were calculated by modification of the equation of McNamara and Alcorn (2002) (equation 7.35), which yields the following:

$$fu_M = \frac{1}{1 + \frac{(1 - fu_H) \times [P]_M}{[P]_H \times fu_H}} \quad (7.52)$$

where $[P]_M$, which is albumin concentration in malnourished children, was derived by a 20.8% decrease from a normal ($[P]_H$) value (Gollan, 1948).

On the basis of the assumption that Kpu_{BC} does not change in malnourished children, as compared to healthy children, R can be obtained by scaling from the latter, using the following equation:

$$R_M = \frac{(R_H + Hct_H - 1)(fu_M \cdot Hct_M)}{fu_H \cdot Hct_H} + 1 - Hct_M \quad (7.53)$$

where Hct_M, which is the Hct level in malnourished children, was derived by a 17.2% decrease from a normal (Hct_H) value (Gollan, 1948).

It has been found that the GFR decreases by 15-70% in malnourished individuals (Arroyave *et al.*, 1961; Alleyne, 1967; Gordillo *et al.*, 1957; Klahr & Alleyne, 1973; Klahr & Tripathy, 1966), and a mean value of 47% was used in the present study. Furthermore, a 19% decrease in tubular secretion has been reported (Pullman *et al.*,

1954). The GFR and tubular secretion rate of healthy children, adjusted by these decreasing values, were used to calculate CL_{GFR} and CL_{TS} for malnourished children as follows:

$$CL_{GFR,M} = \frac{GFR_M}{GFR_H} \times \frac{fu_M}{fu_H} \times CL_{GFR,H} \quad (7.54)$$

$$CL_{TS,M} = \frac{TS_M}{TS_H} \times \frac{fu_M}{fu_H} \times CL_{TS,H} \quad (7.55)$$

where GFR_H and TS_H are those values estimated from equations 7.37 and 7.38, respectively. The intrinsic hepatic activity of the CYP1A2 metabolizing enzyme was also scaled by a 75% decrease from a normal value (Cho *et al.*, 1999). No information with respect to the effect of malnutrition on gut CL was available; therefore, this was scaled from adult data using the three-quarter allometric liver model as follows:

$$CL_{GUT,child,M} = CL_{GUT,adult} \left(\frac{WT_{GUT,child,M}}{WT_{GUT,adult}} \right)^{0.75} \quad (7.56)$$

The Kp values for children of each age group were calculated using the empirical method. There was a lack of information for the V_{ss} of ciprofloxacin in malnourished children, so the median value of the empirical Bayes estimates of 4.49 L/kg, obtained from the previous population analysis, was used. F was sampled from a normal distribution with a mean value of 0.837 and CV of 10%. The value for ka was assumed to be equal to healthy children at 1.27 h^{-1} (SD = 0.381). The lag time was fixed to the result of the population analysis at 0.742 hours.

7D.1.2 Simulation and comparison with experimental data

The simulations were performed for a dosing regimen of 10 mg/kg. A total of 1000 virtual-children, consisting of an equal number of males and females, was generated

for each age group. The MATLAB codes used for the simulation are given in Appendix II (using the parameters for children aged 2 years). The mean concentration was calculated and presented in conjunction with the 95% prediction interval. The concentration-time data predicted from the model were compared with the experimental data, which were obtained from 52 malnourished children aged between 8 and 102 months (29 males; 23 females). The ages of the children used to generate the experimental data were therefore very wide ranging, so in order to make a comparison with the simulated data, the children were divided into five groups, according to their age, as follows:

- Children aged <10 months (n = 2) were assigned to the 6 month group
- Children aged 10-18 months (n = 18) were assigned to the 1 year group
- Children aged 19-42 months (n = 22) were assigned to the 2 year group
- Children aged 43-90 months (n = 8) were assigned to the 5 year group
- Children aged >90 months (n = 2) were assigned to the 10 year group

7D.2 Results

The predicted Kp values for the different age groups of malnourished children are shown in Table 7.12. It was generally observed that these values decreased with age, and were almost identical between males and females. Albumin concentration and Hct level, as well as fu and R, were minimally different between age groups, but were similar between males and females (Table 7.12). All CL values also increased with age. The Kp values predicted for malnourished children were approximately double those of the values estimated for healthy children. However, fu and R, which were adjusted on the basis of the alterations of albumin concentration and Hct, were only slightly different. For example, fu and R for healthy children aged 6 months were 0.74 and 1.022, respectively, and were 0.785 and 1.035 in malnourished children.

The model-predicted plasma concentration-time profiles are illustrated in Figure 7.9. It was found that the predicted concentrations were in agreement with the observed data, with only a few data points lying outside the prediction interval. In the 10 year group, the model predictions tended to be lower than the observed data. Figure 7.10

shows the concentration-time profiles of ciprofloxacin in the different organs of children. The results showed that the profiles of drug for each age group were very similar. The predicted concentrations for 6-month-old children were the highest, although only slightly higher than for the other age groups, followed by the predicted concentrations for 1- and 2-year-old children, respectively. For the majority of organs, the concentration-time profiles of children aged 5 and 10 years were comparable and were generally lower than those profiles obtained for younger children.

The mean concentration-time profiles obtained from the model for malnourished children were compared with the results gleaned from the model of healthy children (Figure 7.11). The profiles for 2-year-old children alone have been presented in this section; the results for the remaining age groups are given in Appendix III. For the majority of organs, drug concentrations in malnourished children were higher than in healthy children, and it was found that the distribution of ciprofloxacin into organ/tissue was rapid. In healthy children, the C_{max} of most organs was reached at approximately 1 hour after dosing, but was slightly delayed in malnourished children (1-2 hours). Drug distribution into adipose tissue, bone, muscle, and skin was slower, compared to distribution into other organs. T_{max} for adipose tissue, bone, and skin was around 2 and 3 hours in healthy and malnourished children, respectively. A longer T_{max} was observed for muscle, being approximately 3.5 hours for healthy children and around 5 hours for malnourished children. In addition, the elimination of drug from these organs was considerably slower, especially in muscle.

Table 7.12 Tissue:plasma partition coefficient (Kp), albumin, haematocrit, fu, R, and clearance used in a WBPBPK model for malnourished children of different age groups

Organs	6 months (M/F)	1 year (M/F)	2 years (M/F)	5 years (M/F)	10 years (M/F)
Kp					
Adipose	1.87/1.91	1.56/1.57	1.56/1.50	1.19/1.20	1.17/1.17
Bone	10.71/10.91	9.07/9.13	9.09/8.77	7.07/7.11	6.96/6.96
Brain	0.57/0.58	0.50/0.51	0.50/0.49	0.42/0.42	0.41/0.41
Gut	7.73/7.82	6.95/6.98	6.96/6.81	5.94/5.96	5.88/5.88
Heart	14.75/15.04	12.43/12.51	12.45/12.00	9.61/9.66	9.45/9.45
Kidney	13.64/13.74	12.74/12.77	12.75/12.56	11.49/11.52	11.42/11.42
Liver	6.89/6.97	6.25/6.27	6.26/6.13	5.39/5.41	5.34/5.34
Muscle	20.50/20.97	16.73/16.86	16.77/16.05	12.34/12.42	12.10/12.10
Skin	10.83/11.00	9.47/9.52	9.48/9.21	7.74/7.77	7.64/7.64
Spleen	20.50/20.97	16.73/16.86	16.77/16.05	12.34/12.42	12.10/12.10
Lungs	15.93/16.22	13.57/13.65	13.59/13.13	10.67/10.72	10.51/10.51
Albumin[1] (g/dL)	3.10	3.46	3.46	3.35	3.35
Haematocrit[1] (%)	29	30	30	31	33
fu[a]	0.785	0.767	0.767	0.772	0.772
R[a]	1.035	1.028	1.028	1.032	1.034
CL_R[b] (L/h)	2.53/2.44	3.36/3.36	5.03/4.79	6.88/6.88	11.27/11.27
CL_{GFR} (L/h)	0.61/0.59	0.86/0.86	1.30/1.26	1.75/1.75	2.48/2.48
CL_{TS} (L/h)	1.92/1.85	2.50/2.50	3.72/3.53	5.12/5.12	8.79/8.79
CL_{NR}[c] (L/h)	1.00/1.02	1.43/1.55	1.97/2.15	3.22/3.56	4.12/4.56
CL_H (L/h)	0.28/0.32	0.39/0.53	0.67/0.84	1.13/1.48	1.37/1.82
CL_{GUT} (L/h)	0.73/0.70	1.03/1.02	1.30/1.31	2.09/2.08	2.74/2.74

[a] the results were similar between male and female.
[b] calculated as the sum of CL_{GFR} and CL_{TS}.
[c] calculated as the sum of CL_H and CL_{GUT}.
M=male, F=female

Figure 7.9 Plasma concentration-time profiles of oral ciprofloxacin predicted using a WBPBPK model for malnourished children of different age groups

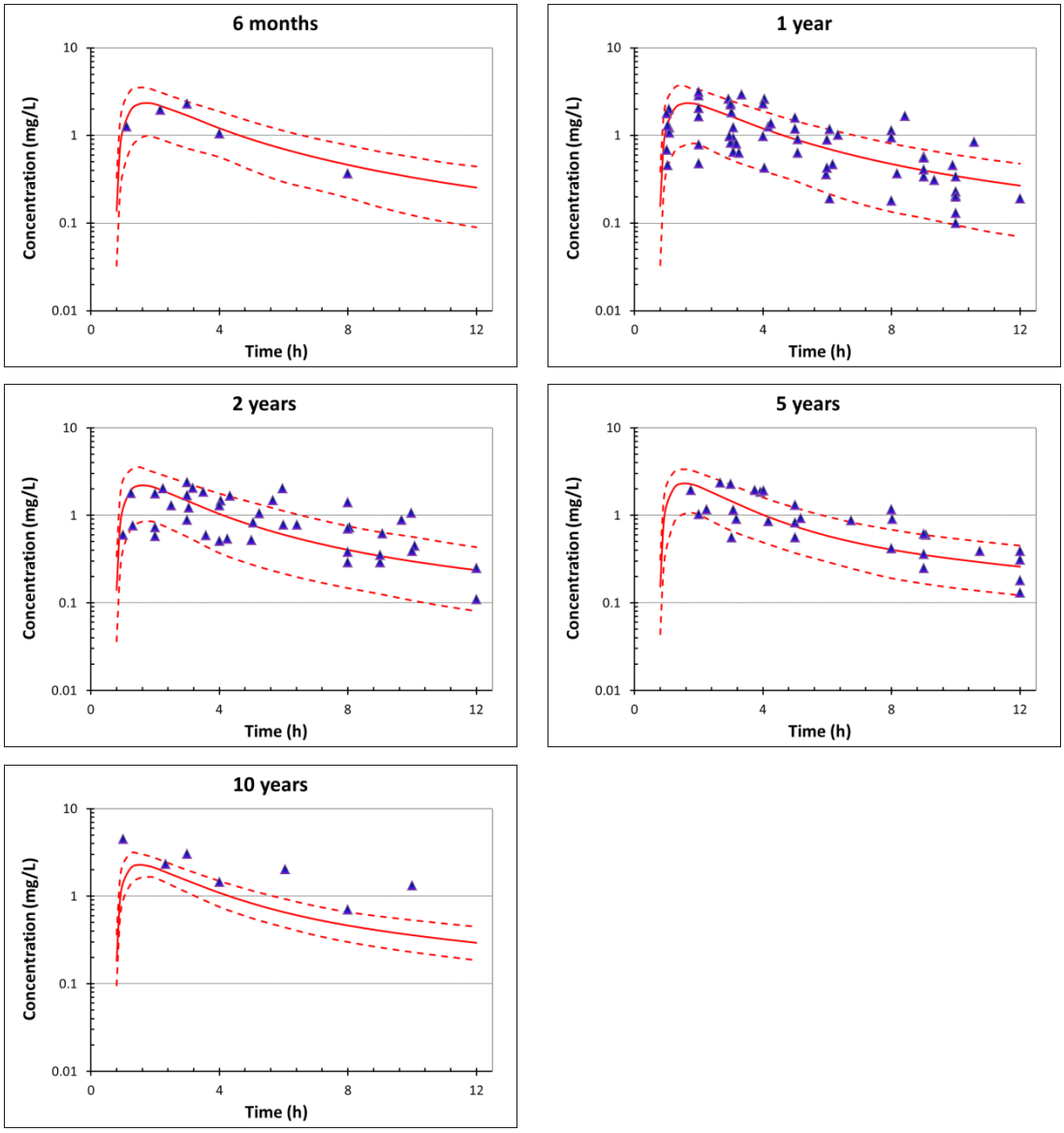

Key: the blue symbols are the observed data, the red solid line is the mean prediction and the red dashed lines are the 2.5th (lower) and 97.5th (upper) percentiles of prediction.

Figure 7.10 Concentration-time profiles of oral ciprofloxacin in different organs of children according to the different age groups

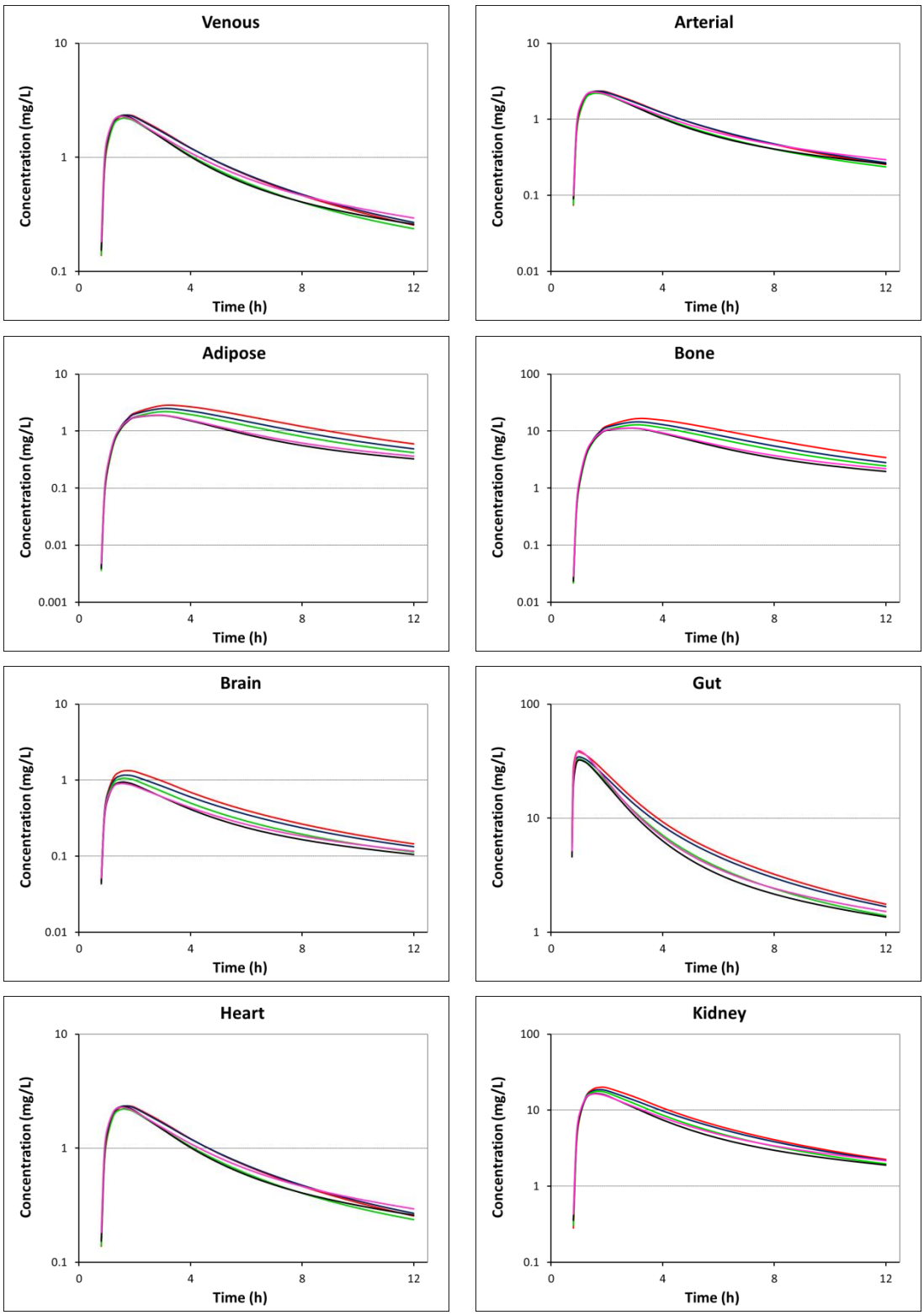

Key: red line = 6 months, blue line = 1 year, green line = 2 years, black line = 5 years, and pink line = 10 years.

Figure 7.10 (continued)

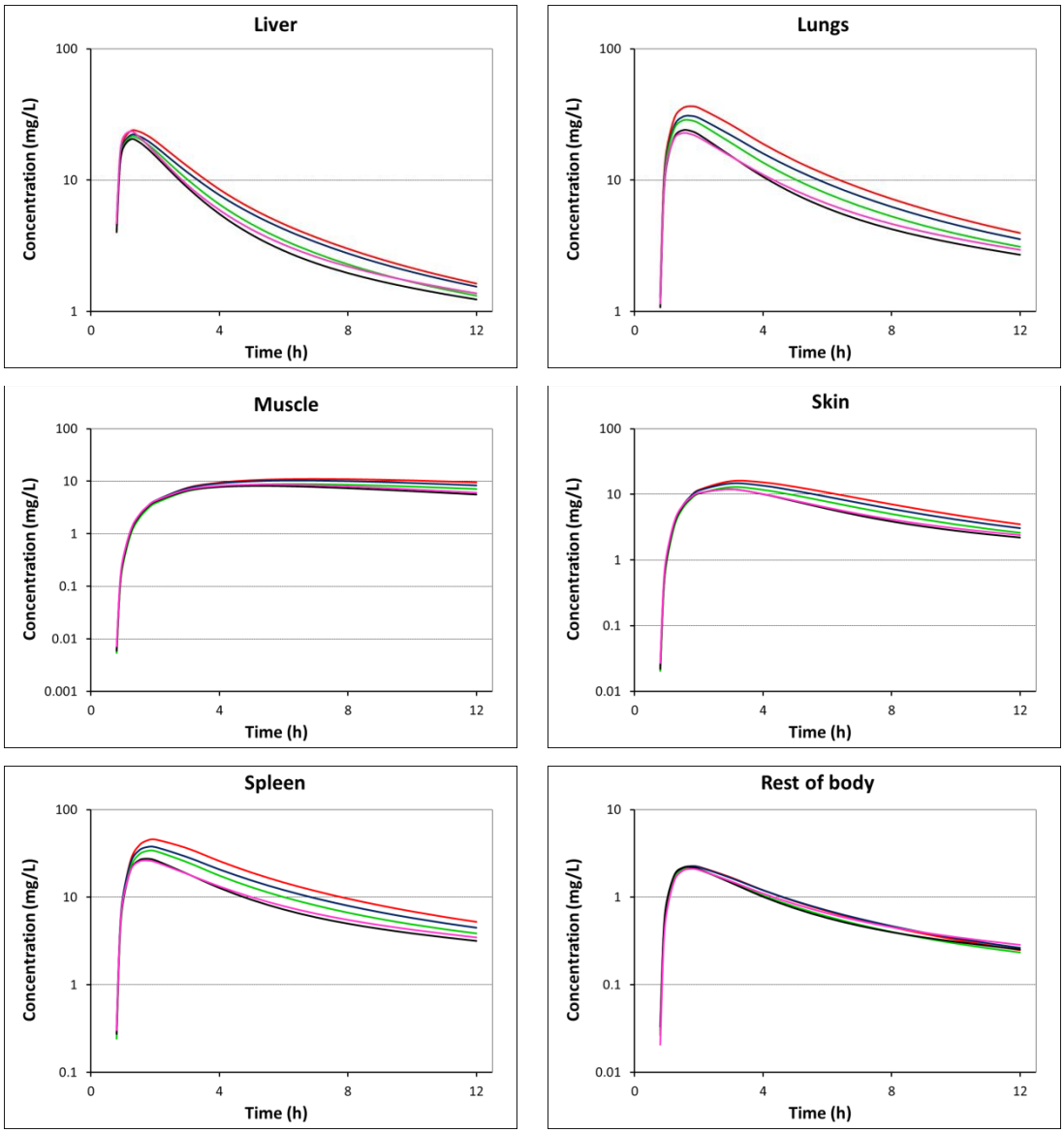

Figure 7.11 Comparison of concentration-time profiles in different organs obtained from a WBPBPK model of healthy children and malnourished children aged 2 years

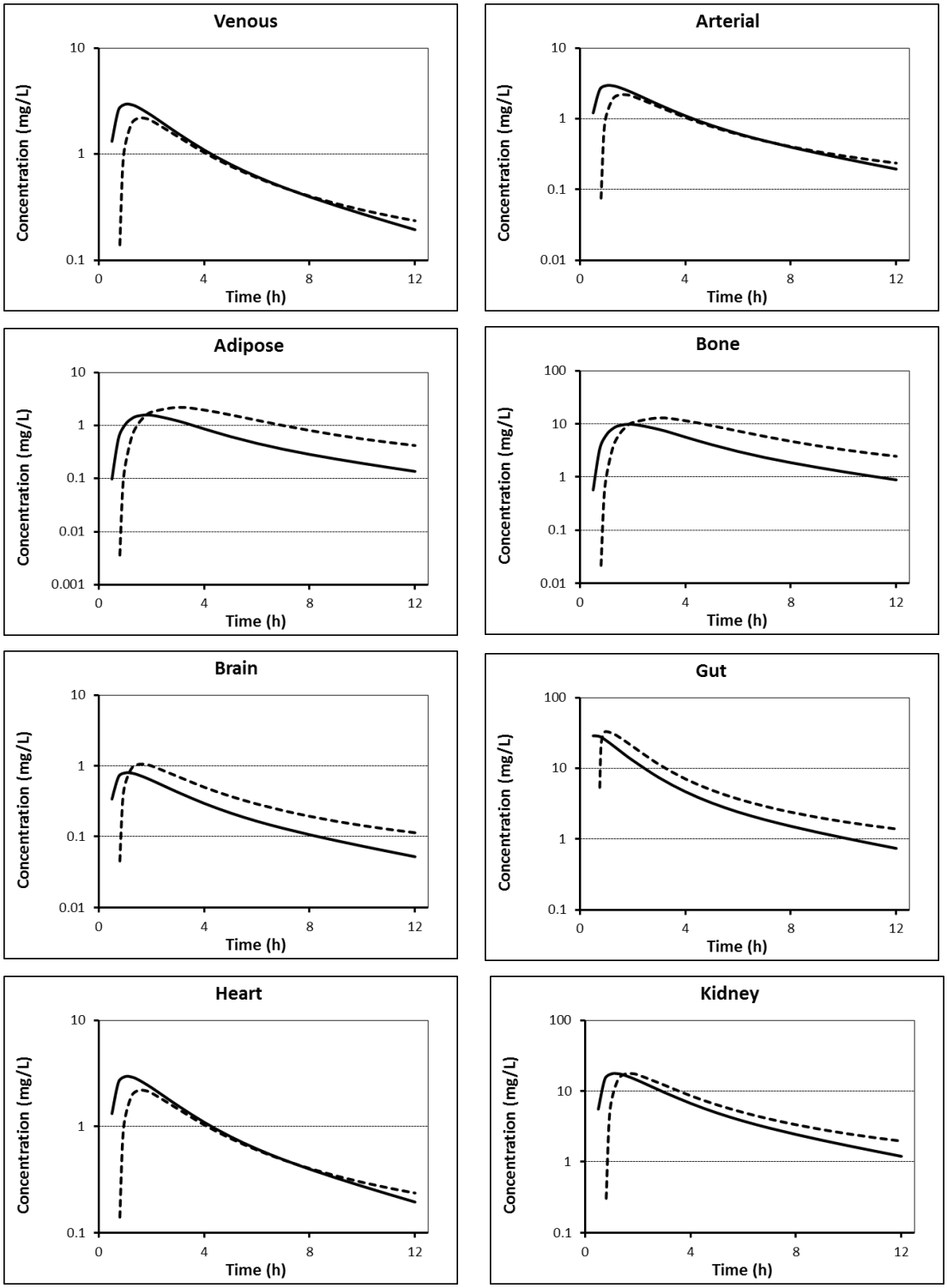

Key: solid line = healthy children, dashed line = malnourished children.

Figure 7.11 (continued)

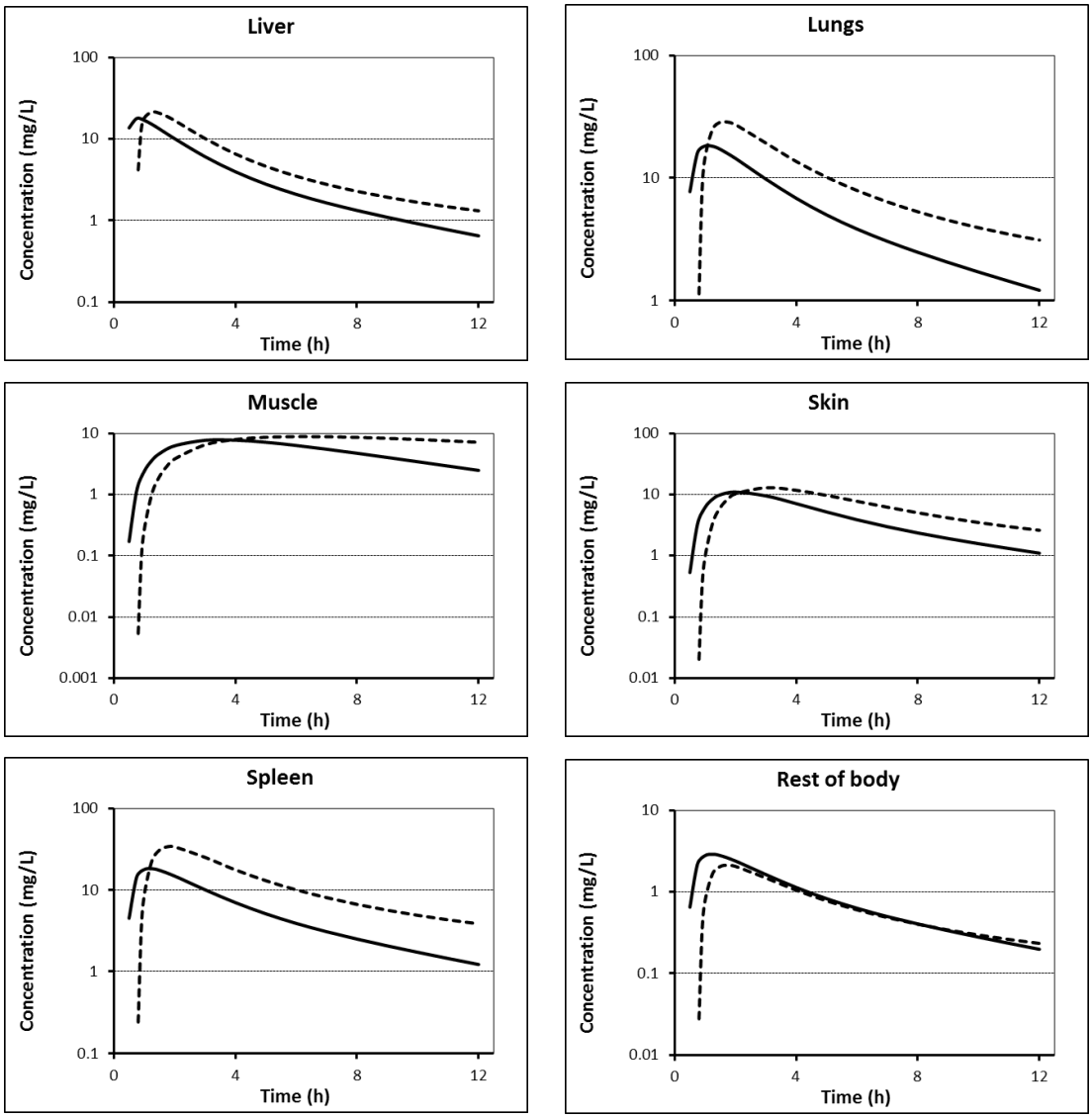

7D.3 DISCUSSION

A WBPBPK model was developed for malnourished children aged 6 months to 10 years. Existing data for this patient population are scant in the available literature, so the majority of parameters were obtained by scaling from the values reported for healthy children. The Kp values predicted from the empirical method decreased with age. In the present study, a target V_{ss} was fixed at 4.49 L/kg for all age groups, therefore the discrepancies in Kp values between age groups may be the result of larger organ volumes being used to estimate Kp in older children. The CL_T values for malnourished children ranged from a minimum of 3.4 L/h in 6-month-old children to a maximum of 15.8 L/h in 10-year-old children. These results were consistent with the values obtained from a previous population PK analysis, which reported a median individual empirical Bayes estimate of 7.19 L/h with a range of 1.83-17.1 L/h.

The results of the present study demonstrated that the model-predicted concentrations were consistent with the observed data, with approximately 95% being in the prediction interval; however, it was found that some data points lay outside this interval. It was noticed that there was particularly high variation in the observed data with regard to malnourished children. This could be explained by the fact that malnutrition is not a single disease, but involves a wide range of pathophysiological changes, e.g., in the gastrointestinal tract, in renal function, and in body water. The observed data used in this study were collected from children with varying degrees of malnutrition, i.e., some children had the presence of oedema (kwashiorkor or marasmus-kwashiorkor), while others had only markedly decreased weight, without the evidence of oedema (pure marasmus). In the present study, the model was primarily developed for those children with oedema and was therefore considered to be applicable for predicting drug disposition in those with kwashiorkor or marasmus-kwashiorkor. In addition, the body weight of malnourished children aged <10 years was predicted using height as a reference; therefore, the model could only account for children with a weight-for-height deficit (wasting). It may be impossible to develop a physiological model that accounts for all possible types of malnutrition because of the difficulty of implementing a model of such complexity, as well as the need for a large number of data.

In the present study, the models were developed for fixed age groups of children, i.e., 6 months, 1, 2, 5, and 10 years, but the observed data for validating the model covered a wide range of ages; from 8-102 months. Therefore, it was requisite that the observed data be grouped into one of five fixed groups of age for comparative purposes. The data points that were outside the prediction interval likely reflect some children whose physiology differed significantly from the children at these fixed ages.

The results showed that the distribution of ciprofloxacin into the majority of organs/tissues was slower in malnourished children than in healthy children. This may be as a result of the delayed lag time that was implemented in the absorption model, as well as a decrease in blood flow rate to these organs. It was found that the tissue concentrations were generally higher in malnourished children, compared to healthy children, which was likely due to decreased total drug CL. A decrease in protein binding concentration may have also contributed to the higher drug concentration found in the majority of organs. It was observed that the distribution of drug to adipose tissue, bone, muscle, and skin was much slower compared to distribution to other organs. This reflected the fact that these organs are represented as the slowly equilibrating tissue with large time constants of the perfusion rate-limited compartments (Nestorov *et al.*, 1998a).

Since the model of malnourished children requires a variety of information that is scarce in the literature, some obstacles were encountered during the model development process. Firstly, as the V_{ss} of ciprofloxacin in malnourished children was not available, the Kp values were predicted from a median value of V derived from a previous population analysis. This value is estimated from concentration-time data after one or two doses, therefore it may be different from the V_{ss}. However, as was demonstrated using a healthy adult model, slight discrepancies in the target V_{ss} had no significant effect on the Kp predictions or the model-predicted concentration-time profiles. The Poulin method and the Rodgers method were not used for predicting Kp values in the present study since they require intensive information regarding the tissue composition of each organ in malnourished individuals. Such

information is scarce in the literature and it may be inappropriate to make an assumption that the tissue composition data relating to malnourished children are similar to those relating to healthy children. Secondly, several parameters, such as binding protein and CL, were scaled from data from healthy children using fixed scaling factors. Indeed, the alteration of these parameters could vary, depending on many factors, e.g., type of malnutrition and severity of disease, as well as unexplained variables. However, for reasons of simplicity, fixed scaling factors were used to estimate PBPK parameters in this study, and the variability was then incorporated in each parameter. It could be assumed that the latter accounted for both the variability of the parameters themselves and the variability of the scaling factors. Finally, the organ weights of malnourished children were predicted by using equations that correlated the change of organ weight with the change of body weight. It was found that a linear model best described this correlation, since these equations were developed from only a small number of data, i.e., between two and eight data points per organ. When using these equations, it is important to note that they cannot be applied to those individuals who have significantly decreased body weight beyond the data points with which these equations were developed. This is due to there being no information to warrant the assumption that correlation of these equations remains linear for these individuals. In the present study, these equations were limited to use for predicting organ weights of those malnourished children with a maximum weight loss of -4 SD.

In summary, the WBPBPK model was developed for malnourished children of differing ages. A reference source of model parameters was compiled as far as possible. Prediction of the disposition of ciprofloxacin in malnourished children generally tallied with observed data. Since there are obvious practical and ethical difficulties in conducting PK studies in paediatric patients, this model may become a useful tool for prediction of drug disposition in this patient population. The application of this model to other drugs and data is required to demonstrate its strengths and weaknesses.

CHAPTER 8

GENERAL CONCLUSIONS AND FUTURE WORK

8.1 GENERAL CONCLUSIONS

The ultimate aim of this thesis was to develop pharmacokinetic models of oral ciprofloxacin for describing and predicting drug disposition in malnourished children. The analysis of a dataset obtained from 52 such children identified that the PK of oral ciprofloxacin is influenced by body weight, serum sodium concentration and the high risk of mortality in this patient population. The physiological explanation for why sodium influenced estimations of CL/F and V/F remains unclear, but since the inclusion of this factor reduced inter-individual variability in CL/F by only 6% and in V/F by 4%, indicating a weak overall effect, it may be an incidental finding. No further clinical factors were identified as having any clinically relevant influence. Due to inadequate drug absorption information, ka was poorly estimated with high variability. However, oral ciprofloxacin absorption was unaffected by the simultaneous administration of nutritional feeds. A current dosage of 10 mg/kg twice daily would be a suitable treatment regimen for patients having septicaemia with *E. coli* and *Salmonella* spp., but a higher dose of 10 mg/kg three times daily should be used for *K. pneumoniae*. Oral ciprofloxacin is unlikely to be an effective treatment for *P. aeruginosa*. Irrespective of the bacterial pathogen, patients with severe illness, and at high risk of mortality, should initially receive intravenous antibiotics.

In this thesis, the optimal design method was used to design future population PK studies of oral ciprofloxacin. Indeed, it may not have been possible, and may be unreasonable, to conduct a further study of the same drug in the same patient population. However, in addition to the development of new study designs, this analysis was also intended to demonstrate the advantages of the optimal design methods and to highlight the importance of sampling times, as well as design structures, when population PK studies are designed.

Since studies of PK in children present obvious practical and ethical difficulties, particularly in those with severe malnutrition, a WBPBPK model was created for a different population, including healthy adults, healthy children and malnourished children, with an age range from 6 months to 10 years. Although there were some

difficulties in the development of the model, due to its complexity and the lack of information available for the changes of both physiological and drug-specific parameters, the predictions derived from the model generally tallied with the experimental data.

8.2 FUTURE WORK

In this thesis, concentration-time data were analysed by using the parametric FOCE-I method, implemented in the NONMEM program. When using the parametric method, the distribution of individual parameter estimates is assumed to be normally distributed around the typical values. In contrast, with non-parametric methods, such as the Non-parametric Adaptive Grid (NPAG) or non-parametric FO and FOCE, which are available in NONMEM, there is no requirement for any assumptions regarding the shape of distribution of model parameter estimates. With this method, a non-parametric population model consisting of discrete support points for each estimate, and the associated probability of that estimate, will be created. In future studies, it might be interesting to compare the results obtained from using a parametric method to those estimated by using a non-parametric method.

In the present study, it was demonstrated that the absorption process of oral ciprofloxacin was not well characterised, due to a lack of available information. If drug absorption is of interest, the optimal study designs for oral ciprofloxacin proposed in this thesis may be useful for guiding optimal sampling times, and sampling windows, as well as design structures in future studies. Nevertheless, in practice, conducting a population PK study is time-consuming task, and a study in special populations, such as severely malnourished children, may be difficult to carry out, due to ethical restrictions. In this circumstance, a WBPBPK model, such as the one developed in this thesis might be a powerful tool for predicting the PK of drugs in this patient population. However, the validity of this model was tested by using ciprofloxacin concentration-time data only. Application of this model to other drugs and data is now required in order to substantiate the predictive performance of the model.

REFERENCES

Adams, D. E., Shekhtman, E. M., Zechiedrich, E. L., Schmid, M. B., & Cozzarelli, N. R. (1992). The role of topoisomerase IV in partitioning bacterial replicons and the structure of catenated intermediates in DNA replication. *Cell*, 71(2), 277–288.

Aigner, K. R., & Dalhoff, A. (1986). Penetration activities of ciprofloxacin into muscle, skin and fat following oral administration. *The Journal of antimicrobial chemotherapy*, 18(5), 644–645.

Akaike, H. (1978). A Bayesian analysis of the minimum AIC procedure. *Annals of the Institute of Statistical Mathematics*, 30(1), 9–14.

Akinyinka, O. O., Sowunmi, A., Honeywell, R., & Renwick, A. G. (2000). The pharmacokinetics of caffeine in Nigerian children suffering from malaria and kwashiorkor. *European journal of clinical pharmacology*, 56(2), 153–158.

Al-Banna, M. K., Kelman, A. W., & Whiting, B. (1990). Experimental design and efficient parameter estimation in population pharmacokinetics. *Journal of pharmacokinetics and biopharmaceutics*, 18(4), 347–360.

Alleyne, G. A. (1967). The effect of severe protein calorie malnutrition on the renal function of Jamaican children. *Pediatrics*, 39(3), 400–411.

Ambrose, P. G., Grasela, D. M., Grasela, T. H., Passarell, J., Mayer, H. B., & Pierce, P. F. (2001). Pharmacodynamics of fluoroquinolones against Streptococcus pneumoniae in patients with community-acquired respiratory tract infections. *Antimicrobial agents and chemotherapy*, 45(10), 2793–2797.

Ambrose, P. G., Bhavnani, S. M., Rubino, C. M., Louie, A., Gumbo, T., Forrest, A., & Drusano, G. L. (2007). Pharmacokinetics-pharmacodynamics of antimicrobial therapy: it's not just for mice anymore. *Clinical infectious diseases: an official publication of the Infectious Diseases Society of America*, 44(1), 79–86.

Anderson, B. J., & Holford, N. H. (2008). Mechanism-based concepts of size and maturity in pharmacokinetics. *Annual review of pharmacology and toxicology*, 48, 303–332.

Anderson, B. J, McKee, A. D., & Holford, N. H. (1997). Size, myths and the clinical pharmacokinetics of analgesia in paediatric patients. *Clinical pharmacokinetics*, 33(5), 313–327.

Anderson, B. J, & Holford, N. H. (2009). Mechanistic basis of using body size and maturation to predict clearance in humans. *Drug metabolism and pharmacokinetics*, 24(1), 25–36.

Andes, D., & Craig, W. A. (1998). In vivo activities of amoxicillin and amoxicillin-clavulanate against Streptococcus pneumoniae: application to breakpoint determinations. *Antimicrobial agents and chemotherapy*, 42(9), 2375–2379.

Andriole, V. T. (2005). The quinolones: past, present, and future. *Clinical infectious diseases : an official publication of the Infectious Diseases Society of America*, *41 Suppl 2*, S113–S119.

Aquino, V. M., Herrera, L., Sandler, E. S., & Buchanan, G. R. (2000). Feasibility of oral ciprofloxacin for the outpatient management of febrile neutropenia in selected children with cancer. *Cancer*, 88(7), 1710–1714.

Arroyave, G., Wilson, D., Behar, M., & Scrimshaw, N. S. (1961). Serum and urinary creatinine in children with severe protein malnutrition. *The American journal of clinical nutrition*, 9, 176–179.

Babirekere-Iriso, E., Musoke, P., & Kekitiinwa, A. (2006). Bacteraemia in severely malnourished children in an HIV-endemic setting. *Annals of tropical paediatrics*, 26(4), 319–328.

Bachou, H., Tylleskär, T., Kaddu-Mulindwa, D. H., & Tumwine, J. K. (2006). Bacteraemia among severely malnourished children infected and uninfected with the human immunodeficiency virus-1 in Kampala, Uganda. *BMC infectious diseases*, 6(160), 1-7.

Balfour, J. A., & Wiseman, L. R. (1999). Moxifloxacin. *Drugs*, 57(3), 363–373.

Ball, P., Mandell, L., Niki, Y., & Tillotson, G. (1999). Comparative tolerability of the newer fluoroquinolone antibacterials. *Drug safety an international journal of medical toxicology and drug experience*, 21(5), 407–421.

Ballard, P, Leahy, D. E., & Rowland, M. (2000). Prediction of in vivo tissue distribution from in vitro data 1. Experiments with markers of aqueous spaces. *Pharmaceutical research*, 17(6), 660–663.

Beal, S. L. (1984). Population pharmacokinetic data and parameter estimation based on their first two statistical moments. *Drug metabolism reviews*, 15(1-2), 173–193.

Beal, S. L., Sheiner, L. B., Boeckmann A. J. (eds.) (1989-2006). *NONMEM Users Guides*, Icon Development Solutions, Ellicott, Maryland, USA.

Berezhkovskiy, L. M. (2004). Volume of distribution at steady state for a linear pharmacokinetic system with peripheral elimination. *Journal of pharmaceutical sciences*, 93(6), 1628–1640.

Bergan, T., Thorsteinsson, S. B., Kolstad, I. M., & Johnsen, S. (1986). Pharmacokinetics of ciprofloxacin after intravenous and increasing oral doses. *European Journal of Clinical Microbiology*, 5(2), 187–192.

Bergan, T., Thorsteinsson, S. B., Solberg, R., Bjornskau, L., Kolstad, I. M., & Johnsen, S. (1987). Pharmacokinetics of ciprofloxacin after intravenous and increasing oral doses. *The American Journal of Medicine*, 5(2), 97–102.

Bergogne-Bérézin, E., Berthelot, G., Even, P., Stern, M., & Reynaud, P. (1986). Penetration of ciprofloxacin into bronchial secretions. *European journal of clinical microbiology*, 5(2), 197–200.

Bergstrand, M., Hooker, A. C., Wallin, J. E., & Karlsson, M. O. (2011). Prediction-corrected visual predictive checks for diagnosing nonlinear mixed-effects models. *The AAPS journal*, 13(2), 143–151.

Björkman, S, Wada, D. R., Berling, B. M., & Benoni, G. (2001). Prediction of the disposition of midazolam in surgical patients by a physiologically based pharmacokinetic model. *Journal of pharmaceutical sciences*, 90(9), 1226–1241.

Björkman, S. (2002). Prediction of the volume of distribution of a drug: which tissue-plasma partition coefficients are needed? *The Journal of pharmacy and pharmacology*, 54(9), 1237–1245.

Björkman, S. (2005). Prediction of drug disposition in infants and children by means of physiologically based pharmacokinetic (PBPK) modelling: theophylline and midazolam as model drugs. *British journal of clinical pharmacology*, 59(6), 691–704.

Black, R. E., Allen, L. H., Bhutta, Z. A., Caulfield, L. E., de Onis, M., Ezzati, M., Mathers, C., et al. (2008). Maternal and child undernutrition: global and regional exposures and health consequences. *Lancet*, 371(9608), 243–260.

Blakey, G. E., Nestorov, I. A., Arundel, P. A., Aarons, L. J., & Rowland, M. (1997). Quantitative structure-pharmacokinetics relationships: I. Development of a whole-body physiologically based model to characterize changes in pharmacokinetics across a homologous series of barbiturates in the rat. *Journal of pharmacokinetics and biopharmaceutics*, 25(3), 277–312.

Blondeau, J. M. (1999). A review of the comparative in-vitro activities of 12 antimicrobial agents, with a focus on five new respiratory quinolones. *The Journal of antimicrobial chemotherapy*, *43 Suppl B*, 1–11.

Boelaert, J., Valcke, Y., Schurgers, M., Daneels, R., Rosseneu, M., Rosseel, M. T., & Bogaert, M. G. (1985). The pharmacokinetics of ciprofloxacin in patients with impaired renal function. *Journal of Antimicrobial Chemotherapy*, 16(1), 87–93.

Bolme, P., Eriksson, M., Habte, D., & Paalzow, L. (1988). Pharmacokinetics of streptomycin in Ethiopian children with tuberculosis and of different nutritional status. *European journal of clinical pharmacology*, 33(6), 647–649.

Bolme, P., Eriksson, M., Paalzow, L., Stintzing, G., Zerihun, G., & Woldemariam, T. (1995). Malnutrition and Pharmacokinetics of Penicillin in Ethiopian Children. *Pharmacology & Toxicology*, 76(4), 259–262.

Bonate, P. L. (2011). *Pharmacokinetic-Pharmacodynamic Modeling and Simulation* (2nd ed.). London: Springer.

Borner, K., Höffken, G., Lode, H., Koeppe, P., Prinzing, C., Glatzel, P., Wiley, R., et al. (1986). Pharmacokinetics of ciprofloxacin in healthy volunteers after oral and intravenous administration. *European Journal of Clinical Microbiology*, 5(2), 179-186.

Bosy-Westphal, A., Reinecke, U., Schlörke, T., Illner, K., Kutzner, D., Heller, M., & Müller, M. J. (2004). Effect of organ and tissue masses on resting energy expenditure in underweight, normal weight and obese adults. *International journal of obesity and related metabolic disorders: journal of the International Association for the Study of Obesity*, 28(1), 72–79.

Box, G. E. P., & Lucas, H. L. (1959). Design of Experiments in Non-Linear Situations. *Biometrika*, 46(1/2), 77–99.

Bravo, M. E., Arancibia, A., Jarpa, S., Carpentier, P. M., & Jahn, A. N. (1982). Pharmacokinetics of gentamicin in malnourished infants. *European journal of clinical pharmacology*, 21(6), 499–504.

Bravo, I. G., Bravo, M. E., Plate, G., Merlez, J., & Arancibia, A. (1984). The pharmacokinetics of cotrimoxazole sulphonamide in malnourished (marasmic) infants. *Pediatric pharmacology*, 4(3), 167–176.

Brendel, K., Comets, E., Laffont, C., Laveille, C., & Mentré, F. (2006). Metrics for external model evaluation with an application to the population pharmacokinetics of gliclazide. *Pharmaceutical research*, 23(9), 2036–2049.

Brendel, K., Dartois, C., Comets, E., Lemenuel-Diot, A., Laveille, C., Tranchand, B., Girard, P., et al. (2007). Are population pharmacokinetic and/or pharmacodynamic models adequately evaluated? A survey of the literature from 2002 to 2004. *Clinical pharmacokinetics*, 46(3), 221–234.

Brendel, K., Comets, E., Laffont, C., & Mentré, F. (2010). Evaluation of different tests based on observations for external model evaluation of population analyses. *Journal of pharmacokinetics and pharmacodynamics*, 37(1), 49–65.

Brewster, D. R. (2006). Critical appraisal of the management of severe malnutrition: 3. Complications. *Journal of paediatrics and child health*, 42(10), 583–593.

Brismar, B., Edlund, C., Malmborg, A. S., & Nord, C. E. (1990). Ciprofloxacin concentrations and impact of the colon microflora in patients undergoing colorectal surgery. *Antimicrobial agents and chemotherapy*, 34(3), 481–483.

Brogard, J. M., Jehl, F., Monteil, H., Adloff, M., Blickle, J. F., & Levy, P. (1985). Comparison of high-pressure liquid chromatography and microbiological assay for the determination of biliary elimination of ciprofloxacin in humans. *Antimicrobial agents and chemotherapy*, 28(2), 311–314.

Brown, R P, Delp, M. D., Lindstedt, S. L., Rhomberg, L. R., & Beliles, R. P. (1997). Physiological parameter values for physiologically based pharmacokinetic models. *Toxicology and industrial health*, 13(4), 407–484.

Buchanan, N. (1977). Drug-protein binding and protein energy malnutrition. *South African medical journal*, 52(18), 733–737.

Buchanan, N., Davis, M. D., & Eyberg, C. (1979). Gentamicin pharmacokinetics in kwashiorkor. *British journal of clinical pharmacology*, 8(5), 451–3.

Butte, N. F., Hopkinson, J. M., Wong, W. W., Smith, E. O., & Ellis, K. J. (2000). Body composition during the first 2 years of life: an updated reference. *Pediatric research*, 47(5), 578–585.

Chen, Q., Tung, E. C., Ciccotto, S. L., Strauss, J. R., Ortiga, R., Ramsay, K. a, & Tang, W. (2008). Effect of the anticoagulant ethylenediamine tetra-acetic acid (EDTA) on the estimation of pharmacokinetic parameters: A case study with tigecycline and ciprofloxacin. *Xenobiotica; the fate of foreign compounds in biological systems*, 38(1), 76–86.

Chiron, C., Raynaud, C., Mazière, B., Zilbovicius, M., Laflamme, L., Masure, M. C., Dulac, O., et al. (1992). Changes in regional cerebral blood flow during brain maturation in children and adolescents. *Journal of nuclear medicine: official publication, Society of Nuclear Medicine*, 33(5), 696–703.

Chiu, W. A., & White, P. (2006). Steady-state solutions to PBPK models and their applications to risk assessment I: Route-to-route extrapolation of volatile chemicals. *Risk analysis: an official publication of the Society for Risk Analysis*, 26(3), 769–780.

Cho, M. K., Kim, Y. G., Lee, M. G., & Kim, S. G. (1999). Suppression of rat hepatic cytochrome P450s by protein-calorie malnutrition: complete or partial restoration by cysteine or methionine supplementation. *Archives of biochemistry and biophysics*, 372(1), 150–158.

Chu, D. T. W., Fernandest, P. B., Laboratories, A., & Park, A. (1989). Structure-Activity Relationships of the Fluoroquinolones, 33(2), 131–135.

Chyský, V., Kapila, K., Hullmann, R., Arcieri, G., Schacht, P., & Echols, R. (1991). Safety of ciprofloxacin in children: worldwide clinical experience based on compassionate use. Emphasis on joint evaluation. *Infection*, 19(4), 289–296.

Clewell, H. J., Gentry, P. R., Covington, T. R., Sarangapani, R., & Teeguarden, J. G. (2004). Evaluation of the potential impact of age- and gender-specific pharmacokinetic differences on tissue dosimetry. *Toxicological sciences : an official journal of the Society of Toxicology*, 79(2), 381–393.

CLSI. (2012). *Performance Standards for Antimicrobial Susceptibility Testing; Twenty-Second Information Supplement M100-S22*. Wayne, PA, USA.

Cogill, B. (2003). *Anthropometric Indicators Measurement Guide*. Washington, DC: Food and Nutrition Technical Assistance (FANTA) Project, FHI 360.

Collins, S. (2007). Treating severe acute malnutrition seriously. *Archives of disease in childhood*, 92(5), 453–461.

Comets, E., Brendel, K., & Mentré, F. (2008). Computing normalised prediction distribution errors to evaluate nonlinear mixed-effect models: the npde add-on package for R. *Computer methods and programs in biomedicine*, 90(2), 154–166.

Committee on Infectious Diseases. (2006). The use of systemic fluoroquinolones. *Pediatrics*, 118(3), 1287–1292.

Costa-Silva, J. H., Silva, P. A., Pedi, N., Luzardo, R., Einicker-Lamas, M., Lara, L. S., Bezerra, A. M., et al. (2009). Chronic undernutrition alters renal active Na+ transport in young rats: potential hidden basis for pathophysiological alterations in adulthood? *European journal of nutrition*, 48(7), 437–445.

Crump, B., Wise, R., & Dent, J. (1983). Pharmacokinetics and tissue penetration of ciprofloxacin. *Antimicrobial Agents and Chemotherapy*, 24(5), 784–786.

Dagan, R. (1995). Fluoroquinolones in paediatrics--1995. *Drugs*, *49 Suppl 2*, 92–99.

Dalhoff, A., & Eickenberg, H. U. (1985). Tissue distribution of ciprofloxacin following oral and intravenous administration. *Infection*, 13(2), 78–81.

Dan, M., Verbin, N., Gorea, A., Nagar, H., & Berger, S. A. (1987). Concentrations of ciprofloxacin in human liver, gallbladder, and bile after oral administration. *European Journal of Clinical Pharmacology*, 32(2), 217–218.

Dan, M., Torossian, K., Weissberg, D., & Kitzes, R. (1993). The penetration of ciprofloxacin into bronchial mucosa, lung parenchyma, and pleural tissue after intravenous administration. *European Journal of Clinical Pharmacology*, 44(1), 101–102.

Daschner, F. D., Westenfelder, M., & Dalhoff, A. (1986). Penetration of ciprofloxacin into kidney, fat, muscle and skin tissue. *European journal of clinical microbiology*, 5(2), 212–213.

Davidian, M., & Giltinan, D. M. (1995). *Nonlinear Models for Repeated Measurement Data*. Boca Raton, FL: Chapman and Hall/CRC.

Davis, R. L., Koup, J. R., Williams-Warren, J., Weber, A., & Smith, A. L. (1985). Pharmacokinetics of three oral formulations of ciprofloxacin. *Antimicrobial Agents and Chemotherapy*, 28(1), 74–77.

Davis, R., Markham, A., & Balfour, J. A. (1996). Ciprofloxacin. An updated review of its pharmacology, therapeutic efficacy and tolerability. *Drugs*, 51(6), 1019-1074.

de Onis, M, Yip, R., & Mei, Z. (1997). The development of MUAC-for-age reference data recommended by a WHO Expert Committee. *Bulletin of the World Health Organization*, 75(1), 11–18.

de Onis, Mercedes, Garza, C., Onyango, A. W., & Borghi, E. (2007). Comparison of the WHO child growth standards and the CDC 2000 growth charts. *The Journal of nutrition*, 137(1), 144–148.

DeRyke, C. A., Kuti, J. L., & Nicolau, D. P. (2007). Reevaluation of current susceptibility breakpoints for Gram-negative rods based on pharmacodynamic assessment. *Diagnostic microbiology and infectious disease*, 58(3), 337–344.

de Wildt, S. N., Kearns, G. L., Leeder, J. S., & van den Anker, J. N. (1999). Cytochrome P450 3A: ontogeny and drug disposition. *Clinical pharmacokinetics*, 37(6), 485–505.

DeWoskin, R. S., & Thompson, C. M. (2008). Renal clearance parameters for PBPK model analysis of early lifestage differences in the disposition of environmental toxicants. *Regulatory toxicology and pharmacology*, 51(1), 66–86.

Dibley, M. J., Goldsby, J. B., Staehling, N. W., & Trowbridge, F. L. (1987). Development of normalized curves for the international growth reference: historical and technical considerations. *The American journal of clinical nutrition*, 46(5), 736–748.

Doherty, J. F., Adam, E. J., Griffin, G. E., & Golden, M. H. (1992). Ultrasonographic assessment of the extent of hepatic steatosis in severe malnutrition. *Archives of disease in childhood*, 67(11), 1348–1352.

Domagala, J. M., Hanna, L. D., Heifetz, C. L., Hutt, M. P., Mich, T. F., Sanchez, J. P., & Solomon, M. (1986). New structure-activity relationships of the quinolone antibacterials using the target enzyme. The development and application of a DNA gyrase assay. *Journal of Medicinal Chemistry*, 29(3), 394–404.

Drabu, Y. J., & Blakemore, P. H. (1991). The post-antibiotic effect of teicoplanin: monotherapy and combination studies. *Antimicrobial agents and chemotherapy*, *27 Suppl B*, 1–7.

Drlica, K., & Zhao, X. (1997). DNA gyrase, topoisomerase IV, and the 4-quinolones. *Microbiology and Molecular Biology Reviews*, 61(3), 377–392.

Drusano, G. L., Standiford, H. C., Plaisance, K., Forrest, A., Leslie, J., & Caldwell, J. (1986a). Absolute oral bioavailability of ciprofloxacin. *Antimicrobial agents and chemotherapy*, 30(3), 444–446.

Drusano, G. L., Plaisance, K. I., Forrest, A., & Standiford, H. C. (1986b). Dose ranging study and constant infusion evaluation of ciprofloxacin. *Antimicrobial agents and chemotherapy*, 30(3), 440–443.

Drusano, G. L., Weir, M., Forrest, A., Plaisance, K., Emm, T., & Standiford, H. C. (1987). Pharmacokinetics of intravenously administered ciprofloxacin in patients with various degrees of renal function. *Antimicrobial agents and chemotherapy*, 31(6), 860–864.

Drusano, G. L., Johnson, D. E., Rosen, M., & Standiford, H. C. (1993). Pharmacodynamics of a fluoroquinolone antimicrobial agent in a neutropenic rat model of Pseudomonas sepsis. *Antimicrobial agents and chemotherapy*, 37(3), 483–490.

Drusano, G. L., Preston, S. L., Hardalo, C., Hare, R., Banfield, C., Andes, D., Vesga, O., et al. (2001). Use of preclinical data for selection of a phase II/III dose for evernimicin and identification of a preclinical MIC breakpoint. *Antimicrobial agents and chemotherapy*, 45(1), 13–22.

Dubois, J., & St-Pierre, C. (2000). In vitro study of the post-antibiotic effect and the bactericidal activity of Cefditoren and ten other oral antimicrobial agents against upper and lower respiratory tract pathogens. *Diagnostic Microbiology and Infectious Disease*, 37(3), 187–193.

Dudley, M. N., Ericson, J., & Zinner, S. H. (1987). Effect of dose on serum pharmacokinetics of intravenous ciprofloxacin with identification and characterization of extravascular compartments using noncompartmental and compartmental pharmacokinetic models. *Antimicrobial agents and chemotherapy*, 31(11), 1782–1786.

Dudley, M. N., Blaser, J., Gilbert, D., Mayer, K. H., & Zinner, S. H. (1991). Combination Therapy with Ciprofloxacin plus Azlocillin against Pseudomonas aeruginosa: Effect of Simultaneous versus Staggered Administration in an In Vitro Model of Infection. *Journal of Infectious Diseases*, 164(3), 499–506.

Duggan, C., Vatkins, J. B., & Walker, W. A. (2008). *Nutrition in paediatrics: Basic Science, Clinical Applications* (4th ed.). Hamilton, Ontario: BC Decker Inc.

D'Argenio, D. Z. (1981). Optimal sampling times for pharmacokinetic experiments. *Journal of pharmacokinetics and biopharmaceutics*, 9(6), 739–756.

D'Argenio, D. Z., & Schumitzky, A. (1979). A program package for simulation and parameter estimation in pharmacokinetic systems. *Computer programs in biomedicine*, 9(2), 115–134.

D'Argenio, D.Z., Schumitzky, A., & Wang, X. (2009). *ADAPT 5 User's Guide: Pharmacokinetic/Pharmacodynamic Systems Analysis Software*, Biomedical Simulations Resource, Los Angeles.

Eagle, H., Fleischman, R., & Musselman, A. D. (1950a). The effective concentrations of penicillin in vitro and in vivo for streptococci, pneumococci, and Treponema pallidum. *Journal of bacteriology*, 59(5), 625–643.

Eagle, H., Fleischman, R., & Musselman, A. D. (1950b). Effect of schedule of administration on the therapeutic efficacy of penicillin; importance of the aggregate time penicillin remains at effectively bactericidal levels. *The American journal of medicine*, 9(3), 280–299.

Edginton, A. N., Schmitt, W., & Willmann, S. (2006a). Development and evaluation of a generic physiologically based pharmacokinetic model for children. *Clinical pharmacokinetics*, 45(10), 1013–1034.

Edginton, A. N., Schmitt, W., Voith, B., & Willmann, S. (2006b). A mechanistic approach for the scaling of clearance in children. *Clinical pharmacokinetics*, 45(7), 683–704.

Edginton, A. N., & Willmann, S. (2008). Physiology-based simulations of a pathological condition: prediction of pharmacokinetics in patients with liver cirrhosis. *Clinical pharmacokinetics*, 47(11), 743–752.

Edwards, K., & Freeman, D. M. (2006). Adolescent and adult pertussis: disease burden and prevention. *Current opinion in pediatrics*, 18(1), 77–80.

Efron, B. (1979). Bootstrap Methods: Another Look at the Jackknife. *The Annals of Statistics*, 7(1), 1–26.

Efron, B., & Tibshirani, R. (1993). *An Introduction to the Bootstrap*. Boca Raton, FL: Chapman & Hall/CRC.

EMEA (2006). Guideline of reporting the results of population pharmacokinetic analyses. Retrieved from http://www.ema.europa.eu/docs/en_GB/document_library/Scientific_guideline/2009/09/WC500003067.pdf

Eriksson, M., Paalzow, L., Bolme, P., & Mariam, T. W. (1983). Chloramphenicol pharmacokinetics in Ethiopian children of differing nutritional status. *European journal of clinical pharmacology*, 24(6), 819–823.

Espié, P., Tytgat, D., Sargentini-Maier, M. L., Poggesi, I., & Watelet, J. B. (2009). Physiologically based pharmacokinetics (PBPK). *Drug metabolism reviews*, 41(3), 391–407.

Esposito, S., Miniero, M., Barba, D., & Sagnelli, E. (1989). Pharmacokinetics of ciprofloxacin in impaired liver function. *International journal of clinical pharmacology research*, 9(1), 37–41.

Ette, E. I. (1997). Stability and performance of a population pharmacokinetic model. *Journal of clinical pharmacology*, 37(6), 486–95.

EUCAST. (2011). *Antimicrobial wild type distributions of microorganisms*. Retrieved from http://mic.eucast.org/Eucast2/SearchController/search.jsp?action=init

Fabre, D., Bressolle, F., Gomeni, R., Arich, C., Lemesle, F., Beziau, H., & Galtier, M. (1991). Steady-state pharmacokinetics of ciprofloxacin in plasma from patients with nosocomial pneumonia: penetration of the bronchial mucosa. *Antimicrobial agents and chemotherapy*, 35(12), 2521–2525.

Farrar, D., Allen, B., Crump, K., & Shipp, A. (1989). Evaluation of uncertainty in input parameters to pharmacokinetic models and the resulting uncertainty in output. *Toxicology letters*, 49(2-3), 371–385.

Fernández, M. A. L., Delchevalerie, P., & Van Herp, M. (2010). Accuracy of MUAC in the detection of severe wasting with the new WHO growth standards. *Pediatrics*, 126(1), e195–201.

Fiserova-Bergerova, V. (1995). Extrapolation of physiological parameters for physiologically based simulation models. *Toxicology letters*, 79(1-3), 77–86.

Fomon, S. J., Haschke, F., Ziegler, E. E., & Nelson, S. E. (1982). Body composition of reference children from birth to age 10 years. *The American journal of clinical nutrition*, 35(5 Suppl), 1169–1175.

Fong, I. W., Ledbetter, W. H., Vandenbroucke, A. C., Simbul, M., & Rahm, V. (1986). Ciprofloxacin concentrations in bone and muscle after oral dosing. *Antimicrobial agents and chemotherapy*, 29(3), 405–408.

FDA (1999). *Guidance for Industry: Population Pharmacokinetics*. Retrieved from http://www.fda.gov/downloads/ScienceResearch/SpecialTopics/WomensHealthResearch/UCM133184.pdf

Forrest, A., Weir, M., Plaisance, K. I., Drusano, G. L., Leslie, J., & Standiford, H. C. (1988). Relationships between renal function and disposition of oral ciprofloxacin. *Antimicrobial agents and chemotherapy*, 32(10), 1537–1540.

Forrest, A, Nix, D. E., Ballow, C. H., Goss, T. F., Birmingham, M. C., & Schentag, J. J. (1993). Pharmacodynamics of intravenous ciprofloxacin in seriously ill patients. *Antimicrobial agents and chemotherapy*, 37(5), 1073–1081.

Frei, C. R., Wiederhold, N. P., & Burgess, D. S. (2008). Antimicrobial breakpoints for gram-negative aerobic bacteria based on pharmacokinetic-pharmacodynamic models with Monte Carlo simulation. *The Journal of antimicrobial chemotherapy*, 61(3), 621–628.

Friedman, S. M., & Lu, T. A. O. (2001). Mutation in the DNA Gyrase A Gene of Escherichia coli That Expands the Quinolone Resistance-Determining Region. *Antimicrobial agents and chemotherapy*, 45(8), 2378–2380.

Frost, R. W., Carlson, J. D., Dietz, A. J., Heyd, A., & Lettieri, J. T. (1989a). Ciprofloxacin pharmacokinetics after a standard or high-fat/high-calcium breakfast. *Journal of clinical pharmacology*, 29(10), 953–955.

Frost, R. W., Lettieri, J. T., Krol, G., Shamblen, E. C., & Lasseter, K. C. (1989b). The effect of cirrhosis on the steady-state pharmacokinetics of oral ciprofloxacin. *Clinical pharmacology and therapeutics*, 45(6), 608–616.

Fu, Y., Guo, L., Xu, Y., Zhang, W., Gu, J., Xu, J., Chen, X., et al. (2008). Alteration of GyrA amino acid required for ciprofloxacin resistance in Klebsiella pneumoniae isolates in China. *Antimicrobial agents and chemotherapy*, 52(8), 2980–2983.

Fukuda, H., Kishii, R., Takei, M., & Hosaka, M. (2001). Contributions of the 8-Methoxy Group of Gatifloxacin to Resistance Selectivity, Target Preference, and Antibacterial Activity against Streptococcus pneumoniae. *Antimicrobial Agents and Chemotherapy*, 45(6), 1649–1653.

Fuursted, K. (1987). Post-antibiotic effect and killing activity of ciprofloxacin against Staphylococcus aureus. *Acta pathologica microbiologica et immunologica Scandinavica Section B Microbiology*, 95(3), 199–202.

Gallicano, K., & Sahai, J. (1996). Lack of gender effect on ciprofloxacin pharmacokinetics in humans. *British Journal of Clinical Pharmacology*, 42(5), 632–634.

Gaohua, L., Abduljalil, K., Jamei, M., Johnson, T. N., & Rostami-Hodjegan, A. (2012). A pregnancy physiologically based pharmacokinetic (p-PBPK) model for disposition of drugs metabolized by CYP1A2, CYP2D6 and CYP3A4. *British journal of clinical pharmacology*, 74(5), 873–885.

Garrow, J. S., Fletcher, K., & Halliday, D. (1965). Body composition in severe infantile malnutrition. *The Journal of clinical investigation*, 44, 417–425.

Gasser, T. C., Ebert, S. C., Graversen, P. H., & Madsen, P. O. (1987). Ciprofloxacin pharmacokinetics in patients with normal and impaired renal function. *Antimicrobial agents and chemotherapy*, 31(5), 709–712.

Gendrel, D., & Moulin, F. (2001). Fluoroquinolones in paediatrics. *Paediatric drugs*, 3(5), 365–377.

Gibbs, J. P., Liacouras, C. A., Baldassano, R. N., & Slattery, J. T. (1999). Up-regulation of glutathione S-transferase activity in enterocytes of young children. *Drug Metabolism Disposition*, 27(12), 1466–1469.

Gibiansky, E., Gibiansky, L. & Bramer, S. (2001). *Comparison of NONMEM, bootstrap, jeckknife and profiling parameter estimates and confidence intervals for the aripiprazole population PK model.* Paper presented the Annual Meeting of the American Association of Pharmaceutical Scientists, Denver, CO. Retrieved from http://www.aapsj.org/abstracts/AM_2001/ 1467.htm

Gibiansky, L., Gibiansky, E., & Bauer, R. (2012). Comparison of Nonmem 7.2 estimation methods and parallel processing efficiency on a target-mediated drug disposition model. *Journal of pharmacokinetics and pharmacodynamics*, 39(1), 17–35.

Giraud, E., Cloeckaert, A., Kerboeuf, D., & Chaslus-Dancla, E. (2000). Evidence for active efflux as the primary mechanism of resistance to ciprofloxacin in Salmonella enterica serovar typhimurium. *Antimicrobial Agents and Chemotherapy*, 44(5), 1223–1228.

Gisbert, S., Gueorguieva, I., Graham, G., & Aarons, L. (2002). *Incorporating uncertainty and variability in the physiological parameters of a PBPK model*. Poster presented at 11th Annual Meeting of the Population Approach Group in Europe (PAGE), Paris, France.

Gogos, C. A., Maraziotis, T. G., Papadakis, N., Beermann, D., Siamplis, D. K., & Bassaris, H. P. (1991). Penetration of ciprofloxacin into human cerebrospinal fluid in patients with inflamed and non-inflamed meninges. *European journal of clinical microbiology & infectious diseases : official publication of the European Society of Clinical Microbiology*, 10(6), 511–514.

Gollan, F. (1948). Blood and extracellular fluid studies in chronic malnutrition in infancy. *The Journal of clinical investigation*, 27(3 Pt 1), 352–363.

Gonzalez, M. A., Uribe, F., Moisen, S. D., Fuster, A. P., Selen, A., Welling, P. G., & Painter, B. (1984). Multiple-dose pharmacokinetics and safety of ciprofloxacin in normal volunteers. *Antimicrobial agents and chemotherapy*, 26(5), 741–744.

Gonzalez, M. A., Moranchel, A. H., Duran, S., Pichardo, A., Magana, J. L., Painter, B., Forrest, A., et al. (1985a). Multiple-dose pharmacokinetics of ciprofloxacin administered intravenously to normal volunteers. *Antimicrobial Agents and Chemotherapy*, 28(2), 235–239.

Gonzalez, M. A., Moranchel, A. H., Duran, S., Pichardo, A., Magana, J. L., Painter, B., & Drusano, G. L. (1985b). Multiple-dose ciprofloxacin dose ranging and kinetics. *Clinical Pharmacology & Therapeutics*, 37(6), 633-637.

Gordillo, G., Soto, R. A., Metcoff, J., Lopez, E., & Antillon, L. G. (1957). Intracellular composition and homeostatic mechanisms in severe chronic infantile malnutrition. III. Renal adjustments. *Pediatrics*, 20(2), 303–316.

Gould, I. M., Milne, K., & Jason, C. (1990). Concentration-dependent bacterial killing, adaptive resistance and post-antibiotic effect of ciprofloxacin alone and in combination with gentamicin. *Drugs under experimental and clinical research*, 16(12), 621–628.

Graf, J. F., Scholz, B. J., & Zavodszky, M. I. (2012). BioDMET: a physiologically based pharmacokinetic simulation tool for assessing proposed solutions to complex biological problems. *Journal of pharmacokinetics and pharmacodynamics*, 39(1), 37–54.

Grasela, T. H., & Sheiner, L. B. (1991). Pharmacostatistical modeling for observational data. *Journal of Pharmacokinetics and Biopharmaceutics*, 19(S3), 25S–36S.

Green, B., & Duffull, S. B. (2003). Prospective Evaluation of a D-Optimal Designed Population Pharmacokinetic Study. *Journal of Pharmacokinetics and Pharmacodynamics*, 30(2), 145–161.

Green, B., & Duffull, S. B. (2004). What is the best size descriptor to use for pharmacokinetic studies in the obese? *British journal of clinical pharmacology*, 58(2), 119–133.

Greer, J. P., Foerster, J., Rodgers, G. M., Paraskevas, F., Glader, B., Arber, D. A., & Means, R. T. (2009). *Wintrobe's Clinical Hematology* (12th ed.). Philadelphia, PA: Lippincott Williams & Wilkins Publishers.

Gueorguieva, I., Nestorov, I. A., Murby, S., Gisbert, S., Collins, B., Dickens, K., Duffy, J., et al. (2004). Development of a whole body physiologically based model to characterise the pharmacokinetics of benzodiazepines. 1: Estimation of rat tissue-plasma partition ratios. *Journal of pharmacokinetics and pharmacodynamics*, 31(4), 269–298.

Gueorguieva, I., Ogungbenro, K., Graham, G., Glatt, S., & Aarons, L. (2007). A program for individual and population optimal design for univariate and multivariate response pharmacokinetic-pharmacodynamic models. *Computer methods and programs in biomedicine*, 86(1), 51–61.

Gomez, F., Ramos Galvan, R., Frenk, S., Cravioto Muñoz, J., Chávez, R., & Vázquez, J. (1956). Mortality in second and third degree malnutrition. *Journal of Tropical Pediatrics*, 2(10), 77–83.

Hacker, M., Bachmann, K., & Messer, W. (2009). *Pharmacology: Principles and Practice*. San Diego, CA: Academic press.

Haddad, S., Restieri, C., & Krishnan, K. (2001). Characterization of age-related changes in body weight and organ weights from birth to adolescence in humans. *Journal of toxicology and environmental health. Part A*, 64(6), 453–464.

Hampel, B., Hullmann, R., & Schmidt, H. (1997). Ciprofloxacin in pediatrics: worldwide clinical experience based on compassionate use--safety report. *The Pediatric infectious disease journal*, 16(1), 127–129.

Hayton, W. L. (2000). Maturation and growth of renal function: dosing renally cleared drugs in children. *AAPS pharmSci*, 2(1), 1-7.

Hendricks, M. K., Van Der Bijl, P., Parkin, D. P., & Donald, P. R. (1995). Pharmacokinetics of amikacin in children with kwashiorkor. *Annals of tropical paediatrics*, 15(4), 295–298.

Hennig, S., Nyberg, J., Fanta, S., Backman, J.T., Hoppu, K., Hooker, A.C., & Karlsson, M.O. (2012). Application of the optimal design approach to improve a pretransplant drug dose finding design for ciclosporin. *Journal of Clinical Pharmacology*, 52(3), 347-360.

Hoffken, G., Lode, H., Prinzing, C., Borner, K., & Koeppe, P. (1985). Pharmacokinetics of ciprofloxacin after oral and parenteral administration. *Antimicrobial agents and chemotherapy*, 27(3), 375–379.

Holford, N. H. (1996). A size standard for pharmacokinetics. *Clinical pharmacokinetics*, 30(5), 329–332.

Honeybourne, D., Andrews, J. M., Ashby, J. P., Lodwick, R., & Wise, R. (1988). Evaluation of the penetration of ciprofloxacin and amoxycillin into the bronchial mucosa. *Thorax*, 43(9), 715–719.

Hooker, A. C., Staatz, C. E., & Karlsson, M. O. (2007). Conditional weighted residuals (CWRES): a model diagnostic for the FOCE method. *Pharmaceutical research*, 24(12), 2187–2197.

Houston, J. B., & Carlile, D. J. (1997). Prediction of hepatic clearance from microsomes, hepatocytes, and liver slices. *Drug metabolism reviews*, 29(4), 891–922.

Hua, M. J., Kun, H. Y., Jie, C. S., Yun, N. Z., De, W. Q., & Yang, Z. (1997). Urinary microalbumin and retinol-binding protein assay for verifying children's nephron development and maturation. *Clinica chimica acta; international journal of clinical chemistry*, 264(1), 127–132.

Höffler, D., Dalhoff, A., Gau, W., Beermann, D., & Michl, A. (1984). Dose- and sex-independent disposition of ciprofloxacin. *European Journal of Clinical Microbiology*, 3(4), 363–366.

ICRP. (2003). *Basic anatomical and physiological data for use in radiological protection: reference values*. ICRP Publication 89. *Annuals of the ICRP*. Amsterdam: Elsevier Science.

Israel, D. S., Stotka, J., Rock, W., Sintek, C. D., Kamada, A. K., Klein, C., Swaim, W. R., et al. (1996). Effect of ciprofloxacin on the pharmacokinetics and pharmacodynamics of warfarin. *Clinical Infectious Diseases*, 22(2), 251-256.

Ito, K., & Houston, J. B. (2005). Prediction of human drug clearance from in vitro and preclinical data using physiologically based and empirical approaches. *Pharmaceutical research*, 22(1), 103–112.

Jacoby, G. A. (2005). Mechanisms of resistance to quinolones. *Clinical Infectious Diseases*, *41 Suppl 2*, S120–S126.

Jaehde, U., Sörgel, F., Reiter, A., Sigl, G., Naber, K. G., & Schunack, W. (1995). Effect of probenecid on the distribution and elimination of ciprofloxacin in humans. *Clinical pharmacology and therapeutics*, 58(5), 532–541.

Jahoor, F., Badaloo, A., Reid, M., & Forrester, T. (2008). Protein metabolism in severe childhood malnutrition. *Annals of tropical paediatrics*, 28(2), 87–101.

Jamei, M., Turner, D., Yang, J., Neuhoff, S., Polak, S., Rostami-Hodjegan, A., & Tucker, G. (2009). Population-based mechanistic prediction of oral drug absorption. *The AAPS journal*, 11(2), 225–237.

Janknegt, R. (1990). Drug interactions with quinolones. *The Journal of antimicrobial chemotherapy*, 26 Suppl D, 7–29.

Jansson, R., Bredberg, U. L. F., & Ashton, M. (2008). Prediction of drug tissue to plasma concentration ratios using a measured volume of distribution in combination with lipophilicity. *Journal of pharmaceutical sciences*, 97(6), 2324-2339.

Johnson, T. N., Rostami-Hodjegan, A., & Tucker, G. T. (2006). Prediction of the clearance of eleven drugs and associated variability in neonates, infants and children. *Clinical pharmacokinetics*, 45(9), 931–956.

Jonsson, E. N., & Karlsson, M. O. (1998). Automated covariate model building within NONMEM. *Pharmaceutical research*, 15(9), 1463–1468.

Jonsson, E. N., & Karlsson, M. O. (1999). Xpose--an S-PLUS based population pharmacokinetic/pharmacodynamic model building aid for NONMEM. *Computer methods and programs in biomedicine*, 58(1), 51–64.

Josephson, B., & Gyllensward, C. (1957). The development of the protein fractions and of cholesterol concentration in the serum of normal infants and children. *Scandinavian journal of clinical and laboratory investigation*, 9(1), 29–38.

Kara, M., Hasinoff, B. B., McKay, D. W., & Campbell, N. R. (1991). Clinical and chemical interactions between iron preparations and ciprofloxacin. *British journal of clinical pharmacology*, 31(3), 257–261.

Karlsson, M. O., & Sheiner, L. B. (1993). The importance of modeling interoccasion variability in population pharmacokinetic analyses. *Journal of pharmacokinetics and biopharmaceutics*, 21(6), 735–750.

Karlsson, M. O., & Savic, R. M. (2007). Diagnosing model diagnostics. *Clinical pharmacology and therapeutics*, 82(1), 17–20.

Kato, M., Tachibana, T., Ito, K., & Sugiyama, Y. (2003). Evaluation of methods for predicting drug-drug interactions by Monte Carlo simulation. *Drug metabolism and pharmacokinetics*, 18(2), 121–127.

Kawai, R., Mathew, D., Tanaka, C., & Rowland, M. (1998). Physiologically based pharmacokinetics of cyclosporine A: extension to tissue distribution kinetics in rats and scale-up to human. *The Journal of pharmacology and experimental therapeutics*, 287(2), 457–468.

Kearns, G. L., Abdel-Rahman, S. M., Alander, S. W., Blowey, D. L., Leeder, J. S., & Kauffman, R. E. (2003). Developmental pharmacology--drug disposition, action, and therapy in infants and children. *The New England journal of medicine*, 349(12), 1157–1167.

Kersting, G., Willmann, S., Würthwein, G., Lippert, J., Boos, J., & Hempel, G. (2012). Physiologically based pharmacokinetic modelling of high- and low-dose etoposide: from adults to children. *Cancer chemotherapy and pharmacology*, 69(2), 397–405.

Khachman, D., Conil, J.-M., Georges, B., Saivin, S., Houin, G., Toutain, P.L., & Laffont, C. M. (2011). Optimizing ciprofloxacin dosing in intensive care unit patients through the use of population pharmacokinetic-pharmacodynamic analysis and Monte Carlo simulations. *The Journal of antimicrobial chemotherapy*, 66(8), 1798–1809.

Khalil, M., Awwad, H., & Hafez, M. (1969). Plasma and red cell iron turnover in protein calorie malnutrition. *Archives of disease in childhood*, 44(233), 124–130.

Kiefer, J., & Wolfowitz, J. (1959). Optimum Designs in Regression Problems. *The Annals of Mathematical Statistics*, 30(2), 271–294.

Klahr, S., & Tripathy, K. (1966). Evaluation of renal function in malnutrition. *Archives of internal medicine*, 118(4), 322–325.

Klahr, S., & Alleyne, G. A. (1973). Effects of chronic protein-calorie malnutrition on the kidney. *Kidney international*, 3(3), 129–141.

Knapp, E. L., & Routh, J. I. (1949). Electrophoretic studies of plasma proteins in normal children. *Pediatrics*, 4(4), 508–514.

Knupp, C. A., & Barbhaiya, R. H. (1997). A multiple-dose pharmacokinetic interaction study between didanosine (Videx) and ciprofloxacin (Cipro) in male subjects seropositive for HIV but asymptomatic. *Biopharmaceutics drug disposition*, 18(1), 65-77.

Ko, W.C., & Hsueh, P.R. (2009). Increasing extended-spectrum beta-lactamase production and quinolone resistance among Gram-negative bacilli causing intra-abdominal infections in the Asia/Pacific region: data from the Smart Study 2002-2006. *The Journal of infection*, 59(2), 95–103.

Kowalski, K. G., & Hutmacher, M. M. (2001). Efficient screening of covariates in population models using Wald's approximation to the likelihood ratio test. *Journal of pharmacokinetics and pharmacodynamics*, 28(3), 253–275.

Kraus, D. M., Fischer, J. H., Reitz, S. J., Kecskes, S. A., Yeh, T. F., McCulloch, K. M., Tung, E. C., et al. (1993). Alterations in theophylline metabolism during the first year of life. *Clinical pharmacology and therapeutics*, 54(4), 351–359.

Krewski, D., Wang, Y., Bartlett, S., & Krishnan, K. (1995). Uncertainty, variability, and sensitivity analysis in physiological pharmacokinetic models. *Journal of biopharmaceutical statistics*, 5(3), 245–271.

Lacy, M. K., Lu, W., Xu, X., Tessier, P. R., Nicolau, D. P., Quintiliani, R., & Nightingale, C. H. (1999). Pharmacodynamic comparisons of levofloxacin, ciprofloxacin, and ampicillin against Streptococcus pneumoniae in an in vitro model of infection. *Antimicrobial agents and chemotherapy*, 43(3), 672–677.

Lagneau, F., Marty, J., Beyne, P., & Tod, M. (2005). Physiological modeling for indirect evaluation of drug tissular pharmacokinetics under non-steady-state conditions: an example of antimicrobial prophylaxis during liver surgery. *Journal of pharmacokinetics and pharmacodynamics*, 32(1), 1–32.

Lares-Asseff, I., Cravioto, J., Santiago, P., & Pérez-Ortíz, B. (1992). Pharmacokinetics of metronidazole in severely malnourished and nutritionally rehabilitated children. *Clinical pharmacology and therapeutics*, 51(1), 42–50.

LeBel, M., Bergeron, M. G., Vallée, F., Fiset, C., Chassé, G., Bigonesse, P., & Rivard, G. (1986). Pharmacokinetics and pharmacodynamics of ciprofloxacin in cystic fibrosis patients. *Antimicrobial agents and chemotherapy*, 30(2), 260–266.

Ledergerber, B., Bettex, J. D., Joos, B., Flepp, M., & Lüthy, R. (1985). Effect of standard breakfast on drug absorption and multiple-dose pharmacokinetics of ciprofloxacin. *Antimicrobial agents and chemotherapy*, 27(3), 350–352.

Leo A, Hansch C, and E. D. (1971). partition coefficients and their uses. *Chemical Reviews*, 71(6), 525–616.

Li, X., Zhao, X., & Drlica, K. (2002). Selection of Streptococcus pneumoniae mutants having reduced susceptibility to moxifloxacin and levofloxacin. *Antimicrobial agents and chemotherapy*, 46(2), 522–524.

Lindbom, L., Ribbing, J., & Jonsson, E. N. (2004). Perl-speaks-NONMEM (PsN)--a Perl module for NONMEM related programming. *Computer methods and programs in biomedicine*, 75(2), 85–94.

Lindbom, L., Pihlgren, P., Jonsson, E. N., & Jonsson, N. (2005). PsN-Toolkit--a collection of computer intensive statistical methods for non-linear mixed effect modeling using NONMEM. *Computer methods and programs in biomedicine*, 79(3), 241–257.

Lindstedt, S. L., & Schaeffer, P. J. (2002). Use of allometry in predicting anatomical and physiological parameters of mammals. *Laboratory animals*, 36(1), 1–19.

Lipman, J., Scribante, J., Gous, A. G., Hon, H., & Tshukutsoane, S. (1998). Pharmacokinetic profiles of high-dose intravenous ciprofloxacin in severe sepsis. *Antimicrobial agents and chemotherapy*, 42(9), 2235–2239.

Lipman, J., Gous, A. G. S., Mathivha, L. R., Tshukutsoane, S., Scribante, J., Hon, H., Pinder, M., et al. (2002). Ciprofloxacin pharmacokinetic profiles in paediatric sepsis: how much ciprofloxacin is enough? *Intensive care medicine*, 28(4), 493–500.

Lipsky, B. A., & Baker, C. A. (1999). Fluoroquinolone toxicity profiles: a review focusing on newer agents. *Clinical Infectious Diseases*, 28(2), 352–364.

Lister, P D, & Sanders, C. C. (1999a). Pharmacodynamics of trovafloxacin, ofloxacin, and ciprofloxacin against Streptococcus pneumoniae in an in vitro pharmacokinetic model. *Antimicrobial agents and chemotherapy*, 43(5), 1118–1123.

Lister, P. D., & Sanders, C. C. (1999b). Pharmacodynamics of levofloxacin and ciprofloxacin against Streptococcus pneumoniae. *Journal of Antimicrobial Chemotherapy*, 43(1), 79–86.

Liu, X., Smith, B. J., Chen, C., Callegari, E., Becker, S. L., Chen, X., Cianfrogna, J., et al. (2005). Use of a physiologically based pharmacokinetic model to study the time to reach brain equilibrium: an experimental analysis of the role of blood-brain barrier permeability, plasma protein binding, and brain tissue binding. *The Journal of pharmacology and experimental therapeutics*, 313(3), 1254–1262.

MacGowan, A. P., White, L. O., Brown, N. M., Lovering, A. M., McMullin, C. M., & Reeves, D. S. (1994). Serum ciprofloxacin concentrations in patients with severe sepsis being treated with ciprofloxacin 200 mg i.v. bd irrespective of renal function. *Journal of Antimicrobial Chemotherapy*, 33(5), 1051–1054.

MacGowan, A., White, L., Reeves, D., & Harding, I. (1996). Retrospective review of serum teicoplanin concentrations in clinical trials and their relationship to clinical outcome. *Journal of Infection and Chemotherapy*, 2(4), 197–208.

Madaras-Kelly, K. J., Ostergaard, B. E., Hovde, L. B., & Rotschafer, J. C. (1996). Twenty-four-hour area under the concentration-time curve/MIC ratio as a generic predictor of fluoroquinolone antimicrobial effect by using three strains of Pseudomonas aeruginosa and an in vitro pharmacodynamic model. *Antimicrobial agents and chemotherapy*, 40(3), 627–632.

Madec, Y., Germanaud, D., Moya-Alvarez, V., Alkassoum, W., Issa, A., Amadou, M., Tchiombiano, S., et al. (2011). HIV prevalence and impact on renutrition in children hospitalised for severe malnutrition in Niger: an argument for more systematic screening. *PloS one*, 6(7), e22787.

Maitland, K., Berkley, J. A., Shebbe, M., Peshu, N., English, M., & Newton, C. R. J. C. (2006). Children with severe malnutrition: can those at highest risk of death be identified with the WHO protocol? *PLoS medicine*, 3(12), e500.

Mandema, J. W., Verotta, D., & Sheiner, L. B. (1992). Building population pharmacokinetic--pharmacodynamic models. I. Models for covariate effects. *Journal of pharmacokinetics and biopharmaceutics*, 20(5), 511–528.

Martínez-Martínez, L., Pascual, A., & Jacoby, G. A. (1998). Quinolone resistance from a transferable plasmid. *Lancet*, 351(9105), 797–799.

McNamara, P. J., & Alcorn, J. (2002). Protein binding predictions in infants. *AAPS pharmSci*, 4(1), 1-8.

Mehta, S., Kalsi, H. K., Jayaraman, S., & Mathur, V. S. (1975). Chloramphenicol metabolism in children with protein-calorie malnutrition. *The American journal of clinical nutrition*, 28(9), 977–981.

Mehta, S., Nain, C. K., Sharma, B., & Mathur, V. S. (1980). Metabolism of sulfadiazine in children with protein calorie malnutrition. *Pharmacology*, 21(6), 369–374.

Mehta, S., Nain, C. K., Yadav, D., Sharma, B., & Mathur, V. S. (1985). Disposition of acetaminophen in children with protein calorie malnutrition. *International journal of clinical pharmacology, therapy, and toxicology*, 23(6), 311–315.

Mei, Z., Grummer-Strawn, L. M., de Onis, M., & Yip, R. (1997). The development of a MUAC-for-height reference, including a comparison to other nutritional status screening indicators. *Bulletin of the World Health Organization*, 75(4), 333–341.

Meibohm, B., Läer, S., Panetta, J. C., & Barrett, J. S. (2005). Population pharmacokinetic studies in pediatrics: issues in design and analysis. *The AAPS journal*, 7(2), E475–E487.

Mentré, F. (1997). Optimal design in random-effects regression models. *Biometrika*, 84(2), 429–442.

Mentré, F., & Escolano, S. (2006). Prediction discrepancies for the evaluation of nonlinear mixed-effects models. *Journal of pharmacokinetics and pharmacodynamics*, 33(3), 345–367.

Mentré, F., Duffull, S., Gueorguieva, I., Hooker, A., Leonov, S., Ogungbenro, K., & Retout, S. (2007, June). *Software for optimal design in population pharmacokinetics and pharmacodynamics: a comparison*. Oral presented at the 16th of the Annual Meeting of the Population Approach Group in Europe (PAGE), København, Denmark.

Metcoff, J. (1967). Biochemical effects of protein-calorie malnutrition in man. *Annual review of medicine*, 18, 377–422.

Milavetz, G., Vaughan, L. M., Weinberger, M. M., & Hendeles, L. (1986). Evaluation of a scheme for establishing and maintaining dosage of theophylline in ambulatory patients with chronic asthma. *The Journal of pediatrics*, 109(2), 351–354.

Mirochnick, M., Capparelli, E., & Connor, J. (1999). Pharmacokinetics of zidovudine in infants: a population analysis across studies. *Clinical pharmacology and therapeutics*, 66(1), 16–24.

Montgomery, M. J., Beringer, P. M., Aminimanizani, A., Louie, S. G., Shapiro, B. J., Jelliffe, R., & Gill, M. A. (2001). Population pharmacokinetics and use of Monte Carlo simulation to evaluate currently recommended dosing regimens of ciprofloxacin in adult patients with cystic fibrosis. *Antimicrobial agents and chemotherapy*, 45(12), 3468–3473.

Mosteller, R. D. (1987). Simplified calculation of body-surface area. *The New England journal of medicine*, 317(17), 1098.

Muchohi, S. N., Thuo, N., Karisa, J., Muturi, A., Kokwaro, G. O., & Maitland, K. (2011). Determination of ciprofloxacin in human plasma using high-performance liquid chromatography coupled with fluorescence detection: application to a population pharmacokinetics study in children with severe malnutrition. *Journal of chromatography. B, Analytical technologies in the biomedical and life sciences*, 879(2), 146–152.

Myatt, M., Khara, T., & Collins, S. (2006). A review of methods to detect cases of severely malnourished children in the community for their admission into community-based therapeutic care programs. *Food and nutrition bulletin*, 27(3 Suppl), S7–S23.

National Health and Nutrition Examination Surveys (NHANES) (2008). Anthropometric Reference Data for Children and Adults: United States, 2003–2006. Retrieved from http://www.cdc.gov/nchs/data/nhsr/nhsr010.pdf

Nestorov, I. A., Aarons, L. J., Arundel, P. A., & Rowland, M. (1998a). Lumping of whole-body physiologically based pharmacokinetic models. *Journal of pharmacokinetics and biopharmaceutics*, 26(1), 21–46.

Nestorov, I. A., Aarons, L., & Rowland, M. (1998b). Quantitative structure-pharmacokinetics relationships: II. A mechanistically based model to evaluate the relationship between tissue distribution parameters and compound lipophilicity. *Journal of pharmacokinetics and biopharmaceutics*, 26(5), 521–545.

Nestorov, I. A. (1999). Sensitivity analysis of pharmacokinetic and pharmacodynamic systems: I. A structural approach to sensitivity analysis of physiologically based pharmacokinetic models. *Journal of pharmacokinetics and biopharmaceutics*, 27(6), 577–596.

Nestorov, I. A. (2003). Whole body pharmacokinetic models. *Clinical pharmacokinetics*, 42(10), 883–908.

Nestorov, I. A. (2007). Whole-body physiologically based pharmacokinetic models. *Expert opinion on drug metabolism & toxicology*, 3(2), 235–249.

Neuhauser, M. M., Weinstein, R. A., Rydman, R., Danziger, L. H., Karam, G., & Quinn, J. P. (2003). Antibiotic resistance among gram-negative bacilli in US intensive care units: implications for fluoroquinolone use. *JAMA*, 289(7), 885–888.

Neuvonen, P. J., Kivistö, K. T., & Lehto, P. (1991). Interference of dairy products with the absorption of ciprofloxacin. *Clinical pharmacology and therapeutics*, 50(5 Pt 1), 498–502.

Öcal, B., Unal, S., Zorlu, P., Tezic, H. T., & Oğuz, D. (2001). Echocardiographic evaluation of cardiac functions and left ventricular mass in children with malnutrition. *Journal of paediatrics and child health*, 37(1), 14–17.

Ogungbenro, K., Graham, G., Gueorguieva, I., & Aarons, L. (2005). The use of a modified Fedorov exchange algorithm to optimise sampling times for population pharmacokinetic experiments. *Computer methods and programs in biomedicine*, 80(2), 115–125.

Ogungbenro, K., Matthews, I., Looby, M., Kaiser, G., Graham, G., & Aarons, L. (2009). Population pharmacokinetics and optimal design of paediatric studies for famciclovir. *British journal of clinical pharmacology*, 68(4), 546–560.

Ogungbenro, K., Gueorgueiva, I., & Aarons, L. (2011). *PopDes manual*. Retrieved from http://www.pharmacy.manchester.ac.uk/capkr/popdes/PopDes_Manual_4.0.pdf

Oshikoya, K. A., & Senbanjo, I. O. (2009). Pathophysiological changes that affect drug disposition in protein-energy malnourished children. *Nutrition & metabolism*, 6(50), 1-7.

Oshikoya, K. A., Sammons, H. M., & Choonara, I. (2010). A systematic review of pharmacokinetics studies in children with protein-energy malnutrition. *European journal of clinical pharmacology*, 66(10), 1025–1035.

O'Reilly, C. E., Jaron, P., Ochieng, B., Nyaguara, A., Tate, J. E., Parsons, M. B., Bopp, C. A., et al. (2012). Risk Factors for Death among Children Less than 5 Years Old Hospitalized with Diarrhea in Rural Western Kenya, 2005-2007: A Cohort Study. *PLoS medicine*, 9(7), e1001256.

Pacifici, G. M., Taddeucci-Brunelli, G., & Rane, A. (1984). Clonazepam serum protein binding during development. *Clinical pharmacology and therapeutics*, 35(3), 354–359.

Pacifici, G. M., Viani, A., & Taddeucci-Brunelli, G. (1987). Serum protein binding of furosemide in newborn infants and children. *Developmental pharmacology and therapeutics*, 10(6), 413–421.

Paganini, H., Gómez, S., Ruvinsky, S., Zubizarreta, P., Latella, A., Fraquelli, L., Iturres, A. S., et al. (2003). Outpatient, sequential, parenteral-oral antibiotic therapy for lower risk febrile neutropenia in children with malignant disease: a single-center, randomized, controlled trial in Argentina. *Cancer*, 97(7), 1775-1780.

Pariente-Khayat, A., Tréluyer, J. M., Rey, E., Mokhtari, M., Werner, E., Jouvet, P., d'Athis, P., et al. (1999). Pharmacokinetics and tolerance of flunitrazepam in neonates and in infants. *Clinical pharmacology and therapeutics*, 66(2), 136–139.

Parry, M. F., Smego, D. A., & Digiovanni, M. A. (1988). Hepatobiliary kinetics and excretion of ciprofloxacin. *Antimicrobial Agents and Chemotherapy*, 32(7), 982–985.

Payen, S., Serreau, R., Munck, A., Aujard, Y., Aigrain, Y., Bressolle, F., & Jacqz-Aigrain, E. (2003). Population pharmacokinetics of ciprofloxacin in pediatric and adolescent patients with acute infections. *Antimicrobial agents and chemotherapy*, 47(10), 3170–3178.

Peltola, H., Väärälä, M., Renkonen, O. V, & Neuvonen, P. J. (1992). Pharmacokinetics of single-dose oral ciprofloxacin in infants and small children. *Antimicrobial agents and chemotherapy*, 36(5), 1086–1090.

Peltola, H., Ukkonen, P., Saxén, H., & Stass, H. (1998). Single-dose and steady-state pharmacokinetics of a new oral suspension of ciprofloxacin in children. *Pediatrics*, 101(4 Pt 1), 658–662.

Perry, C. M., Balfour, J. A., & Lamb, H. M. (1999). Gatifloxacin. *Drugs*, 58(4), 683–696.

Peters, R. H. (1986). *The Ecological Implications of Body Size (Cambridge Studies in Ecology)*. Cambridge: Cambridge University Press.

Peters, S. A. (2012). *Physiologically Based Pharmacokinetic (PBPK) Modeling and Simulations: Principles, Methods, and Applications in the Pharmaceutical Industry*. Hoboken, NJ: John Wiley & Sons.

Plaisance, K. I., Drusano, G. L., Forrest, A., Bustamante, C. I., & Standiford, H. C. (1987). Effect of dose size on bioavailability of ciprofloxacin. *Antimicrobial agents and chemotherapy*, 31(6), 956–958.

Plaisance, K. I., Drusano, G. L., Forrest, A., Weir, M. R., & Standiford, H. C. (1990). Effect of renal function on the bioavailability of ciprofloxacin. *Antimicrobial Agents and Chemotherapy*, 34(6), 1031–1034.

Polk, R. E., Healy, D. P., Sahai, J., Drwal, L., & Racht, E. (1989). Effect of ferrous sulfate and multivitamins with zinc on absorption of ciprofloxacin in normal volunteers. *Antimicrobial Agents and Chemotherapy*, 33(11), 1841–1844.

Polk, R. E., Johnson, C. K., McClish, D., Wenzel, R. P., & Edmond, M. B. (2004). Predicting hospital rates of fluoroquinolone-resistant Pseudomonas aeruginosa from fluoroquinolone use in US hospitals and their surrounding communities. *Clinical infectious diseases: an official publication of the Infectious Diseases Society of America*, 39(4), 497–503.

Poulin, P., & Theil, F. P. (2000). A priori prediction of tissue:plasma partition coefficients of drugs to facilitate the use of physiologically-based pharmacokinetic models in drug discovery. *Journal of pharmaceutical sciences*, 89(1), 16–35.

Poulin, P., Schoenlein, K., & Theil, F. P. (2001). Prediction of adipose tissue: plasma partition coefficients for structurally unrelated drugs. *Journal of pharmaceutical sciences*, 90(4), 436–447.

Poulin, P., & Theil, F.P. (2002). Prediction of pharmacokinetics prior to in vivo studies. 1. Mechanism-based prediction of volume of distribution. *Journal of pharmaceutical sciences*, 91(1), 129–156.

Poulin, P., & Theil, F. P. (2009). Development of a Novel Method for Predicting Human Volume of Distribution at Steady-State of Basic Drugs and Comparative Assessment With Existing Methods. *Journal of pharmaceutical science*, 98(12), 4941–4961.

Poulin, P., Ekins, S., & Theil, F. P. (2011). A hybrid approach to advancing quantitative prediction of tissue distribution of basic drugs in human. *Toxicology and applied pharmacology*, 250(2), 194–212.

Price, K., Haddad, S., & Krishnan, K. (2003). Physiological modeling of age-specific changes in the pharmacokinetics of organic chemicals in children. *Journal of toxicology and environmental health. Part A*, 66(5), 417–433.

Prost, M.A., Jahn, A., Floyd, S., Mvula, H., Mwaiyeghele, E., Mwinuka, V., Mhango, T., et al. (2008). Implication of new WHO growth standards on identification of risk factors and estimated prevalence of malnutrition in rural Malawian infants. *PloS one*, 3(7), e2684.

Pullman, T. N., Alving, A. S., Dern, R. J., & Landowne, M. (1954). The influence of dietary protein intake on specific renal functions in normal man. *The Journal of laboratory and clinical medicine*, 44(2), 320–332.

Radandt, J. M., Marchbanks, C. R., & Dudley, M. N. (1992). Interactions of fluoroquinolones with other drugs: mechanisms, variability, clinical significance, and management. *Clinical Infectious Diseases*, 14(1), 272–284.

Rajagopalan, P., & Gastonguay, M. R. (2003). Population pharmacokinetics of ciprofloxacin in pediatric patients. *Journal of clinical pharmacology*, 43(7), 698–710.

Rane, A., Lunde, P. K., Jalling, B., Yaffe, S. J., & Sjöqvist, F. (1971). Plasma protein binding of diphenylhydantoin in normal and hyperbilirubinemic infants. *The Journal of pediatrics*, 78(5), 877–882.

Reid, M, Badaloo, A., Forrester, T., Morlese, J. F., Frazer, M., Heird, W. C., & Jahoor, F. (2000). In vivo rates of erythrocyte glutathione synthesis in children with severe protein-energy malnutrition. *American journal of physiology. Endocrinology and metabolism*, 278(3), E405–E412.

Reid, Marvin, Badaloo, A., Forrester, T., Morlese, J. F., Heird, W. C., & Jahoor, F. (2002). The acute-phase protein response to infection in edematous and nonedematous protein-energy malnutrition. *The American journal of clinical nutrition*, 76(6), 1409–1415.

Ribbing, J., Nyberg, J., Caster, O., & Jonsson, E. N. (2007). The lasso--a novel method for predictive covariate model building in nonlinear mixed effects models. *Journal of pharmacokinetics and pharmacodynamics*, 34(4), 485–517.

Robson, R. A. (1992). The effects of quinolones on xanthine pharmacokinetics. *The American Journal of Medicine*, 92(4A), 22S–25S.

Rodgers, T., Leahy, D., & Rowland, M. (2005). Physiologically based pharmacokinetic modeling 1: predicting the tissue distribution of moderate-to-strong bases. *Journal of pharmaceutical sciences*, 94(6), 1259–1276.

Rodgers, T., & Rowland, M. (2006). Physiologically based pharmacokinetic modelling 2: predicting the tissue distribution of acids, very weak bases, neutrals and zwitterions. *Journal of pharmaceutical sciences*, 95(6), 1238–1257.

Rodgers, T., & Rowland, M. (2007). Mechanistic approaches to volume of distribution predictions: understanding the processes. *Pharmaceutical research*, 24(5), 918–933.

Rodvold, K. A. (2001). Pharmacodynamics of antiinfective therapy: taking what we know to the patient's bedside. *Pharmacotherapy*, 21(11 Pt 2), 319S–330S.

Rohwedder, R. W., Bergan, T., Thorsteinsson, S. B., & Scholl, H. (1990). Transintestinal elimination of ciprofloxacin. *Chemotherapy*, 36(2), 127–133.

Rolston, K. V. I., Frisbee-Hume, S., LeBlanc, B., Streeter, H., & Ho, D. H. (2003). In vitro antimicrobial activity of moxifloxacin compared to other quinolones against recent clinical bacterial isolates from hospitalized and community-based cancer patients. *Diagnostic Microbiology and Infectious Disease*, 2(2), 13S–20S.

Roos, J. F., Kirkpatrick, C. M. J., Tett, S. E., McLachlan, A. J., & Duffull, S. B. (2008). Development of a sufficient design for estimation of fluconazole pharmacokinetics in people with HIV infection. *British journal of clinical pharmacology*, 66(4), 455–466.

Rosenson, R. S., McCormick, A., & Uretz, E. F. (1996). Distribution of blood viscosity values and biochemical correlates in healthy adults. *Clinical chemistry*, 42(8 Pt 1), 1189–1195.

Ross, D. L., Elkinton, S. K., & Riley, C. M. (1992). Physicochemical properties of the fluoroquinolone antimicrobials. III. 1-Octanol/water partition coefficients and their relationships to structure. *International Journal of Pharmaceutics*, 88(1-3), 379–389.

Rowland, M. & Tozer, T. N. (1995). Clinical Pharmacokinetics: Concepts and Applications (3rd ed.). Media, PA: Williams & Wilkins.

Rowland, M., Peck, C., & Tucker, G. (2011). Physiologically-based pharmacokinetics in drug development and regulatory science. *Annual review of pharmacology and toxicology*, 51, 45–73.

Rubio, T. T., Miles, M. V, Lettieri, J. T., Kuhn, R. J., Echols, R. M., & Church, D. A. (1997). Pharmacokinetic disposition of sequential intravenous/oral ciprofloxacin in pediatric cystic fibrosis patients with acute pulmonary exacerbation. *The Pediatric infectious disease journal*, 16(1), 112–117.

Ruiz, J. (2003). Mechanisms of resistance to quinolones: target alterations, decreased accumulation and DNA gyrase protection. *Antimicrobial agents and chemotherapy*, 51(5), 1109–1117.

Russell, S. J. M. (1949). Blood volume studies in healthy children. *Archives of disease in childhood*, 24(118), 88–98.

Salako, L. A., Sowunmi, A., & Akinbami, F. O. (1989). Pharmacokinetics of quinine in African children suffering from kwashiorkor. *British journal of clinical pharmacology*, 28(2), 197–201.

Samotra, K., Gupte, S., & Raina, R. K. (1985). Pharmacokinetics of gentamicin in protein-energy malnutrition. *European journal of clinical pharmacology*, 29(2), 255–256.

Savic, R. M., Jonker, D. M., Kerbusch, T., & Karlsson, M. O. (2007). Implementation of a transit compartment model for describing drug absorption in pharmacokinetic studies. *Journal of pharmacokinetics and pharmacodynamics*, 34(5), 711–726.

Savic, R. M., & Karlsson, M. O. (2009). Importance of shrinkage in empirical bayes estimates for diagnostics: problems and solutions. *The AAPS journal*, 11(3), 558–569.

Schaefer, H. G., Stass, H., Wedgwood, J., Hampel, B., Fischer, C., Kuhlmann, J., & Schaad, U. B. (1996). Pharmacokinetics of ciprofloxacin in pediatric cystic fibrosis patients. *Antimicrobial agents and chemotherapy*, 40(1), 29–34.

Schlenkhoff, D., Dalhoff, A., Knopf, J., & Opferkuch, W. (1986). Penetration of ciprofloxacin into human lung tissue following intravenous injection. *Infection*, 14(6), 299–300.

Schwartz, G. J., Haycock, G. B., Edelmann, C. M., & Spitzer, A. (1976). A simple estimate of glomerular filtration rate in children derived from body length and plasma creatinine. *Pediatrics*, 58(2), 259–263.

Schwartz, G. J., Feld, L. G., & Langford, D. J. (1984). A simple estimate of glomerular filtration rate in full-term infants during the first year of life. *The Journal of pediatrics*, 104(6), 849–854.

Schwartz, G. J., & Gauthier, B. (1985). A simple estimate of glomerular filtration rate in adolescent boys. *The Journal of pediatrics*, 106(3), 522–526.

Scott, C. S., Riggs, K. W., Ling, E. W., Fitzgerald, C. E., Hill, M. L., Grunau, R. V, Solimano, A., et al. (1999). Morphine pharmacokinetics and pain assessment in premature newborns. *The Journal of pediatrics*, 135(4), 423–429.

Seal, A., & Kerac, M. (2007). Operational implications of using 2006 World Health Organization growth standards in nutrition programmes: secondary data analysis. *BMJ*, 334(7596), 733.

Seaton, C., Ignas, J., Muchohi, S., Kokwaro, G., Maitland, K., & Thomson, A. H. (2007). Population pharmacokinetics of a single daily intramuscular dose of gentamicin in children with severe malnutrition. *The Journal of antimicrobial chemotherapy*, 59(4), 681–689.

Sendzik, J., Lode, H., & Stahlmann, R. (2009). Quinolone-induced arthropathy: an update focusing on new mechanistic and clinical data. *International Journal of Antimicrobial Agents*, 33(3), 194–200.

Shah, A., Lettieri, J., Kaiser, L., Echols, R., & Heller, A. H. (1994). Comparative pharmacokinetics and safety of ciprofloxacin 400 mg i.v. thrice daily versus 750 mg po twice daily. *Journal of Antimicrobial Chemotherapy*, 33(4), 795–801.

Shah, A., Liu, M. C., Vaughan, D., & Heller, A. H. (1999). Oral bioequivalence of three ciprofloxacin formulations following single-dose administration: 500 mg tablet compared with 500 mg/10 mL or 500 mg/5 mL suspension and the effect of food on the absorption of ciprofloxacin oral suspension. *The Journal of antimicrobial chemotherapy*, *43 Suppl A*, 49–54.

Sheiner, L. B., Rosenberg, B., & Marathe, V. V. (1977). Estimation of population characteristics of pharmacokinetic parameters from routine clinical data. *Journal of pharmacokinetics and biopharmaceutics*, 5(5), 445–479.

Sheiner, L. B., & Beal, S. L. (1981). Some suggestions for measuring predictive performance. *Journal of pharmacokinetics and biopharmaceutics*, 9(4), 503–512.

Shibata, N., Gao, W., Okamoto, H., Kishida, T., Iwasaki, K., Yoshikawa, Y., & Takada, K. (2002). Drug interactions between HIV protease inhibitors based on physiologically-based pharmacokinetic model. *Journal of pharmaceutical sciences*, 91(3), 680–689.

Sholler, G. F., Celermajer, J. M., Whight, C. M., & Bauman, A. E. (1987). Echo Doppler assessment of cardiac output and its relation to growth in normal infants. *The American Journal of Cardiology*, 60(13), 1112–1116.

Sherwin, C. M., Ding, L., Kaplan, J., Spigarelli, M. G., & Vinks, A. A. (2011) Optimal study design for pioglitazone in septic pediatric patients. *Journal of pharmacokinetics and pharmacodynamics*, 38(4), 433-447.

Silverman, S. H., Johnson, M., Burdon, D. W., & Keighley, M. R. (1986). Pharmacokinetics of single dose intravenous ciprofloxacin in patients undergoing gastrointestinal surgery. *Journal of antimicrobial chemotherapy*, 18(1), 107–112.

Silverman, W. A., Andersen, D. H., Blanc, W. A., & Crozier, D. N. (1956). A Difference in mortality rate and incidence of kernicterus among premature infants allotted to two prophylactic antibacterial regimens. *Pediatrics*, 18(4), 614–625.

Simmons, J. E., Evans, M. V, & Boyes, W. K. (2005). Moving from external exposure concentration to internal dose: duration extrapolation based on physiologically based pharmacokinetic derived estimates of internal dose. *Journal of toxicology and environmental health. Part A*, 68(11-12), 927–950.

Singh, B. N. (2005). A quantitative approach to probe the dependence and correlation of food-effect with aqueous solubility, dose/solubility ratio, and partition coefficient (LogP) for orally active drugs administered as immediate-release formulations. *Drug Development Research*, 65(2), 55–75.

Smith, K. (1918). On the standard deviations of adjusted and interpolated values of an observed polynomial function and its constants and the guidance they give towards a proper choice of the distribution of observations. *Biometrika*, 12(1-2), 1–85.

Sonnier, M., & Cresteil, T. (1998). Delayed ontogenesis of CYP1A2 in the human liver. *European Journal of Biochemistry*, 251(3), 893–898.

Stahlmann, R., & Schwabe, R. (1997). Safety profile of grepafloxacin compared with other fluoroquinolones. *The Journal of antimicrobial chemotherapy*, 40 Suppl A, 83–92.

Stein, G. E. (1988). The 4-quinolone antibiotics: past, present, and future. *Pharmacotherapy*, 8(6), 301–314.

Stewart, C. F., & Hampton, E. M. (1987). Effect of maturation on drug disposition in pediatric patients. *Clinical pharmacy*, 6(7), 548–64.

Strolin Benedetti, M., & Baltes, E. L. (2003). Drug metabolism and disposition in children. *Fundamental & clinical pharmacology*, 17(3), 281–299.

Ståhlberg, M. R., Hietanen, E., & Mäki, M. (1988). Mucosal biotransformation rates in the small intestine of children. *Gut*, 29(8), 1058–1063.

Sun, H., Fadiran, E. O., Jones, C. D., Lesko, L., Huang, S. M., Higgins, K., Hu, C., et al. (1999). Population pharmacokinetics. A regulatory perspective. *Clinical pharmacokinetics*, 37(1), 41–58.

Takei, M., Fukuda, H., Kishii, R., & Hosaka, M. (2001). Target preference of 15 quinolones against Staphylococcus aureus, based on antibacterial activities and target inhibition. *Antimicrobial Agents and Chemotherapy*, 45(12), 3544–3547.

Takács-Novák, K., Józan, M., Hermecz, I., & Szász, G. (1992). Lipophilicity of antibacterial fluoroquinolones. *International Journal of Pharmaceutics*, 79(1-3), 89–96.

Tam, V. H., Louie, A., Fritsche, T. R., Deziel, M., Liu, W., Brown, D. L., Deshpande, L., et al. (2007). Impact of drug-exposure intensity and duration of therapy on the emergence of Staphylococcus aureus resistance to a quinolone antimicrobial. *The Journal of Infectious Diseases*, 195(12), 1818–1827.

Tanaka, C., Kawai, R., & Rowland, M. (1999). Physiologically based pharmacokinetics of cyclosporine A: reevaluation of dose-nonlinear kinetics in rats. *Journal of pharmacokinetics and biopharmaceutics*, 27(6), 597–623.

Tartaglione, T. A., Raffalovich, A. C., Poynor, W. J., Espinel-Ingroff, A., & Kerkering, T. M. (1986). Pharmacokinetics and tolerance of ciprofloxacin after sequential increasing oral doses. *Antimicrobial agents and chemotherapy*, 29(1), 62–66.

Teorell T. (1937). Kinetics of distribution of substances administered to the body. I. The extravascular modes of administration. *Archives Internationales de Pharmacodynamie et de Therapie*, 57, 202–205.

The Wellome Trust Working Party. (1970). Classification of infantile malnutrition. *Lancet*, 2(7667), 302–303.

Thompson, C. M., Sonawane, B., Barton, H. A., DeWoskin, R. S., Lipscomb, J. C., Schlosser, P., Chiu, W. A., et al. (2008). Approaches for applications of physiologically based pharmacokinetic models in risk assessment. *Journal of toxicology and environmental health. Part B, Critical reviews*, 11(7), 519–547.

Tod, M., Mentré, F., Merlé, Y., & Mallet, a. (1998). Robust optimal design for the estimation of hyperparameters in population pharmacokinetics. *Journal of pharmacokinetics and biopharmaceutics*, 26(6), 689–716.

Tran, J. H., Jacoby, G. A., & Hooper, D. C. (2005). Interaction of the plasmid-encoded quinolone resistance protein QnrA with Escherichia coli topoisomerase IV. *Antimicrobial Agents and Chemotherapy*, 49(7), 3050–3052.

Uchimura, T., Kato, M., Saito, T., & Kinoshita, H. (2010). Prediction of human blood-to-plasma drug concentration ratio. *Biopharmaceutics & drug disposition*, 31(5-6), 286–297.

Ullmann, U., Giebel, W., Dalhoff, A., & Koeppe, P. (1986). Single and multiple dose pharmacokinetics of ciprofloxacin. *European Journal of Clinical Microbiology*, 5(2), 193–196.

van Zanten, A. R. H., Polderman, K. H., van Geijlswijk, I. M., van der Meer, G. Y. G., Schouten, M. A., & Girbes, A. R. J. (2008). Ciprofloxacin pharmacokinetics in critically ill patients: a prospective cohort study. *Journal of critical care*, 23(3), 422–430.

Vance-Bryan, K., Guay, D. R., & Rotschafer, J. C. (1990). Clinical pharmacokinetics of ciprofloxacin. *Clinical Pharmacokinetics*, 19(6), 434–461.

Vidal, L., Shavit, M., Fraser, A., Paul, M., & Leibovici, L. (2005). Systematic comparison of four sources of drug information regarding adjustment of dose for renal function. *BMJ*, 331(7511), 263.

Vinks, A. A. (2002). The application of population pharmacokinetic modeling to individualized antibiotic therapy. *International journal of antimicrobial agents*, 19(4), 313–322.

Wald, A. (1943). On the Efficient Design of Statistical Investigations. *The Annals of Mathematical Statistics*, 14(2), 134–140.

Walker, O., Dawodu, A. H., Salako, L. A., Alván, G., & Johnson, A. O. (1987). Single dose disposition of chloroquine in kwashiorkor and normal children--evidence for decreased absorption in kwashiorkor. *British journal of clinical pharmacology*, 23(4), 467–472.

Wang, J. C. (1996). DNA topoisomerases. *Annual review of biochemistry*, 65, 635–692.

Waterhouse, T. H., Redmann, S., Duffull, S. B., & Eccleston, J. A. (2005). Optimal design for model discrimination and parameter estimation for itraconazole population pharmacokinetics in cystic fibrosis patients. *Journal of pharmacokinetics and pharmacodynamics*, 32(3-4), 521–545.

Waterlow, J. C. (1973). Note on the assessment and classification of protein-energy malnutrition in children. *Lancet*, 2(7820), 87–89.

Waterlow, J. C. (2006). *Protein-Energy Malnutrition*. London: Smith-Gordon.

Webb, D. B., Roberts, D. E., Williams, J. D., & Asscher, A. W. (1986). Pharmacokinetics of ciprofloxacin in healthy volunteers and patients with impaired kidney function. *The Journal of antimicrobial chemotherapy*, 18 suppl D, 83–87.

Were, T., Davenport, G. C., Hittner, J. B., Ouma, C., Vulule, J. M., Ong'echa, J. M., & Perkins, D. J. (2011). Bacteremia in Kenyan children presenting with malaria. *Journal of clinical microbiology*, 49(2), 671–676.

White, D. L., Li, D., Nurgalieva, Z., & El-Serag, H. B. (2008). Genetic variants of glutathione S-transferase as possible risk factors for hepatocellular carcinoma: a HuGE systematic review and meta-analysis. *American journal of epidemiology*, 167(4), 377–389.

WHO. (1999). *Management of Severe Malnutrition: A Manual for Physicians and Other Senior Health Workers*. Retrieved from http://www.who.int/nutrition/publications/severemalnutrition/en/manage_severe_malnutrition_eng.pdf

WHO Multicentre Growth Reference Study Group. (2006). WHO Child Growth Standards based on length/height, weight and age. *Acta paediatrica (Oslo, Norway : 1992). Supplement*, 450, 76–85.

WHO Global Database on Child Growth and Malnutrition (2012). Retrieved from http://www.who.int/nutgrowthdb/en/

Willmott, C. J., & Maxwell, A. (1993). A single point mutation in the DNA gyrase A protein greatly reduces binding of fluoroquinolones to the gyrase-DNA complex. *Antimicrobial Agents and Chemotherapy*, 37(1), 126–127.

Wingender, W., Graefe, K. H., Gau, W., Forster, D., Beermann, D., & Schacht, P. (1984). Pharmacokinetics of ciprofloxacin after oral and intravenous administration in healthy volunteers. *European Journal of Clinical Microbiology*, 3(4), 355–359.

Wintermark, M., Lepori, D., Cotting, J., Roulet, E., van Melle, G., Meuli, R., Maeder, P., et al. (2004). Brain perfusion in children: evolution with age assessed by quantitative perfusion computed tomography. *Pediatrics*, 113(6), 1642–1652.

Wise, R., Lockley, R. M., Webberly, M., & Dent, J. (1984). Pharmacokinetics of intravenously administered ciprofloxacin *Antimicrobial agents and chemotherapy*, 26(2), 208–210.

Wolff, M., Boutron, L., Singlas, E., Clair, B., Decazes, J. M., & Regnier, B. (1987). Penetration of ciprofloxacin into cerebrospinal fluid of patients with bacterial meningitis. *Antimicrobial agents and chemotherapy*, 31(6), 899–902.

Wolfson, J. S., & Hooper, D. C. (1989). Fluoroquinolone antimicrobial agents. *Clinical Microbiology Reviews*, 2(4), 378–424.

Woodnutt, G., & Berry, V. (1999). Two pharmacodynamic models for assessing the efficacy of amoxicillin-clavulanate against experimental respiratory tract infections caused by strains of Streptococcus pneumoniae. *Antimicrobial agents and chemotherapy*, 43(1), 29–34.

Wählby, U., Jonsson, E. N., & Karlsson, M. O. (2001). Assessment of actual significance levels for covariate effects in NONMEM. *Journal of pharmacokinetics and pharmacodynamics*, 28(3), 231–252.

Xu, L., Eiseman, J. L., Egorin, M. J., & D'Argenio, D. Z. (2003). Physiologically-based pharmacokinetics and molecular pharmacodynamics of 17-(allylamino)-17-demethoxygeldanamycin and its active metabolite in tumor-bearing mice. *Journal of pharmacokinetics and pharmacodynamics*, 30(3), 185–219.

Yang, F., Tong, X., McCarver, D. G., Hines, R. N., & Beard, D. A. (2006). Population-based analysis of methadone distribution and metabolism using an age-dependent physiologically based pharmacokinetic model. *Journal of pharmacokinetics and pharmacodynamics*, 33(4), 485–518

Yang, J., Jamei, M., Yeo, K. R., Rostami-Hodjegan, A., & Tucker, G. T. (2007). Misuse of the well-stirred model of hepatic drug clearance. *Drug metabolism and disposition: the biological fate of chemicals*, 35(3), 501–502.

Yee, C. L., Duffy, C., Gerbino, P. G., Stryker, S., & Noel, G. J. (2002). Tendon or joint disorders in children after treatment with fluoroquinolones or azithromycin. *The Pediatric infectious disease journal*, 21(6), 525–529.

Yokoi, T. (2009). Essentials for starting a pediatric clinical study (1): Pharmacokinetics in children. *The Journal of toxicological sciences*, 34 Suppl 2, SP307–SP312.

Yoshida, H., Bogaki, M., Nakamura, M., Yamanaka, L. M., & Nakamura, S. (1991). Quinolone resistance-determining region in the DNA gyrase gyrB gene of Escherichia coli. *Antimicrobial Agents and Chemotherapy*, 35(6), 1647–1650.

Young, J. F., Luecke, R. H., Pearce, B. A., Lee, T., Ahn, H., Baek, S., Moon, H., et al. (2009). Human organ/tissue growth algorithms that include obese individuals and black/white population organ weight similarities from autopsy data. *Journal of toxicology and environmental health. Part A*, 72(8), 527–540.

Yu, L. X., & Amidon, G. L. (1999). A compartmental absorption and transit model for estimating oral drug absorption. *International journal of pharmaceutics*, 186(2), 119–125.

Yuk, J. H., Nightingale, C. H., Sweeney, K. R., Quintiliani, R., Lettieri, J. T., & Frost, R. W. (1989). Relative bioavailability in healthy volunteers of ciprofloxacin administered through a nasogastric tube with and without enteral feeding. *Antimicrobial agents and chemotherapy*, 33(7), 1118–1120.

APPENDICES

Appendix I: Modified scripts of PopDes program used to account for the covariates in the model

Code 1: PopDes.m file

```
%% Covariates (No covariate Cov=[])
nsim_cov=25;

%% (1) WT
WTlb=4.1;
WTub=14.5;
xx = lhsdesign(nsim_cov,1);
WT = WTlb + (WTub-WTlb)*xx;

%% (2) Na conc
Naconclb=120;
Naconcub=160;
Naconc = Naconclb + (Naconcub-Naconclb)*xx;

%% (3) Mort
Mort_prob=0.31;
% Mort = binornd(1,Mort_prob,[nsim_cov,1]);

for ij=1:nsim_cov
    if xx(ij) > Mort_prob
        Mort(ij)=0;
    else
        Mort(ij)=1;
    end
end
Mort=Mort';

Cov=[WT Naconc Mort];
```

Code 2: ext_model.m file

```
%% Covariates
WT=Cov(1);
Naconc=Cov(2);
Mort=Cov(3);

%% Parameters and other variables
Dose=D(idose)*WT;
di=Di(idose);

ka=THETA(1)*exp(ETA(1));
cl=(THETA(2)*((WT/70)^0.75)*(1+THETA(5)*(Naconc-136))*(1+THETA(6)*Mort))
*exp(ETA(2));
v=(THETA(3)*(WT/70)^1*(1+THETA(7)*(Naconc-136)))*exp(ETA(3));
lag=THETA(4);

for i=1:length(TT)
    nd=0;
    ff=0;
    hh=0;
    while TT(i) > hh
        nd=nd+1;        % calculate number of doses
        ta=TT(i)-hh;

        if ta <= lag
            f1=0;
        else
            f1=(Dose*ka/(v*ka-cl))*(exp(-cl*(ta-lag)/v)-exp(-ka*(ta-lag)));
        end
        ff=ff+f1;
        hh=hh+di;
    end
    f(i)=ff;
end
f;
```

Appendix II: MATLAB codes used for simulating concentration-time profile in malnourished children aged 2 years

Code 1: BWdis.m file

```
%% Lognormal distribution
% m=0.39; %mean of lognormal distribution
% sd=0.3*m; %sd of lognormal distribution
% v=sd^2;
% mu = log((m^2)/sqrt(v+m^2)); %parameter MU
% sigma = sqrt(log(v/(m^2)+1)); %parameter SIGMA
% x = lognrnd(mu,sigma,1000,1);

% x=normrnd(m,sd,1000,1);
% Trunctated normal distribution
m=1000;
mu=0.39;
sigma=0.3*mu;
x=normrnd(mu,sigma,1000,1);
xTrunc=1;
x=x(x<xTrunc);
xTrunc2=0;
x(x<xTrunc2)=[];
start=[mean(x),std(x)];
pdf_truncnorm=@(x,mu,sigma)normpdf(x,mu,sigma)./(normcdf(xTrunc,mu,sigma)-
normcdf(xTrunc2,mu,sigma));
[paramEsts,paramCIs]=mle(x,'pdf',pdf_truncnorm,'start',start,'lower',[-Inf
0])

% X=normrnd(m,sd,1000,1);
% figure;
histfit(x);
skewness(x)
```

Code 2: ciprofloxacin.m file

```
function Ciprofloxacin
tic
n_param=75;
p=[];
Concsim=[];
K1=[];
K2=[];
K3=[];
K4=[];
K5=[];
K6=[];
K7=[];
K8=[];
K9=[];
K10=[];
K11=[];
K12=[];
K13=[];
K14=[];
Vad=[];
Qad=[];
t=[];

%% Mean and variance for organ volumes
%venous,lungs,arterial,liver,gut,spleen,kidney,muscle,adipose,skin,heart,bra
in,bone
% Male volume (%CV=20)
mean=[1.1367,0.1739,0.5684,0.4479,0.2128,0.0405,0.0857,2.7185,3.9328,0.3981,
0.0833,1.0783,0.4250];
var=[0.06482210855165020000 0.00691576314156197000  0.02183040583176030000
0.01736016061873680000  0.00842625636949377000  0.00163474593911444000
0.00344305396558435000  0.09950450568867420000  0.14615383303435500000
0.01549549834571710000  0.00334708016009699000  0.04029516064647930000
0.01650334565577190000
0.00691576314156197000  0.00127329316228680000  0.00360044865421591000
0.00287029960763607000  0.00140026864600248000  0.00027272775026738700
0.00057381026104437300  0.01585584498033730000  0.02297266732385080000
0.00256468578218948000  0.00055784648880660000  0.00658143079776849000
0.00272994731080860000
0.02183040583176030000  0.00360044865421591000  0.01488028156557260000
0.00900778189354282000  0.00438468729764304000  0.00085253869750137700
0.00179453192016534000  0.05057906439056490000  0.07373274625723280000
0.00804499100235702000  0.00174456466313488000  0.02076549862923640000
0.00856551516285766000
0.01736016061873680000  0.00287029960763607000  0.00900778189354282000
0.00901999729722708000  0.00349510764087085000  0.00067991658673648500
0.00143098177640442000  0.04009844229236320000  0.05834995953098610000
0.00640946470085042000  0.00139114723267087000  0.01651554786839280000
0.00682366748822325000
0.00842625636949377000  0.00140026864600248000  0.00438468729764304000
0.00349510764087085000  0.00192572867536575000  0.00033196122563560100
0.00069846824351309100  0.01934006892304910000  0.02803880308378860000
0.00312282022273679000  0.00067903471931267700  0.00801852007472496000
0.00332413138082000000
0.00163474593911444000  0.00027272775026738700  0.00085253869750137800
0.00067991658673648500  0.00033196122563560100  0.00006635491736618740
0.00013609440136494800  0.00373359137047424000  0.00539708163143716000
0.00060762346792476200  0.00013230931872545000  0.00155597700167120000
0.00064671911111676200
0.00344305396558435000  0.00057381026104437300  0.00179453192016534000
0.00143098177640442000  0.00069846824351309100  0.00013609440136494800
0.00030170940422235700  0.00787400123561411000  0.01139117937871500000
```

```
0.0012787578948378300  0.0002783436349569420  0.0032769647821176600
0.0013610774458522100
0.0995045056886742000  0.0158558449803373000  0.0505790643905649000
0.0400984422923632000  0.0193400689230491000  0.0037335913704742400
0.0078740012356141100  0.4074760607698872000  0.3582585669965040000
0.0357448693894095000  0.0076539794682346400  0.0944765458277765000
0.0380966221582186000
0.1461538330343550000  0.0229726673238508000  0.0737327462572328000
0.0583499595309861000  0.0280388030837886000  0.0053970816314371600
0.0113911793787150000  0.3582585669965040000  0.8553035880386760000
0.0519752612648505000  0.0110724176026790000  0.1386694308377370000
0.0554176732762600000
0.0154954983457171000  0.0025646857821894800  0.0080449910023570200
0.0064094647008504200  0.0031228202227367900  0.0006076234679247620
0.0012787578948378300  0.0357448693894095000  0.0519752612648505000
0.0070512263636424900  0.0012431645870723300  0.0147424478066891000
0.0060953091852504100
0.0033470801600969900  0.0005578464888066000  0.0017445646631348800
0.0013911472326708700  0.0006790347193126770  0.0001323093187254500
0.0002783436349569420  0.0076539794682346400  0.0110724176026790000
0.0012431645870723300  0.0002847564501176290  0.0031856303554968000
0.0013231906741516900
0.0402951606464793000  0.0065814307977684900  0.0207654986292364000
0.0165155478683928000  0.0080185200747249600  0.0015559770016712000
0.0032769647821176600  0.0944765458277765000  0.1386694308377370000
0.0147424478066891000  0.0031856303554968000  0.0579190097144506000
0.0157008302229346000
0.0165033456557719000  0.0027299473108086000  0.0085655151628576600
0.0068236674882232500  0.0033241313808200000  0.0006467191111167620
0.0013610774458522100  0.0380966221582186000  0.0554176732762600000
0.0060953091852504100  0.0013231906741516900  0.0157008302229346000
0.0080815985668408000];

%venous,lungs,arterial,liver,gut,spleen,kidney,muscle,adipose,skin,heart,bra
in,bone
% Female volume (%CV=20)
%mean=[1.2566,0.1739,0.6283,0.4149,0.2143,0.0361,0.0873,2.7185,3.8960,0.3845
,0.0683,0.9602,0.41];
% var=[0.080389389016047000000   0.00759095522862768000
0.0264027457205114000  0.0177068091944353000  0.0093148532469163200
0.0016024485373488800  0.0038492688380417900  0.1097403101869360000
0.1598576915791730000  0.0164522265138477000  0.0030193531075243300
0.0396435211266906000  0.0175046984980640000
% 0.00759095522862768000    0.00127385092388430000  0.0039560469070345200
0.0026661902864792400  0.0014094429269466300  0.0002435768680419320
0.0005843207308172600  0.0158429359981125000  0.0227381785073122000
0.0024790736956355100  0.0004585647407298010  0.0058976316088566800
0.0026360640491970200
% 0.02640274572051140000    0.00395604690703452000  0.0184076234467615000
0.0091980999906567700  0.0048517521497231600  0.0008367520358788950
0.0020085010349789000  0.0557172098884055000  0.0805190449350990000
0.0085497764742344500  0.0015758882277350100  0.0204578502559482000
0.0090936902103884300
% 0.01770680919443530000    0.00266619028647924000  0.0091980999906567700
0.0076919292077801400  0.0032691722983334000  0.0005643420746121780
0.0013542503749217900  0.0371799739686763000  0.0535639929647949000
0.0057560251112726400  0.0010626644633742900  0.0137367037129308000
0.0061214442595598200
% 0.00931485324691632000    0.00140944292694663000  0.0048517521497231600
0.0032691722983334000  0.0019554320422383900  0.0002985453636539510
0.0007162255702854180  0.0194612165452454000  0.0279495887957395000
0.0030396449316585200  0.0005620697784518880  0.0072351421910447800
0.0032322168869043000
% 0.00160244853734888000    0.00024357686804193100  0.0008367520358788950
0.0005643420746121780  0.0002985453636539510  0.0000528225634138852O
```

```
0.00012382806428363600  0.00333217221545134000  0.00477135622605706000
0.00052479169660924400  0.00009718508771753840  0.00124609390723684000
0.00055797492754462000
% 0.00384926883804179000    0.00058432073081726000  0.00200850103497890000
0.00135425037492179000  0.00071622557028541800  0.00012382806428363600
0.00031343793343460700  0.00801535877256463000  0.01148727491441380000
0.00125929105421068000  0.00023310438566684100  0.00299226378295091000
0.00133896253005925000
% 0.10974031018693600000    0.01584293599811250000  0.05571720988840550000
0.03717997396867630000  0.01946121654524540000  0.00333217221545134000
0.00801535877256463000  0.40805662480673100000  0.35462125242030000000
0.03452016538793590000  0.00628400931753088000  0.08426152611597320000
0.03675123007988330000
% 0.15985769157917300000    0.02273817850731220000  0.08051904493509900000
0.05356399296479480000  0.02794958879573950000  0.00477135622605706000
0.01148727491441380000  0.35462125242030000000  0.84054270527912000000
0.04970924648061240000  0.00900307653224238000  0.12230684534218500000
0.05294240721881030000
% 0.01645222651384770000    0.00247907369563551000  0.00854977647423445000
0.00575602511127264000  0.00303964493165852000  0.00052479169660924400
0.00125929105421068000  0.03452016538793590000  0.04970924648061240000
0.00656275310918714000  0.00098816558642132100  0.01276571267536310000
0.00569084314124382000
% 0.00301935310752433000    0.00045856474072980100  0.00157588822773501000
0.00106266446337429000  0.00056206977845188800  0.00009718508771753840
0.00023310438566684100  0.00628400931753088000  0.00900307653224239000
0.00098816558642132100  0.00019089535150449000  0.00234741062736786000
0.00105067076647467000
% 0.03964352112669060000    0.00589763160885668000  0.02045785025594820000
0.01373670371293080000  0.00723514219104478000  0.00124609390723684000
0.00299226378295091000  0.08426152611597320000  0.12230684534218500000
0.01276571267536310000  0.00234741062736786000  0.04529972797860520000
0.01358030195540450000
% 0.01750469849806400000    0.00263606404919702000  0.00909369021038843000
0.00612144425955982000  0.00323221688690430000  0.00055797492754462000
0.00133896253005925000  0.03675123007988320000  0.05294240721881030000
0.00569084314124382000  0.00105067076647467000  0.01358030195540450000
0.00750323361743787000];

%% ---------- START ---------- %%
n=14;
% VENOUS
model1.param(1).name = 'Venous volume [L]';
model1.param(1).type = 4;
model1.param(1).value = 0;
model1.param(2).name = 'Venous flow [L/h]';
model1.param(2).type = 5;
model1.param(2).value = 0;
model1.param(3).name = 'Venous Kp';
model1.param(3).type = 3;
model1.param(3).value = [1 0.1];
model1.param(4).name = 'Venous Clearance';
model1.param(4).type = 0;
model1.param(4).value = 0;
model1.param(5).name = 'Venous Initial Condition';
model1.param(5).type = 0;
model1.param(5).value = 0;
% LUNGS
model1.param(6).name = 'Lung volume [L]';
model1.param(6).type = 4;
model1.param(6).value = 0;
model1.param(7).name = 'Lung flow [L/h]';
model1.param(7).type = 5;
model1.param(7).value = 0;
model1.param(8).name = 'Lung Kp';
```

```
model1.param(8).type = 3;
model1.param(8).value = [13.59 1.359];     %male
% model1.param(8).value = [13.13 1.313];   %female
model1.param(9).name = 'Lung Clearance';
model1.param(9).type = 0;
model1.param(9).value = 0;
model1.param(10).name = 'Lung Initial Condition';
model1.param(10).type = 0;
model1.param(10).value = 0;
% ARTERIAL
model1.param(11).name = 'Arterial volume [L]';
model1.param(11).type = 4;
model1.param(11).value = 0;
model1.param(12).name = 'Arterial flow [L/h]';
model1.param(12).type = 5;
model1.param(12).value = 0;
model1.param(13).name = 'Arterial Kp';
model1.param(13).type = 3;
model1.param(13).value = [1 0.1];
model1.param(14).name = 'Arterial Clearance';
model1.param(14).type = 0;
model1.param(14).value = 0;
model1.param(15).name = 'Arterial Initial Condition';
model1.param(15).type = 0;
model1.param(15).value = 0;
% LIVER
model1.param(16).name = 'Liver volume [L]';
model1.param(16).type = 4;
model1.param(16).value = 0;
model1.param(17).name = 'Liver flow [L/h]';
model1.param(17).type = 5;
model1.param(17).value = 0;
model1.param(18).name = 'Liver Kp';
model1.param(18).type = 3;
model1.param(18).value = [6.26 0.626];    %male
% model1.param(18).value = [6.13 0.613];  %female
model1.param(19).name = 'Liver Clearance';
model1.param(19).type = 2;
model1.param(19).value = [0.064 0.0192];   %Male
% model1.param(19).value = [0.084 0.0252]; %Female
model1.param(20).name = 'Liver Initial Condition';
model1.param(20).type = 0;
model1.param(20).value = 0;
% GUT
model1.param(21).name = 'Gut volume [L]';
model1.param(21).type = 4;
model1.param(21).value = 0;
model1.param(22).name = 'Gut flow [L/h]';
model1.param(22).type = 5;
model1.param(22).value = 0;
model1.param(23).name = 'Gut Kp';
model1.param(23).type = 3;
model1.param(23).value = [6.96 0.696];   %male
% model1.param(23).value = [6.13 0.613]; %female
model1.param(24).name = 'Gut Clearance';
model1.param(24).type = 2;
model1.param(24).value = [0.134 0.0402];   %Male
% model1.param(24).value = [0.141 0.0423]; %Female
model1.param(25).name = 'Gut Initial Condition';
model1.param(25).type = 0;
model1.param(25).value = 0;
% SPLEEN
model1.param(26).name = 'Spleen volume [L]';
model1.param(26).type = 4;
model1.param(26).value = 0;
```

```
model1.param(27).name = 'Spleen flow [L/h]';
model1.param(27).type = 5;
model1.param(27).value = 0;
model1.param(28).name = 'Spleen Kp';
model1.param(28).type = 3;
model1.param(28).value = [16.77 1.677];     %male
% model1.param(28).value = [16.05 0.1605];  %female
model1.param(29).name = 'Spleen Clearance';
model1.param(29).type = 0;
model1.param(29).value = 0;
model1.param(30).name = 'Spleen Initial Condition';
model1.param(30).type = 0;
model1.param(30).value = 0;
% KIDNEY
model1.param(31).name = 'Kidney volume [L]';
model1.param(31).type = 4;
model1.param(31).value = 0;
model1.param(32).name = 'Kidney flow [L/h]';
model1.param(32).type = 5;
model1.param(32).value = 0;
model1.param(33).name = 'Kidney Kp';
model1.param(33).type = 3;
model1.param(33).value = [12.75 1.275];   %male
% model1.param(33).value = [12.56 1.256]; %female
model1.param(34).name = 'Kidney Clearance';
model1.param(34).type = 2;
model1.param(34).value = [0.517 0.1551];   %Male
% model1.param(34).value = [0.515 0.1545]; %Female
model1.param(35).name = 'Kidney Initial Condition';
model1.param(35).type = 0;
model1.param(35).value = 0;
% MUSCLE
model1.param(36).name = 'Muscle volume [L]';
model1.param(36).type = 4;
model1.param(36).value = 0;
model1.param(37).name = 'Muscle flow [L/h]';
model1.param(37).type = 5;
model1.param(37).value = 0;
model1.param(38).name = 'Muscle Kp';
model1.param(38).type = 3;
model1.param(38).value = [16.77 1.677];    %male
% model1.param(38).value = [16.05 1.605];  %female
model1.param(39).name = 'Muscle Clearance';
model1.param(39).type = 0;
model1.param(39).value = 0;
model1.param(40).name = 'Muscle Initial Condition';
model1.param(40).type = 0;
model1.param(40).value = 0;
% ADIPOSE
model1.param(41).name = 'Adipose volume [L]';
model1.param(41).type = 4;
model1.param(41).value = 0;
model1.param(42).name = 'Adipose flow [L/h]';
model1.param(42).type = 5;
model1.param(42).value = 0;
model1.param(43).name = 'Adipose Kp';
model1.param(43).type = 3;
model1.param(43).value = [1.56 0.156];   %male
% model1.param(43).value = [1.50 0.150]; %female
model1.param(44).name = 'Adipose Clearance';
model1.param(44).type = 0;
model1.param(44).value = 0;
model1.param(45).name = 'Adipose Initial Condition';
model1.param(45).type = 0;
model1.param(45).value = 0;
```

```
% SKIN
model1.param(46).name = 'Skin volume [L]';
model1.param(46).type = 4;
model1.param(46).value = 0;
model1.param(47).name = 'Skin flow [L/h]';
model1.param(47).type = 5;
model1.param(47).value = 0;
model1.param(48).name = 'Skin Kp';
model1.param(48).type = 3;
model1.param(48).value = [9.48 0.948];   %male
% model1.param(48).value = [9.21 0.921]; %female
model1.param(49).name = 'Skin Clearance';
model1.param(49).type = 0;
model1.param(49).value = 0;
model1.param(50).name = 'Skin Initial Condition';
model1.param(50).type = 0;
model1.param(50).value = 0;
% HEART
model1.param(51).name = 'Heart volume [L]';
model1.param(51).type = 4;
model1.param(51).value = 0;
model1.param(52).name = 'Heart flow [L/h]';
model1.param(52).type = 5;
model1.param(52).value = 0;
model1.param(53).name = 'Heart Kp';
model1.param(53).type = 3;
model1.param(53).value = [12.45 1.245];    %male
% model1.param(53).value = [12.00 1.2];    %female
model1.param(54).name = 'Heart Clearance';
model1.param(54).type = 0;
model1.param(54).value = 0;
model1.param(55).name = 'Heart Initial Condition';
model1.param(55).type = 0;
model1.param(55).value = 0;
% BRAIN
model1.param(56).name = 'Brain volume [L]';
model1.param(56).type = 4;
model1.param(56).value =0;
model1.param(57).name = 'Brain flow [L/h]';
model1.param(57).type = 5;
model1.param(57).value = 0;
model1.param(58).name = 'Brain Kp';
model1.param(58).type = 3;
model1.param(58).value = [0.50 0.05];    %male
% model1.param(58).value = [0.49 0.049]; %female
model1.param(59).name = 'Brain Clearance';
model1.param(59).type = 0;
model1.param(59).value = 0;
model1.param(60).name = 'Brain Initial Condition';
model1.param(60).type = 0;
model1.param(60).value = 0;
% BONE
model1.param(61).name = 'Bone volume [L]';
model1.param(61).type = 4;
model1.param(61).value = 0;
model1.param(62).name = 'Bone flow [L/h]';
model1.param(62).type = 5;
model1.param(62).value = 0;
model1.param(63).name = 'Bone Kp';
model1.param(63).type = 3;
model1.param(63).value = [9.09 0.909];     %male
% model1.param(63).value = [8.77 0.877];   %female
model1.param(64).name = 'Bone Clearance';
model1.param(64).type = 0;
model1.param(64).value = 0;
```

```
model1.param(65).name = 'Bone Initial Condition';
model1.param(65).type = 0;
model1.param(65).value = 0;
% REST COMPARTMENT
model1.param(66).name = 'Rest volume [L]';
model1.param(66).type = 4;
model1.param(66).value = 0;
model1.param(67).name = 'Rest flow [L/h]';
model1.param(67).type = 5;
model1.param(67).value = 0;
model1.param(68).name = 'Rest Kp';
model1.param(68).type = 3;
model1.param(68).value = [1 0.1];
model1.param(69).name = 'Rest Clearance';
model1.param(69).type = 0;
model1.param(69).value = 0;
model1.param(70).name = 'Rest Initial Condition';
model1.param(70).type = 0;
model1.param(70).value = 0;
% FRACTION UNBOUND
model1.param(71).name = 'Fraction unbound in blood';
model1.param(71).type = 1;
model1.param(71).value = [0.767 0.0767];  %Male and female

%% PARAMETER FOR ORAL MODEL %%
% ABSORPTION RATE CONSTANT
model1.param(72).name = 'Absorption rate (KA)';
model1.param(72).type = 6;
model1.param(72).value =[1.27 0.381];
% BIOAVAILABILITY
model1.param(73).name = 'Bioavailability (FA)';
model1.param(73).type = 1;
model1.param(73).value =[0.837 0.0837];
% LAG TIME
model1.param(74).name = 'Absorption lag (h)';
model1.param(74).type = 0;
model1.param(74).value =0.742;
% BLOOD-TO-PLASMA RATIO
model1.param(75).name = 'Blood-to-Plasma ratio';
model1.param(75).type = 0;
model1.param(75).value =1.028;

%% ---------- START ---------- %%
%% ---------- MONTE CARLO SIMULATION START ----------%%
S_smp_BWm=[];
S_smp_Vve=[];
S_smp_Vlu=[];
S_smp_Vart=[];
S_smp_Vli=[];
S_smp_Vgut=[];
S_smp_Vspl=[];
S_smp_Vki=[];
S_smp_Vmu=[];
S_smp_Vad=[];
S_smp_Vsk=[];
S_smp_Vht=[];
S_smp_Vbr=[];
S_smp_Vbo=[];
S_smp_Vre=[];
S_smp_COm=[];
S_smp_Qli=[];
S_smp_Qgut=[];
S_smp_Qspl=[];
S_smp_Qki=[];
S_smp_Qmu=[];
```

```
S_smp_Qad=[];
S_smp_Qsk=[];
S_smp_Qht=[];
S_smp_Qbr=[];
S_smp_Qbo=[];
S_smp_Qre=[];

for i=1:500
i
p=[];
[ff,bb,smp_BWn,smp_BWm,smp_COn,smp_COm] = samCO(mean,var)
 %ff=organ volume for malnutrition
 %bb=organ blood flow for malnutrition
fre=smp_BWm-sum(ff)
ffre=smp_COm-sum(bb)
S_smp_Vve=[S_smp_Vve; ff(1)]
S_smp_Vlu=[S_smp_Vlu; ff(2)]
S_smp_Vart=[S_smp_Vart; ff(3)]
S_smp_Vli=[S_smp_Vli; ff(4)]
S_smp_Vgut=[S_smp_Vgut; ff(5)]
S_smp_Vspl=[S_smp_Vspl; ff(6)]
S_smp_Vki=[S_smp_Vki; ff(7)]
S_smp_Vmu=[S_smp_Vmu; ff(8)]
S_smp_Vad=[S_smp_Vad; ff(9)]
S_smp_Vsk=[S_smp_Vsk; ff(10)]
S_smp_Vht=[S_smp_Vht; ff(11)]
S_smp_Vbr=[S_smp_Vbr; ff(12)]
S_smp_Vbo=[S_smp_Vbo; ff(13)]
S_smp_BWm=[S_smp_BWm; smp_BWm]
S_smp_Qli=[S_smp_Qli; bb(1)]
S_smp_Qgut=[S_smp_Qgut; bb(2)]
S_smp_Qspl=[S_smp_Qspl; bb(3)]
S_smp_Qki=[S_smp_Qki; bb(4)]
S_smp_Qmu=[S_smp_Qmu; bb(5)]
S_smp_Qad=[S_smp_Qad; bb(6)]
S_smp_Qsk=[S_smp_Qsk; bb(7)]
S_smp_Qht=[S_smp_Qht; bb(8)]
S_smp_Qbr=[S_smp_Qbr; bb(9)]
S_smp_Qbo=[S_smp_Qbo; bb(10)]
S_smp_COm=[S_smp_COm; smp_COm]

for j=1:75
if model1.param(j).type==4
if j==1 %venous volume
smp=ff(1);
elseif j==6 %lung volume
smp=ff(2);
elseif j==11 %arterial volume
smp=ff(3);
elseif j==16 %liver volume
smp=ff(4);
elseif j==21 %gut volume
smp=ff(5);
elseif j==26 %spleen volume
smp=ff(6);
elseif j==31 %kidney volume
smp=ff(7);
elseif j==36 %muscle volume
smp=ff(8);
elseif j==41 %adipose volume
smp=ff(9);
elseif j==46 %skin volume
smp=ff(10);
elseif j==51 %heart volume
smp=ff(11);
```

```
elseif j==56 %brain volume
smp=ff(12);
elseif j==61 %bone volume
smp=ff(13);
elseif j==66 %rest compartment
smp=fre;
end

elseif model1.param(j).type==5;
    if j==2 %venous flow
        smp=smp_COm;
    elseif j==7 %lung flow
        smp=smp_COm;
    elseif j==12 %arterial flow
        smp=smp_COm;
    elseif j==17 %liver flow
        smp=bb(1);
    elseif j==22 %gut flow
        smp=bb(2);
    elseif j==27 %spleen flow
        smp=bb(3);
    elseif j==32 %kidney flow
        smp=bb(4);
    elseif j==37 %muscle flow
        smp=bb(5);
    elseif j==42 %adipose flow
        smp=bb(6);
    elseif j==47 %skin flow
        smp=bb(7);
    elseif j==52 %heart flow
        smp=bb(8);
    elseif j==57 %brain flow
        smp=bb(9);
    elseif j==62 %bone flow
        smp=bb(10);
    elseif j==67 %rest flow
        smp=ffre;
    end

% TYPE=0 IS FIXED VALUES
elseif model1.param(j).type==0;
    smp=model1.param(j).value;
% TYPE=1 IS NORMAL DISTRIBUTION FOR fu and F
elseif model1.param(j).type==1
    while model1.param(j).value(1)>0
        m=model1.param(j).value(1);
        v=model1.param(j).value(2);
        smpx= normrnd(m,v);
        if (any (smpx<=0))
            smpx= normrnd(m,v);
        elseif (any (smpx>1))
            smpx= normrnd(m,v);
        else
            smp=smpx;
            break
        end
    end
% TYPE=2 IS LOGNORMAL DISTRIBUTION FOR CLEARANCE
elseif model1.param(j).type==2
    m=model1.param(j).value(1);
    sd=model1.param(j).value(2);
    v=sd^2;
    mu = log((m^2)/sqrt(v+m^2));
    sigma = sqrt(log(v/(m^2)+1));
    smpCL = lognrnd(mu,sigma);
```

```
    smpCLwt=(smpCL*smp_BWm)/1.028; %CLb=CLp/R
    smp=smpCLwt;
% TYPE=3 IS LOGNORMAL DISTRIBUTION FOR Kp
elseif model1.param(j).type==3
    m=model1.param(j).value(1);
    sd=model1.param(j).value(2);
    v=sd^2;
    mu = log((m^2)/sqrt(v+m^2));
    sigma = sqrt(log(v/(m^2)+1));
    smpKp = lognrnd(mu,sigma);
    smp=smpKp;
% TYPE=6 IS LOGNORMAL DISTRIBUTION FOR KA
elseif model1.param(j).type==6
    m=model1.param(j).value(1);
    sd=model1.param(j).value(2);
    v=sd^2;
    mu = log((m^2)/sqrt(v+m^2));
    sigma = sqrt(log(v/(m^2)+1));
    smpKA = lognrnd(mu,sigma);
    smp=smpKA;
end

dose=10*smp_BWm;
p=[p;smp];
end
p;

%%-----ODE start-----
t=[0 0.25 0.5 0.75 0.8 0.9 1 1.25 1.5 1.75 2 3 4 5 6 7 8 9 10 11 12];
% t=[0 0.5 1 1.5 2 3 4 6 8 12];
% t=[0:0.1:12];
[z, A, b]=matrix(p,n,dose);
[t,y]=ode23s('PKmodel',t,z);
Conc=y'; %transpose matrix
kk=size(Conc); %return array dimension - kk= 1 14
m=kk(1,2); %m=14
%zint=y(:,m);
Concsim=[Concsim; Conc];
end
Concsim;
n_comp=14;
ss=size(Concsim);
ss1=ss(1,1);
M=Concsim;

for j=1:n_comp
    for i=j:n_comp:ss1
        if j==1
            sim.comp1=M(i,:);
            K1=[K1;sim.comp1];
        elseif j==2
            sim.comp2=M(i,:);
            K2=[K2;sim.comp2];
        elseif j==3
            sim.comp3=M(i,:);
            K3=[K3;sim.comp3];
        elseif j==4
            sim.comp4=M(i,:);
            K4=[K4;sim.comp4];
        elseif j==5
            sim.comp5=M(i,:);
            K5=[K5;sim.comp5];
        elseif j==6
            sim.comp6=M(i,:);
            K6=[K6;sim.comp6];
```

```
        elseif j==7
            sim.comp7=M(i,:);
            K7=[K7;sim.comp7];
        elseif j==8
            sim.comp8=M(i,:);
            K8=[K8;sim.comp8];
        elseif j==9
            sim.comp9=M(i,:);
            K9=[K9;sim.comp9];
        elseif j==10
            sim.comp10=M(i,:);
            K10=[K10;sim.comp10];
        elseif j==11
            sim.comp11=M(i,:);
            K11=[K11;sim.comp11];
        elseif j==12
            sim.comp12=M(i,:);
            K12=[K12;sim.comp12];
        elseif j==13
            sim.comp13=M(i,:);
            K13=[K13;sim.comp13];
        elseif j==14
            sim.comp14=M(i,:);
            K14=[K14;sim.comp14];
        end
    end
end
K11=K1';
Volume=[S_smp_BWm S_smp_Vve S_smp_Vlu S_smp_Vart S_smp_Vli S_smp_Vgut
S_smp_Vspl S_smp_Vki S_smp_Vmu S_smp_Vad S_smp_Vsk S_smp_Vht S_smp_Vbr
S_smp_Vbo];
Bloodflow=[S_smp_COm S_smp_Qli S_smp_Qgut S_smp_Qspl S_smp_Qki S_smp_Qmu
S_smp_Qad S_smp_Qsk S_smp_Qht S_smp_Qbr S_smp_Qbo];

save DV_venous.dat K1 /ASCII
save DV_venous2.dat K11 /ASCII
save DV_lungs.dat K2 /ASCII
save DV_arterial.dat K3 /ASCII
save DV_liver.dat K4 /ASCII
save DV_gut.dat K5 /ASCII
save DV_spleen.dat K6 /ASCII
save DV_kidney.dat K7 /ASCII
save DV_muscle.dat K8 /ASCII
save DV_adipose.dat K9 /ASCII
save DV_skin.dat K10 /ASCII
save DV_heart.dat K11 /ASCII
save DV_brain.dat K12 /ASCII
save DV_bone.dat K13 /ASCII
save DV_rest.dat K14 /ASCII
save Volume.dat Volume /ASCII
save Bloodflow.dat Bloodflow /ASCII
save WT.dat S_smp_BWm /ASCII
save CO.dat S_smp_COm /ASCII
toc
```

Code 3: samBW.m file

```
function [ff,hh,smp_HT,smp_SDn,smp_SDm,smp_BWn,smp_BWm,fBW] =samBW(mean,var)
ff=[]; %organ volume (malnutrition)
hh=[]; %organ volume (healthy)
sum_alln=[];
sum_allm=[];
smp_HT=[];
smp_SDn=[];
smp_SDm=[];
smp_BWn=[];
smp_BWm=[];
fBW=[];

%%HEIGHT
%Male
m=91.9;
sd=0.1*m;
%Female
% m=90.2;
% sd=0.1*m;
v=sd^2;
mu = log((m^2)/sqrt(v+m^2));
sigma = sqrt(log(v/(m^2)+1));
xx = lognrnd(mu,sigma);
smp_HT=xx;
%%SEVERITY (SD)
lb=-4;
ub=-3;
x = lhsdesign(1,1);
smp_SDn = 0;
smp_SDm = lb + (ub-lb)*x;
%%GENDER (0=male, 1=female)
SEX=0;
%%CALCULATE BW
smp_BWn = exp(0.773+(0.0197*smp_HT)+(0.0880*smp_SDn)-(0.0123*SEX));
smp_BWm = exp(0.773+(0.0197*smp_HT)+(0.0880*smp_SDm)-(0.0123*SEX));
fBW=smp_BWm/smp_BWn;
while (mean>0)
    h=mvnrnd(mean,var,1);
    f(1)=h(1)*fBW;
    f(2)=h(2)*(0.7027*fBW + 0.2836);
    f(3)=h(3)*fBW;
    f(4)=h(4)*(0.7436*fBW + 0.2254);
    f(5)=h(5)*fBW;
    f(6)=h(6)*(0.8942*fBW + 0.0269);
    f(7)=h(7)*(0.5368*fBW + 0.4092);
    f(8)=h(8)*(1.3571*fBW - 0.3401);
    f(9)=h(9)*(1.9*fBW - 0.9);
    f(10)=h(10)*(1.5945*fBW - 0.5945);
    f(11)=h(11)*(0.5384*fBW + 0.3824);
    f(12)=h(12)*0.9;
    f(13)=h(13)*(0.2*fBW + 0.8);
    sum_alln=sum(h);
    sum_allm=sum(f);
    if (any (h<=0))
        h = mvnrnd(mean,var,1);
        f(1)=h(1)*fBW;
        f(2)=h(2)*(0.7027*fBW + 0.2836);
        f(3)=h(3)*fBW;
        f(4)=h(4)*(0.7436*fBW + 0.2254);
        f(5)=h(5)*fBW;
        f(6)=h(6)*(0.8942*fBW + 0.0269);
        f(7)=h(7)*(0.5368*fBW + 0.4092);
```

```
        f(8)=h(8)*(1.3571*fBW - 0.3401);
        f(9)=h(9)*(1.9*fBW - 0.9);
        f(10)=h(10)*(1.5945*fBW - 0.5945);
        f(11)=h(11)*(0.5384*fBW + 0.3824);
        f(12)=h(12)*0.9;
        f(13)=h(13)*(0.2*fBW + 0.8);
    elseif sum_alln>=smp_BWn
        h = mvnrnd(mean,var,1);
        f(1)=h(1)*fBW;
        f(2)=h(2)*(0.7027*fBW + 0.2836);
        f(3)=h(3)*fBW;
        f(4)=h(4)*(0.7436*fBW + 0.2254);
        f(5)=h(5)*fBW;
        f(6)=h(6)*(0.8942*fBW + 0.0269);
        f(7)=h(7)*(0.5368*fBW + 0.4092);
        f(8)=h(8)*(1.3571*fBW - 0.3401);
        f(9)=h(9)*(1.9*fBW - 0.9);
        f(10)=h(10)*(1.5945*fBW - 0.5945);
        f(11)=h(11)*(0.5384*fBW + 0.3824);
        f(12)=h(12)*0.9;
        f(13)=h(13)*(0.2*fBW + 0.8);
    elseif sum_allm>=smp_BWm
        h = mvnrnd(mean,var,1);
        f(1)=h(1)*fBW;
        f(2)=h(2)*(0.7027*fBW + 0.2836);
        f(3)=h(3)*fBW;
        f(4)=h(4)*(0.7436*fBW + 0.2254);
        f(5)=h(5)*fBW;
        f(6)=h(6)*(0.8942*fBW + 0.0269);
        f(7)=h(7)*(0.5368*fBW + 0.4092);
        f(8)=h(8)*(1.3571*fBW - 0.3401);
        f(9)=h(9)*(1.9*fBW - 0.9);
        f(10)=h(10)*(1.5945*fBW - 0.5945);
        f(11)=h(11)*(0.5384*fBW + 0.3824);
        f(12)=h(12)*0.9;
        f(13)=h(13)*(0.2*fBW + 0.8);
    else
        ff=f; %organ volume (malnutrition)
        hh=h; %organ volume (healthy)
        break
    end
end
```

Code 4: samCO.m file

```
function [ff,bb,smp_BWn,smp_BWm,smp_COn,smp_COm] = samCO(mean,var)
smp_COn=[];
smp_COm=[];
sum_all=[];
bb=[]; %organ blood flow (malnutrition)
while (mean>0)
 [ff,hh,smp_HT,smp_SDn,smp_SDm,smp_BWn,smp_BWm,fBW] =samBW(mean,var)
 %ff=organ volume for malnutrition
 %hh=organ volume for healthy
    a=9.164;
    b=-0.0291;
    c=0.000391;
    d=-0.00000191;
    CO=9119-exp(a+(b*smp_BWn)+(c*(smp_BWn^2))+(d*(smp_BWn^3)));
    smp_COn=(CO/1000)*60; %L/h
    BSAn=sqrt((smp_BWn*smp_HT)/3600); %BSA for healthy children
    CI=smp_COn/BSAn; %CI of healthy and malnourished children is similar
    BSAm=sqrt((smp_BWm*smp_HT)/3600); %BSA for malnourished children
    smp_COm=CI*BSAm; %L/h
%% Male organ volume %%
    aa(1)=((hh(4)*0.05777*smp_COn)/0.4479)*(ff(4)/hh(4));     %liver
    aa(2)=((hh(5)*0.14219*smp_COn)/0.2128)*(ff(5)/hh(5));     %gut
    aa(3)=((hh(6)*0.02666*smp_COn)/0.0405)*(ff(6)/hh(6));     %spleen
    aa(4)=((hh(7)*0.09324*smp_COn)/0.0857)*(ff(7)/hh(7));     %kidney
    aa(5)=((hh(8)*0.03921*smp_COn)/2.7185)*(ff(8)/hh(8));     %muscle
    aa(6)=((hh(9)*0.03496*smp_COn)/3.9328)*(ff(9)/hh(9));     %adipose
    aa(7)=((hh(10)*0.01868*smp_COn)/0.3981)*(ff(10)/hh(10));  %skin
    aa(8)=((hh(11)*0.02927*smp_COn)/0.0833)*(ff(11)/hh(11));  %heart
    aa(9)=((hh(12)*0.31561*smp_COn)/1.0783)*(ff(12)/hh(12));  %brain
    aa(10)=((hh(13)*0.02175*smp_COn)/0.4250)*(ff(13)/hh(13)); %bone

%% Female %%
%     aa(1)=((hh(4)*0.06040*smp_COn)/0.4149)*(ff(4)/hh(4));      %liver
%     aa(2)=((hh(5)*0.16726*smp_COn)/0.2143)*(ff(5)/hh(5));      %gut
%     aa(3)=((hh(6)*0.02788*smp_COn)/0.0361)*(ff(6)/hh(6));      %spleen
%     aa(4)=((hh(7)*0.09274*smp_COn)/0.0873)*(ff(7)/hh(7));      %kidney
%     aa(5)=((hh(8)*0.04086*smp_COn)/2.7185)*(ff(8)/hh(8));      %muscle
%     aa(6)=((hh(9)*0.04250*smp_COn)/3.8960)*(ff(9)/hh(9));      %adipose
%     aa(7)=((hh(10)*0.02448*smp_COn)/0.3845)*(ff(10)/hh(10));   %skin
%     aa(8)=((hh(11)*0.03748*smp_COn)/0.0683)*(ff(11)/hh(11));   %heart
%     aa(9)=((hh(12)*0.29287*smp_COn)/0.9602)*(ff(12)/hh(12));   %brain
%     aa(10)=((hh(13)*0.02729*smp_COn)/0.4100)*(ff(13)/hh(13));  %bone
    smp_COm;
    sum_all=sum(aa);
    if (any (aa<=0))
    elseif sum_all>=smp_COm
        ko=1
    else
        bb=aa; %ff are organ blood flow
        break
    end
end
sum(bb);
```

Code 5: matrix.m file

```
function [z, A, b]=matrix(p,n,dose)
global A
global z
global b
global c
global d
global e
A=zeros(14,14); %matrix for PBPK equations
z=zeros(14,1);  %initial condition (inside)
b=zeros(14,1);
c=zeros(1,1); %matrix for KA
d=zeros(1,1);
e=zeros(1,1); %matrix for Tlag
%% -----PBPK MODEL START------
Vven = p(1) ; Qven = p(2) ; Kpven = p(3); CLven = p(4); Cven0 = p(5);
Vlu = p(6) ; Qlu = p(7) ; Kplu = p(8); CLlu = p(9); Clu0 = p(10);
Vart = p(11); Qart = p(12); Kpart = p(13); CLart = p(14); Cart0 = p(15);
Vli = p(16); Qli = p(17); Kpli = p(18); CLli = p(19); Cli0 = p(20);
Vgut = p(21); Qgut = p(22); Kpgut = p(23); CLgut = p(24); Cgut0 = p(25);
Vspl = p(26); Qspl = p(27); Kpspl = p(28); CLspl = p(29); Cspl0 = p(30);
Vki = p(31); Qki = p(32); Kpki = p(33); CLki = p(34); Cki0 = p(35);
Vmu = p(36); Qmu = p(37); Kpmu = p(38); CLmu = p(39); Cmu0 = p(40);
Vad = p(41); Qad = p(42); Kpad = p(43); CLad = p(44); Cad0 = p(45);
Vsk = p(46); Qsk = p(47); Kpsk = p(48); CLsk = p(49); Csk0 = p(50);
Vht = p(51); Qht = p(52); Kpht = p(53); CLht = p(54); Cht0 = p(55);
Vbr = p(56); Qbr = p(57); Kpbr = p(58); CLbr = p(59); Cbr0 = p(60);
Vbo = p(61); Qbo = p(62); Kpbo = p(63); CLbo = p(64); Cbo0 = p(65);
Vre = p(66); Qre = p(67); Kpre = p(68); CLre = p(69); Cre0 = p(70);
fu=p(71); KA=p(72); F=p(73); TLag=p(74); R=p(75);
Qtot=Qlu;
Qhe = Qli + Qgut + Qspl;
%Hepatic clearance
fup=fu*R;
if (Qhe>CLli)
    CLint=(Qhe*CLli)/(fup*(Qhe-(CLli/R)));
else
    CLint=Qhe;
end
CLH=CLint*fu; %corrected to obtain Kpu
CLR=CLki/R;
CLT=CLgut/R;
A(1,1) = -Qtot/Vven;
A(2,1) = Qtot/Vlu;
A(4,1) = Qli/Vli;
A(5,1) = Qgut/Vgut;
A(6,1) = Qspl/Vspl;
A(7,1) = Qki/Vki;
A(8,1) = Qmu/Vmu;
A(9,1) = Qad/Vad;
A(10,1)= Qsk/Vsk;
A(11,1)= Qht/Vht;
A(12,1)= Qbr/Vbr;
A(13,1)= Qbo/Vbo;
A(14,1)= Qre/Vre;
A(1,4) = Qhe/(Vven*(Kpli/R));
A(1,7) = Qki/(Vven*(Kpki/R));
A(1,8) = Qmu/(Vven*(Kpmu/R));
A(1,9) = Qad/(Vven*(Kpad/R));
A(1,10)= Qsk/(Vven*(Kpsk/R));
A(1,11)= Qht/(Vven*(Kpht/R));
A(1,12)= Qbr/(Vven*(Kpbr/R));
A(1,13)= Qbo/(Vven*(Kpbo/R));
```

```
A(1,14)= Qre/(Vven*(Kpre/R));
A(3,2) = Qtot/(Vart*(Kplu/R));
A(4,5) = Qgut /(Vli*(Kpgut/R));
A(4,6) = Qspl/(Vli*(Kpspl/R));
A(2,2) = -(Qtot)/(Vlu*(Kplu/R));
A(3,3) = -Qtot / Vart;
A(4,4) = -(Qhe+CLH)/(Vli*(Kpli/R));
A(5,5) = -(Qgut+CLT)/(Vgut*(Kpgut/R));
A(6,6) = -(Qspl)/(Vspl*(Kpspl/R));
A(7,7) = -(Qki+CLR)/(Vki*(Kpki/R));
A(8,8) = -(Qmu)/(Vmu*(Kpmu/R));
A(9,9) = -(Qad)/(Vad*(Kpad/R));
A(10,10) = -(Qsk)/(Vsk*(Kpsk/R));
A(11,11) = -(Qht)/(Vht*(Kpht/R));
A(12,12) = -(Qbr)/(Vbr*(Kpbr/R));
A(13,13) = -(Qbo)/(Vbo*(Kpbo/R));
A(14,14) = -(Qre)/(Vre*(Kpre/R));
%% ---------- PBPK END ----------%%
c=KA;
d=(F*dose)/Vgut;
e=TLag;
end
```

Code 6: PKmodel.m file

```
function [dydt] = PKmodel(t,y)
global A;
global b;
global c;
global d;
global e;
f=zeros(14,1);
f(5)=(c*d)*exp(-c*(t-e));
if t<=e
    [dydt]=A*y+0.00000001;
else
    [dydt]=A*y+f;
end
end
```

Appendix III: Comparison of concentration-time profiles in different organs obtained from a WBPBPK model of healthy children and malnourished children

A: children aged 6 months (1/2)

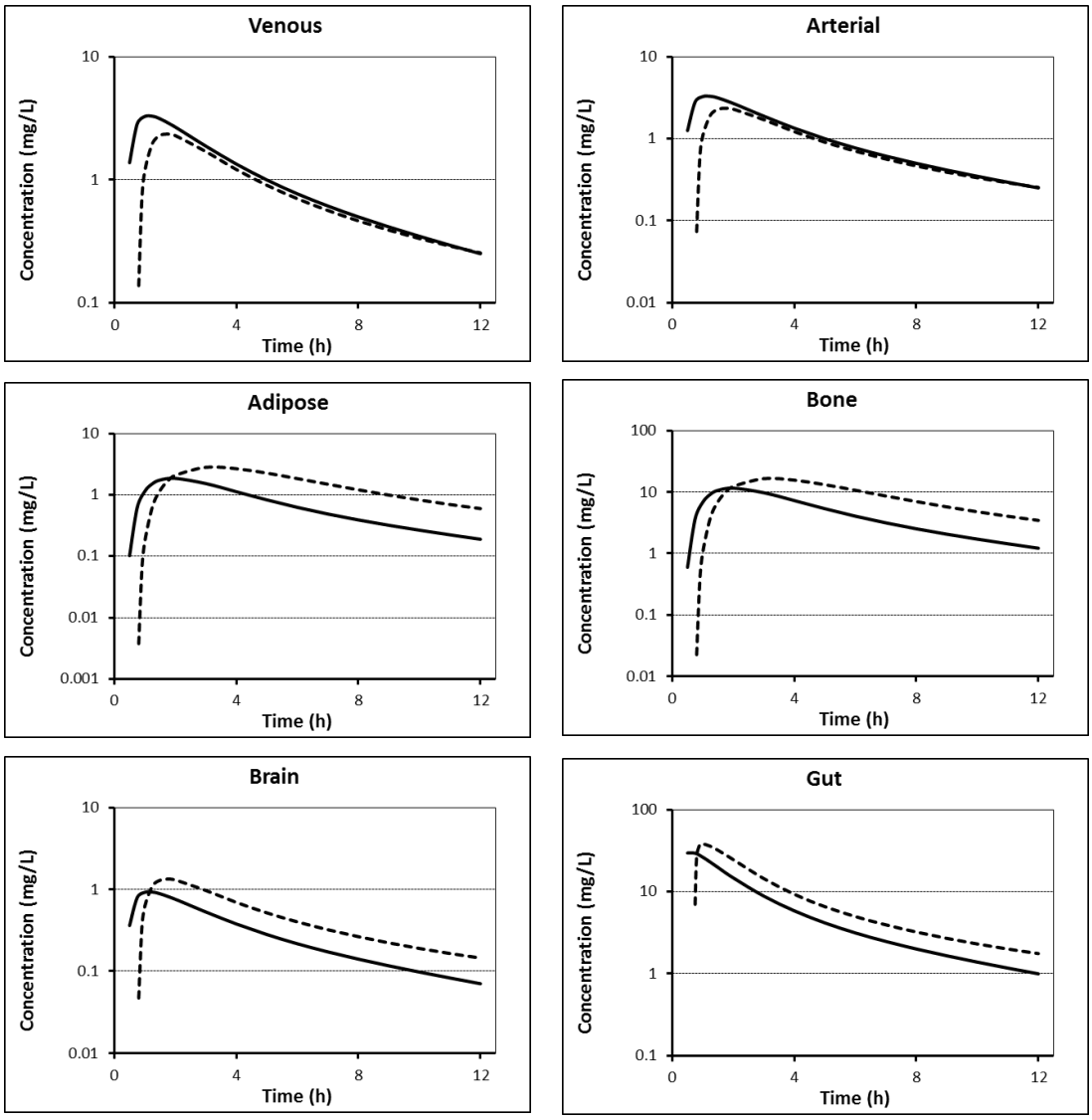

Key: solid line = healthy children, dashed line = malnourished children.

A: children aged 6 months (2/2)

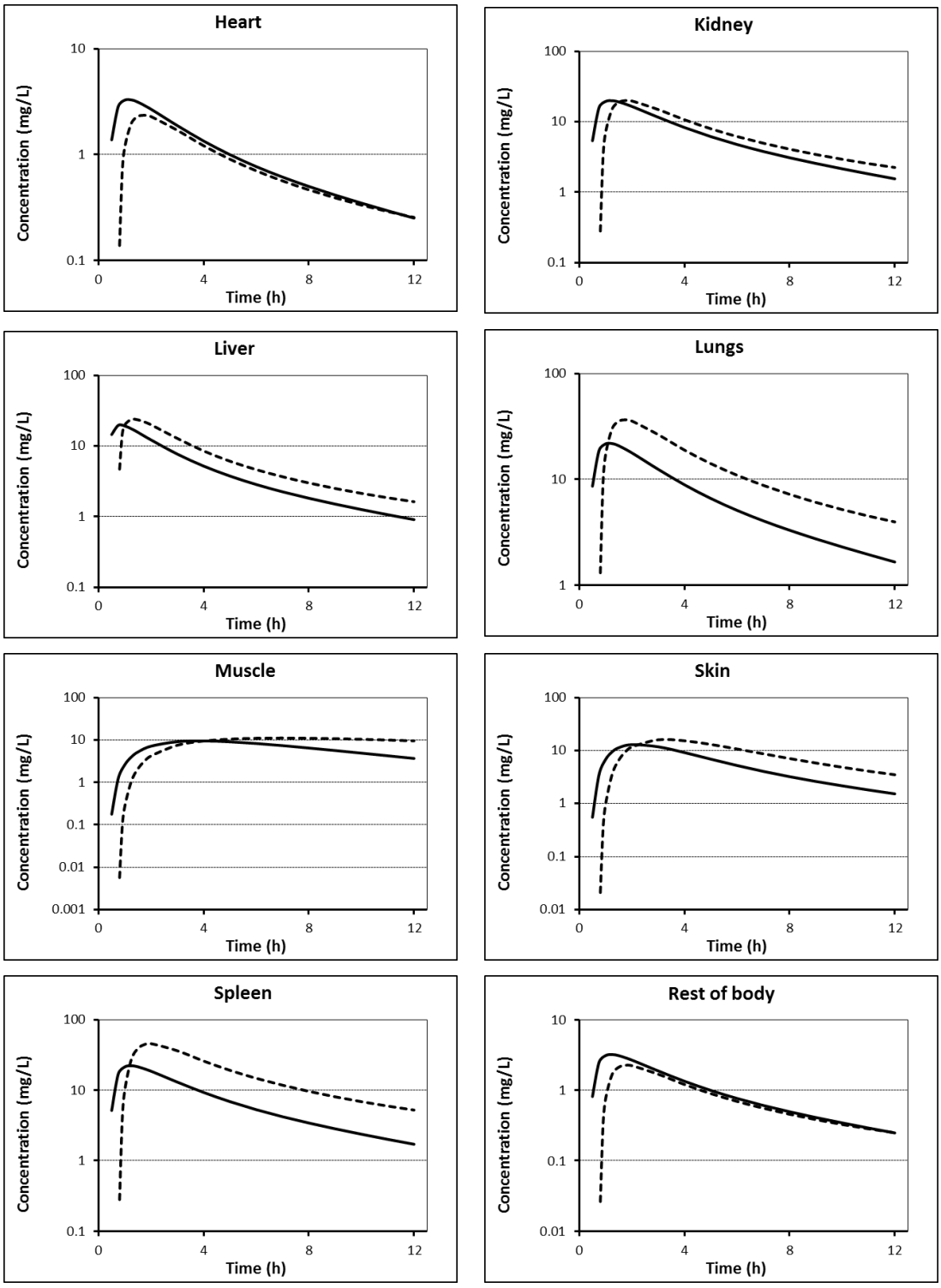

B: children aged 1 year (1/2)

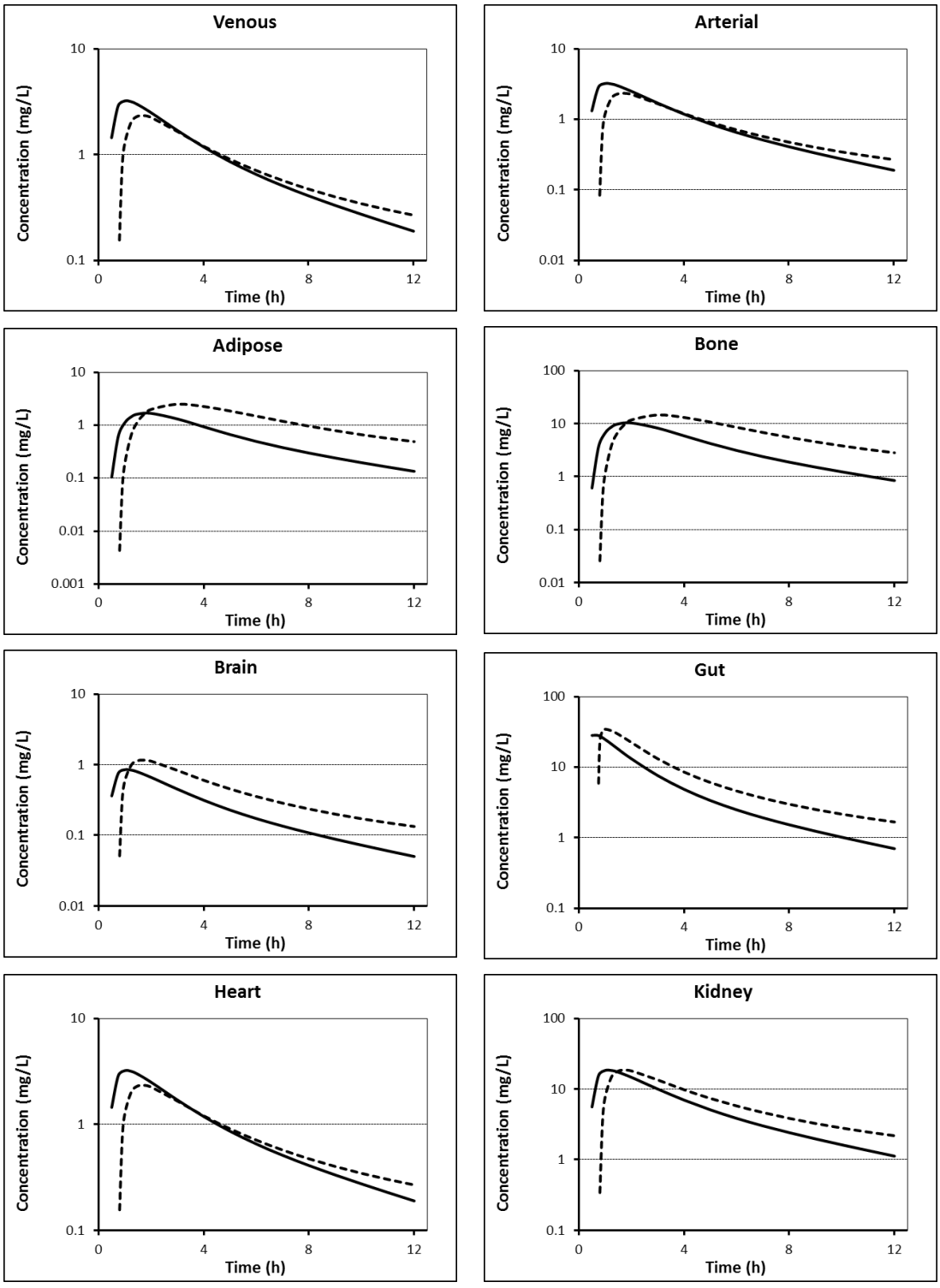

Key: solid line = healthy children, dashed line = malnourished children.

B: children aged 1 year (2/2)

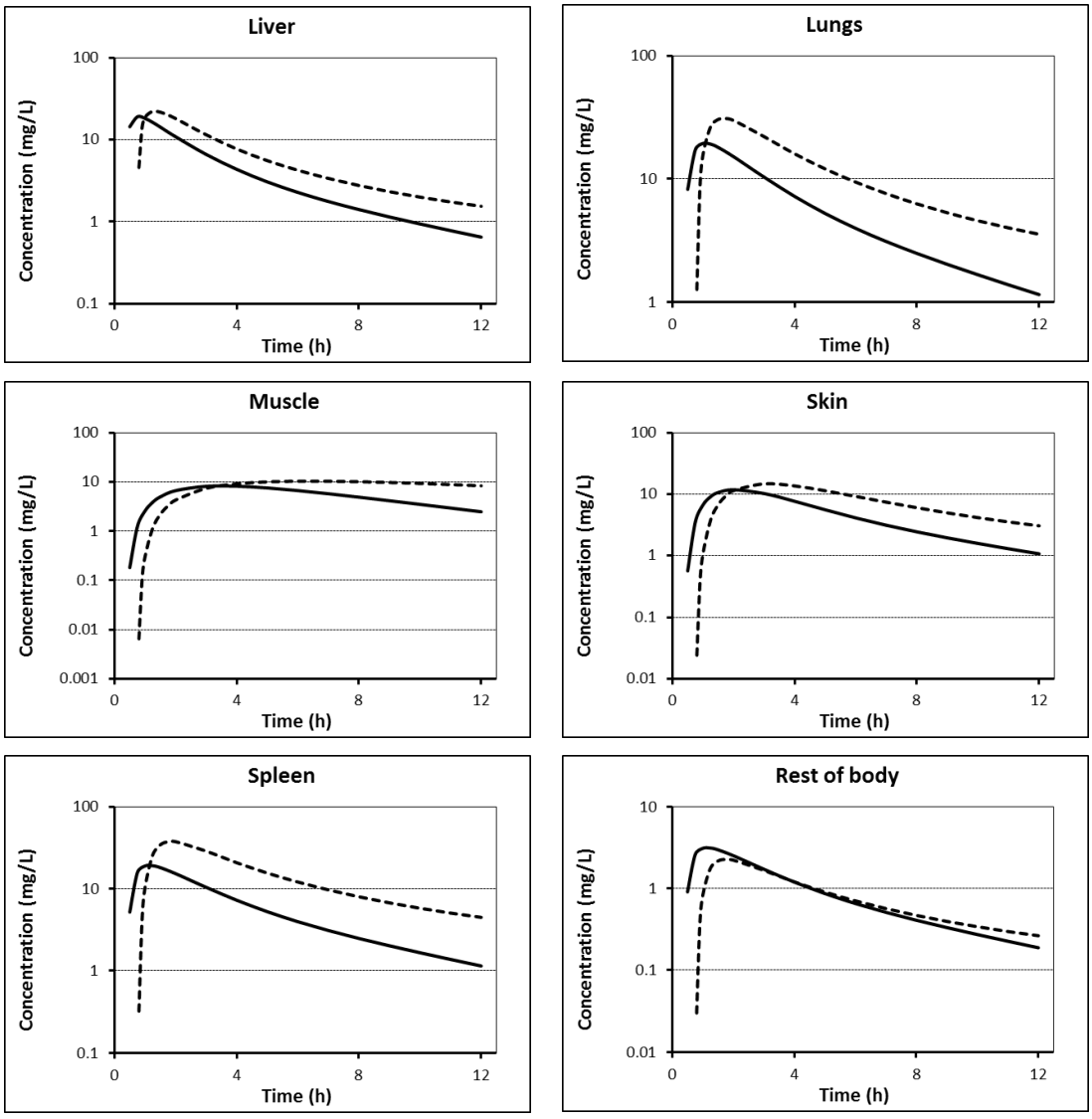

C: children aged 5 years (1/2)

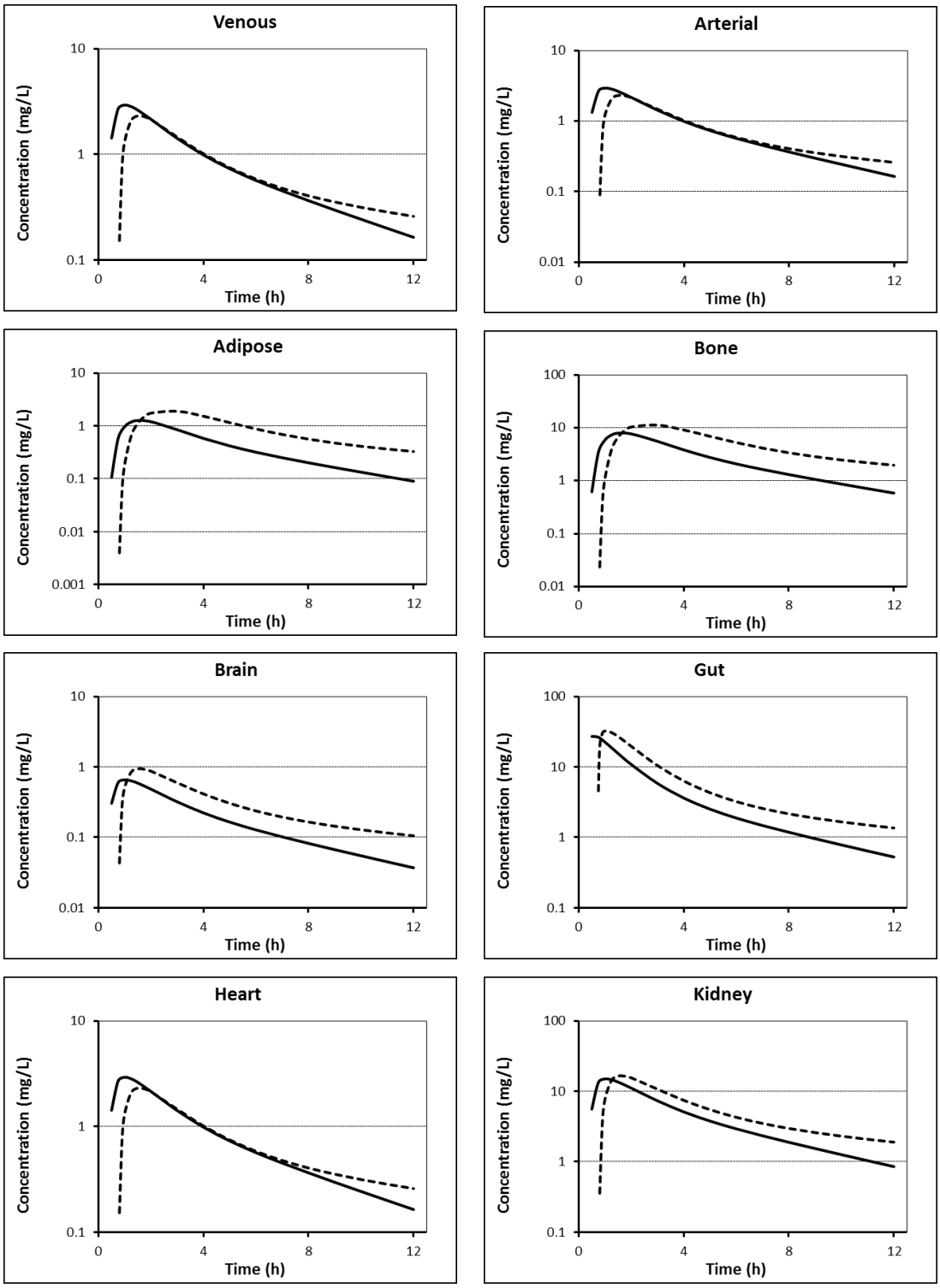

Key: solid line = healthy children, dashed line = malnourished children.

C: children aged 5 years (2/2)

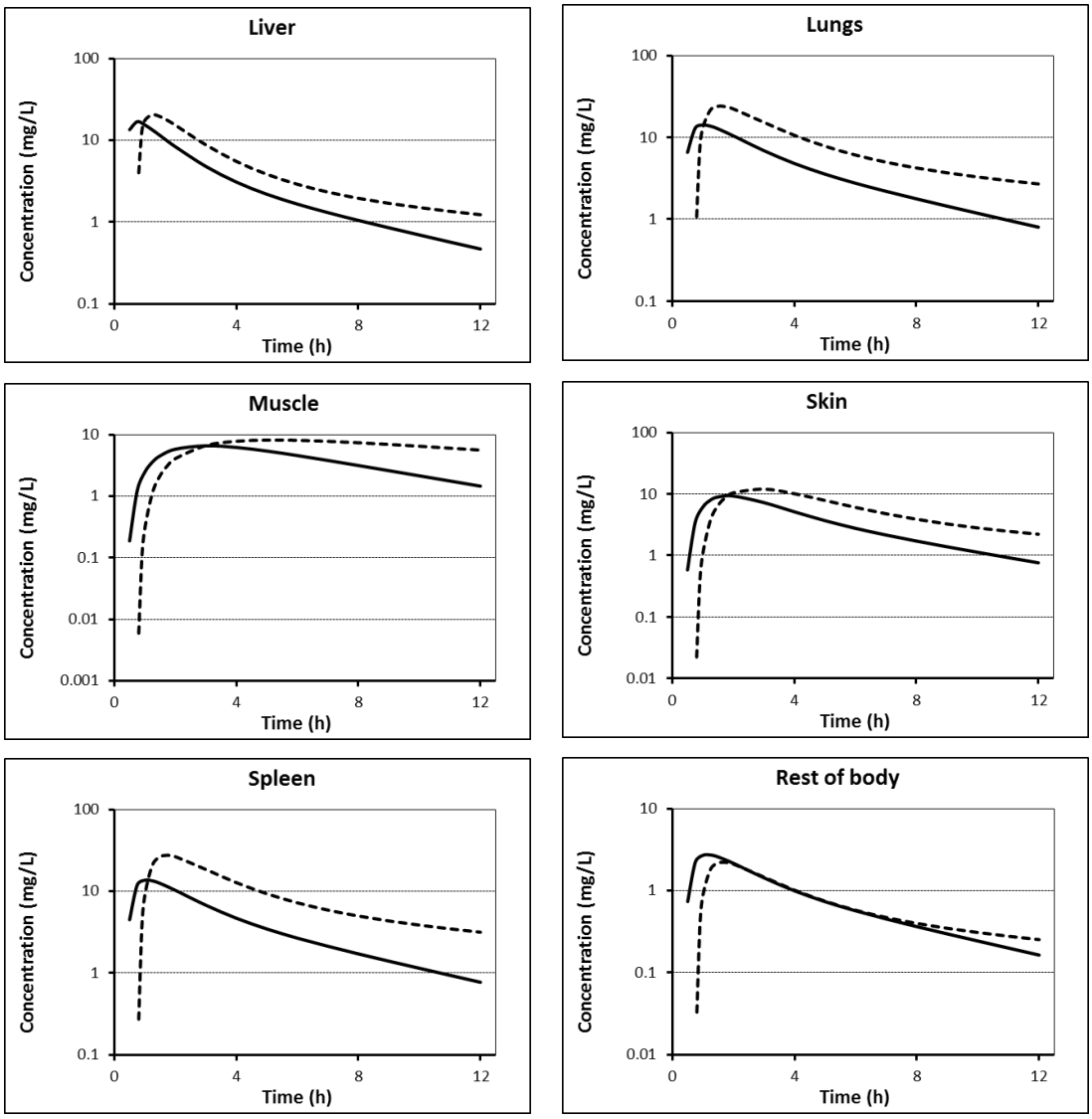

D: children aged 10 years (1/2)

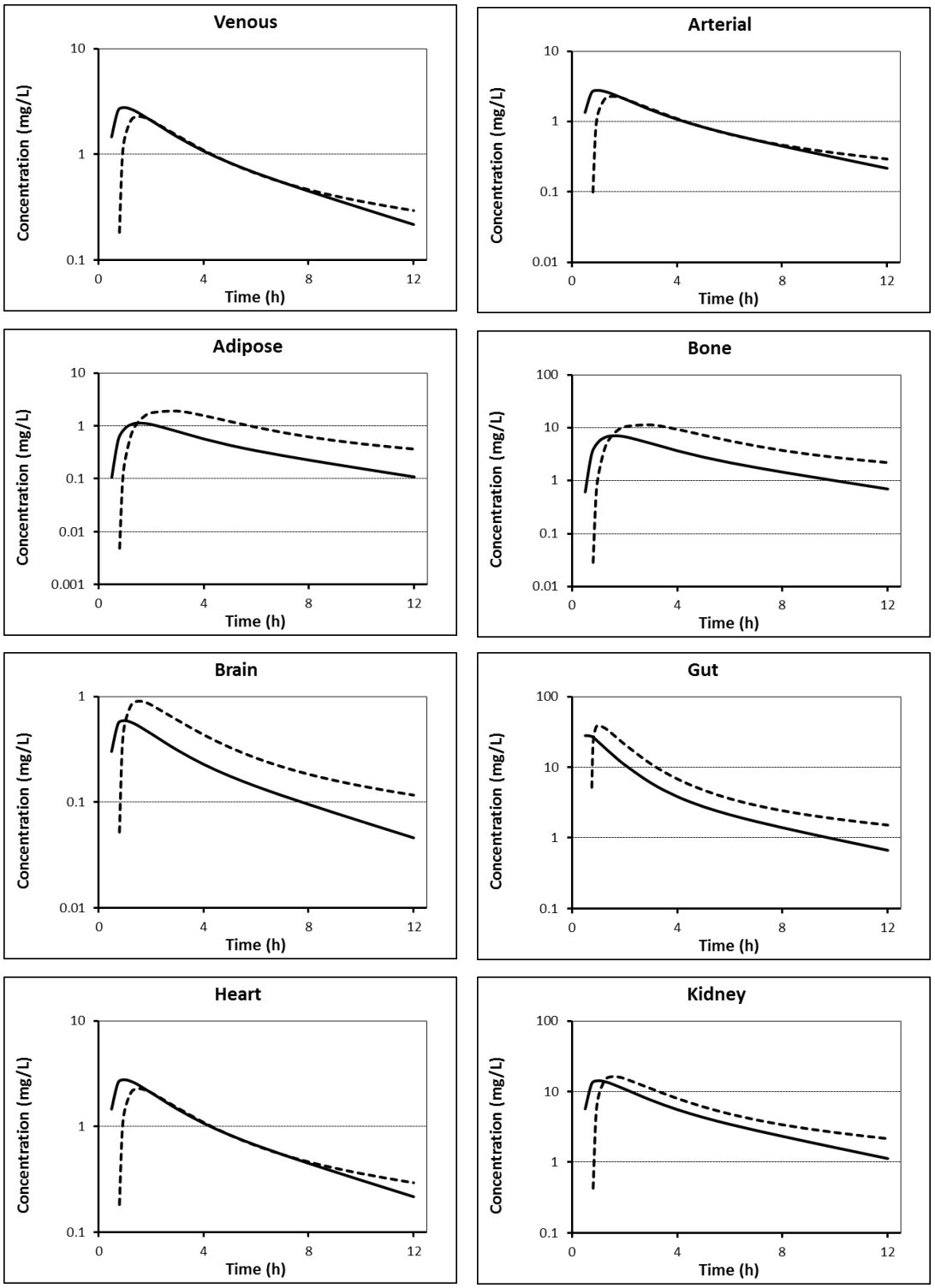

Key: solid line = healthy children, dashed line = malnourished children.

D: children aged 10 years (2/2)